DEVELOPMENT AND EVALUATION OF MOUSE MONOCLONAL ANTIBODIES AGAINST HUMAN C1Q

JOSEPH WILLIAM WRIN

Adelaide Medical School
Faculty of Health and Medical Science
The University of Adelaide

August 2022

A thesis submitted to The University of Adelaide in fulfillment of the requirements for the admission to the degree of Doctor of Philosophy

TABLE OF CONTENTS

LIST OF FIGURES

LIST OF TABLES

ABSTRACT

The complement protein C1q plays an important role in breast cancer susceptibility, development, and progression. Mice genetically deficient in C1qA exhibit an eighty-five percent decrease in mammary tumour incidence when administered the chemical carcinogen DMBA. Similarly, in the aggressive MMTV-PyMT model of mouse mammary cancer, *C1qA* null mutant mice exhibit two thirds of the tumour burden seen in wild type mice and a third of the late-stage carcinoma at eighteen weeks of age. There may also be a role for C1q in human breast cancer as women genetically deficient in C1q have a decreased incidence of breast cancer. C1q plays a key role in macrophage-mediated efferocytic uptake of dying mammary epithelial cells, thereby preventing apoptotic cells from becoming necrotic and releasing pro-inflammatory cytoplasmic components. Persistence of necrotic cells alters the immune response during cancer initiation, as evidenced by an increase in cytotoxic T cells mobilised to the mammary gland of C1q null mutant mice in response to carcinogen DMBA. The over-arching goal of this research project was to generate and characterise an inhibitor of C1q-mediated efferocytosis. A monoclonal antibody was chosen as the C1q inhibitor, to further explore the role of C1q in breast cancer and as a potential first step in development of a new breast cancer therapeutic.

Human C1q was inoculated into *C1qA* null mutant mice to generate an antibody-mediated immune response to C1q. Three fusions of immune splenocytes from these mice yielded a total of 2,776 cultures of which 2,017 contained viable hybridomas. Antibody binding by enzyme-linked immunosorbent assay (ELISA) included both linear epitopes (contiguous amino acids) and conformational epitopes (binding to a three-dimensional structure), making this an ideal screening strategy. Screening of these cultures by ELISA identified eight hybridomas that bound C1q. Of these, four were successfully expanded and cultures established from single cells. Thus, four candidate monoclonal antibodies were generated: BHI1-1G4, BHI1-4D3, BHI3-3F6, and BHI3-8B9.

Characterisation of these antibodies was performed to determine the specificity of their binding conditions. Binding of the monoclonal antibodies in assays that involve denaturation of proteins and presentation of linear epitopes was not observed. These assays included western blotting, immunohistochemistry on normal breast sections, and immunocytochemistry on a fixed macrophage cell line. An assay with potential to display conformational epitopes, immunocytochemistry on unfixed macrophages, also did not demonstrate monoclonal binding. The antibodies were also tested for binding to C1q by immunoprecipitation. This assay can detect conformational epitopes, and all four monoclonal antibodies were demonstrated to bind soluble C1q by this method. Combined, these studies suggested that all four candidate monocloncal antibodies bind only to intact native C1q and do not bind to denatured antigen.

Identification of a monoclonal antibody that inhibits C1q-mediated efferocytosis required development of a bioassay that quantifies the functional activity of candidate antibodies. An *in vitro* efferocytosis assay was developed involving fluorescent green-labelled macrophages co-cultured with fluorescent red-labelled MDA-MB-231 breast cancer cells induced to undergo apoptosis by cross-linking the TRAIL receptor 2. Co-localisation of red and green fluorescence as an indicator of efferocytosis was investigated in bone marrow-derived macrophages from *C1qA* replete and null mice. Reduced efferocytosis was observed in macrophages where C1q was absent and was quantified using ImageJ software involving digital masking of images and Boolean calculation of overlap. Hybridoma supernatants from candidate antibodies BHI1-1G4 and BHI1-4D3 were tested in the assay using the mouse macrophage cell line RAW 264.7 labelled green and dying breast cancer cells labelled red. Commercially available anti-C1q antibody 9A7 and hybridoma supernatant from non-C1q binding cell line BHI3-2C12 were also assessed. The antibodies exhibited variable capacity to affect C1q-mediated phagocytosis however whether a specific candidate monoclonal antibody could effectively inhibit C1q was inconclusive due to a high degree of variability in the timing of apoptotic cell uptake.

This research led to the generation of four candidate monoclonal antibodies with potential for further pre-clinical research. Future work should concentrate on purification of the antibodies in order to improve investigation of their inhibitory capacity in C1q-mediated efferocytosis bioassays. Studies in mouse mammary cancer models would also provide valuable data on the potential of these candidate antibodies for downstream clinical applications in breast cancer patients.

DECLARATION

I certify that this work contains no material that has been accepted for the award of any other degree or diploma in my name in any university or other tertiary institution and, to the best of my knowledge and belief, contains no material previously published or written by another person, except where due reference has been made in the text. In addition, I certify that no part of this work will in the future be used in a submission in my name for any other degree or diploma in any university or other tertiary institution without the prior approval of the University of Adelaide and, where applicable, any partner institution responsible for the joint award of this degree.

The author acknowledges that published works contained within this thesis resides with the copyright holder(s) of those works. I give permission for the digital version of my thesis to be made available on the web, via the University's digital research repository, the Library search, and through web search engines, unless permission has been granted by the University to restrict access for a period of time. I acknowledge the support I have received for my research through the provision of an Australian Government Research Training Program Scholarship.

……..
Joseph William Wrin
August 2022

STATEMENT OF AUTHOR CONTRIBUTION

I conducted 99% of the experiments reported in this thesis with the assistance and guidance of my principal supervisor Associate Professor Wendy Ingman, as well as invaluable input from my co-supervisor Andreas Evdokiou. Additional advice and assistance are noted in the individual chapters.

Chapter three

I completed the majority of the work in chapter three, including the C1q enrichment procedures, PAGE gels, and western blots, as well as the three hybridoma fusions, screening ELISAs and single cell cloning. I received two units of patient blood from the Outpatient Cancer Clinic at the Queen Elizabeth Hospital for use in C1q isolation. I received training in the use of the Acta FPLC situated at the Flinders Proteomic Centre from Tim Chataway and Nusha Chegeni. I obtained the animal ethics approval for the immunisation of mice for the production of monoclonal antibodies. Mouse husbandry was overseen by the staff of Laboratory Animal Services at the Helen Mayo Barrier Facility, University of Adelaide, as well as the collection of blood samples from immunised mice.

Chapter four

I completed the majority of the work in chapter four that included the design and performance of a variety of monoclonal antibody binding assays: ELISA, immunoprecipitation, western blotting, immunohistochemistry on FFPE tissue blocks, Immunocytochemistry and antibody isotyping. I received advice on reducing background staining in western blots from Bill Panagopoulos of the Breast Cancer Research Unit and help cutting FFPE section from Leigh Hodson of the Breast Biology and Cancer Unit.

Chapter five

I completed the majority of the work for chapter five, which concentrated on development of an *in vitro* efferocytosis assay. This included work with different breast cancer cell lines, different sources of phagocytes, cell labelling dyes, timing of assay assembly, and method of fluorescent frame acquisition. I was assisted in the set-up of the Zeiss LSM700 confocal microscope by Benjamin Ung, territory manager for Zeiss. I attended a workshop on the use of the FIJI suite of software presented by Cameron Nowell of Monash University that allowed me to analyse colocalisation of fluorescent images for the efferocytosis assays. I received advice on the use of the pHrodo dye from Eugene Roscioli and Rhys Hamon of the Royal Adelaide Hospital and University of Adelaide Lung Research Laboratory.

ACKNOWLEDGEMENTS

I must first acknowledge the invaluable role my partner Cristina Puglia played during the course of my PhD studies. Cristina picked me up innumerable times when I was feeling overwhelmed and helped me to settle and focus on my work. She believed in me more than I believed in myself. Without her unremitting support I doubt I would have finished my project. She is my rock and my love. Thank you, Cristina.

I cannot say enough about my supervisor Wendy Ingman. Wendy took on a mature age PhD student at literally the last minute for scholarship applications and never looked back. Ever calm, ever helpful, never discouraging and always supportive, Wendy guided me through the rough patches and exasperations of PhD study, always with a smile. She was as much a friend to me as a supervisor and we invariably wandered into unrelated tangents during our weekly meetings. She taught me the difference between doing experiments and conducting a research project and for that I will be forever grateful. Wendy is a rare sort of person, intelligent, kind and wise, and I have been privileged to have worked with her.

My co-supervisor Andreas Evdokiou helped to reinforce the knowledge Wendy was conveying to me about conducting a research project. At critical junctures in my project, Andreas was able to see past my confusion and point in me in the right direction. He saved me from countless hours of work when a different approach was more appropriate.

Sarah Bernhardt, my “PhD buddy”. We cast off into the great PhD River within a week of each other, in separate rafts but ever side by side. We navigated all the bends, rapids, deadfalls and snags in the shape of innumerable MDT meeting, endless patient records, seminars, conferences, symposia, and presentations. We even served as student representatives for the BHI together. Sarah was always there with her good cheer, pictures of her beautiful dogs, and a plate of delicious cookies. I will ever hold her in warm regard.

Vahid Atashgaran, who lived “down the street” from me, which translates to a few desks down. Vahid had irrepressible good humour, smiling and laughing and could snap his fingers in a way I never figured out. Professionally, we only collaborated on his review paper so he was mainly a guy who would always lighten the mood and could be counted on to give Amita endless grief. The place was quieter and less jovial when Vahid finished.

Amita Ghadge, my next-door neighbour, turned up when I was well along in my studies and quickly became a good friend. Amita had a difficult project and I would commiserate with her over the difficulties she encountered. Difficulties aside, Amita never lost her pleasant demeanour and was always good for a chat and a laugh.

Pallave Dasari, the post-doc down the road, was the anchor for us students, the rich repository of knowledge in all things Breast Biology and Cancer Unit and the Basil Hetzel Institute. She was also philosophically sound, politically astute, a computing wizard, and a darned good cook. She started all the students down the PhD road, settled our anxieties, offered sound advice, and provided an Indian feast to help take the sting out of Bill Shorten’s election defeat. I knew her vaguely when she was doing her PhD (not many people wore saris at CHRI), was pleased to run into her again, and so suspect I will see more of her in the future. Adelaide is just that kind of place.

Maddison Archer, down the road and hang a right, did not have much to do with me since she was not sitting nearby. But she was always helpful when I needed it, especially in the early days when I was getting started. I am forever grateful that she settled my nerves and got me going on my project.

Leigh Hodson, down the road with the post-doc, put up with years of my requests for lab supplies and reagents. I shared her own quest, ultimately successful, to become a mammographer and although this is her primary occupation now, she is still around to help out and keep the lab organised. Without Leigh, chaos.

Dr. Tim Chataway at Flinders Proteomics Facility, who helped me get started with my ill-fated purification of C1q from human plasma, was unstinting of his time and offered helpful advice. And Nusha Chegeni who oriented me to the facility and help me with the operation of the FPLC.

Dr Eugene Roscioli and Rhys Hamon helped me with advice on the use of pHrodo dye in phagocytosis assays. I had been undecided on the best approach to take for my efferocytosis assay and their advice decided the choice of dye.

Kathryn Hudson I first met at the Biochemistry Department at the University of Adelaide many years ago is now the facility manager for the Basil Hetzel Institute. Kathryn has helped me sort out many problems. No problem was too big for her to solve and Kathryn always helped out cheerfully.

And finally, music has always been important to me, so I will acknowledge the bands that have helped me through the PhD process. The live shows I saw during my PhD helped me unwind and blow off steam. These include Arch Enemy, The Used, Suicide Silence, Cradle of Filth, L7, Everclear, Sepultura, AFI, Spiderbait, Machine Head, Motionless in White, Veruca Salt, Dead Letter Circus, Karnivool, Deftones, Death Angel, Dead Kennedys, Parkway Drive, Helmet, Limp Bizkit, and Seether.

PUBLICATIONS ARISING FROM THIS THESIS

Manuscript in preparation

Noor Din, S, Wrin J, Woodford L, Evdokiou A, Robertson SA, Ingman WV. C1q-mediated phagocytosis promotes mouse mammary gland regression. To be submitted to Biology of Reproduction

ABSTRACTS ARISING FROM THIS THESIS

2019

Wrin JW, Evdokiou A, Ingman WV. C1q and Immune Tolerance During Mammary Carcinogenesis. ASMR Adelaide Conference. Adelaide, SA. Oral presentation.

2018

Wrin JW, Evdokiou A, Ingman WV. Complement Protein C1q: The Key to a New Breast Cancer Treatment? ASI National Scientific Meeting. Perth, WA. Poster presentation.

Wrin JW, Evdokiou A, Ingman WV. C1q and Immune Tolerance in Mammary Carcinogenesis: A Therapeutic Approach. Florey Postgraduate Conference. Adelaide, SA. Poster presentation.

Wrin JW, Evdokiou A, Ingman WV. C1q and Immune Tolerance in Mammary Carcinogenesis: A Therapeutic Approach. ASI Adelaide Immunology Retreat. Victor Harbour SA. Oral presentation.

Wrin JW, Evdokiou A, Ingman WV. C1q and Immune Tolerance During Mammary Carcinogenesis. ASMR Adelaide Conference. Adelaide, SA. Oral presentation.

Wrin JW, Evdokiou A, Ingman WV. Breast Cancer: Prevention Beats Treatment Every Time. ASI Day of Immunology. Basil Hetzel Institute, Woodville, SA. Oral presentation.

2017

Wrin JW, Evdokiou A, Ingman WV. Breaking Immune Tolerance During Mammary Carcinogenesis Robinson Research Institute Symposium, Adelaide, SA. Poster presentation.

Wrin JW, Evdokiou A, Ingman WV. Breaking C1q-mediated Immune Tolerance in Mammary Carcinogenesis. Florey Postgraduate Conference. Adelaide, SA. Poster presentation.

Wrin JW, Evdokiou A, Ingman WV. C1q and Immune Tolerance in Breast Carcinogenesis. ASI Adelaide Immunology Retreat. Barossa Valley, SA. Oral presentation.

Wrin JW, Evdokiou A, Ingman WV. Breaking Immune Tolerance During Breast Carcinogenesis. ASMR Adelaide Conference. Adelaide, SA. Poster presentation.

2016

Wrin JW, Evdokiou A, Ingman WV. C1q in Menstrual Cycle-Associated Breast Cancer Risk. ASI Adelaide Immunology Retreat. Wirrina Cove, SA. Oral presentation.

ABBREVIATIONS

ADCP	Antibody-Dependent Cellular Phagocytosis
ANA	Anti-Nuclear Antibody
AnV	Annexin V
Arg1	Arginase 1
ATM	Ataxia Telangiectasia Mutated
ATP	Adenosine Triphosphate
BAI1	Brain-specific angiogenesis inhibitor 1
Bcl-2	B-cell Lymphoma-2
bFGF	Basic Fibroblast Growth Factor
BH3	Bcl-2 Homology 3 Domain
BRCA1	Breast Cancer gene 1
BRCA2	Breast Cancer gene 2
BrdU	5-Bromo-2'-deoxyuridine
Br-dUTP	5-Bromo-2´-deoxyuridine 5´-Triphosphate
Btk	Bruton's tyrosine kinase
CAF	Cancer-Associated Fibroblast
CCL	CC-motif Chemokine Ligand
CDC	Complement-Dependent Cytotoxicity
Chek2	Checkpoint Kinase 2
CMFDA	5-Chloromethylfluorescein Diacetate
CR1	Complement Receptor 1
CRT	Calreticulin
CSF1	Colony Stimulating Factor 1
DAB	3,3'-diaminobenzidine
DCIS	Ductal Carcinoma in situ

DDR	DNA Damage Response
DIC	Differential Interference Contrast
DMBA	Dimethylbenz(a)anthracene
DMEM	Dulbecco's Modified Eagle Medium
DMSO	Dimethyl Sulfoxide
DR5	Death Receptor 5
ECM	Extracellular Matrix
EDTA	Ethylenediaminetetraacetic acid
EGF	Epidermal Growth Factor
ELISA	Enzyme-linked Immunosorbent Assay
ER	Estrogen Receptor
ERet	Endoplasmic Reticulum
FACS	Fluorescence-Activated Cell Sorting
FasL	Fas cell surface death receptor ligand
FCS	Fetal Calf Serum
FFPE	Formalin-Fixed Paraffin Embedded
FITC	Fluorescein Isothiocyanate
FoxP3	Forkhead box P3
FPLC	Fast Protein Liquid Chromatography
Gas6	Growth Arrest Specific 6
GFP	Green Fluorescent Protein
GTPase	Guanosine Triphosphate Hydrolase
HBSS	Hanks' Buffered Salt Solution
HDGF	Hepatoma-Derived Growth Factor
HEPES	4-(2-Hydroxyethyl)-1-Piperazineethanesulfonic acid
HGF	Hepatocyte Growth Factor

HMGB1	High Mobility Group Box Protein 1
HNP-1	Human Neutrophil Peptide 1
HPRT	Hypoxanthine Phosphoribosyltransferase
HRP	Horseradish Peroxidase
HRT	Hormone Replacement Therapy
HSP	Heat Shock Protein
ICAM3	Intracellular Adhesion Molecule 3
IFNG	Interferon γ
Ig	Immunoglobulin
IGF1	Insulin-like Growth Factor 1
IGF2	Insulin-like Growth Factor 2
IL	Interleukin
iNOS	Inducible Nitrogen Oxide Synthase
kD	Kilodalton
LAIR1	Leukocyte-Associated Immunoglobulin-like Receptor 1
LAIR2	Leukocyte-Associated Immunoglobulin-like Receptor 2
LDL	Low-Density Lipoprotein
LOX-1	Lectin-like oxidized LDL receptor-1
LPS	Lipopolysaccharide
MAC	Membrane Attack Complex
MaSC	Mammary Stem Cell
MGF-E8	Milk Fat Globule Epidermal Growth Factor 8
MHC	Major Histocompatibility Complex
MMP	Matrix Metalloproteinase
MMTV	Mouse Mammary Tumour Virus
MSCRAMM	Microbial Surface Components Recognizing Adhesive Matrix Molecules

NK	Natural killer
NKG2D	Natural Killer Group 2D
OPD	O-phenylenediamine
P/S	Penicillin/streptomycin
PAGE	Polyacrylamide Gel Electrophoresis
PALB2	Partner and Localizer of BRCA2
PBS	Phosphate Buffered Saline
PEG	Polyethylene Glycol
PI	Propidium Iodide
PI3K	Phosphatidylinositol 3-Kinase
PLC-γ1	Phospholipase C-γ1
PMSF	Phenylmethylsulphonyl Fluoride
PP2A	Protein Phosphatase 2
PR	Progesterone Receptor
PS	Phosphatidylserine
PVDF	Polyvinylidene Fluoride
PyMT	Polyomavirus Middle T antigen
Rac1	Ras-related C3 botulinum toxin substrate 1
RAGE	Receptor for advanced glycation end products
RANK	Receptor Activator of Nuclear Factor-κ B
RANKL	Receptor Activator of Nuclear Factor-κ B Ligand
RhoA	Ras Homolog Family Member A
RPMI	Roswell Park Memorial Institute
SAS	Saturated Ammonium Sulphate
SCARF1	Scavenger Receptor Class F Member 1
scFv	Single-chain fragment, antibody variable region

SDS	Sodium Dodecyl Sulphate
SERM	Selective Estrogen Receptor Modulator
ShcA	Src homology and collagen A adaptor Protein
SLE	Systemic Lupus Erythematosus
SR-A1	Scavenger Receptor A1
SREC1	Scavenger Receptor Expressed by Endothelial Cells 1
SR-PSOX	Scavenger Receptor for Phosphatidylserine and Oxidized Low-Density Lipoprotein
STAT3	Signal Transducer and Activator of Transcription 3
TBS	Tris Buffered Saline
TBST	Tris Buffered Saline + Tween 20
TBSTM	Tris Buffered Saline + Tween 20 + Milk
TdT	Terminal deoxynucleotidyl Transferase
TGFB	Transforming Growth Factor β
TIM4	T-cell immunoglobulin and mucin domain containing protein 4
TLR	Toll-like receptor
TMB	3,3',5,5'-tetramethylbenzidine
TNFA	Tumour Necrosis Factor α
Tp53	Tumour protein p53
TRAIL	TNF-Related Apoptosis-Inducing Ligand
UV	Ultraviolet

CHAPTER ONE: LITERATURE REVIEW

1.1 INTRODUCTION TO THE PROJECT

This project had the following aims:
1. To immunise mice with C1q for the purpose of performing hybridoma fusions and isolating anti-C1q monoclonal antibodies.
2. To investigate C1q binding capacity of anti-human C1q monoclonal antibodies.
3. Tom develop an *in vitro* efferocytosis assay to test the ability of the monoclonal antibodies to neutralise C1q efferocytic activity.

As will be detailed in this thesis, C1q is a vital element in the process of efferocytosis. Previous work in our lab with C1q-null mutant mice showed C1q is functional in the development and progression of carcinoma in the mammary tissue. C1q null-mutant mice were less susceptible to mammary cancer development and progression in two different mouse models.

This led to the hypothesis:

Monoclonal antibodies developed to C1q may have the capacity to inhibit C1q-mediated efferocytosis, with implications for inhibiting mammary carcinogenesis.

Of the possible means of inhibiting C1q activity, production of monoclonal antibodies (MAbs) was chosen as the most accessible method. The author had extensive experience in monoclonal antibody production and monoclonal antibodies are currently essential therapeutics for many cancers.

Monoclonals are used to target blood cells and blood cancers, from the frist Mab approved directed to CD3 (Muronomab) to MAbs for treatment of B cell lymphoma (Rituximab), T cell lymphoma (Mogamulizumab), multiple myeloma (Isatuximab, Elatuzumab, Daratumumab) and chronic lymphocytic leukaemia (Olaratumab, Ofatumumab). Exciting new monoclonals to immune checkpoint proteins have offered treatments for previously treatment-refractory cancers. These include Mabs directed to PD-1 which target melanoma (Pembrolizumab, Nivolumab), renal cancer (Nivolumab), lung cancer (Nivolumab), and squamous cell carcinoma (Cemiplimab). A monoclonal to checkpoint inhibitor CTLA-4, Ipilimumab, is useful in treatment of melanoma and renal cell carcinoma. In breast cancer, the monoclonals Trastuzumab and Pertuzumab are treatments for ER/PR negative, Her2 positive cancers, a subtype previously without targeted therapy (Zahavi, 2020). This list covers only a few of the monoclonal cancer therapies available, which have become indispensable therapies and have saved many lives.
At the commencement of the project, many monoclonals to C1q were available commercially but little investigation of the role of C1q in health and disease was being conducted. In fact, only two groups were working on the role of C1q in autoimmune inflammation of CNS tissue, using monoclonal antibodies (Phuan 2013), (McGonigal, 2016). An attempt to procure one of these monoclonals for use in the project was met with no reply from the lab in question. To date, no searches have found another lab working on inhibition of C1q with monoclonal antibodies to study impact on carcinogenesis.

1.2 BREAST CANCER: INCIDENCE AND RISK FACTORS

Breast cancer is a major cause of morbidity and mortality for women in modern society. It is the most frequently diagnosed cancer in women with estimates projecting 19,866 new cases of breast cancer in Australian women in 2021, comprising 12.3% of all cancers diagnosed and 6.5% of cancer deaths (Cancer Australia: www.canceraustralia.gov.au). The outlook becomes even bleaker when males, who make up

<1% of breast cancer patients, are removed from the figures, showing that breast cancer accounts for 27.3% of cancers in women (Cancer Australia: www.canceraustralia.gov.au). And while the incidence of breast cancer has been decreasing in women over the age of 50 since 2000, there has been no corresponding decline in incidence for women under 40; rather there has been an increase in occurrence for this age group (Bouchardy, 2007), (Anders, 2009). And although women under 40 make up only 6.7% of breast cancer cases, breast cancer accounts for 40% of all the cancers seen in this generally healthier age group. In addition, women under 40 have a poorer prognosis, with the five-year survival for 25-30 year olds at 72% compared with 84-86% for 50-80 year old women (Anders, 2009). The prognosis is equally poor for pregnancy-associated and post-partum breast cancers (Mathelin, 2008). This suggests there are inherent differences between the biology underlying pre-menopausal and post-menopausal breast cancers, and these differences are not all associated with hormone receptor status, tumour size, or stage (Lian, 2017), (Ryu, 2017), (Alabdulkareem, 2018).

The risk factors for developing breast cancer can be divided into two broad categories: modifiable and non-modifiable. Modifiable risk factors are under the control of the individual and include alcohol consumption and sedentary lifestyle that can contribute generally to poorer health. Use of oral contraceptives or hormone replacement therapy (HRT) also increases breast cancer risk, highlighting the role of estrogen and progesterone in the development of breast cancer (Breast Cancer Network Australia: www.bcna.org.au), (Yue, 2010), (Mohammed, 2015)' On the other hand, non-modifiable factors are beyond the control of the individual and include being female, advancing age, family history of breast cancer, high mammographic density, benign breast disease, and diagnosed ductal carcinoma in situ (DCIS) (National Breast and Ovarian Cancer Centre), (Maas, 2016). Early onset of menarche and late onset of menopause are also factors for increased risk and this is likely due to an increased number of menstrual cycles experienced over a woman's reproductive life (Chavez-MacGregor, 2005), (Collaborative Group on Hormonal Factors in Breast Cancer, 2012). And while childbirth and lactation have overall protective effects for breast cancer, there exists a window of increased susceptibility post-partum, persisting for up to 10-15 years after parity for women under 25 (Lyons, 2009).

The concept of mutations as causative agents for breast cancer was brought to the attention of the mainstream public when Angelina Jolie chose to have a prophylactic bilateral mastectomy upon receiving the diagnosis of a germline BRCA1 mutation. Much attention and research has been focussed on the role of BRCA-1 and BRCA-2 gene mutations (King, 2003), but other germline mutations can also play a significant role in breast carcinogenesis. The common element amongst these genes is the sensing and/or repair of DNA damage, thereby safeguarding cells from carcinogenesis due to genetic abnormalities. BRCA-1 and BRCA-2 are both involved with the cell's DNA damage response (DDR), with BRCA-1 functioning in both mitotic checkpoint activation and DNA repair while BRCA-2 is required for homologous recombination repair of damaged DNA (Roy, 2012). Mutations in other proteins involved in the DDR include Partner and Localizer of BRCA2 (PALB2) (Southey, 2016), ataxia-telangiectasia mutated (ATM) (Ahmed, 2006), and checkpoint kinase 2 (Chek-2) (Nevanlinna, 2006) and are all associated with increased breast cancer incidence. Mutations in tumour protein p53 (Tp53) is the basis for Li-Fraumeni syndrome, an autosomal dominant condition that predisposes affected individuals to the development of sarcomas, as well as cancers of the breast, brain, and adrenal glands (Masciari, 2012). Tp53 is a vital protein in protecting cells from malignant transformation by promoting DNA repair, halting cell cycle progression of damaged cells at the G1/S checkpoint and initiating apoptosis in cells with irreparable DNA damage. However, despite the high penetrance of the various germline mutations detailed above, these mutations are quite rare in the population and are associated with approximately 5% of all breast cancers (Wang, 2018).

The majority of breast cancer cases are not due to germline mutations; they are the result of random somatic mutations and are considered to be sporadic. But the ties between breast cancer, menstrual cycling, and other risk factors complicate the notion of purely random sporadic disease incidence. The

association between circulating estrogen, mammary epithelial cell proliferation and breast cancer risk is well established (Wilson, 2006), (Yue, 2010) and to understand breast cancer risk it is first necessary to better understand the role of hormones in normal breast development.

1.3 HORMONAL REGULATION OF MAMMARY EPITHELIAL CELLS

During the menstrual cycle, mammary epithelial cell proliferation and regression is driven by fluctuations in circulating estrogen and progesterone. This is a finely tuned process requiring both proliferative and inhibitory inputs that are ultimately regulated by estrogen and progesterone. In humans, a biphasic profile of estrogen concentration is observed, with a peak at the follicular phase followed by a second lower peak at the luteal phase, while progesterone is present as a single peak during the luteal phase (Need, 2014). In the mouse, estrogen peaks during the estrus phase (similar to the follicular phase in humans) and progesterone at diestrus (similar to the luteal phase in humans) (Hodson, 2013). Estrogen and progesterone exert effects on the mammary gland epithelium both through direct regulation of these cells, and indirectly through regulation of stromal cells (Polyak, 2010), (Unsworth, 2014). The increased circulating concentration of these hormones drives proliferation of epithelial cells, resulting in the formation of alveolar buds on the mammary gland ductal tree (Hodson, 2013) (Figure 1.1). Estrogen induces the expression of progesterone receptors through paracrine signalling of Receptor Activator of Nuclear Factor Kappa-B Ligand (RANKL) (Russo, 1999), (Visvader, 2009), (Beleut, 2010), (Need, 2014). Macrophages play an important role in both the proliferation of mammary epithelium and, if no pregnancy is established, in the removal of the regressing alveolar bud structures. Progesterone is necessary for the maintenance of alveolar buds, and when the concentration of progesterone drops, the alveolar epithelial cells become apoptotic and are scavenged by macrophages (Chua, 2010), (Noor Din, 2017). This process of alveolar cell senescence is known as regression and bears some resemblance to the more dramatic remodelling of the mammary gland that occurs during involution when the lactating mammary gland returns to its non-pregnant state following weaning (Watson, 2006), (Atabai, 2007), (Stein, 2007), (Flanders, 2009).

Mammary epithelial cells are a heterogeneous cell population, with different subsets expressing estrogen receptor, progesterone receptor, or RANK (Visvader, 2009). This makes the study of mammary epithelium in isolation problematic, especially when grown *in vitro* in a monolayer culture. Mammary epithelial cells in monolayer culture will differentiate into either luminal epithelium or myoepithelium, but individual colonies never contain both cell types (Graham,1997). It is the paracrine signalling between proximal mammary epithelial cells that is crucial for estrogen and progesterone to exert their effects on cell proliferation. Estrogen drives progesterone receptor (PR) expression, and while mammary epithelial cells can be positive for either estrogen receptor (ER) or PR, they do not express both. In addition, ER- or PR-expressing cells do not express the proliferation marker Ki67, indicating epithelial cells not expressing hormone receptors are the proliferative component of the mammary gland, (Russo, 1999), (Clarke, 2004), (Arendt, 2015),.

However, there is evidence that some PR positive epithelial cells are able to proliferate (Beleut, 2010). In the mammary gland, estrogen acts to promote epithelial cell proliferation and up-regulate pro-inflammatory cytokine secretion (Wilson, 2006), (Dasari, 2014). Progesterone induces mouse mammary epithelial cell proliferation in PR-positive cells via Cyclin D1 expression as well as in PR negative cells through RANKL signalling (Beleut, 2010). In a matrigel-imbedded organoid culture system, progesterone in the presence of estrogen stimulated epithelial cell proliferation and the expansion of epithelial progenitors (Graham, 1997). And in an ovariectomised mouse model, treatment with estrogen and progesterone induced an expansion of mammary stem cells as well as differentiated cells (Joshi, 2010).

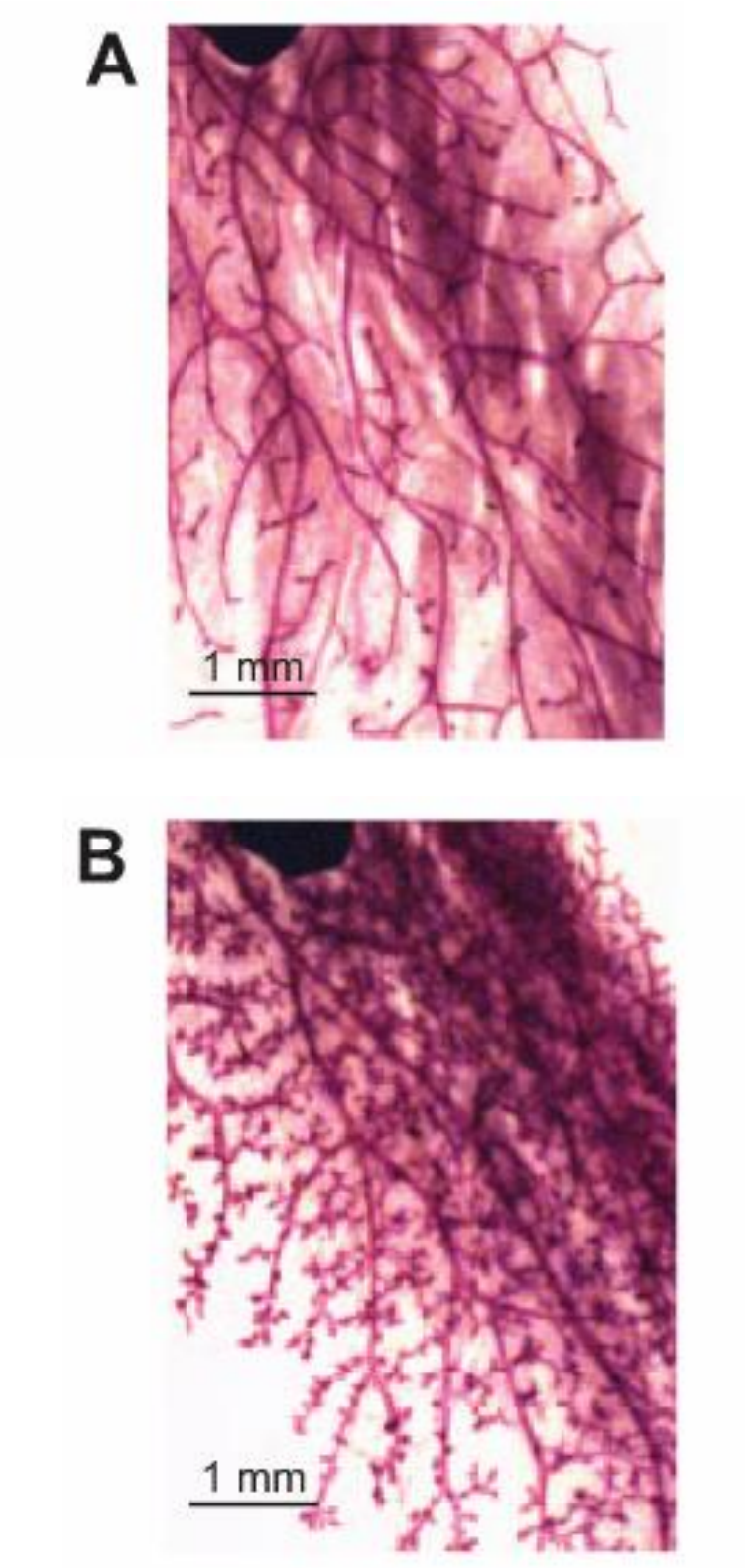

Figure 1.1 Formation of alveolar buds in response to elevated hormone levels

Increased concentration of circulating estrogen and progesterone drive proliferation of mouse mammary gland epithelial cells and the formation of alveolar buds. (A) At estrus, the mammary gland exhibits a basic architecture. (B) At diestrus, the mammary gland exhibits alveolar buds, which are structures that will further develop into milk-producing lobules in the event of successful embryo implantation and subsequent pregnancy. Figure from Hodson et al, Biol Reprod 89(3):65, 1–8, (2013).

Another factor, prolactin, acts in association with estrogen and progesterone to stimulate epithelial cell proliferation and survival (Tworoger, 2006).

An important cytokine in the regulation of mammary epithelial cell proliferation is transforming growth factor beta 1 (TGFB1), which is produced by epithelial cells and acts in an autocrine manner to restrict epithelial cell proliferation at diestrus (Moses, 2011). A lack of epithelial cell-derived TGFB1 leads to increased rate of epithelial cell turnover (Sun, 2013). TGFB1 is also produced by other cell types in the breast and exerts indirect effects on the mammary epithelium. Through actions on mammary gland macrophage populations, TGFB1 can inhibit progesterone-induced epithelial cell differentiation during diestrus (Sun, 2021). Stromal modulation of the epithelium by other growth factors has also been studied using a number of different null mutation mouse models. Many autocrine/paracrine signals that regulate mammary epithelial cell proliferation have been identified including Insulin-like Growth Factor 1 (IGF-1), Insulin-like Growth Factor-2 (IGF-2), and Hepatocyte Growth Factor (HGF) (Gouon-Evans, 2000). Expression of some of these factors is regulated by estrogen and progesterone, and cytokines such as colony-stimulating factor 1 (CSF1) and interferon gamma (IFNG) that fluctuate across the estrous cycle and regulate epithelial cell function (Sun, 2013), (Dasari, 2014).

1.4 IMMUNE CELLS IN THE MAMMARY GLAND MICROENVIRONMENT

Another major component necessary for development and mature function of the mammary gland are cells of the immune system. Different types of leukocytes are present in mammary tissue, including B and T lymphocytes, neutrophils, basophils, and eosinophils; but of most significance to mammary gland function is the macrophage. Macrophages are phenotypically plastic and are able to shift from the pro-inflammatory M1 type to the anti-inflammatory M2 type (Mantovani, 2013), (Das, 2015). Macrophage phenotypes shift over the course of the estrous cycle in mice, with the M1 phenotype predominating during the epithelial proliferative phase of metestrus, characterised by Natural Killer Group 2D (NKG2D) and Inducible Nitrogen Oxide Synthase (iNOS) expression while the M2 phenotype is more prevalent during the regression phase of proestrus and are characterised by CD204 and arginase 1 (Arg-1) expression, and increased major histocompatibility complex (MHC) class II (Hodson, 2013), (Sun, 2013). M1 macrophages perform immune surveillance of the proliferating epithelial cells to detect and remove damaged or cancerous cells, whereas the M2 macrophages suppress inflammation during the removal of dying alveolar cells to prevent a breakdown in tolerance to self-antigens that could lead to the development of autoimmune disease (Roos, 2001), (Macedo, 2016).

While it is simple to classify macrophages by the M1/M2 dichotomy, they more likely exist as an M1/M2 continuum *in vivo*, from the pro-inflammatory M1 that promote a vigorous immune response, to the wound-healing response of M2 that are essentially immunologically silent (Italiani, 2014), (Martinez 2014). Yet even the M1/M2 concept is overly simplistic. M2 macrophages can be further broken down into several subtypes induced by different factors and conditions, including M2a, M2b, M2c, M2d, and M2 tissue resident phenotypes, all of which secrete different factors (Röszer, 2015).

Macrophage numbers fluctuate throughout the ovarian cycle, being most abundant at diestrus (Chua, 2010). Macrophages in close contact with mammary epithelial cells induce ductal expansion and branching, and facilitate the removal of alveolar structures during regression (Chua, 2010). Colony-stimulating factor 1 (CSF1) is an important cytokine in the recruitment and proliferation of macrophages and macrophage-precursor monocytes. Mice deficient in CSF1 expression exhibit impaired mammary gland development during puberty and pregnancy (Gouon-Evans, 2000). CSF1 is also important in the interaction of macrophages with mammary stem cells (MaSCs). Not only do normal MaSCs fail to develop

into alveolar structures in CSF1 null mice, but MaSCs from null mice also fail to develop into alveolar structures when transplanted into CSF1 replete mice (Gyorki, 2009).

Estrogen and progesterone directly affect macrophages throughout the ovarian cycle, with estrogen stimulating a more inflammatory phenotype (M1) while progesterone induces an alternative wound-healing activation (M2) (Need, 2014). In an *in vitro* mouse macrophage system, progesterone was found to dampen production of both inflammatory nitric oxide and anti-inflammatory arginase while up-regulating mannose receptor (CD206) expression, which demonstrates the complexity of immune interactions in the mammary gland (Menzies, 2011).

1.5 APOPTOSIS AND AUTOPHAGY IN MAMMARY GLAND REGRESSION

Mammary gland regression occurs when circulating progesterone drops at the end of the luteal phase of the ovarian cycle. Following development of the mammary gland into a highly-branched system of alveolar buds, in the absence of pregnancy this network of cells becomes senescent and must be removed to avoid undue inflammation. The newly formed alveolar buds undergo apoptosis and the gland is remodelled back to its basal architecture (Figure 1A), ready for commencement of the next cycle (Fata, 2001), (Chua, 2010). It has been suggested that the regression phase of the ovarian cycle is significant in relation to breast cancer development as rats injected with a chemical carcinogen during proestrus when mammary gland regression occurs are more likely to develop mammary tumours than mice injected at diestrus when mammary epithelium proliferates (Nagasawa, 1976), (Ratko, 1985).

Mammary gland regression during the ovarian cycle bears resemblance to the process of involution, which occurs at the cessation of lactation and leads to the remodelling of the ductal tree back to its basic architecture. There is a difference in scale though, with involution involving the removal of the more extensive milk-producing lobules. There has been significantly more research on the biology of involution compared to research on mammary regression during the ovarian cycle. A mouse model for involution induced by forced weaning of pups involves two distinct phases: a reversible phase of up to 48 hours and an irreversible phase beyond 48 hours. The first phase initiates apoptosis via Signal Transducer and Activator of Transcription 3 (STAT3) signalling while the second phase centres on matrix metalloproteinase (MMP) production and phagocytosis of the now-surplus dying epithelium (Watson, 2006). The involuting mammary gland is populated with interleukin 10 (IL10) secreting alternatively activated M2 macrophages and immunosuppressive Forkhead box P3 (Foxp3) positive regulatory T cells (Martinson, 2015). An analysis of three microarray studies in mice confirms the activation of STAT3 and death receptor-linked extrinsic apoptotic pathways early in involution, followed at a later stage by expression of MMPs and phagocyte-attracting chemokines such as CC-motif Chemokine Ligand (CCL) 6, 7 and 8 (Stein, 2007). It is also apparent there is a lag between the onset of apoptosis and the arrival of immune phagocytes. In this interval, mammary epithelial cells can act as “amateur” phagocytes and begin the process of removing apoptotic cells prior to the arrival of “professional” phagocytic macrophages (Atabai, 2007).

But are all the regressing mammary epithelial cells necessarily undergoing apoptosis? The process of cell death comprises at least 11 different modes (Melino, 2005) with more mechanisms emerging such as necroptosis and charontosis (Nikoletopoulou, 2013), (Tichy, 2013). Apoptosis, whether triggered by factors such as Tumour Necrosis Factor Alpha (TNF-α), Fas cell surface death receptor ligand (FASL) or TNF-related apoptosis-inducing ligand (TRAIL) (extrinsic apoptosis) or by events such as growth factor withdrawal or DNA damage (intrinsic apoptosis), involves the engagement of a caspase cascade. Caspase activation mediates the hallmarks of apoptosis, namely mitochondrial leakage of cytochrome c,

chromatin condensation and fragmentation, apoptotic body formation, and membrane blebbing (Elmore, 2007). Necroptosis is the process of organelle swelling and cell membrane rupture, leaving the nucleus intact, which leads to a release of inflammatory mediators such as High Mobility Group Box 1 (HMGB1) and Hepatoma-derived growth factor (HDGF), and activation of the inflammasome (Iyer, 2009). Charontosis is a Tp53-dependant mode of programmed cell death that is independent of caspase activation (Tichy, 2013).

Autophagy is another mechanism for the removal of senescent cells in regressing mammary gland tissue. Autophagy involves the recycling of organelles into autophagosomes and is a useful mechanism for temporary preservation of cells from death during times of stress, such as hypoxia or nutrient deprivation (Glick, 2010). The key player in initiating autophagy is the bcl-2 homology 3 (BH3) domain protein beclin-1, involved in interactions with members of the B-cell lymphoma 2 (BCL-2) family. Beclin-1 assembles the components of the autophagosome, which sequesters organelles prior to fusion with lysosomes and breaking down of the organelles (Kang, 2011). Studies in cattle (Gajewska, 2008) have shown autophagy to be an important process in involuting mammary epithelial cells. Studies in mice have shown induction of autophagy by growth factor deprivation involving STAT3 activation of lysosomal proteases cathepsin B and L (Kreuzaler, 2011). So, the possibility exists that involuting or regressing mammary epithelium undergoes autophagy before the arrival of phagocytes and the onset of apoptosis.

1.6 PROTEINS THAT MEDIATE RECOGNITION AND EFFEROCYTOSIS OF DYING EPITHELIUM

Efferocytosis is the process of removing dying cells by phagocytosis to prevent an inflammatory response. Cells age and become senescent, experience damage through DNA errors, viral infection, T cell education or bystander damage during inflammation and undergo cell death by several different mechanisms (Melino 2005). Removal of dying cells before they become necrotic prevents the release of pro-inflammatory mediators that could potentially trigger inappropriate response by leukocytes. Necrotic cells also release many self-antigens that can be processed by antigen-presenting cells to trigger anti-self immune reactions capable of leading to auto-immune disease (Elmore, 2007). Efferocytosis potentially involves a variety of cell surface molecules with the most important including phosphatidylserine, C1q, SCARF-1, calreticulin and Btk signalling (Byrne, 2013), (Barth, 2017).

During involution and menstrual cycle-associated regression, the mammary gland sheds an abundance of epithelial cells. And while the processes of mammary involution and regression are distinct, there is some overlap in their mechanisms, such as the exposure of phosphatidylserine (PS) on the outer leaflet of the plasma membrane (Melino, 2005) and release of the “find me” signal adenosine triphosphate (ATP) (Wang, 2013), (Medina, 2016). During the process of apoptosis, dying cells release a number of “find me” signals that attract phagocytes while at the same time they display a number of “eat me” signals on the cell membrane, primarily PS, calreticulin (CRT), thrombospondin and altered Intercellular adhesion molecule 3 (ICAM3) (Lauber, 2004), (Arandjelovic, 2015). These signals can be displayed in conjunction with “don’t eat me” signals such as CD47 and/or the “keep out” factor lactoferrin (Poon, 2010), ((Poon, 2014), Barth, 2017). Macrophages attracted into proximity with dying cells display a diverse array of receptors for binding these cells. Many of these molecules recognise PS displayed on the dying cell surface, including Brain-specific angiogenesis inhibitor 1 (BAI1), T-cell immunoglobulin and mucin domain containing protein 4 (TIM4), stabilin-2, and Receptor for advanced glycation end products (RAGE) (Armstrong, 2011), (Tang, 2012), (Canton, 2013), (Penberthy, 2016), (Barth, 2017). Upon engagement of the PS receptors, signalling occurs in the phagocyte via guanosine triphosphate hydrolases (GTPases), Ras homolog family member A (RhoA), and Ras-related C3 botulinum toxin substrate 1 (Rac-1) to initiate

phagocytic cup formation (Kim, 2017). The Tyro3, Axl and MerTK (TAM) family and αv integrins also bind PS through the bridging molecules growth arrest-specific 6 (Gas-6), protein S, and milk fat globule epidermal growth factor 8 (MGF-E8) respectively (Lauber, 2004), (Arandjelovic, 2015). Scavenger receptors CD36, scavenger receptor A1 (SR-A1), scavenger receptor for phosphatidylserine and oxidized low-density lipoprotein (SR-PSOX) and the lipopolysaccharide (LPS) receptor CD14 are also capable of binding antigens on dying cells (Poon, 2010), (Canton, 2013), (Penberthy. 2016). Despite the multiplicity of efferocytic receptors, C1q is a very important protein capable of binding several target molecules on apoptotic cells (Noor Din, 2017), (Hodson, manuscript in preparation). This is not to discount the efficacy of the other efferocytic receptors but points up an important role for C1q in efferocytosis, perhaps as a tethering molecule that brings the apoptotic target into proximity with other receptors.

Another protein important for the phagocytosis of apoptotic cells is CRT, which binds calcium in the lumen of the endoplasmic reticulum and acts as a molecular chaperone during protein folding (Groenendyk, 2004), (Gelebart, 2005). Normally restricted to the endoplasmic reticulum (Eret), signals from toll-like receptors (TLRs) via Bruton's tyrosine kinase (Btk) will induce translocation of CRT to the cell surface (Byrne, 2013). Loss of Btk function is associated with X-linked agammaglobulinemia, an autoimmune condition linked to a deficiency in clearance of apoptotic cells (Mattsson, 1996). Once on the cell surface, CRT binds CD91 where it facilitates the uptake of the molecular chaperones heat shock protein (HSP) 70, HSP90 and HSP90B1, and the subsequent loading of antigens to MHC class I (Basu, 2001), (Gardai, 2005). CRT also mediates efferocytosis via binding PS expressed on the outer membrane leaflet of apoptotic cells (Wijeyesakere, 2016) as well as being expressed on apoptotic cells where it interacts with C1q globular domains (Verneret, 2014).

The complement component C1q binds to CRT on the surface of the phagocyte (Peerschke, 2014) and the C1q-CRT complex in association with CD91 has been shown to be important, if not essential, for the clearance of dying cells (Ogden, 2001), (Vandivier, 2002), (Galvan, 2012), (Barth, 2017). One study has indicated that although CRT, CD91 and C1q are found as a complex, C1q-mediated efferocytosis can occur in the absence of CD91 (Lillis, 2008).

C1q facilitates the immunologically-silent removal of apoptotic cells, thereby avoiding local or systemic inflammation (Galvan, 2012), (Arandjelovic, 2015). SLE is an autoimmune disorder that involves perturbation of the classical complement cascade, particularly C1q. The varied presentations of SLE make it a less than perfect disease for studying hypocomplementaemia; however, the generally low levels of C1q seen in these patients allow for some observations to be drawn. Inactivating mutations of C1q are rare, but when present they lead to the development of systemic lupus erythematosus (SLE) with a penetrance of 93% (Roumenina, 2011), (Schejbel, 2011), (Jlajla, 2014), (Macedo, 2016). in which improper clearance of dying cells in the body leads to the formation of an autoimmune anti-nuclear antibody (ANA) response, resulting in deposition of immune complexes in the kidneys and initiation of glomerulonephritis (Walport, 1998), (Toong, 2011). Anti-C1q autoantibodies have long been noted in SLE, although it is unclear whether these antibodies are causative or occur after disease onset to exacerbate its severity (Katsumata, 2011). A recent study has linked a neutralising epitope on C1q with a similar epitope on Epstein-Barr virus nuclear antigen 1, offering an interesting possible mechanism for the onset of SLE (Csorba, 2019).

In vivo data confirm the importance of C1q for the removal of dying cells in the mammary gland. Ovariectomised mice reconstituted with estrogen and progesterone exhibit a build-up of apoptotic cells when macrophages are depleted (Chua, 2010) and a similar accumulation of apoptotic cells is observed in C1q null mutant mice (Noor Din, 2017). Taken together, these studies suggest the importance of macrophages and C1q in the clearance of dying epithelium in the mammary gland.

1.7 C1q

The classical complement pathway is a proteolytic cascade of enzymes similar to the clotting cascade. C1q is the initiating component of the classic cascade but not the alternative or lectin clotting pathways. The classical pathway involves the modification of complement components into active enzymes capable of altering the next component in the cascade. The classical complement pathway begins when C1q binds to a target cell, either directly via a number of different molecules on the target or through binding to immunoglobulin present on the target surface, leading to antibody-dependent cellular phagocytosis (ADCP) or complement-dependant cytotoxicity (CDC) (Golay 2020), (Wang 2020). C1q combines with C1s and C1r to form an enzyme that cleaves C2 and C4 into a and b fragments. C2a and C4b associate to form C3 convertase that acts on C3 to make C3a and C3b. C3b then binds to the C4bC2a complex to form C5 convertase. C5b binds the target cell surface and nucleates the membrane attack complex (MAC) by binding C6, C7, C8 and multiple copies of C9. The MAC forms a pore in the target that leaks cellular contents, killing the target and supporting an inflammatory response. C3b and C4b on the target cell surface act as opsonins to mediate ADCP. C4a, C3a and C5a are known as anaphylatoxins, causing local inflammation via mast cell deregulation and increased vascular permeability as well as being chemotactic for pro-inflammatory leukocytes.

C1q is the first component in the classical complement cascade, capable of binding antibody Fc regions and bacterial mannans, making it an early link in the inflammatory response for both the innate and adaptive immune systems (Markiewski, 2007). C1q is an aggregate of three protein structures, each consisting of A, B and C chains disulphide-linked into A-B and C-C dimers. These subunits fold one C-C dimer and two A-B dimers into structures containing two globular domains with a collagen-like triple helical tail. The collagenous tails of three of these structures in turn combine into a triple helix to produce the “bunch of tulips” quaternary structure, featuring six globular heads and an entwined collagen-like tail. (Frachet, 2015), (Figure 1.2). The globular domain consists of a “jelly-roll fold” of anti-parallel beta sheets, a fold characteristic of the TNF superfamily that demonstrates an evolutionary link between innate and adaptive immunity (Shapiro, 1998). The globular regions of C1q recognise a wide variety of ligands on various target cells while the collagen-like tail interacts with phagocytic cells (Kishore, 2000), (Galvan, 2012), (Thielens, 2017).

C1q performs functions that can be roughly grouped into three categories: the classical complement cascade, efferocytosis, and immune regulation. The classical complement cascade involves the combination of one C1q molecule with two C1r and two C1s molecules to form the C1 protein. C1 binds to immune complexes for the opsonisation of dying cells and/or killing of microorganisms (Lu, 2008), (Nayak, 2012). Phagocytosis of bacteria can be initiated through the interaction of phagocytes with the opsonins C1q, C3b or C4b (Figure 1.3). Alternately, assembly of the membrane attack complex on membrane-bound C5b can mediate bacterial cell lysis through loss of membrane integrity and creation of a channel for cytoplasmic access of granzyme B (Lubbers, 2017), (Figure 1.4). The classical complement cascade is an inherently pro-inflammatory process that derives the anaphylatoxins C3a and C5a, and recruits inflammatory leukocytes (Lubbers, 2017).

In contrast to the classical complement cascade, C1q-mediated efferocytosis of dying cells and their pro-inflammatory cellular contents induces production of IL10 and TGFB by phagocytes, which suppress the activation of inflammatory leukocytes (Lauber, 2004). The globular heads of the C1q protein are able to bind PS exposed on the outer membrane leaflet of apoptotic cells, as well as to immune complexes, bacterial and viral pathogens, free DNA, myelin, and β-amyloid (Lauber, 2004), (Galvan, 2012). The C1q collagen-like tail binds to CRT on phagocytes and, in association with CD91, helps facilitate efferocytosis (Verneret, 2014). Interestingly, CRT is also transported to the surface of apoptotic cells where it is recognised by C1q globular domains, describing another ligand operative in C1q clearance of regressing epithelial cells (Wijeyesakere, 2016), (Figure 1.5).

CD91/CRT is not the only mechanism of C1q-assisted phagocytosis. Scavenger receptor class F member 1 (SCARF-1), also known as scavenger receptor expressed by endothelial cells (SREC-1), was originally characterised as a receptor for chaperone proteins and CRT, much in the manner of CD91 (Berwin, 2004). SCARF-1 is a scavenger receptor for low density lipoprotein (LDL) but also is capable of binding C1q collagen-like tails and mediating phagocytosis of apoptotic cells. Paralleling the characteristics of C1q or Btk deficiency, SCARF-1 null mutant mice develop autoimmune disease characterised by the appearance of ANA, a defining clinical feature of SLE (Ramirez-Ortiz, 2013). SCARF-1 is also capable of interaction with phagocyte TLRs, triggering an inflammatory response in the presence of dsRNA and CpG DNA (Murshid, 2016). Thus SCARF-1 represents an alternate C1q–mediated mechanism of efferocytosis, perhaps prior to CRT exposure on the phagocyte surface.

C1q-mediated phagocytosis down-regulates macrophage production of the pro-inflammatory cytokines and up-regulates the tissue remodelling cytokine IL10 (Lu, 2007). An *in vitro* phagocytosis model also demonstrated that phagocytosis of apoptotic epithelium induced production of TGFB, a potent immunosuppressive factor (Monks, 2005). In common with various scavenger receptors, C1q can assist in macrophage clearance of oxidised/acetylated LDL through CD36 and Lectin-like oxidized LDL receptor-1 (LOX1) as well as increasing cholesterol efflux, thereby reducing the accumulation and growth of atherosclerotic plaques (Spivia,2014).

The role of C1q in breast cancer might be different from other cancers. Breast epithelium proliferates in response to hormone fluctuations to form epithelial buds, buds that become senescent if no pregnancy is established. Tissues of the colon, skin and bone marrow also display a high rate of proliferation but the fate of the cells in each case differs from the breast. Colonic epithelium cells are shed into the lumen of the colon when they become senescent. Skin cells cornify to become the non-viable stratum corneum. Blood cells mature and are released into circulation to be scavenged by different cells or organs. Breast epithelial cells remain in place to undergo apoptosis and are phagocytosed by macrophages. Efferocytosis by macrophages creates an immunosuppressive environment in the mammary tissue that interferes with cytotoxic T cell activity and allows for the establishment of mammary tumours.

Generally, the role of C1q in response to cancer is dependent on the cancer. Just as there is no single disease known as cancer, so the response of the immune system is dependent on the individual cancer; not simply the tissue type but the mutations that drive the cancer's growth and ability to metastasise. For example, implants of B16 melanoma cells into C1qA-null mice displayed slower tumour growth and prolonged survival compared to wild type mice (Bulla, 2016). C1q was detected binding blood vessels and stroma, without C3 activation, indicating a non-complement cascade mechanism. However, prostate cells treated with C1q-containing serum underwent apoptosis through activation of p53 and *WWOX* (Hong, 2009). Neu-T transgenic mice null for C1q activity displayed more rapid carcinoma progression and lung metastasis (Bandini, 2016), featuring an increased infiltration of the tumour by blood vessels. The receptor gC1qR, which is present on nearly all cells, binds the globular domains of C1q and has been observed to increase tumour cell survival, proliferation, and metastasis (Peerschke 2014). However, gC1q also binds several other ligands so its role is far from clear. Bioinformatic analysis of Oncomine data has shown C1q to be protective for basal and HER2 breast cancers while being pro-tumourigenic for lung and renal carcinomas (Magogna, 2019). Clearly, the context of the cancer niche is vital to determining the role C1q plays in in suppression or promotion of cancer growth.

C1q-meditated efferocytosis suppresses inflammatory activity in B and T cells via secretion of IL10 and TGFB (Lauber, 2004). Immobilised C1q can inhibit the production of the TH2 factor IL4 but enhance IL10 secretion by T cells *in vitro* suggesting similar immune regulation *in vivo* (Lu, 2007) (Figure 1.6). C1q is also able to dampen immune responses by inhibiting the differentiation of monocytic and plasmacytoid

dendritic cells through binding the leukocyte-associated immunoglobulin-like receptor 1 (LAIR-1) and LAIR-2 receptors via its collagenous tail (Son, 2012), (Kouser, 2015), (Son, 2017).

The C1q globular domain may well have other unrecognised functions as this domain occurs in at least 31 proteins with many, but not all, containing collagen-like regions (Tang, 2005). The functions of most of these proteins have been described in cursory fashion, with only adiponectin found to trigger cell signalling; however, the extreme conservation of the globular domain suggests an important role for these proteins that may serve to bridge innate immunity with adaptive immune function (Tang, 2005).

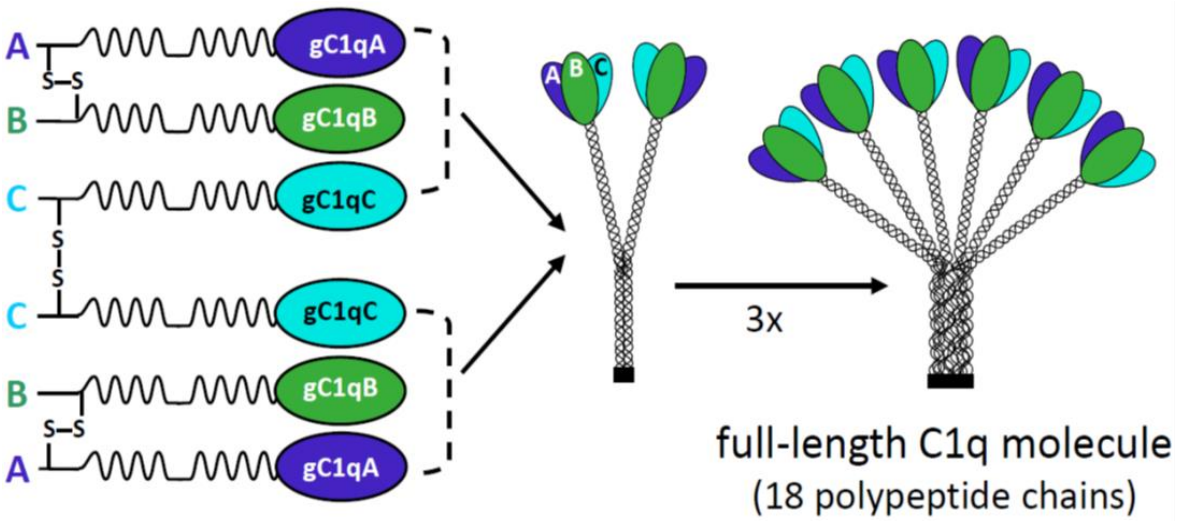

Figure 1.2 Structure of the C1q protein

Two disulphide-linked A- B dimers and one C-C protein dimer assemble into the tertiary structure of the C1q protein. Two heads are formed by the globular regions of the A, B, and C chains while the collagen-like tails form triple-helices that entwine the tail. Three of these tertiary structures form a further triple helix at the collagenase tail to form the quaternary structure, yielding a protein with six globular heads attached to a collagen-like tail. This figure is taken from Role of C1q in Efferocytosis and Self-Tolerance. Frachet et al. In: Autoimmunity: Pathogenesis, Clinical Aspects and Therapy of Specific Autoimmune Diseases. Katerina Chatzidionysiou ed. (2015).

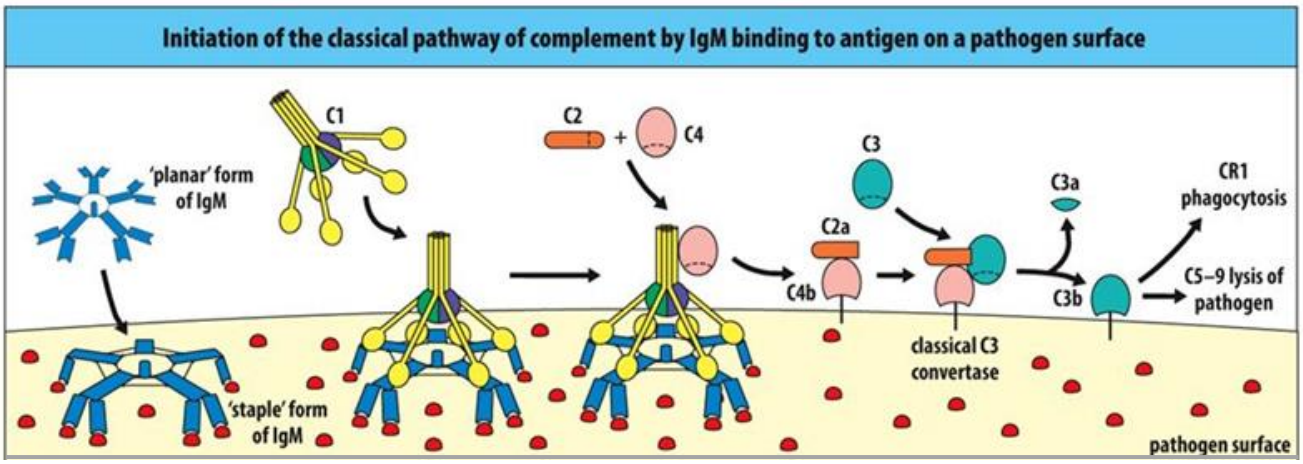

Figure 1.3 The role of C1q in initiation of the classical complement cascade

The six globular heads of C1q bind to repetitive motifs such as CH2 domains on IgM, bacterial mannans, and viral proteins displayed by infected cells. C1q assembles with C1r and C1s for form the C1 protein that cleaves C2 and C4 thereby initiating the complement cascade. Downstream in the cascade, opsonins are deposited on the target cell to facilitate phagocytic uptake, and anaphylatoxins are released that attract inflammatory leukocytes to the site. From Parham, P. The Immune System, 4th edition 2014.Garland Science, New York.

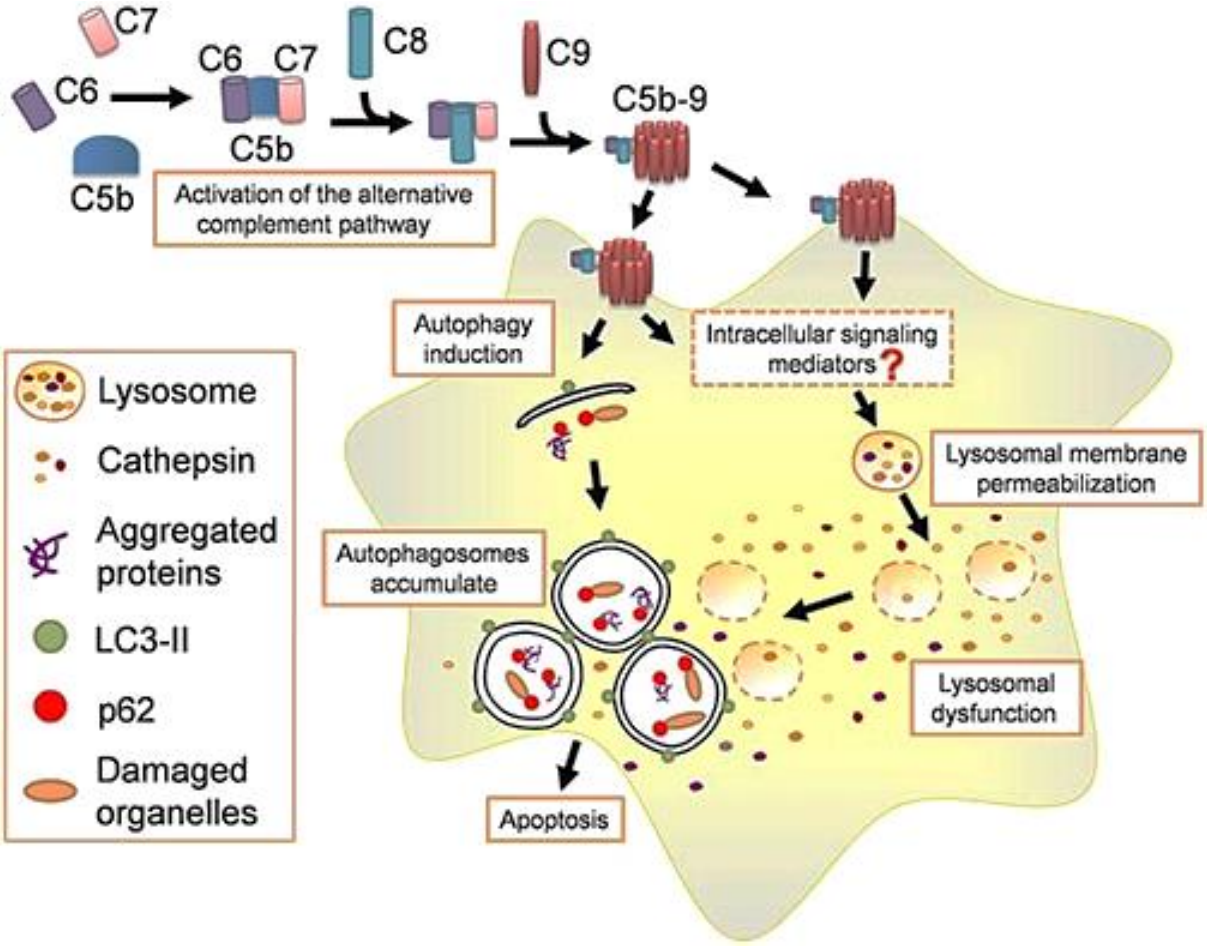

Figure 1.4 Formation of the membrane attack complex leads to cell lysis

Nucleation of complement factors downstream of C5b on the target cell membrane leads to the assembly of a trans-membrane channel of C9 proteins. This membrane attack complex disrupts the membrane integrity of the cell with consequent leakage of pro-inflammatory cytoplasmic components and creation of cytoplasmic access for granzyme b with subsequent activation of the caspase cascade. Figure from Liu et al, Sci Rep 7:8643. (2017).

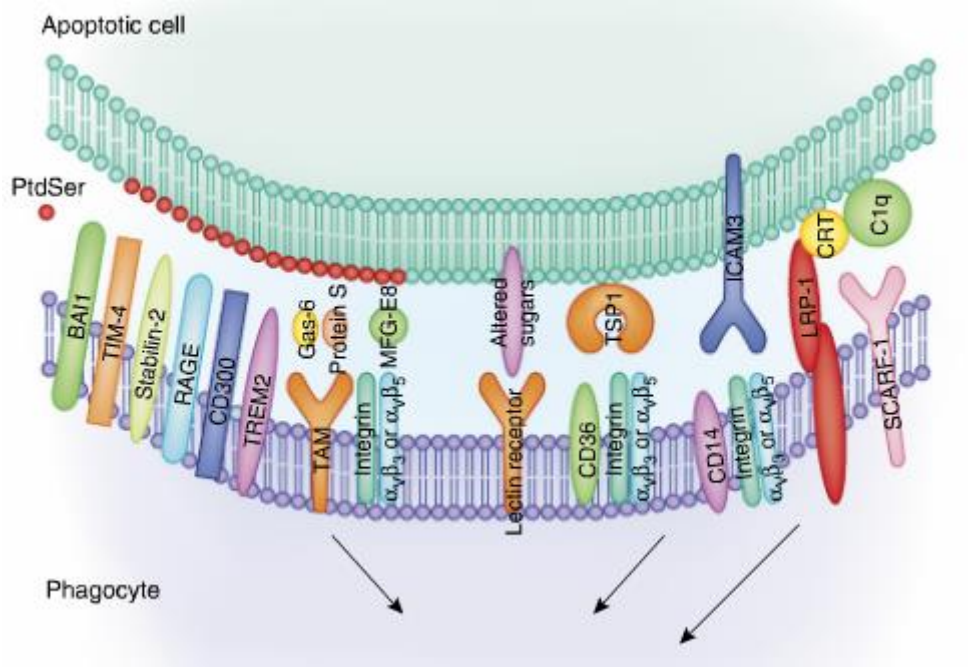

Cell signalling

Figure 1.5 C1q and the efferocytic synapse

An assortment of molecules function in the recognition, engagement, and engulfment of apoptotic cells. While all of these molecules play a role in efferocytosis, C1q plays a central role in the uptake of dying cells. Deletion of C1q through null mutation leads to a build-up of apoptotic epithelial cells in the mammary gland. Figure from Arandjelovic and Ravichandran Nat Immunol 16(9): 909, (2015).

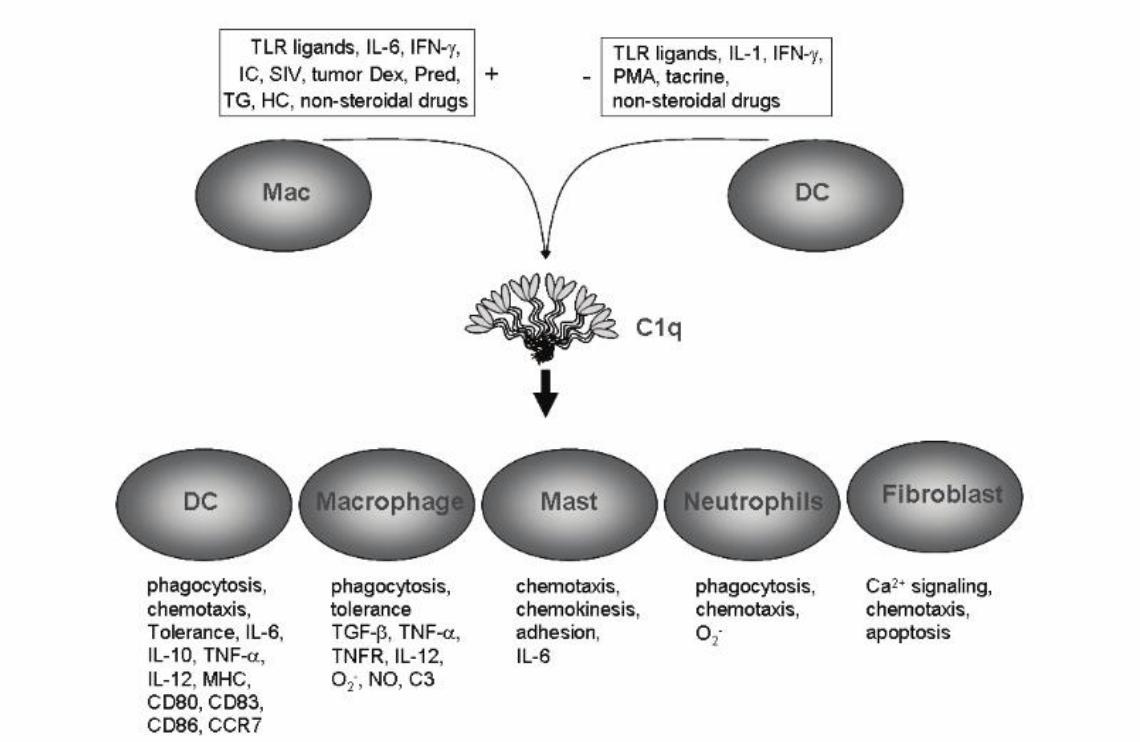

Figure 1.6 Immunoregulatory functions of C1q

C1q produced by macrophages and/or dendritic cells engages in the regulation of various immune cells. These different regulatory functions can promote an inflammatory or anti-inflammatory phenotype depending on the target cell and the immune environment. Figure from Lu et al. Cell Mol Immunol 5(1): 14 (2008).

1.8 MENSTRUAL CYCLING, C1Q, AND BREAST CANCER RISK

As discussed in Section 1.1, an increased lifetime number of menstrual cycles is associated with increased breast cancer risk (Chavez-MacGregor, 2005), (Collaborative Group on Hormonal Factors in Breast Cancer, 2012). Studies in rats have demonstrated an increased incidence of mammary cancer with carcinogen exposure during proestrus, the regression phase of the cycle, as compared to exposure at diestrus, the proliferation phase (Nagasawa, 1976), (Ratko, 1985). C1q appears to have a significant role in removal of dying cells during mammary gland regression, as C1q null mice exhibit increased abundance of dying cells during regression compared to C1q replete controls (Noor Din, 2017). Given the importance of this protein in the mammary gland and in regulating immune system responses, there has been much interest in the role of C1q in mammary cancer risk.

Hodson et al (manuscript in preparation) studied the incidence of mammary tumours initiated by treatment with the carcinogen dimethylbenz(a)anthracene (DMBA) in wild type C57Bl/6 mice and C1qA null mutant mice. C1q replete mice developed mammary tumours in 61% of mice while 10% of C1qA null mice developed tumours, a six-fold lower incidence of mammary carcinogenesis ($p = 0.02$). DMBA is a highly lipophilic compound that accumulates in the mammary fat pad of mice and leads to the formation of mammary tumours (Kerdelhué, 2016); however, DMBA can also accumulate in other fatty tissues in the mouse, leading to off-target malignancies and making this a less-than-ideal model of mammary cancer.

Noor Din explored the role of C1q with the MMTV-PyMT transgenic model of mammary cancer in mice (Noor Din, 2017). In the MMTV-PyMT mouse model, the mouse mammary tumour virus (MMTV) promotor drives polyoma middle T (PyMT) antigen expression in the mammary gland (Guy, 1992). PyMT interacts with and inactivates protein phosphatase 2 (PP2A), as well as interacting with and activating signalling by the proto-oncogene tyrosine-protein kinase c-Src, Src homology and collagen adaptor protein (ShcA), phosphatidylinositol 3-kinase (PI3K), and phospholipase C-γ1 (PLC-γ1) (Zhou, 2011). Activation of these multiple signalling pathways is highly transforming and results in aggressive mammary tumours with a short latency period.

Crossing MMTV-PyMT mice with C1q null mice to produce MMTV-PyMT/C1q-null double mutants produced a new model for studying the interaction of C1q with mammary epithelium during tumourigenesis (Chua, 2010). Measurements taken at 15 weeks of age indicated the wild type mice had developed more tumours than the C1q null mice, 4.8 v 3.2 ($P < 0.05$) and a similar but non-significant increase at 18 weeks, 5.8 v 4.8. Total tumour weight at 15 weeks was also higher for the C1q replete mice than the null mutants, 1.8 g v 0.8 g ($P < 0.05$) and at 18 weeks, 3.7 g v 2.4 g ($p<0.05$). The more aggressive disease was reflected not only in tumour size, but also tumour grade. Tumours from C1q replete mice had a higher frequency of late carcinoma grade compared to C1q null mice 44 v 10% ($p<0.05$) at 15 weeks and 72 v 28% at 18 weeks ($p<0.05$). Thus, the lack of C1q not only retarded mammary tumour formation, but it also slowed the progression to late carcinoma in the tumours that developed in this highly aggressive model.

Another example of the role of C1q in mammary carcinogenesis can be drawn from lupus patients. A hallmark of SLE is the development of ANA and the formation of immune complexes that deposit in the joints and kidney, thereby inciting arthritis and glomerulonephritis respectively (Walport, 1998). It is also of interest that in addition to ANA, SLE patients also develop antibodies to C1q protein thereby neutralising its activity (El-Hawala, 2011), (Katsumata, 2011). And while SLE patients are more susceptible to some haematological malignancies, they have a lower incidence of breast, ovarian, and endometrial cancers (Bernatsky, 2013), (Cloutier, 2013). Not only are anti-C1q antibodies a feature of SLE, mutations in C1q are sufficient to cause SLE as shown by patients with one of twelve mutations to C1q alleles (Schejbel, 2011). Thus, the role of C1q with efferocytosis-linked diseases as well as breast cancer incidence is well

established. Inhibition of C1q activity during ovarian cycling has the potential to decrease neoplastic transformation in mammary tissue and thereby function as a preventative for breast cancer.

However, carcinogenesis is a complex process with many inputs from the tissue microenvironment. Extracellular matrix (ECM) plays a role in altering epithelial cell phenotype, an interaction particularly obvious in cancer. ECM can have opposing actions in carcinogenesis, from an enriched collagen I environment that promotes cancer invasion (Nguyen-Ngoc, 2015) to an orderly scaffold of extracellular matrix that restrains cancer initiation and progression (Bissel, 2011). And as cancer cells influence the stromal niche in the mammary gland, so does the converse happen with stromal modulation of cancer cell proliferation and migration (Polyak, 2010). Thus, the functioning of healthy mammary gland tissue during menstrual cycling requires a finely-balanced network of epithelium, stromal cells, leukocytes and other interacting factors.

Other cell types in the tissue microenvironment also contribute to the process of carcinogenesis, cancer progression, and metastatic spread. Stromal fibroblasts can adopt an altered phenotype that contributes to cancer development and progression. These cancer-associated fibroblasts (CAFs) have been shown to produce a number of growth factors and pro-inflammatory chemokines such as epidermal growth factor (EGF), basic fibroblast growth factor (bFGF), IL6, IL17a, CCL5 and CCL7 (Öhlund, 2014). However, as in many other biological systems, CAFs have been found to have different phenotypes, some with cancer-promoting properties while others that inhibit cancer progression (Gieniec, 2019). Further, adipocytes and vascular endothelial cells are also able to contribute to the progression and spread of cancerous cells (Gieniec, 2019), (Wu, 2019).

Despite this complexity in the cancer cell microenvironment, the striking impact of C1q depletion in mammary gland regression, and in cancer susceptibility and progression demonstrates the importance of this protein in carcinogenesis. Inhibition of C1q therefore presents an opportunity for devising an intervention to reduce breast cancer risk. Inhibitors of C1q activity are quite varied in their size and source. These include the endogenous neutrophil defensin human neutrophil peptide 1 (HNP-1) (Van den Berg, 1998) and the microbial surface components recognising adhesive matrix molecules (MSCRAMMs) produced by gram-positive bacteria (Kang, 2011). A monoclonal antibody capable of disrupting C1q function has been derived for the study of acute motor axonal neuropathy (McGonigal, 2016). A soluble form of complement receptor 1 (CR1, CD35) has been investigated as a potential therapeutic for inflammatory diseases (Morgan, 1996). A highly active 15mer peptide has been derived from a 787 residue capsid protein from an astrovirus and intended for treatment of haemolytic anaemia (Sharp, 2014). Inhibitors of C1q have been synthetically derived through a phage-display library screened for binding to C1q (Lauvrak, 1997). This same library was screened for peptides that inhibited C1q-mediated haemolysis and the peptide 2J selected for further characterisation of its anti-C1q activity (Roos, 2001). While the research on C1q inhibition has focused on the inhibition of inflammatory processes, such molecules could possibly inhibit C1q-mediated efferocytosis and the attendant promotion of breast cancer progression during the regression phase of the ovarian cycle.

1.9 CONCLUSION

Macrophages play several important roles in mammary gland development and function, and while most studies have been performed in mice, many of these observations have been shown to be consistent in human biology as well. Macrophages are essential for the proliferation and budding of mammary gland epithelium, and for removal of apoptotic alveoli in the regression phase of the ovarian cycle. Macrophage abundance changes throughout the cycle with peak numbers at diestrus and lowest numbers at proestrus. In addition, macrophages alter their overall phenotype from M1 immune surveillance at diestrus to M2

wound healing/tissue remodelling at proestrus. It is the tissue-remodelling M2 macrophages that clear the apoptotic cells of the breast alveoli and the complement component C1q appears to play a vital role in this clearance.
But this mechanism of epithelial proliferation and regression does not always proceed smoothly. The menstrual cycle itself is contributory to the development of breast cancer, as seen in women who have experienced a greater number of cycles over their lifetime. In addition, increased cancer susceptibility is linked to the regression phase compared to the proliferation phase, as seen in rat carcinogen studies. The regression phase is populated with tissue remodelling M2 macrophages that secrete immunosuppressive cytokines. Absence of C1q in the mouse null mutant model results in delayed cancer development and progression.

While there have been numerous studies of macrophages in the post-lactational involuting mammary tissue and tumour-associated macrophages in breast cancer, there has been negligible investigation of macrophage function and the role of C1q in normal cycling, especially vis-a-vis cancer susceptibility. Noor Din has demonstrated the importance of C1q in the clearance of apoptotic mammary epithelial cells and the development of mammary cancer (Noor Din, 2017). This has led to the hypothesis that a monoclonal antibody capable of blocking C1q function in efferocytosis would inhibit the anti-inflammatory microenvironment during regression and lead to a decreased incidence of mammary cancer.

Monoclonal antibodies are able to act in a therapeutic capacity is several ways: antibody-dependent cellular cytotoxicity (ADCC), complement-dependent cytotoxicity (CDC), molecular blockade, receptor activation, or in the case of antibody-drug conjugates, cellular targeting (Suzuki, 2015). In ADCC and CDC, the therapeutic antibody supplies the immunoglobulin that binds the target cell and directs innate immune system killing, via leukocyte killing for ADCC or assembly of the membrane attack complex for CDC. The proposed monoclonal antibodies to C1q would act in a blocking capacity, stopping the binding of C1q to its cognate receptors. Since the activity of C1q in efferocytosis requires two interactions, viz. binding the apoptotic cell via interaction with the globular domain and interaction with a phagocytic cell by way of the collagen-like domain. this provides an opportunity for a monoclonal antibody to target either of two areas on C1q: the globular domain or the collagen-like domain. This can either involve directly blocking a receptor-binding domain, or by binding in proximity to such a domain and sterically hindering access to the target receptor. At 150 kD, an immunoglobulin molecule is a relatively large protein and a good candidate for blocking the activity of a molecule from a non-receptor-binding epitope.

Monoclonal antibodies to C1q were developed and their ability to block efferocytic uptake of apoptotic cells was studied *in vitro*, with the intention of studying a potential anti-cancer effect in a preclinical mouse model in both C1q replete and C1q null backgrounds. Efficacy seen in preclinical models would provide an opportunity to move to clinical studies of a potential treatment for breast cancer, providing new and alternative treatment options particularly for treatment refractory cancers such as the triple negative cancers for which there are currently limited options. Such a novel therapeutic would represent a significant step forward in the treatment of breast cancer.

CHAPTER TWO: MATERIALS AND METHODS

2.1 TISSUE CULTURE

This project utilised several different cell lines in the study of macrophage efferocytosis and the production of monoclonal antibodies. Table 2.1 lists the cell lines employed in this project and the different media used for culturing these cells.

2.1.1 CULTURE TECHNIQUES

2.1.1.1 Sub-cultivation using trypsin

Cells were grown in a 75 cm^2 flask (Greiner 658 175) at 37°C + 5% CO_2 in culture medium of either DMEM (Life Technologies 12430-054) or RPMI 1640 (Life Technologies 11875-093), 10% fetal calf serum (FCS) (Serana S-FBS-AU-015, lot no 18010617FBS), 100 U/mL penicillin plus 100 µg/mL streptomycin (Life Technologies 15140-163). When cells covered 80%-100% of the flask surface area (80-100% confluence), the culture medium was removed and the flask rinsed briefly with 7 mLs of phosphate buffered saline (PBS) (Life Technologies 14190-144) to remove the remnants of the culture medium. The PBS was discarded, 1 mL of trypsin (Life Technologies 25200-056) added, and the flask then incubated for 5 minutes at room temperature. The flask was tapped to loosen the cells and 9 mLs of DMEM or RPMI growth medium added to neutralise the trypsin. The cells were sub-cultivated at a 1:5 to 1:10 split ratio, in 15 mLs of culture media for a 75 cm^2 flask.

2.1.1.2 Sub-cultivation using Accutase and scraping

Cells were grown in a 75 cm^2 flask at 37°C and 5% CO_2 in RPMI growth medium until the cells reached 80-100% confluence. The culture media was removed and the flask rinsed briefly with 7 mLs of PBS (Life Technologies 14190-144) to remove the remnants of the culture medium. The PBS rinse was discarded and 1 mL of Accutase (Sigma A6964) added. The flask was incubated for 10 minutes at 37°C then tapped several times with the palm of the hand to remove the lightly adherent cells from the flask. The remaining adherent cells were dislodged with a cell scraper (Sigma CLS 3010) and resuspended in 9 mLs of RPMI growth medium. The cells were sub-cultivated at a 1:5 to 1:10 split ratio in 15 mLs of culture media and transferred to a 75 cm^2 flask.

2.1.1.3 Sub-cultivation of SP2/0 suspension cells

Suspension cell lines do not require enzymatic treatment during sub-cultivation. However, SP2/0 cells were lightly adherent and required dislodging with a few taps on the flask. Once all cells were in suspension, the culture was sub-cultivated by diluting into fresh growth medium at split ratios between 1:10 and 1:50.

Cell	Species	Tissue	Medium	Cultivation method
T47D	Human	Breast Cancer	DMEM + 10% FCS + p/s	Trypsin
MDA-MB-231	Human	Breast Cancer	DMEM + 10% FCS + p/s	Trypsin
RAW264.7	Mouse	Macrophage	RPMI + 10% FCS + p/s	Accutase + scraping
L cells	Mouse	Connective tissue	RPMI + 10% FCS + p/s	Trypsin
Sp2/0-Ag14 clone 4	Mouse	Myeloma	RPMI + 10% FCS + p/s	Dilution of suspension culture
Hybridoma	Mouse	Myeloma/B cell hybrid	Fusion medium	Dilution of suspension culture
Bone marrow-derived macrophages	Mouse	Differentiated bone marrow	Macrophage medium	N/A

Table 2.1 Cells used in the study and their culture conditions

This table details the species and tissue of origin of the cells utilised in this project, as well as their growth media and techniques for sub-cultivation. Fusion medium = RPMI + 20% FCS + 100 U/mL penicillin + 100 µg/mL streptomycin + 1.1 mM oxaloacetic acid (Sigma O9504) + 1 mM sodium pyruvate (Life technologies 11360070) + 0.5 U/mL bovine insulin (Sigma I5500) + 200 µM hypoxanthine (Sigma H9636) + 1 µg/mL azaserine (Sigma A1164). Macrophage medium = RPMI + 10% fetal calf serum + 100 U/mL penicillin and 100ug/mL streptomycin + 20% L cell conditioned medium. p/s = penicillin/streptomycin (Life Technologies 15140-163).

2.1.1.4 Preservation of cell lines in liquid nitrogen

If the cell line was adherent, cells were first detached from the flask using trypsin or Accutase plus scraping. The suspended cells were centrifuged at 200 x g then resuspended in freezing medium (5% dimethyl sulfoxide (DMSO) (Sigma D2660) in FCS) at 2 mLs per 75 cm^2 flask, or approximately 5 x 10^6 cells/mL. 1 mL aliquots were distributed into 2 mL cryovials and placed into a Mr Frosty (Sigma C1562) filled with isopropanol (Sigma 190764) at room temperature then placed into a -80° C ultra-cold freezer overnight, before being transferred within a week to a liquid nitrogen tank for long-term storage.

2.1.1.5 Thawing cryovials of cell lines from liquid nitrogen storage

Cryovials retrieved from liquid nitrogen were held on dry ice prior to thawing. The vial was removed from dry ice then swirled in a 37°C water bath until the ice in the vial had nearly melted. The cells were slowly diluted with growth medium to a final volume of 10 mLs. The cell suspension was then plated directly into a flask with the growth medium changed the following day or pelleted at 200 x g and resuspended in growth medium for culturing.

2.1.2 CELL LINES

2.1.2.1 T47D

T47D (ATCC HTB133) is a ductal breast adenocarcinoma line of epithelial morphology. This cell line was derived from the metastatic pleural effusion in a 54 year old woman and expresses receptors for estrogen and progesterone (Keydar, 1979). The karyotype for this line is hypotriploid (modal chromosome number = 65).

2.1.2.2 MDA-MB-231 TXSA-S

MDA-MB-231 (ATCC HTB-26) is a ductal breast adenocarcinoma line of epithelial morphology. This cell line was derived from the metastatic pleural effusion in a 51 year old female and is negative for both estrogen and progesterone receptors. The karyotype for this line is aneuploid (modal chromosome number = 64, range = 52 to 68). The MDA-MB-231 TXSA-S variant was derived from passage through nude mice and isolating metastatic deposits for sequential passaging, creating an aggressively metastatic cell line (Zinonos, 2009).

2.1.2.3 RAW 264.7

RAW 264.7 (ATCC TIB 71) is a macrophage cell line derived from a male BALB/c mouse infected with Abelson murine leukaemia virus and recovered from the resultant ascitic effusion. Abelson leukaemia virus is a class VI retrovirus capable of inducing aggressive lymphosarcomas in mice (Raschke, 1978). RAW cells have the ability to lyse erythrocytes and phagocytose zymosan and latex beads.

2.1.2.4 L cells

L cells (ATCC CRL-2648) are a subcutaneous connective tissue cell line derived from a male C3H/An mouse. This cell line displays fibroblastic morphology and inherent to its enteroendocrine lineage, it secretes CSF1. These cells are tumorigenic in mice having a modal karyotype of 45 chromosomes with a range of 42 to 48.

2.1.2.5 SP2/0-Ag14 clone 4

SP2/0-Ag14 (ATCC CRL-1581) is a mouse hybridoma derived from a fusion of splenocytes from a BALB/c mouse immunised with sheep red blood cells and the myeloma line P3X63Ag8. This cell line has been selected to be negative for immunoglobulin (Ig) production and positive for the hypoxanthine phosphoribosyltransferase (HPRT) gene, which forms the basis for hypoxanthine and aminopterin/azaserine selection during hybridoma derivation (Shulman, 1978). Clone 4 of this cell line was selected at Cetus Corporation for its ability to maximise fusion with splenocytes to produce hybridoma cell lines.

2.1.3 CONDITIONED MEDIA

2.1.3.1 L cell conditioned medium

Fifteen mLs of fresh RPMI growth medium was added to a confluent 75 cm^2 flask of l cells and incubated at 37°C + 5% CO_2 for a week. The conditioned medium was removed, retained at 4°C, and the culture refreshed with a further 15 mLs of RPMI growth medium. After incubating for a further week, the conditioned medium was collected and the RPMI growth medium refreshed again. After a third week of incubation, the conditioned medium was harvested and pooled with the previous two lots collected then stored at 4°C.

2.1.3.2 SP2/0 spent medium

A culture of SP2/0 at optimal density for passaging was allowed to grow for a further three days. The cells were pelleted ay 200 x g, and the supernatant retained and stored at 4°C.

2.1.4 PRIMARY CELL CULTURE

2.1.4.1 Mouse bone marrow derived macrophages

2.1.4.1.1 Harvesting bone marrow

A C57Bl/6 mouse was sacrificed by cervical dislocation and soaked with 70% ethanol (Pfizer 155412). The skin was removed from the hind limbs and, proceeding from the distal end, the muscles removed from the tibia. The foot was removed and the tibia separated from the leg at the knee joint. The isolated bone was placed into a tube of RPMI containing penicillin/streptomycin and held on ice. The muscles were removed from the femur, the bone disarticulated from the hip and placed in RPMI containing penicillin/streptomycin with the tibia. The procedure was repeated for the other hind leg.

A 5 mL syringe (BD cat no 302130) was filled with cold RPMI containing penicillin/streptomycin and fitted with a 26g needle (BD 302002) bent to a 45-degree angle. A marrow-free section of bone was trimmed from the distal end and a small opening clipped into the proximal end with fine scissors. The needle was placed into the opening and the marrow flushed from bone with RPMI until the bone blanched. This procedure was repeated until all bones were flushed.

In a biosafety cabinet, the clumps of marrow were disaggregated by passing the cell suspension through a 21g needle (BD 302015) three times, followed by three passes through a 23g needle (BD 301810). An aliquot of the cells was counted by mixing 1:1 with Türk's solution (2% acetic acid (Merck 6.10001.2500) + 0.1% crystal violet (Sigma C0775)). The bone marrow yield from one mouse varied between $5x10^7$ and $1 x 10^8$ cells. The cells were pelleted and frozen in portions of $5 x 10^6$ cells in fetal calf serum + 5% DMSO.

2.1.4.1.2 Differentiating bone marrow into macrophages

On day 1, cultures of mouse bone marrow were plated into an Ibidi 8-chamber slide (Ibidi cat no 80826) at 200 µL/well of a $1.5 x 10^7$ cells/mL suspension in macrophage medium. On day 4, 100 µL/well of fresh macrophage medium was added and by day 7 the cultures contained fully differentiated macrophages.

2.1.4.1.3 Activating macrophages into different phenotypes

Cultured macrophages were differentiated into different phenotypes with various factors and/or cytokines. For M1 cells, macrophage cultures were treated with 200 ng/mL lipopolysaccharide (LPS) (Sigma L4391) and 20 ng/mL IFNG (Peprotech 200-02). For the M2a, macrophage cultures were treated with 20 ng/mL IL4 (Peprotech 214-14). M2c cells were differentiated by treatment with 20 ng/mL TGFB1 (Peprotech 100-21). All differentiation treatments were conducted for 24 hours prior to assay or staining protocols.

2.2 MOUSE MODELS

2.2.1 CARE OF MOUSE COLONIES

All animal experiments were conducted with the approval of the University of Adelaide animal ethics committee (ethics approval numbers M088/2015 and M-2017-015) and all experimental procedures followed the Australian Code of Practice for the Use of Animals for Scientific Purposes (8th edition, 2013). All mice were obtained from breeding colonies maintained by the University of Adelaide Laboratory Animal Services. Mice were maintained in a barrier facility under specific pathogen free conditions, with a 12 hour light / 12 hour dark cycle and temperature control at the University of Adelaide Helen Mayo South animal facility. Food and water were provided ad libitum.

2.2.2 MACGREEN TRANSGENIC MICE (c-fms-Gfp)

MacGreen mice are transgenic mice expressing the green fluorescent protein (GFP) linked to the c-fms (CSF1 receptor) promoter. The c-fms promotor drives expression of GFP protein in CSF1 responsive cells, primarily myeloid cells of the monocyte/macrophage lineage although receptor expression can also be found in trophoblast tissue during pregnancy (Sasmono, 2012).

2.2.3 C1q NULL MUTANT MICE

Targeted insertion of the neomycin-resistance gene into the first exon of the *C1qA* gene through homologous recombination disrupted expression of C1qA protein in an embryonic stem cell line (Botto, 1998). The resultant *C1qA*-null stem cell lines were injected into 129/C57Bl/6 F1 blastocysts prior to transfer of the embryos into pseudo-pregnant recipient females. C1qA-targeted stem cells were able to incorporate into the inner cell mass of blastocyst embryos and contributed to the tissues of the developing mouse embryo, thereby producing a chimaera of donor and injected cells. Chimaeric mice were identified by the different coat colour derived from injected ES cells compared to the wild-type coat colour. Chimaeric progeny that transmitted the mutant C1qA allele through the germline were backcrossed onto a C57Bl/6 background. These mice exhibit anti-nuclear antibodies (ANA) and develop glomerulonephritis, a hallmark

of the human disease systemic lupus erythematosus (SLE). Approximately fifty per cent of C1qA mutant mice produced an anti-nuclear antigen antibody response at one year of age (Botto, 1998); however, the mice used in this project were not maintained to this age and these younger mice were normal by visual inspection.

2.3 INDUCTION OF APOPTOSIS

2.3.1 ULTRAVIOLET IRRADIATION

A confluent 75 cm^2 flask of T47D cells was serum-starved by growing in DMEM + p/s overnight to synchronise the cells in G1 phase of the cell cycle. The cells were then trypsinised, resuspended in 10 mLs of DMEM growth medium, and counted with a Neubauer haemocytometer. The cell suspension was adjusted to 1 x 10^6 cell/mL with growth medium and 2 mLs placed into a well of a 6-well tray (Greiner 657 160). The tray was placed into a biosafety cabinet, the lid removed and the tray exposed to 254 nm ultraviolet (UV) light (UVC) for 30 minutes to initiate apoptosis. The cell suspension was removed from the well, placed in a 10 mL tube and maintained on ice until stained and analysed by flow cytometry.

2.3.2 DOXORUBICIN TREATMENT

On day 0, a 75 cm^2 flask was serum starved in DMEM overnight to synchronise the cells in G1 phase of the cell cycle. On day 1, a confluent of T47D cells was trypsinised, resuspended in 10 mLs of DMEM growth medium and counted with a Neubauer haemocytometer. The cell suspension was adjusted to 1 x 10^6 cell/mL, 2 mLs was placed into a well of a 6-well tray and the tray was incubated at 37°C + 5% CO_2 overnight. On day 2, the growth medium was removed and replaced with serum-free DMEM to serum-starve the culture. On day 3, doxorubicin (Hospira cat no 8145) was added to a final concentration of 0.5 and 5 µM and the tray incubated at 37°C in 5% CO_2 for 24 hours. On day 4, the cells were trypsinised, resuspended in 10 mLs of DMEM growth medium and counted with a Neubauer haemocytometer. The cell suspension was then adjusted to 1 x 10^6 cell/mL and the cells maintained on ice until stained and analysed by flow cytometry.

2.3.3 ESTROGEN DEPRIVATION

On day 1, DMEM growth medium was removed from a 75 cm^2 flask of T47D at approximately 75% confluence and replaced with serum-free DMEM to serum-starve the culture. On day 2, cells were plated to a 75 cm^2 flask at a 1:3 split ratio in DMEM growth medium containing 1nM estradiol. On day 4, cells were trypsinised, counted with a Neubauer haemocytometer and resuspended in growth medium at 1 x 10^6 cells/mL. The cells were plated into a 24-well tray at 300 µL/well, tamoxifen was added to a final concentration 2 or 5 µM and the tray was placed at 37°C in 5% CO_2 for 30 minutes. The cells were then trypsinised, resuspended and maintained on ice until stained and analysed by flow cytometry.

2.3.4 DROZITUMAB CROSS-LINKING

Apoptosis in MDA-MB-231 cells can be induced through binding of the death receptor 5 (DR5) with Drozitumab cross-linked with anti-Fc antibody. Cross-linking Drozitumab promotes clustering of DR5 molecules on the plasma membrane and enhanced cytoplasmic signalling, leading to a more rapid onset of apoptosis (Liu, 2015). A Drozitumab (Genentech) stock solution (50 mg/mL) was diluted to 100 µg/mL and a goat anti-human Fc (Jackson ImmunoResearch 109-005-008) stock solution (2.3 mg/mL) was diluted to 100 µg/mL, both in DMEM growth medium. To cross-link Drozitumab, 100 µg/mL Drozitumab was mixed with 100 µg/mL anti-Fc antibody at a 1:1 ratio and incubated on ice for 30 minutes. The cross-

linked Drozitumab was added at a final concentration of 200 ng/mL to co-cultures of either bone marrow-derived macrophages or RAW 264.7 cells and MDA-MB-231 cells plated into Ibidi 8 well chamber slides (see efferocytosis protocols, section 2.4).

2.3.5 ANALYSIS OF APOPTOSIS BY FLOW CYTOMETRY

2.3.5.1 Early apoptosis

Apoptotic T47D cells were placed into 1.5 mL tubes (Axygen MCT-150-C) at 5 x 10^5 cells/tube in 500 µL DMEM growth medium. Cells were washed with cold binding buffer (0.1 M 4-(2-hydroxyethyl)-1-piperazineethanesulfonic acid (HEPES) (Life Technologies 15630-080) + 1.4 M NaCl (Sigma S9888) + 25 mM $CaCl_2$ (Sigma C3306), pH 7.4), and centrifuged at 200 x g for 5 minutes. The cells were resuspended at 1x10^6/mL in binding buffer and placed on ice for 30-60 minutes. 1x10^5 cells (100 µL) were aliquoted into FACS tubes (Falcon 352052) and 5 µL of fluorescein isothiocyanate (FITC) Annexin V (BD Biosciences 556419) and/or 10 µL propidium iodide (PI) (BD Biosciences 556463) was added. The cells were gently mixed and incubated for 15 minutes at room temperature in the dark. 100 µL of binding buffer was added to each tube and fluorescent staining was analysed by flow cytometry on a BD FACSCanto II within one hour of staining.

2.3.5.2 Late apoptosis

T47D cells were centrifuged at 200 x g for 5 minutes and resuspended at 1 x 10^6 cells/mL in 1% formalin (Australian Biostains ANBCF). The cells were placed on ice for 30-60 minutes, then centrifuged at 200 x g for 5 minutes and washed twice with 5 mLs of PBS. The PBS was tipped off and the cells were gently resuspended in the residual PBS. Ice cold ethanol (Sigma E7023) was added to the cells to restore the concentration of 1 x 10^6 cells/mL and the tubes were incubated for 30 minutes on ice. The cells were centrifuged at 200 x g for 5 minutes and resuspended in 1 mL of wash buffer (BD Bioscience 51-6579AZ). The cells were washed twice with 1 mL of wash buffer and each tube resuspended in 50 µL of DNA labelling solution containing 10 µL reaction buffer (BD Bioscience 51-6580AZ), 0.75 µL terminal deoxynucleotidyl transferase (TdT) enzyme (BD Bioscience 51-6581AZ), 8 µL 5-bromo-2´-deoxyuridine 5´-triphosphate (Br-dUTP) (BD Bioscience 51-6582AZ), and 32.25 µL deionised water (Life Technologies 10977-023). The cells were incubated for 60 minutes in a 37°C water bath with the tubes shaken every 15 minutes to resuspend cells.

Cells were washed twice with 1 mL per tube of rinse buffer and resuspended in 100 µL per tube of antibody staining solution containing 5 µL Anti-('-bromo-2'-deoxyuridine) (BrdU) fluorescein isothiocyanate (FITC) (BD Bioscience 51-6584AZ), and 95 µL rinse buffer (BD Bioscience 51-6583AZ). The cells were incubated for 30 minutes in the dark at room temperature and then 500 µL of PI/RNase staining buffer (BD Bioscience 51-6585AZ) was added and the cells incubated for 30 minutes at room temperature in the dark. The cells were analysed by flow cytometry on a BD FACSCanto II within 3 hours of staining.

2.4 EFFEROCYTOSIS ASSAYS

2.4.1 EFFEROCYTOSIS OF MDA-MB-231 CANCER CELLS BY RAW 264.7 MACROPHAGES

On day 1, a confluent 75 cm^2 flask of RAW 264.7 cells was Accutase-treated, the cells counted by Neubauer haemocytometer and 6 x 10^4 cells/well in 200 µL RPMI growth medium were plated into an Ibidi 8 well slide. RAW cells were incubated at 37°C for 4-6 hours prior to enable adherence to the Ibidi slide prior to labelling. CellTracker Green 5-chloromethylfluorescein diacetate (CMFDA) (Life Technologies C2925) dye was dissolved in DMSO to a final concentration of 10 mM then diluted to 5 µM in serum-free RPMI. The growth medium was removed from the RAW 264.7 cultures and 200 µL/well of 5 µM dye was added and incubated for 30 minutes at 37ºC with 5% CO_2. The dye-containing medium was removed and 100 µL/well of RPMI growth medium added.

On day 2, a confluent 75 cm^2 flask of MDA-MB-231 TXSA-S cells was trypsinised, counted on a Neubauer haemocytometer, and then diluted to 2 x 10^5/mL in 2 mLs of RPMI growth medium. pHrodo SE dye (Life Technologies P36600) was diluted from 1.5 mM to a final concentration of 0.2 µM in Hank's buffered salt solution (HBSS) (Life Technologies 14170-112). The MB-231 cells were centrifuged at 200 x g for 5 minutes then 2 mLs of 0.2 µM pHrodo in HBSS was added. The MB-231 cells were resuspended and incubated for 15 minutes in the dark at room temperature. The cells were pelleted, the pHrodo dye-containing medium removed and replaced with 2 mL of RPMI growth medium. The labelled MB-231 were plated at 100 µL/well onto Ibidi slides containing the CellTracker-labelled RAW cells.

Cross-linked Drozitumab was prepared, incubated on ice for 30 minutes and then added to the Ibidi slide containing RAW/MB-231 co-culture to a final concentration of 200 ng/mL. The slide was placed on a Zeiss LSM700 confocal microscope which was set up to detect two-colour fluorescence (CellTracker in the green channel; pHrodo in the red channel). Images were acquired through either time lapse frame acquisition at five minute intervals or through manual acquisition of multiple frames (typically eight) at two hour intervals. Data analysis was undertaken using the FIJI suite of image analysis software.

2.4.2 EFFEROCYTOSIS OF MDA-MB-231 CANCER CELLS BY MOUSE BONE MARROW-DERIVED MACROPHAGES

On day 1, a culture of mouse bone marrow was set up in an Ibidi 8-chamber slide at 3 x 10^6 cells/well in 200 µL/well macrophage medium. On day 3, 100 µL of fresh macrophage medium was added to each well.

On day 6, the CellTracker green CMFDA dye was dissolved in DMSO to a final concentration of 10 mM and then diluted to 5 µM in serum-free RPMI. The macrophage medium was removed from the chamber slide wells and retained, then 100 µL/well of CellTracker dye was added to the macrophages and incubated for 30 minutes at 37ºC with 5% CO_2. The dye-containing medium was removed and 100 µL/well of the retained macrophage medium was added along with 100 µL/well of fresh macrophage medium.

On day 7, a confluent 75 cm^2 flask of MDA-MB-231 cells was trypsinised, counted with a Neubauer haemocytometer and diluted to 2 x 10^5/mL in 2 mLs of RPMI growth medium. CellTracker red CMTPX dye was diluted from a 10 mM stock in DMSO to a final concentration of 5 µM in serum free RPMI. The MB-231 cells were centrifuged at 200 x g for 5 minutes, resuspended in 2 mLs of the CellTracker red dye in RPMI and incubated for 30 minutes at 37ºC with 5% CO_2. The cells were centrifuged and the dye solution replaced with 2 mL of RPMI growth medium. From the macrophage cultures, 100 µL/well of RPMI

growth medium was removed and 100 µL/well of labelled MB-231 cells were added. Alternatively, experiments were also performed with MDA-MB-231 cells expressing red fluorescent protein (RFP).

Cross-linked Drozitumab was prepared by incubation on ice for 30 minutes and then added to the Ibidi slide containing RAW/MB-231 co-culture at a final concentration of 200 ng/mL. The slide was placed on a Zeiss LSM700 confocal microscope which was set-up for 2-colour fluorescence (CellTracker green in the green channel; CellTracker red in the red channel). Images were acquired through either time lapse frame acquisition at five minute intervals or through manual acquisition of multiple frames (typically eight) at two hour intervals. Data analysis was undertaken with the FIJI suite of image analysis software.

2.4.3 QUANTIFICATION OF EFFEROCYTOSIS

Fluorescent co-localisation of green CellTracker-labelled macrophages and red pHrodo-labelled dying MDA-MB-231 cells was used to quantify efferocytosis. FIJI is an open-source image processing package based on ImageJ that employs the Java programming language. Images from the Zeiss LSM700 confocal microscope saved as czi files can be opened by FIJI directly. FIJI employs digitisation of analogue images for the purpose of quantifying many aspects of the image. In the case of analysing efferocytosis assay images, the aspect sought to be quantified was the degree of apoptotic cellular material ingested by phagocytic macrophages. The degree of efferocytosis would involve calculating the amount of overlap of the red and green dyes, i.e., the amount of apoptotic cells within the phagocyte. The digitisation allowed the entire phagocyte to be viewed in the image, making it possible to view overlap with apoptotic material even when there was no overlap of red and green dyes. The analogue images were split into red and green channels, followed by application of a thresholding algorithm to create a digital image for each channel. The two channels required different threshold algorithms: Li for the green channel and Triangle for the red channel. The area of overlap between the red and green masks was determined using the image calculator function and the Boolean operator ‘AND’. The area of overlap was then expressed as a proportion of the macrophage (green) area and labelled the phagocytic index. Figure 2.1 illustrates the steps in the analysis of an image visually. Figure 2.2 lists the FIJI commands used in the analysis.

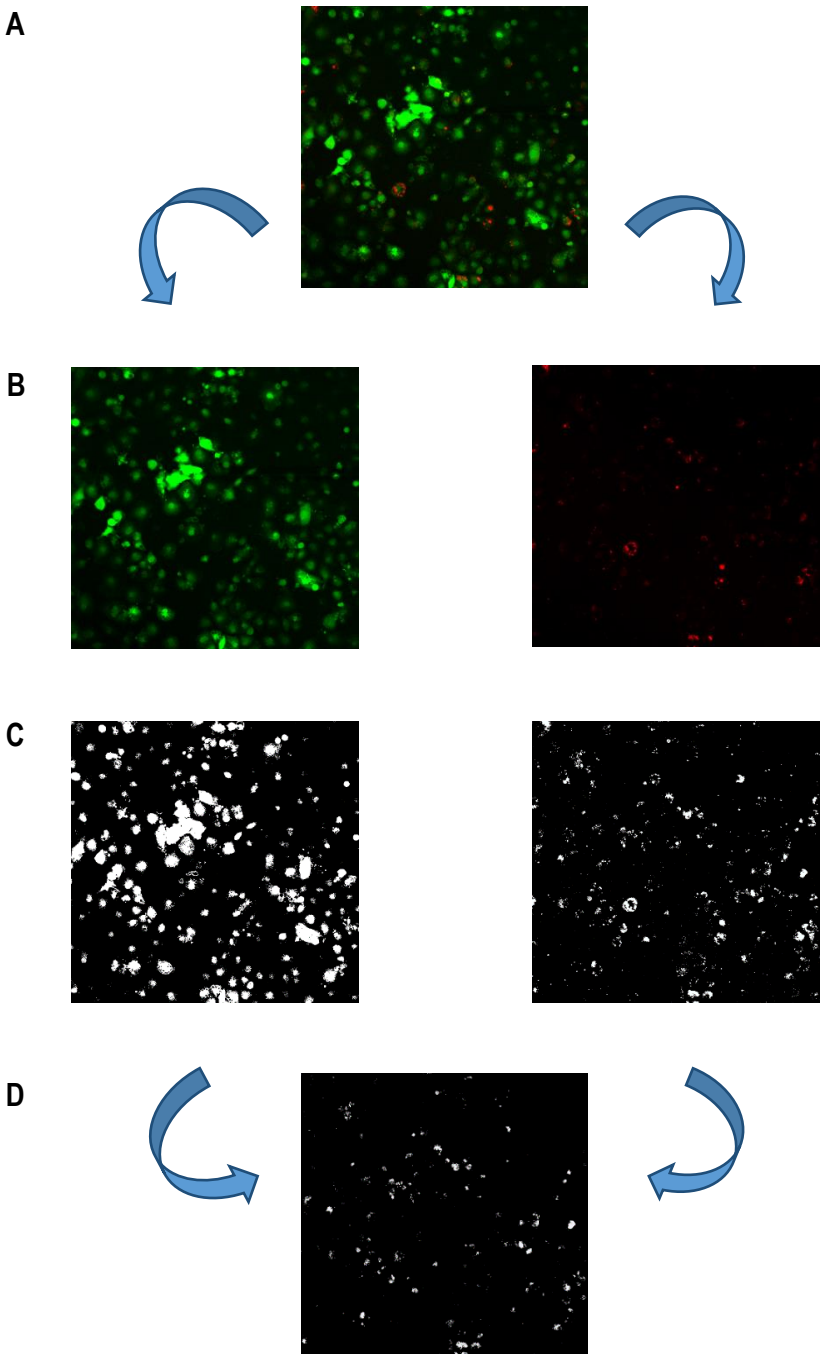

Figure 2.1 Analysis of efferocytic uptake of MB-MDA-231 cells with FIJI

A two colour image (A) from an efferocytosis assay consisting of green-labelled RAW 264.7 macrophages and red-labelled apoptotic MB-MDA-231 breast cancer cells. The image is split into green and red channels (B), then a digital mask is produced for each image (C). Finally, the area of overlap for the two masks is calculated (D), representing the uptake of dying cancer cells by macrophages.

A

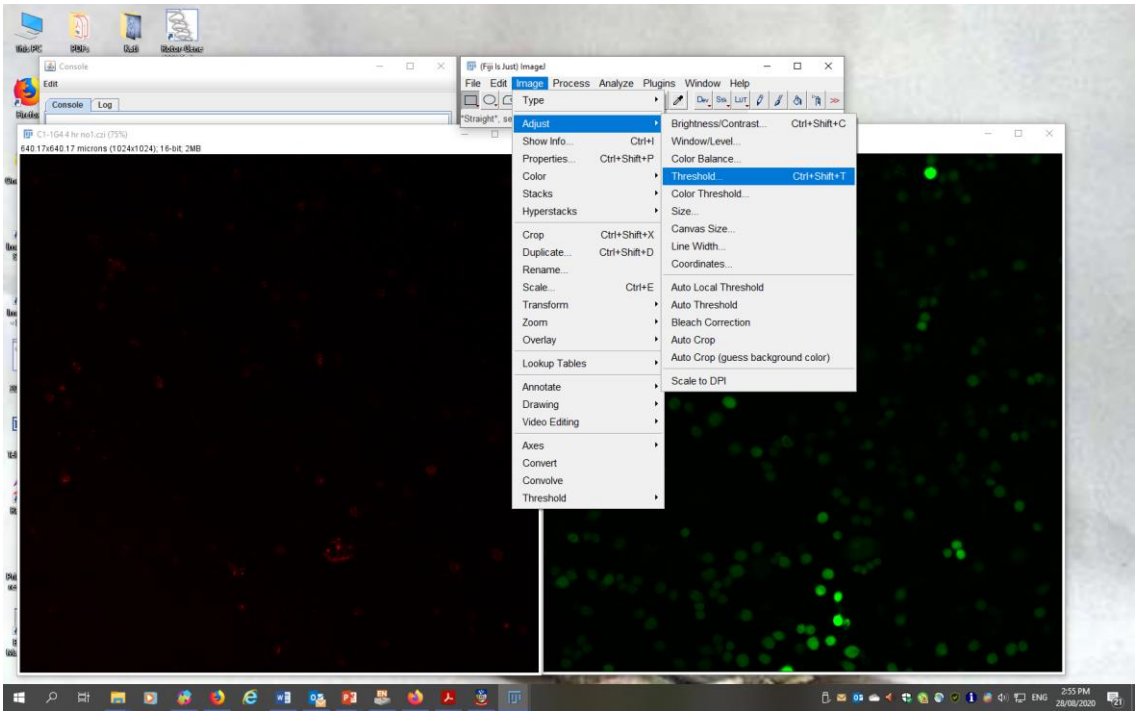

B

1. File: open
2. Image: colour: split channels
3. Select green channel
4. Image: adjust: threshold: Li
5. Analyse: measure
6. Select red channel
7. Image: adjust: threshold: triangle
8. Process: image calculator
9. Select c1 and c2
10. Select operator: AND
11. Tick create new window box and click OK
12. Analyse: measure
13. Efferocytic index = area of red and green mask overlap/area of green mask (Excel calculation)

Figure 2.2 FIJI commands for co-localisation analysis

An example of the FIJI program with a two-colour image split into red and green channels. The tool bar is displaying the commands in drop-down menus for applying a threshold to an image. (B) The full list of FIJI commands for determining the efferocytic index. The final calculation of the efferocytic index from the mask areas was performed in Excel.

2.5 C1Q PURIFICATION

2.5.1 PREPARATION OF SERUM FROM WHOLE BLOOD

Blood was sourced from two patients at The Queen Elizabeth Hospital being treated for either haemochromatosis or polycythaemia vera whose disease was not disclosed. On day 1, 500 µL of 100 mM phenylmethylsulphonyl fluoride (PMSF) (Sigma P7626) was added to 500 mL of citrated blood, to make a final concentration of 0.1 mM and stored overnight at 4°C. On day 2, the blood was centrifuged at 1200 x g for 10 minutes to separate the plasma from the blood cells. The isolated plasma was centrifuged again to remove residual red blood cells. Fresh PMSF was added to a final concentration of 0.1 mM, the plasma was aliquoted, and stored at -80°C.

2.5.2 SATURATED AMMONIUM SULPHATE PRECIPITATION

A saturated ammonium sulphate (BDH 10030) solution (SAS) was chilled to 4°C prior to the precipitation of plasma to achieve 20, 30, 40, and 50% ammonium sulphate saturation. Plasma was thawed and maintained on ice. The plasma was placed into an Erlenmeyer flask held in a water-ice slurry and the SAS added dropwise with continuous mixing. The SAS/plasma mixture was incubated at 4°C for either 4 hours or overnight to allow for complete precipitation of proteins from the plasma. The precipitated proteins were centrifuged from the SAS/plasma mixture at 3,000 x g for 30 minutes. The supernatant was removed from above the pellet and was used for the addition of SAS to achieve the next level of saturation. The pelleted precipitate from each saturation step was resuspended and dissolved in 0.5 volume of 50 mM sodium phosphate (Sigma cat S3264) containing 10 mM Ethylenediaminetetraacetic acid (EDTA) (Sigma E9884) at pH 6.8.

2.5.2.1 Dialysis of saturated ammonium sulphate protein precipitate

Lengths of Snakeskin dialysis tubing (ThermoFisher 68100) were cut at 1 cm of tubing for every 3.7 mLs of dissolved SAS precipitate, including extra length for clipping the tubing shut. The SAS precipitated protein solution was added to the tubing and air pushed out prior to clipping the end shut. The dialysis tubing was then placed in 20 volumes of 50 mM sodium phosphate + 10 mM EDTA at pH 6.8 (1 volume equals the volume of the protein solution). The tubing bag was dialysed with stirring for 2 hours at 4°C. The sodium phosphate dialysate was discarded, fresh dialysate added and then incubated for 2 hours or overnight. The sodium phosphate dialysate was refreshed a further 3 times, for a total of 80 volumes of dialysate buffer exchange. The dialysed sample was recovered, passed through a 0.2 µm filter and stored at 4°C.

2.5.3 ION EXCHANGE CHROMATOGRAPHY

2.5.3.1 Source 30S chromatography on an Akta FPLC

A Tricorn 10/100 column (GE Healthcare 28406415) was packed with cation exchanger Source 30S beads (GE Healthcare 17-1273-01) to a total bed volume of 7.6 mL. Pumps A and B of an Akta fast protein liquid chromatography (FPLC) were equilibrated with deionised water. The flow rate was set to 2 mLs/minute then pump A was primed with 20 mM Tris (Sigma 252859) at pH 8, and pump B with 20 mM Tris + 1 M NaCl at pH 8. The sample was injected onto the column and the flow rate set to 1.5 mL/minute. The column was washed with 5 column volumes of 50 mM Tris prior to running an elution gradient of 0 to 1M NaCl with collection of 2 mL fractions. Upon completion of the gradient, the column was washed with 5 volumes of 20 mM Tris + 1 M NaCl followed by 5 volumes of deionised water. The column was washed with 5 volumes of 20% ethanol and stored at 4°C.

2.5.3.2 Source 30S chromatography by batch method

Eight mLs of the cation exchange resin Source 30S was placed in a 50 mL tube. The resin was equilibrated by washing 3 times with 40 mLs of 50 mM sodium phosphate + 10 mM EDTA at pH 6.8, centrifuging between washes at 200 x g for 5 minutes. Eight mLs of dialysed 30% SAS precipitate was added to the resin and incubated for 30 minutes at room temperature on a rocking platform. The resin was pelleted and the eight mLs of supernatant collected as "flow-through" i.e., the solution containing the non-binding protein species. The 30S beads were washed 3 times with 7.5 mL of 50 mM sodium phosphate buffer + 10 mM EDTA. To elute the bound protein, eight mLs of 50 mM sodium phosphate buffer + 10 mM EDTA + 1 M NaCl was added to the resin beads and incubated for 30 minutes at room temperature on a rocking platform. The 30S beads were pelleted and the eight mLs of supernatant collected as the eluate. The resin was regenerated by washing 3 times with 40 mLs of 50 mM sodium phosphate buffer + 10 mM EDTA + 1M NaCl, followed by 3 washes with 40 mLs of ultrapure water and then 3 washes with 40 mLs of 20% ethanol. The final pellet of resin was resuspended in eight mLs of 20% ethanol and stored at 4°C.

2.5.4 REMOVAL OF IgG WITH PROTEIN A

Four mLs of protein A agarose beads were equilibrated with 50 mM sodium phosphate buffer + 10 mM EDTA at pH 6.8 by washing 3 times with 20 mLs of the buffer, pelleting the resin at 200 x g for 5 minutes between washes. Eight mLs of C1q 30S eluate was mixed with the protein A agarose beads and incubated for 30 minutes at room temperature on a rocking platform. The protein A beads were centrifuged at 200 x g for 5 minutes and the supernatant removed. Bound IgG was eluted by incubation with 8 mLs of 50 mM sodium phosphate + 10 mM EDTA + 100 mM glycine (Sigma G8898) at pH 3 for 30 minutes at room temperature on a rocking platform. The eluted beads were regenerated by washing 3 times with 40 mLs of phosphate/glycine buffer followed by 3 washes with 40 mLs of 50 mM sodium phosphate buffer + 10 mM EDTA. The pelleted beads were resuspended in 4 mLs 50 mM sodium phosphate buffer + 10 mM EDTA + 0.02% NaN_3 and stored at 4°C.

2.5.5 ANALYSIS OF C1Q PURIFICATION BY POLYACRYLAMIDE GEL ELECTROPHORESIS

2.5.5.1 Polyacrylamide gel electrophoresis (PAGE)

Protein samples were prepared for electrophoresis by adding 4x Laemmli loading buffer (Bio-Rad 161-0747) containing 10% β-mercaptoethanol (Sigma M6250) followed by heating to 95°C for 10 minutes. Protein samples were loaded onto 12% Mini-Protean TGX stain-free gel (Bio-Rad 456-8044) along with 10 µL of pre-stained Western C standards (Bio-Rad 1610385). The mini-Protean gel tank (Bio-Rad 1658004) was filled with tris/glycine/sodium dodecyl sulphate (SDS) Buffer (Bio-Rad 1610732) and gels were run at 30 mA for 30 minutes.

2.5.5.2 Coomassie brilliant blue staining

Following PAGE electrophoresis, the gel was placed in a tray and 25 mLs of 0.25% Coomassie Brilliant Blue R250 (Sigma B0149) in 50% methanol (VWR 152506X) + 10% acetic acid was added. The gel was stained for 4 hours at room temperature and then destained through 3 changes of 50% methanol + 10% acetic acid to clear background staining until specific protein bands were clearly visible. The gel was then swelled with 10% acetic acid and imaged on the Bio Rad Gel Doc EZ.

2.6 GENERATION OF MONOCLONAL ANTIBODIES

2.6.1 IMMUNISATION OF MICE

The immunisation of C1qA null mice used a C1q immunogen (Abcam 96363) mixed with AddaVax adjuvant (Invivogen Vac-adx-10) at a 1:1 ratio to form a water-in-oil emulsion. C57Bl/6 C1qA null mutant mice were injected intraperitoneally with 100 µL of the immunogen and boosted twice at three week intervals before the first test bleed was taken by cheek bleed. Antigen doses were tapered down (10, 5, and 2 µg) to engender a stronger immune response (Figure 2.4). Subsequent boosts were performed for two mice with C1q cross-linked by 0.11% glutaraldehyde treatment for 2.5 minutes prior to quenching the reaction with 1M tris-HCl pH 8. Mice selected for fusion were given a final intraperitoneal boost of 1 or 2 µg 3 days prior to sacrificing the mouse and recovering the spleen.

2.6.1.1 Test bleeds for immune sera

Blood sampling was performed by a technician from Laboratory Animal Services at the Helen Mayo animal facility by puncturing the submandibular vein with a 26 g needle. The blood was allowed to clot on ice for 3 hours prior to centrifugation at 12,000 x g for 5 minutes followed by removal of the serum from above the blood cell pellet.

2.6.2 HYBRIDOMA FUSION

On day 1, an immunised mouse was sacrificed by cervical dislocation, the spleen removed and placed in RPMI + penicillin/streptomycin (p/s) medium. Concurrently, the spleen was removed from an unimmunised mouse to provide splenocyte feeder cells for the fused hybridoma cells. An SP2/0-Ag14 culture in mid-log growth (5-8 $x10^5$/mL) with was mixed 1:1 with trypan blue and counted on a Neubauer haemocytometer to confirm a minimum 90% viability. The immunised and non-immune spleens were placed in separate 100 mm petri dishes and the fat and extraneous connective tissue trimmed away. Both spleens were rinsed in RPMI + p/s and homogenised in 10 mLs of RPMI + p/s between the frosted ends of sterile glass microscope slides.

The cell suspensions were transferred into separate 50 mL tubes and the dishes washed twice with 10 mLs of RPMI and pooled with their respective cell suspension in the 50 mL tubes. An aliquot of immune spleen cells and feeder spleen cells were counted 1:1 in Türk's solution (crystal violet in 2% acetic acid) and the number of SP2/0 cells required was calculated based on a 5:1 spleen cell to SP2/0 ratio. The immune spleen cells were washed twice with 50 mLs of RPMI by centrifuging at 200 x g for 5 minutes. The feeder spleen cells were pelleted, resuspended at $1x10^7$ cells/mL and maintained in a 37°C water bath.

The SP2/0 cells were pelleted, resuspended in 50 mLs of RPMI and combined with the washed immunised spleen cell pellet. This combined cell suspension was centrifuged at 200 x g for 5 minutes and the resultant SP2/spleen pellet loosened. Working in a class II biosafety cabinet, the spleen/SP2/0 tube was held in a 500 mL beaker of water at 37°C and 1 mL of 50% polyethylene glycol (PEG) (Sigma 10783641001) was added dropwise with stirring by a pipette over a 1 minute interval to initiate cell:cell fusion. The cells and PEG were stirred for an additional minute, then 2 mLs of RPMI added over 2 minutes and a further 7 mLs over 3 minutes, all with constant stirring by pipette.

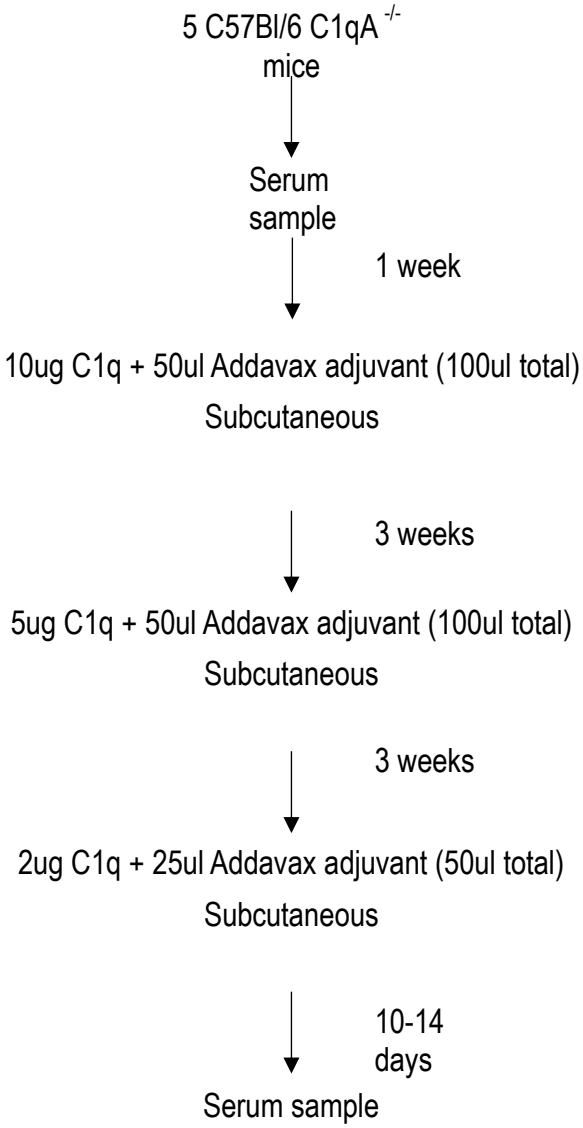

Figure 2.3 Immunisation scheme for C1q -/- mice

C1q knockout mice were immunised with a tapering dose of C1q in Addavax adjuvant. Tapering of the antigen dose was performed to stimulate maturation of B cells secreting higher affinity antibodies. A 10 µg priming dose was followed by boosts of 5 and 2 µg and a serum sample was taken to assess antibody titres.

The fusing cells were centrifuged at 200 x g for 5 minutes and resuspended in fusion medium (RPMI + 20% FCS + 1mM sodium pyruvate (Life Technologies cat11360-070) + 1.1mM oxalacetic acid (Sigma O9504) + 0.5 U/mL insulin (Sigma I5500) + 100 µM hypoxanthine (Sigma H9636) + 10,000 U/mL penicillin, and 10,000 µg/mL streptomycin) to a concentration of $2x10^6$ cells/mL. Feeder spleen cells were centrifuged, resuspended in fusion medium, and added to the fusion suspension. The fusion/feeder cell suspension was plated into 96 well flat-bottom plates at 100 µL/well and incubated at 37°C in 5% CO_2.

On day 2, 100 µL/well of selection medium (fusion medium + 2 µg/mL azaserine (Sigma cat no A1164)) was added to the wells. Every 3-4 days, the cultures were refreshed with 100 µL/well of fusion medium containing 1 µg/mL azaserine until individual cultures covered 20-50% of the well surface, at which point they were ready to screen for the presence of specific antibodies by ELISA. The cultures continued to be fed and screened until all cultures had been screened for antibodies, approximately day 25.

2.6.3 SINGLE CELL CLONING BY LIMITING DILUTION

A mid-log phase hybridoma culture (5-8 x 10^5/mL) was counted and if viability was determined to be >90%, the culture was suitable for single cell cloning. The cells were diluted to 40 cells/mL in cloning medium (fusion medium + 25% SP2/0 spent medium). Five mLs of the cell suspension was placed in a sterile trough and 24 wells were plated at 100 µL/well into a 96-well U-bottom tray (Costar 3799), equivalent to approximately 4 cells per well. Cloning medium (2.5 mLs) was added sequentially to the trough and 24 wells were plated to yield 2, 1 and 0.5 cells/well. 1 µL of the culture being cloned was added to one well as a control for specific antibody secretion in that culture.

2.7 IMMUNOASSAYS

2.7.1 C1q ENZYME-LINKED IMMUNOSORBENT ASSAY (ELISA)

C1q at 1 µg/mL in PBS was coated onto polystyrene 96 well ELISA plates (Nunc 442404), 50 µL/well, for 1 hour at room temperature. The antigen solution was removed and the wells blocked with tris buffered saline (TBS) + 0.2% Tween 20 (Sigma P1379) + 5% skim milk (Black and Gold) at 400 µL/well for 1 hour at room temperature. The blocking solution was removed, hybridoma supernatants were added, 50 µL/well, and incubated for 1 hour at room temperature. The hybridoma supernatants were removed and the plate washed 3 times with 200 µL/well of PBS + 0.1% Tween 20. Rabbit anti-mouse IgG horseradish peroxidase (HRP) (abcam 97046) was added at 1:5,000 in PBS containing 0.1% Tween 20, 50 µL/well, and incubated for 30 minutes at room temperature. The plate was then washed 3 times with 200 µL/well of PBS/Tween. O-phenylenediamine (OPD) (Sigma P9029) was dissolved at 1 mg/mL in 100 mM citrate buffer (Sigma 251275) at pH 6.5 + 0.03% H_2O_2 (Chem Supply HA154). The OPD solution was added to the ELISA plate, 100 µL/well, and incubated at room temperature for 5-10 minutes, until background colour levels began to rise. The reaction was quenched with 100 ul/well of 1 M H_2SO_4 (Sigma 258105) and read at 490 nm.

2.7.2 WESTERN BLOTTING

2.7.2.1 Transfer of PAGE gel

Protein samples were run on a PAGE gel at 30 mA per gel for 30 minutes and the gel placed onto Bio-Rad Trans-Blot Turbo Mini Polyvinylidene Fluoride (PVDF) Transfer pack (Bio-Rad 170-4156). The transfer pack sandwich consisted of a stack of blotting paper, the PVDF membrane, the PAGE gel, and a second stack of blotting paper, with the blotting paper saturated in transfer buffer. The transfer pack-gel sandwich was placed into the Trans Blot Turbo cell, inserted into the Trans Blot Turbo instrument (Bio-Rad 170-4155) and run on the Mixed MW program for 7 minutes. The membrane was removed from the transfer cell and placed in a tray for probing with antibody and subsequent chemiluminescent development.

2.7.2.2 Detection of C1q

The transferred membrane was placed in a small tray containing 25 mL of TBS + 0.2% Tween 20 (TBST) for 3 minutes. The membrane was then blocked with 25 mL of TBST + 5% dry skim milk (TBSTM) on a rocking platform overnight at 4°C. The blocking solution was discarded and the blot inserted into a 50 mL tube. Either mouse anti-human C1qA antibody 9A7 (Abcam 71089) at 1:1000 in 3 mL of TBSTM or a hybridoma supernatant was added to the blot in the tube and incubated for 1 hour at room temperature on a rocking platform. The membrane was removed from the tube and washed in a small tray with 25 mL of TBSTM 3 times for 15 minutes each on a rocking platform at room temperature.

Rabbit anti-mouse IgG HRP at 1:20,000 and StrepTactin-HRP (Bio-Rad 161-0381) at 1:10,000 were added to the blot in 20 mLs of TBSTM and incubated on a rocking platform for 30 minutes at room temperature. The blot was washed in a small tray on a rocking platform with 25 mLs of TBST 3 times for 15 minutes each at room temperature. The chemiluminescent solution was prepared by mixing the two substrate components of the Clarity Western ECL Substrate (Bio-Rad 170-5060) at a 1:1 ratio in a 5 mL tube. The membrane was placed onto the imaging tray and 1 mL of ECL substrate solution was added onto membrane. The membrane was incubated in the dark for 1 minute and then imaged for chemiluminescence with a Fuji LAS4000 for 30sec, 1 minute, and 2 minutes.

2.7.3 IMMUNOHISTOCHEMISTRY ON FFPE SECTIONS

Glass slides containing 5 micron formalin-fixed paraffin-embedded (FFPE) sections were placed on a hotplate at 60°C and incubated for 1 hour. The sections were dewaxed with two 5 minute changes of xylene (Fronine FFJJ028/5) and then rehydrated with 3 changes of 3 minutes each in 100% ethanol (Fronine FFJJ0027P), and single 3 minute changes of each of 90%, 70%, 50% and 0% ethanol in deionised water.

The slides were placed into staining pots with pH 9.0 antigen retrieval solution (Agilent 8004) pre-heated to 95°C and incubated for 20 minutes at 95°C. The slides in the pots were placed at room temperature and allowed to cool for 20 minutes. The slides were removed from the antigen retrieval solution, washed once for 5 minutes in Envision wash buffer (Agilent K8007) and the sections on the slides circled with a pap pen. Endogenous peroxidase block (Agilent S2023) was added for 10 minutes at room temperature and then the slides were washed 3 times for 3 minutes each with wash buffer.

The sections were incubated with mouse anti-human C1qA antibody 9A7 at 1:1000 in antibody diluent (Agilent cat no K8006) or neat hybridoma supernatant for 30 minutes at room temperature. The slides were washed 3 times for 3 minutes each with wash buffer. Anti-mouse Ig HRP polymer conjugate (Agilent cat no DM842) was added to the slides and incubated for 30 minutes at room temperature. The slides were washed 3 times for 3 minutes each with wash buffer.

The 3, 3'-diaminobenzidine (DAB) substrate was prepared by adding 1 drop of chromogen (Agilent K3468) into 1 mL of DAB buffer (Agilent K4065). The DAB substrate was added to the slides and incubated for 10 minutes at room temperature. The DAB substrate was removed, the slides washed in tap water, and then incubated in haematoxylin stain (Agilent CS700) for 5 minutes at room temperature. Slides were washed with tap water and then sections were dehydrated through a series of changes in 90% ethanol for 3 minutes, 2 changes of 100% ethanol for 3 minutes, and 2 changes of xylene for 5 minutes. Slides were mounted with Entellan (Merck 1079610500), cover-slipped and allow to dry before assessment on a Nikon TE200 microscope.

2.7.4 IMMUNOCYTOCHEMISTRY ON RAW 264.7 CELLS

On day 1, a 75 cm^2 culture flask of RAW 264.7 cells in RPMI growth medium were treated with Accutase and scraped into RPMI growth medium. The cells were counted with a Neubauer haemocytometer and plated onto coverslips in 6 well plates at 5 x 10^5 cells/well in 2 mLs RPMI growth medium. On day 2, the growth medium was removed from the cover slips and wells washed once with 2 mLs/well of PBS.

In some experiments, cells were fixed prior to staining. The cells on the coverslips were fixed for 5 minutes with 2 mLs/well of 10% acetic acid in methanol and washed once with 2 mLs of PBS. Fixed or unfixed cells were then incubated with antibody. Two mLs of anti-C1q antibody 9A7 at 1:1000 in fusion medium or neat hybridoma supernatant was added to the wells and incubated for 1 hour at room temperature. The wells were washed 3 times with 2 mLs PBS and then 2 mLs/well of rabbit anti-mouse IgG HRP at 1:1,000 in fusion medium was added to the wells and incubated for 30 minutes at room temperature.

DAB substrate was prepared by adding 1 drop of substrate to 1 mL of substrate buffer and then the wells were washed 3 times with 2 mL/well of PBS. The DAB solution was added at 1 mL/well and incubated for 10 minutes at room temperature. The substrate was removed and the wells washed with deionised water before blotting the cover slips dry and mounting them onto glass slides with 10 µL of 1:1 PBS/glycerol (Sigma G9012). The coverslips were sealed with nail polish then visualised on a Nikon TE200 microscope.

CHAPTER THREE: GENERATION OF C1Q ANTIBODY-SECRETING HYBRIDOMAS FOR PRE-CLINICAL AND THERAPEUTIC APPLICATIONS

3.1 INTRODUCTION

The C1q protein performs an essential role in initiation of the classical complement cascade, the facilitation of phagocytosis of apoptotic cells, and the regulation of immune homeostasis (Lu, 2007), (Lu, 2008), (Thielens, 2017). In addition, C1q has also been linked to increased cancer susceptibility in the mammary gland, with mice genetically deficient in C1q exhibiting reduced cancer development and progression in DMBA and MMTV-PyMT models compared to C1q replete controls (Noor Din, 2017). This lower rate of mammary tumour development in the absence of C1q presents the intriguing possibility that inhibition of C1q activity could lead to a reduction in breast cancer initiation and progression. Monoclonal antibodies are an important class of therapeutic agents in the modern clinic, as such this project was focussed on the generation of monoclonal antibodies capable of neutralising C1q as the first step in development of a potential cancer therapeutic.

Monoclonal antibodies are produced by cells called hybridomas, which are generated by polyethylene glycol-induced fusion of antigen-specific B cells with a malignant B cell line known as a myeloma (Köhler, 1975), (Figure 3.1). This fusion event derives hybridoma cell lines capable of growing indefinitely in culture while producing antibodies of a single specificity, i.e. monoclonal. Selection of fused B-cell:myeloma hybrids from myeloma cells is centred on purine synthesis pathways. Purines are nitrogen-rich bases necessary for DNA replication and cell growth. Unfused myeloma cells are unable to synthesise purines from phosphoribosyl pyrophosphate in the presence of the glutamine amidotransferase inhibitor azaserine. Fused hybridoma cells are able to utilise the purine salvage pathway in the presence of azaserine in which the HPRT enzyme transforms hypoxanthine into the purine precursor inosine monophosphate (Gershfield, 1976). Selection of fused B-cell:myeloma hybrids from unfused B cells is relatively simple as unfused B cells do not proliferate in culture.

In order to generate a monoclonal antibody-secreting hybridoma specific for C1q, a source of abundant, pure, and functionally intact human C1q protein was required for injection into mice to induce an antibody response. C1q is a large protein requiring post-translational assembly, making recombinant production of fully-assembled and functional C1q a difficult proposition. C1q purified from human serum was commercially available, however the cost for a sufficient quantity for immunisation of mice and screening monoclonals was not feasible. Therefore, purification of C1q from human plasma using protein chemistry techniques was attempted. Previous experience with protein chemical purification techniques led to the expectation that isolation of C1q from plasma was a feasible approach. C1q has molecular characteristics which are advantageous from the perspective of purification from a complex mixture of proteins. First, C1q is and highly basic protein at physiological pH with an isoelectric point (pI) of 9.3, which makes it a good candidate for cation exchange chromatography. Cation exchange would be able to exclude a large number of proteins from plasma, making it a good first step in isolation of C1q. C1q also has a large molecular weight at 410-462 kD. Separation with gel filtration chromatography would allow the removal of smaller molecular weight proteins, further enriching the C1q fraction.

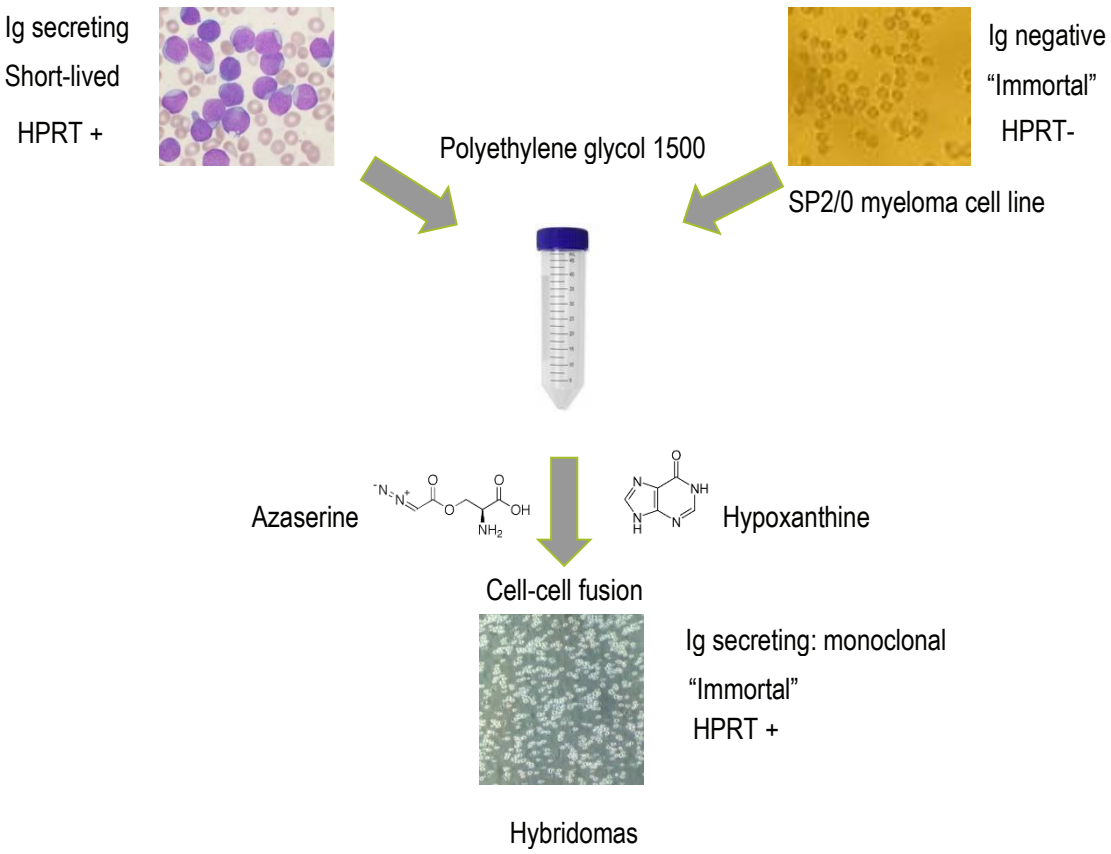

Figure 3.1 Generation of hybridomas by fusion of B cells and myeloma cells

Splenic B cells from C1qA null mutant mice immunised with human C1q were fused to mouse B cell myeloma cells to produce hybridomas. Unfused myeloma cells, which lack the HPRT gene, die in the presence of azaserine, a *de novo* purine pathway antagonist, while the hybridoma cells, which contain the HPRT gene from the B cell the myeloma cell fused with, can utilise hypoxanthine in a salvage pathway to synthesise purines and proliferate in culture. Hybridomas acquire the ability to grow in culture from the myeloma cell while secreting antibodies of a single specificity coded for by the B cell.

However, the multiplicity of proteins contained in plasma was such that the final product obtained from the purification scheme was not sufficiently pure for optimal monoclonal antibody generation. Eventually, a less expensive commercial source of purified human C1q protein was identified and mouse immunisations proceeded using this protein. It is possible this source of pure protein was overlooked prior to commencing C1q isolation from plasma, but by the time this source was found this became a moot point.

This chapter describes the successful generation of four hybridoma cultures secreting anti-C1q antibodies. The steps involved in this process were C1q purification from human blood, immunisation of mice, and hybridoma generation. Also described in this chapter is the development of an ELISA for the purpose of measuring anti-C1q antibody titres in immunised mice and for identifying specific antibody in hybridoma cultures. The anti-C1q monoclonal antibodies generated here will require further testing of C1q binding specificity and their capacity to neutralise C1q activity *in vitro*. If any of these antibodies display C1q neutralising activity, scale-up cultures could be used to generate quantities sufficient for proof-of-concept studies in preclinical and potentially clinical settings.

3.2 RESULTS

3.2.1 ISOLATION OF C1Q FROM HUMAN BLOOD

3.2.1.1 Introduction to approach

The rationale employed for the purification of C1q from human blood took advantage of its distinctive biochemical characteristics (Kozlowski, 2017). C1q is a highly basic protein with a strong positive charge at physiological pH that mediates its binding to negatively charged molecules such as nucleic acids (Gaboriaud, 2012). This positive charge made C1q a good candidate for cation exchange chromatography, which employs a negatively charged resin to bind protein species with a net positive charge. In addition, C1q is a large protein, 420-462 kD, which made gel filtration chromatography a good technique for enriching a C1q-containing protein mixture. Gel filtration beads contain pores that retard the progress of protein molecules able to pass through the pores such that resin porous to proteins 100 of less kD would allow the much larger C1q to pass through the column in the void volume (the volume of the buffer in the column) to be followed by concentration through centrifugal concentration.

A method of monitoring the abundance of C1q during the purification process was required. Native PAGE electrophoresis to monitor the high molecular weight species of intact C1q (410-460 kD) by was impractical due to the highly positive charge of C1q. Non-denaturing and denaturing SDS PAGE electrophoresis breaks C1q into nine disulphide-linked subunits or eighteen individual chains respectively. These bands would run amongst abundant protein species in plasma at approximately 55 or 25-30 kD, rendering this technique also impractical. Detecting the C1qA band at 30 kD by western blotting of denaturing PAGE was chosen as the method for monitoring C1q during the purification process.

With the plasma concentration of C1q in the range of 12-22 mg/dl, C1q is the twentieth most abundant protein in plasma (Figure 3.2), with 10 mL yielding 1.2-2.2 mg of protein (https://www.mayocliniclabs.com/test-catalog/Clinical+and+Interpretive/8851). Therefore, 60-110 mg of protein was expected to be contained within a single unit of 500 mL of venesected blood. However, the actual yield following purification was anticipated to be less as it is not possible to recover 100% of a particular protein from each purification step.

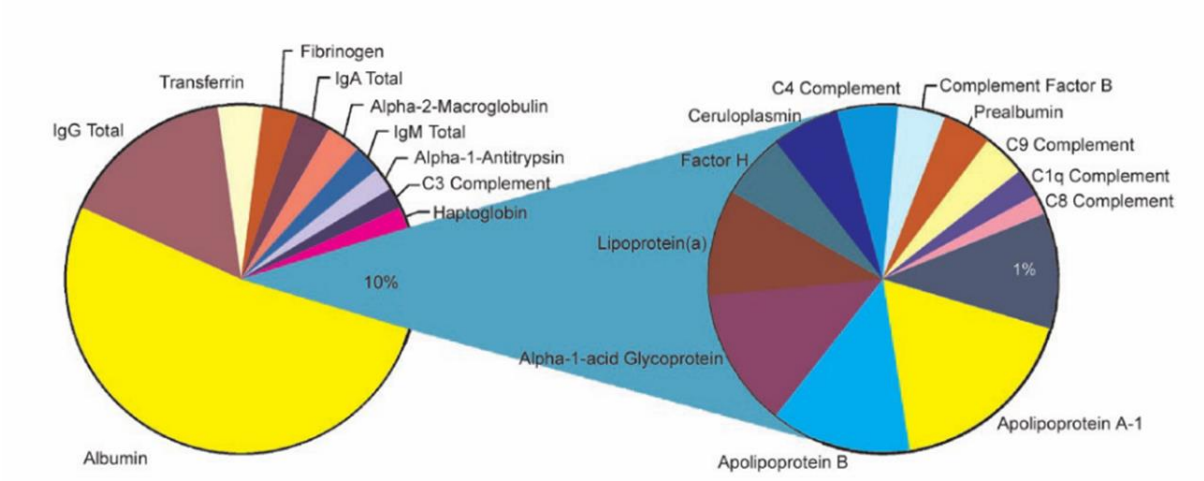

Figure 3.2 Relative abundance of C1q in plasma

A graphical representation of plasma proteins in order of their abundance. The ten most abundant proteins make up 90% of serum proteins with albumin alone comprising approximately 50% of the total protein. C1q represents the twentieth most abundant protein with a relative of prevalence of approximately 0.2% of serum proteins. Figure reproduced from Molecular & Cellular Proteomics, (2003), 2(10):1096-1103.

Isolation of C1q from human blood was a four-step process. First, plasma was isolated from patient blood. The next step involved fractionation of the C1q component in the plasma sample through saturated ammonium sulphate (SAS) precipitation. The C1q-containing fraction was then enriched using 30S cation exchange resin capable of binding strongly positive proteins like C1q. The eluted C1q appeared quite pure on western blot but for a contamination of bands at 50 and 25 kD, likely to be immunoglobulin. Therefore, the fraction was passed over protein A agarose to remove the IgG. Although the results appeared quite positive by western blotting, Coomassie staining showed a lack of purity of the final product.

3.2.1.2 Isolation of plasma from human blood

Blood was sourced from two patients at The Queen Elizabeth Hospital being treated for either haemochromatosis or polycythaemia vera whose disease was not disclosed. These patients undergo venesection of a 500 mL unit of blood three to five times a year to manage their symptoms. Polycythaemia vera is a myeloproliferative disease that features an increased haematocrit, increased white cell counts – particularly granulocytes — and increased platelet(https://www.msdmanuals.com/professional/hematology-and-oncology/myeloproliferative-disorders/polycythemia-vera?query=polycythemia%20vera#v974284). Hemochromatosis is an iron storage disease caused by increased iron uptake by the gut and iron accumulation in (https://www.msdmanuals.com/professional/hematology-and-oncology/iron-overload/hereditary-hemochromatosis?query=haemochromatosis#v976425). C1q is synthesised by monocytes, macrophages, mast cells and dendritic cells (van Schaarenburg, 2016), cells not associated with either disease process. While polycythaemia increases white cell counts, there is no clinical correlation with C1q levels in either disease. Therefore, 2 x 500 mL units were collected from these patients for C1q purification.

Following the method of Kojouharova, isolation of serum from human blood was attempted. Blood was collected into 4% sodium citrate as anticoagulant (Kojouharova, 2014). Citrate chelates the ionic calcium necessary for thrombin to cleave fibrinogen and produce a clot (Dahlbäck, 2000). Addition of calcium to citrated plasma to a final concentration of 20 mM restored the thrombogenic capacity of the plasma and resulted in a fibrin clot. Once the clot formed, the serum was filtered through muslin cheesecloth thereby removing the clot (Kojouharova, 2014). However, there were persistent difficulties with the serum clotting following calcium addition, and this led to a shift to the use of plasma as starting material for the isolation of C1q.

3.2.1.3 Fractionation of plasma with saturated ammonium sulphate

The first step of C1q purification was fractionation of plasma using saturated ammonium sulphate (SAS) in a process known as “salting out”. Proteins precipitate in the presence of ammonium sulphate based on their relative solubility; the more soluble a protein is, the greater the concentration of ammonium sulphate required to precipitate it. As progressively greater amounts of ammonium sulphate are added to a protein solution, more water molecules interact with the ammonium sulphate salt rather than the proteins in solution. When the protein loses contact with the water solute, it self-aggregates and precipitates or “salts out”. This is an effective method for removing albumin, an abundant protein in plasma which remains soluble in high levels of ammonium sulphate.

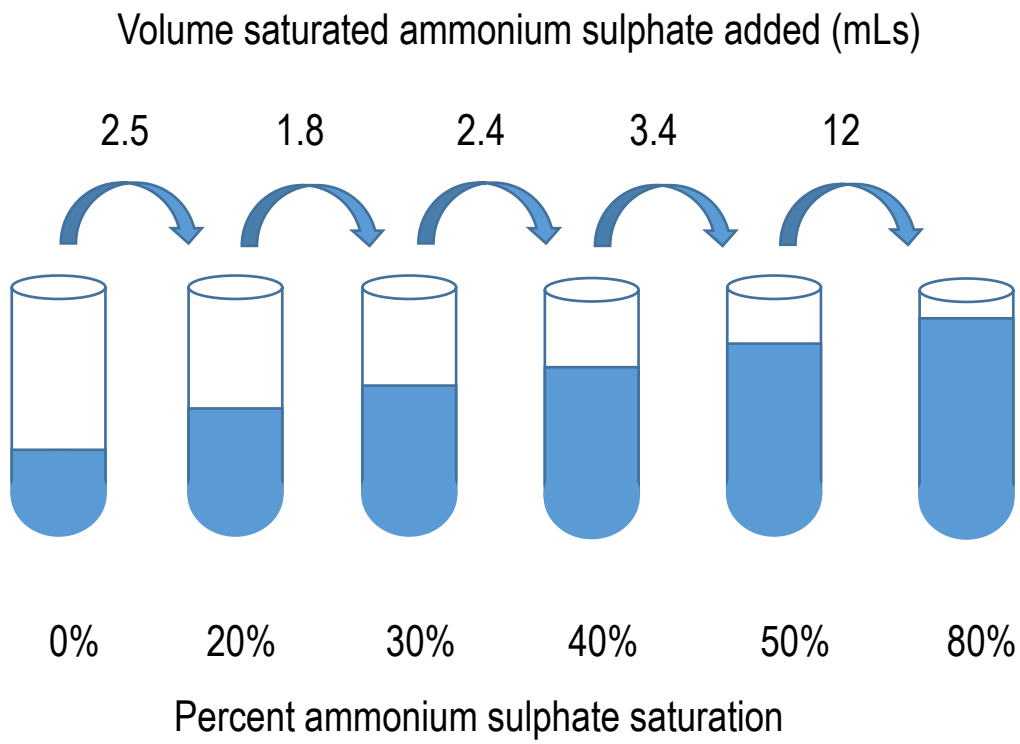

Figure 3.3 Stepwise addition of SAS to achieve increasing levels of saturation

Illustrating the sequential addition of saturated ammonium sulphate into plasma to produce a stepwise precipitation of proteins based on their relative solubility. The saturation levels achieved were 20, 30, 40, 50, and 80% ammonium sulphate, with precipitated proteins pelleted by centrifugation between each addition of ammonium sulphate solution.

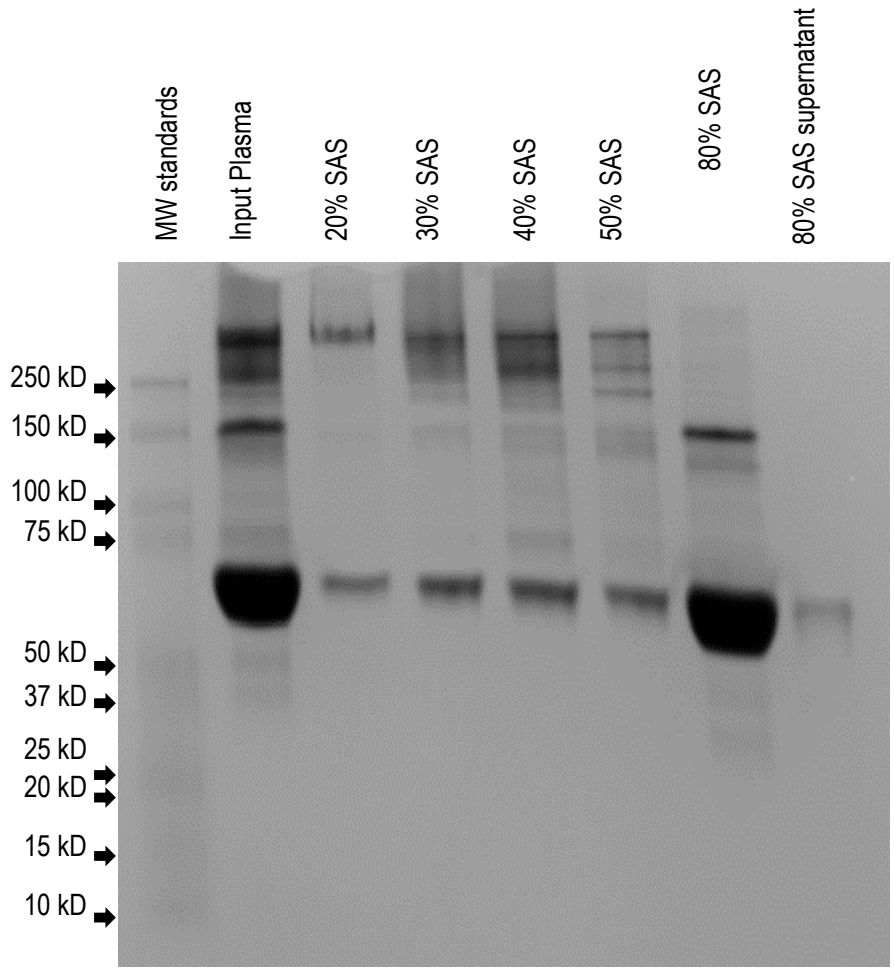

Figure 3.4 Coomassie blue staining of a non-reducing polyacrylamide gel loaded with saturated ammonium sulphate (SAS) fractionated plasma

A 12% PAGE gel of 10 µL of each SAS fraction was run under non-reducing conditions and stained with Coomassie brilliant blue R250 to assess the protein content of the fractions. Most of the larger proteins precipitate between 20 and 50% saturation while the abundant protein albumin (68 kD) precipitates at 80% saturation, leaving the other fractions relatively albumin free.

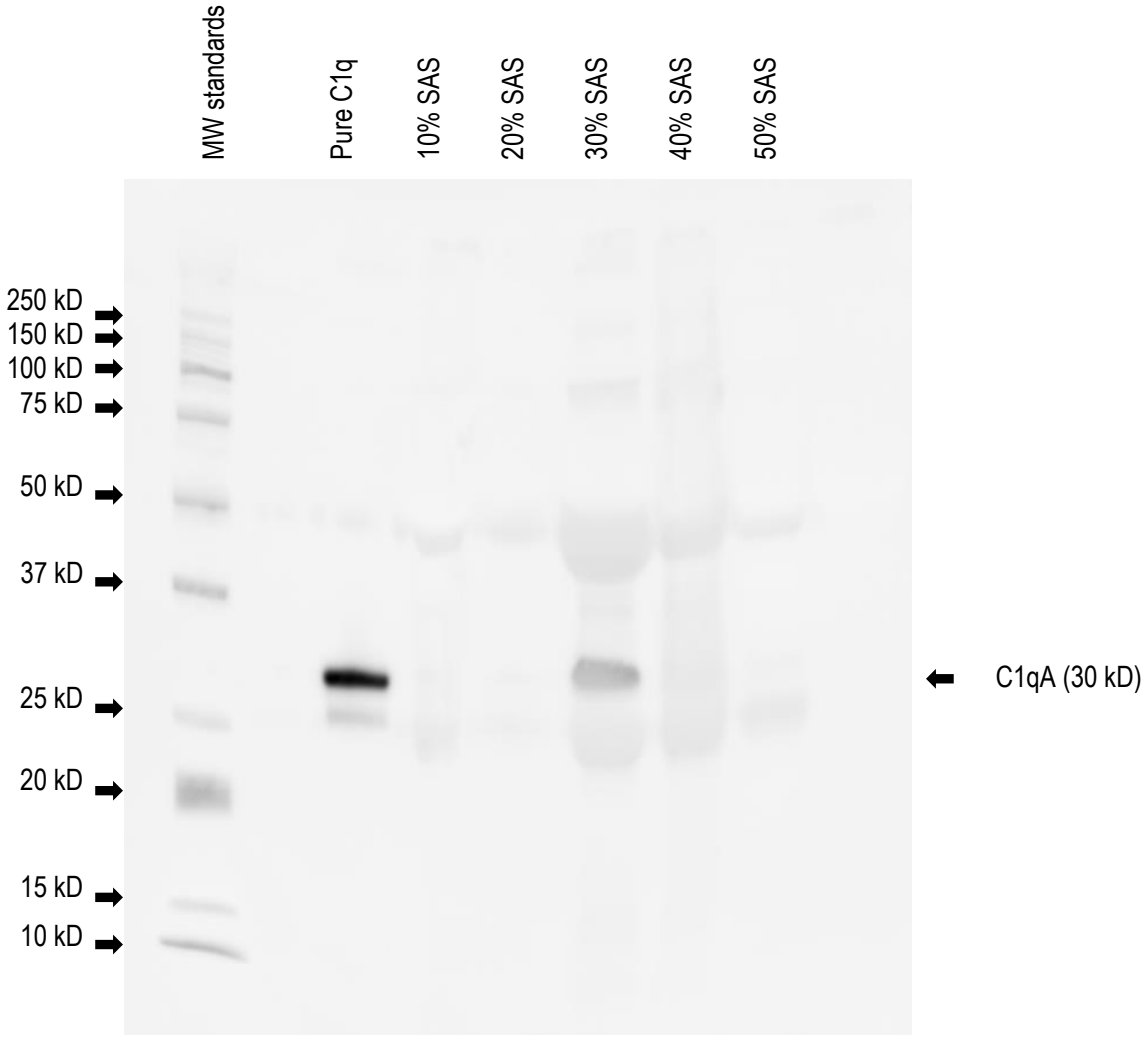

Figure 3.5 Western blotting for identification of C1q in SAS fractions

Western blot of 10 µL of the SAS fractions was run on a 12% reducing PAGE gel, probed with Abcam anti-C1qA antibody 9A7 and developed with chemiluminescent substrate. C1qA was observed at 30 kD in the Abcam pure C1q sample, a band also present exclusively in the 30% fraction. The rabbit anti-mouse IgG HRP antibody showed some non-specific binding to other proteins in the sample.

3.2.1.4 Enrichment of C1q with the Source 30S cation exchange resin

Having established the 30% SAS fraction of the plasma sample was the sole fraction to contain C1q, the next step was enrichment of the sample by ion exchange chromatography on the strong cation exchanger Source 30S. An intermediate pore size of 30 microns was used to enable a high buffer flow rate suitable for use on a fast protein liquid chromatography (FPLC) apparatus.

Following dialysis of the 30% fraction to remove the ammonium sulphate, the sample was ultracentrifuged to remove insoluble particulate matter and loaded onto the 30S column on an Akta FLPC located at Proteomics Facility at Flinders University. Elution of the protein employed a 0-1000 mM sodium chloride gradient. Anticipating that the majority of C1q would elute at 200 mM sodium chloride (Kojouharova, 2014) it was surprising that no material eluted from the column. Subsequent attempts at enrichment did not yield any better results, so it was decided to batch purify on the 30S resin.

Batch purification involves conducting the incubations in a tube with sequential washes matching the volumes and sodium chloride concentrations that had been employed for FPLC, with centrifugation to pellet the resin between washes and elution steps. In this procedure, material bound to the resin and eluted with stepwise increasing sodium chloride concentration, providing an enrichment of the C1q protein. Enrichment for C1q was assessed by western blot using the 9A7 anti-C1q antibody. Comparing two buffer systems, C1q was detected at 30 kD in the 500-1000 mM range of sodium chloride elution when HEPES buffer was used, but also carried over non-specific bands at 50 and 25 kD on the western blot, compatible with the heavy and light chains of immunoglobulin respectively (Figure 3.6). In comparison, the phosphate buffer system eluted over a wider range of sodium chloride concentrations but yielded a much purer product.

3.2.1.5 Removal of contaminating immunoglobulin from the C1q fraction using protein A agarose

Enrichment of C1q using the 30S ion exchange resin with HEPES buffer yielded contaminating bands of 50 and 25 kD in size that were likely to be immunoglobulins. It was anticipated that their removal would result in a C1q preparation pure enough for the immunisation of mice. Immunoglobulin G (IgG) isotypes can be readily removed from a protein preparation using protein A coupled to agarose beads. Protein A is a Staphylococcus aureus virulence factor that binds immunoglobulins via the CH3 region of the heavy chain (Keener, 2017). Protein A binds well to most mouse immunoglobulin G isotypes, slightly less to immunoglobulin G1. The 30S eluate was then incubated with protein A agarose beads, washed and eluted with 100 mM glycine at pH 3 followed by western blot detection of C1q (Figure 3.7). The protein A flow-through showed a promising amount of C1q had been successfully recovered with little immunoglobulin contamination.

To investigate the purity of the protein A flow-through, the purification samples were run on reducing PAGE gel and stained with Coomassie brilliant blue. Unfortunately, the Coomassie staining revealed a number of proteins that had not been removed from the plasma (Figure 3.8). The 30% SAS eluate contained a decreased amount of proteins, particularly albumin; however the protein A flow-through contained many contaminating proteins in addition to C1q observed at 30 kD. At this point, a commercial source of C1q was purchased for the immunisation of mice and downstream screening of monoclonal antibodies.

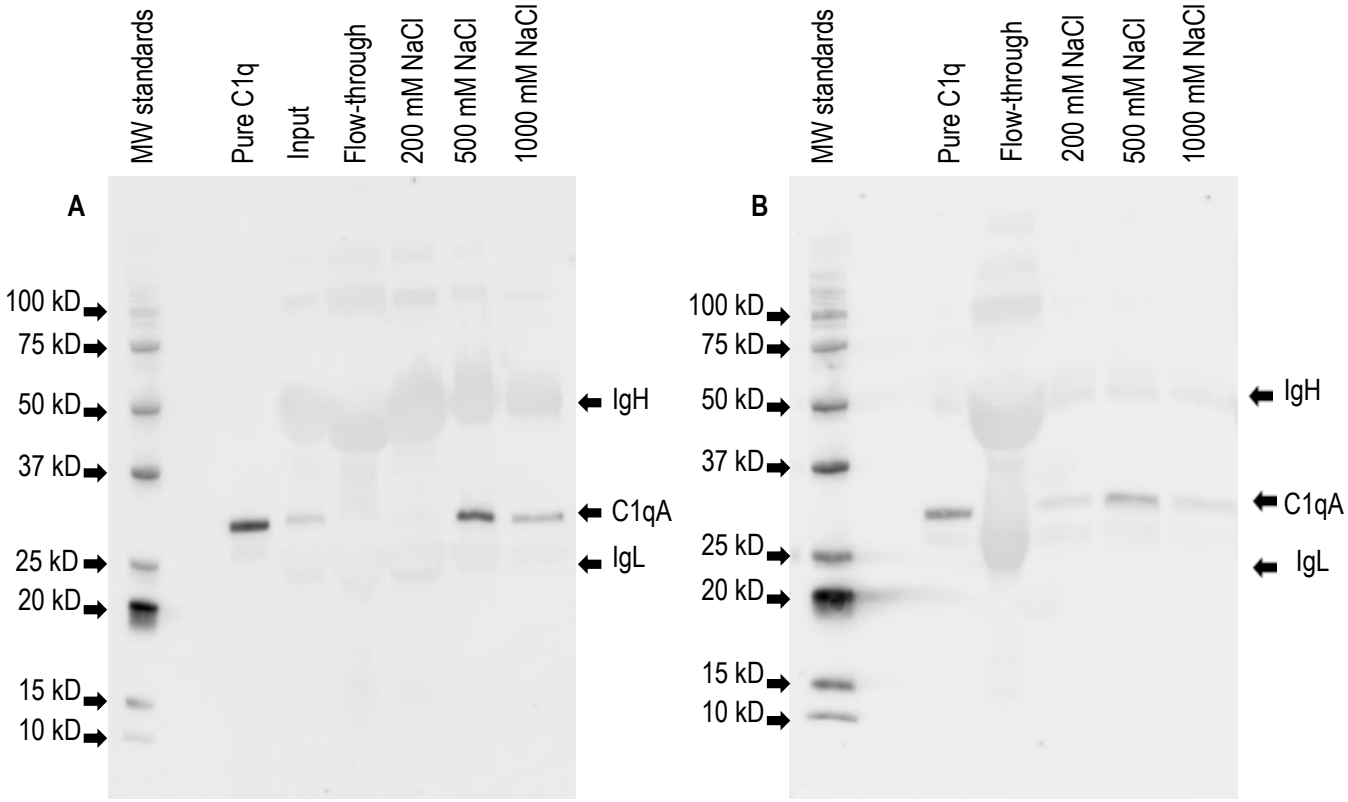

Figure 3.6 Enrichment of 30% SAS fraction by ion exchange chromatography using HEPES or phosphate buffers

Western blots of the C1q-containing 30% SAS fraction probed with 9A7 anti-C1qA antibody. Two concurrent batch separations were sequentially eluted with 200, 500, and 1000 mM sodium chloride (NaCl) in either 20 mM HEPES buffer (A) or 50 mM phosphate buffer (B). The elution profile of C1q in the phosphate buffer was spread over all three salt concentrations, compared with the sharper elution at 500 and 1000 mM NaCl for the HEPES buffer. However, more presumably immunoglobulin (IgH and IgL) contamination in the HEPES buffer elution was observed.

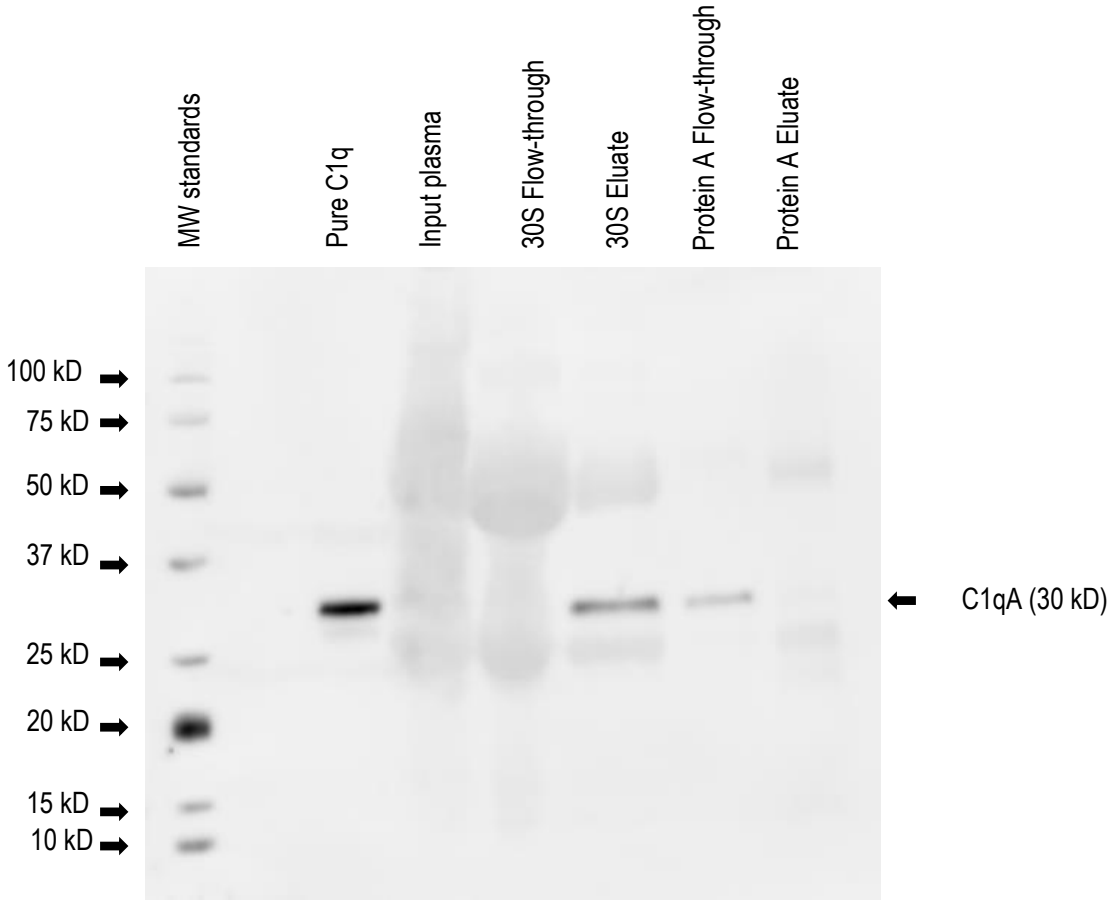

Figure 3.7 Western blot of the steps involved in purification of C1q from plasma

Western blot of C1q purified from plasma and probed with 9A7 anti-C1qA antibody. C1q was precipitated from plasma with 30% ammonium sulphate saturation, bound to Source 30S cation exchange resin and eluted with HEPES buffer + 1000 mM sodium chloride. To remove contaminating immunoglobulin, the protein eluted from the 30S resin was passed onto protein A agarose beads. The C1q-containing fraction was collected as non-adherent flow-through and the immunoglobulin was eluted with 100 mM glycine at pH 3. The C1q is present as a single band in the protein A flow-through.

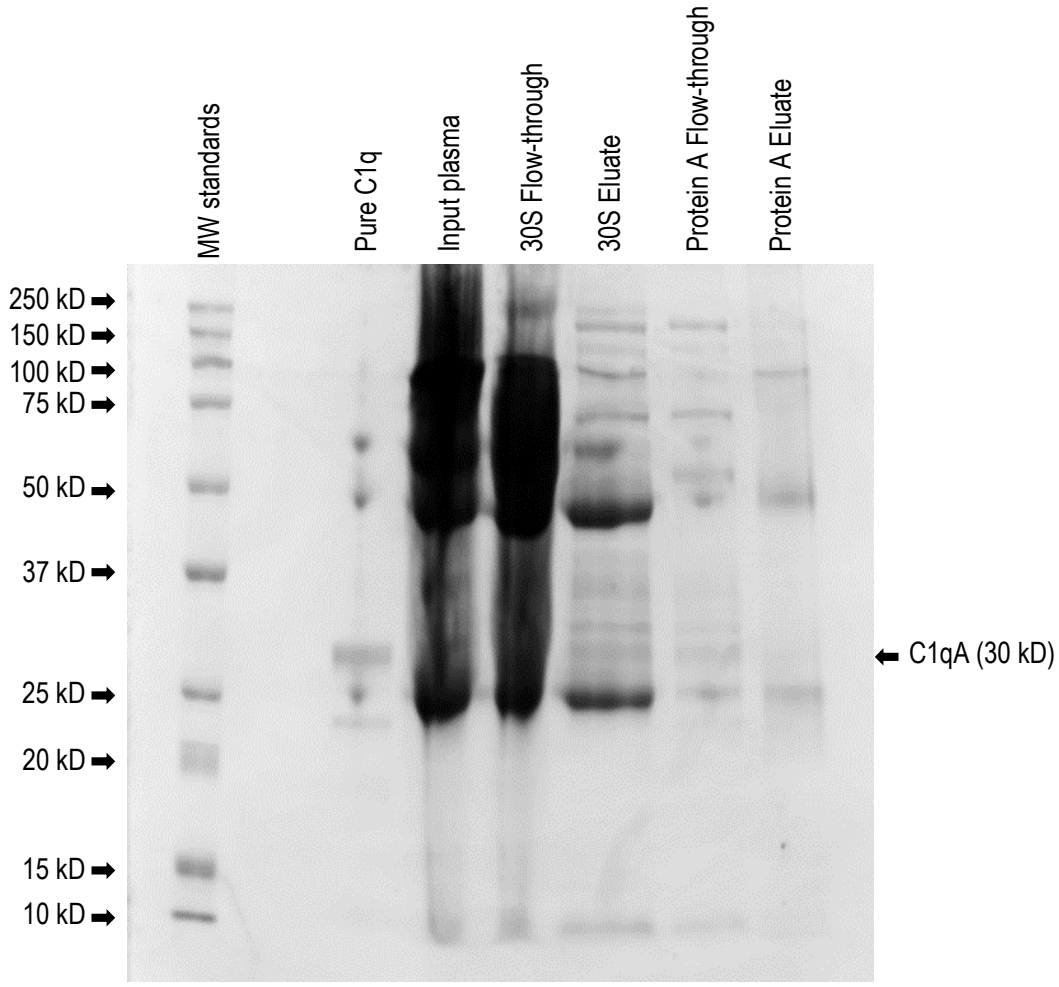

Figure 3.8 Coomassie blue-stained reducing polyacrylamide gel of the steps involved in enrichment of C1q from plasma

Reducing 12% PAGE gel of the full C1q purification scheme followed by Coomassie brilliant blue R250 staining. The purification consisted of passing the 30% SAS plasma fraction over a Source 30S cation exchange column followed by the removal of immunoglobulin with protein A agarose. The plasma input and 30S flow-through is indicative of the high protein load at the start of the process. C1q was a small portion of the proteins not adherent to protein A, indicating the purification scheme was not effective.

3.2.2 DEVELOPMENT OF AN ENZYME-LINKED IMMUNOSORBENT ASSAY FOR THE DETECTION OF C1q SPECIFIC ANTIBODIES

Prior to immunisation of mice and hybridoma generation, it was necessary to develop an enzyme-linked immunosorbent assay (ELISA) to assess antibody titres in the immunised mice and screen for anti-C1q antibodies produced by hybridomas. ELISA is a format capable of screening large numbers of samples in a timely fashion, making it an ideal assay for hybridoma screening.

In order to obtain a source of C1q specific antibodies with which to develop the ELISA, five mice were immunised with pure C1q and serum obtained for testing according to the immunisation schedule shown in Figure 3.9. Pure C1q was coated onto polystyrene plates at 10 µg/mL. The test serum was titrated and applied with the commercial 9A7 antibody included in duplicate wells at 10 µg/mL as positive control. Following washing, rabbit anti-mouse IgG HRP secondary antibody and anti-C1q binding assessed by the HRP substrate 3,3',5,5'-tetramethylbenzidine (TMB). The 9A7 positive control showed an OD of 0.315. Signal strength was low but ran at twice background level from a non-immunised mouse and indicated all immunised mice were responding well to the C1q immunogen (Figure 3.10).

The ELISA appeared to have been adequately validated and ready for screening hybridomas; however when the first wells of a hybridoma fusion were tested, all the wells displayed positive signals to the same degree. Since C1q can bind to antibody through the CH2 region, it seemed likely that either the primary and/or the secondary antibody were binding C1q via this mechanism, more likely the latter since not all hybridoma wells contain antibody. A titration of the concentration of C1q used to coat the ELISA plate showed a two-fold decrease in background with each doubling dilution. The optimal concentration for ELISA coating was determined to be a concentration of 1 µg/mL of C1q, adequate for showing antibody binding to C1q without allowing secondary antibody binding via its heavy chain (data not shown).

The low signal strength seen with the TMB substrate when screening the hybridomas led to the substitution of o-phenylenediamine (OPD) for TMB. Ordinarily, TMB is a more sensitive substrate than OPD, but in this circumstance this was not the case. A repeat of the titration of the immune mouse sera directly compared TMB with OPD, showing OPD to be superior to TMB in signal strength and the change to OPD was made. (Figure 3.11). The 9A7 positive control showed an OD of 1.15.

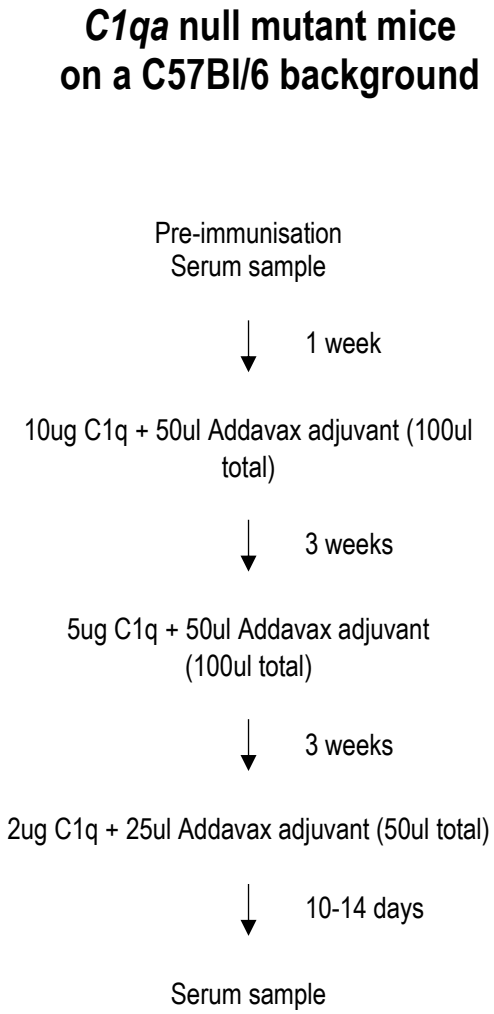

Figure 3.9 Immunisation schedule for C1q null mice

C1qA null mice were immunised with a tapering dose of C1q in Addavax adjuvant, a squalene-based oil-in water emulsion. A priming dose of 10 µg was followed by boosts of 5 and 2 µg prior to taking a serum sample. The interval between boosts was three weeks and serum was sampled at ten to fourteen days post boost.

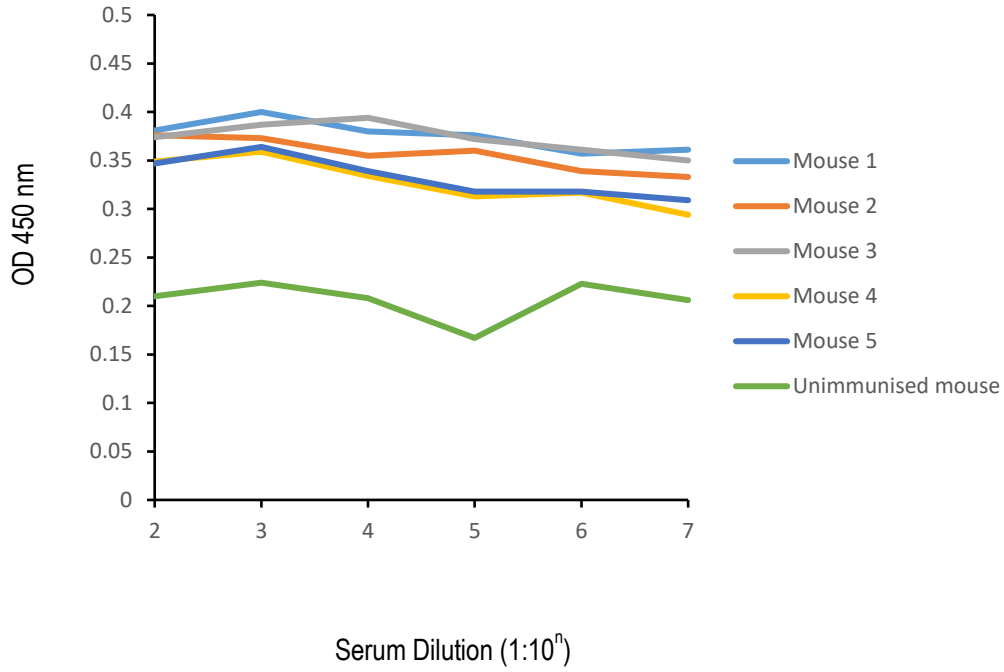

Figure 3.10 Test ELISA to measure C1q antibody titres in serum from immunised mice

C1q was coated onto polystyrene wells at 10 µg/mL for 1 hour and then blocked with 5% dry milk in tris buffered saline. Serum from immunised mice was titrated 10-fold in PBS and incubated for 1 hour followed by washing three times with PBS + 0.01% Tween 20. Rabbit anti-mouse IgG HRP at 1:1000 was incubated for thirty minutes followed by final washing. 3, 3', 5 5'-tetramethylbenzidine substrate at 20 µg/mL was incubated for five minutes, quenched with 1M sulphuric acid and read at 450 nm. Signal strength was twice background level and indicated a good immune response in all mice.

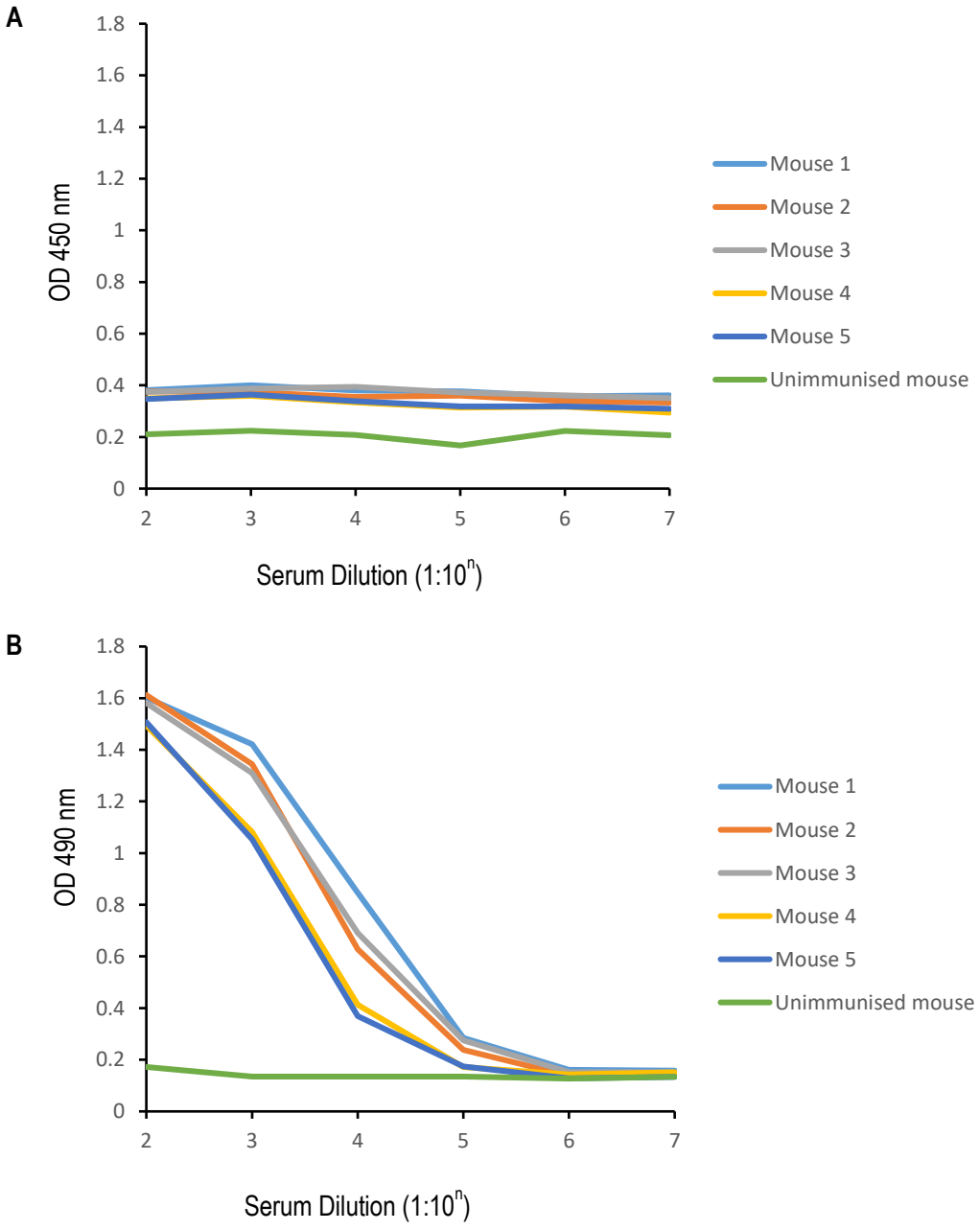

Figure 3.11 Comparison of TMB and OPD substrates in C1q antibody ELISA

Mouse sera were titrated on ELISA plate coated with 1 µg/mL C1q, probed with rabbit anti-mouse IgG HRP and then developed with either TMB (A) or OPD (B) substrate. Peak signal intensity at 1:100 dilution yielded approximately a 4-fold increase in signal with OPD compared to TMB. This changed the assumed $1:10^7$ titre seen with TMB to a lower $1:10^4$ titre with OPD substrate.

3.2.3 IMMUNISATION OF MICE WITH HUMAN C1q

Immunisation involves the introduction of a foreign antigen into an animal or human that is then recognised by the adaptive immune system through antigen presentation. B cell and helper T cells are stimulated leading to lymph node germinal centre formation. Subsequent exposure to the antigen will lead to immunoglobulin class switching and affinity maturation(Mishra, 2018), (Palm, 2019).

The degree of sequence identity of the immunogen to host proteins dictates the ease or difficulty of generating an antibody response (Simkins, 2011). Human C1qA has 71% sequence identity to the mouse protein at the amino acid level, human C1qB has 79% sequence identity with mouse C1qB, and human C1qC has 74% sequence identity with mouse C1qC (BLAST search: blast.ncbi.nlm.nih.gov). Use of a mouse line that was null for C1qA due to targeted genetic mutation would produce an increased sequence disparity, aiding in the formation of a C1q specific immune response and increase the likelihood of generating antibodies to C1qA chain.

Adjuvants are added to immunogens to increase immune stimulation and antigen persistence, resulting in a more vigorous immune response. Squalene-based oil-in-water adjuvants are effective and easily prepared. The adjuvant Addavax used for this project is similar to the MF59 adjuvant in current use for the human influenza vaccine (Calabro, 2013). C1q protein was injected into C1qA null mutant mice with tapering down of the dose from 10 to 2 µg to promote affinity maturation, thereby selecting for higher affinity B cell clones stimulated at lower antigen concentrations (Figure 3.9).

The five mice immunised with pure human C1q used to develop the ELISA presented in Section 3.2.2 were also used as a source of splenocytes for fusion with myeloma cells. Serum obtained from each mouse was assessed for C1q antibody titre using the custom-designed ELISA and the mouse with the highest titre used as the splenocyte donor for hybridoma fusion. Optimally, a minimum antibody titre of 1:10,000 in serum was required before mouse splenocytes were used for hybridoma generation.

3.2.4 PRODUCTION OF MOUSE MONOCLONAL ANTIBODIES TO HUMAN C1q

3.2.4.1 Introduction to approach

C1qA null mutant mice were immunised according to Figure 3.9 and antibody titres were assessed to select the best candidate mouse for hybridoma fusion. Immune splenocytes were induced to fuse to SP2/0-Ag14 myeloma cells in the presence of 50% polyethylene glycol 1500 and were plated into 96 well plates laid with normal splenocyte feeder cells (Fendly, 1987). Hypoxanthine/azaserine selection was added on the following day and the first hybridomas screened on day 10.

In summary, three fusion experiments were conducted, and modifications to the immunisation and boost protocol were made throughout the three fusions to maximise hybridoma generation. Fusions yielded a moderate number of wells but the fusion efficiencies were good indicating robust fusion. That the fusions did not produce a larger number of plated wells is likely due to sequence similarity between human and mouse C1q. Immunisations and attendant titres are represented in Table 3.1. Over the course of the three experiments, a total of 2,776 wells were plated that ultimately generated four C1q antibody-secreting hybridoma cell lines (Table 3.2). These cultures were screened again by ELISA to confirm stable antibody production and stored in liquid nitrogen for future studies. The resulting hybridomas were named “BHI” in recognition of the Basil Hetzel Institute where they were created, followed by the fusion experiment number and well number of the 96 well plate in which they were derived.

	Mouse 1	Mouse 2	Mouse 3
Boost	1 µg	1 µg	1 µg
Titre	1:10,000	1:10,000	1:10,000
	Fusion BHI1		
Boost		5 µg	5 µg
Titre		1:100,000	1:10,000
Boost		2.5 µg	2.5 µg
		Fusion BHI2	
Boost			2 µg
Titre			1:10,000
Boost			5 µg 2 µg
			Fusion BHI3

Table 3.1 Antigen boosts and antibody titres for mice selected for fusion

Following on from the immunisation schedule presented in Figure 3.9, mice were boosted with doses of C1q protein in Addavax adjuvant and antibody titres determined at various intervals. ELISAs were performed prior to hybridoma fusion to select the mouse responding with the highest antibody titre.

Fusion	Wells plated	Wells growing	Wells positive	Fusion efficiency	Specific efficiency
BHI #1	816	505	2 (BHI1-1G4 and BHI1-4D3)	61.9%	0.4%
BHI #2	904	785	0	86.8%	0%
BHI #3	1,056	727	2 (BHI3-3F6 and BHI3-8B9)	68.8%	0.3%
TOTAL	2,776	2,017	4	72.6%	0.2%

Table 3.2 Summary of the three BHI fusions for identifying anti-C1q hybridomas

The BHI fusions were quite successful, producing a good number of viable hybridomas for screening and, with the exception of BHI2, producing C1q-specific antibodies. The fusion efficiency refers to the proportion of wells containing growing hybridoma cultures while the specific efficiency indicates the proportion of growing wells that were positive for binding C1q in ELISA.

3.2.4.2 Generation of anti-C1q hybridomas - BHI fusion #1

For BHI fusion #1, splenocytes from Mouse 1 were used. Mouse 1 was selected from the data obtained with TMB substrate (Figure 3.10) and was later determined to have an antibody titre of 1:10,000, the highest titre of the five mice immunised (Figure 3.11B). Prior to harvesting the spleen, Mouse 1 was boosted with 1 µg of C1q four days prior to fusion. This first hybridoma fusion resulted in 816 plated cell cultures of which 505 produced growing hybridomas, representing a fusion efficiency of 61.9%. Of the 505 growing wells, 3 hybridomas were identified as binding to C1q by ELISA and selected for single-cell cloning. Two of These hybrids yielded stable cell lines positive for anti-C1q antibody secretion as determined by ELISA. The two monoclonal lines derived were named BHI1-1G4 and BHI1-4D3.

3.2.4.3 Generation of anti-C1q hybridomas - BHI fusion #2

Although an antibody titre of 1:10,000 can produce hybridomas, the immunisation protocol employed was anticipated to result in titres of 1:100,000 to 1:1,000,000 (Halenbeck, 1989). The lower titres produced by the immunisation protocol raised concerns that the tissues of the C1qA null mutant mice could be sequestering the C1q immunogen in the complement cascade, efferocytosis mechanisms or other immune regulatory roles. *C1qA* null mice lack the capacity to assemble a functional C1q molecule and, as such, cannot initiate classical complement cascade, promote efferocytosis or modulate the maturation and function of various leukocytes. It is theoretically possible for human C1q to fill the niche filled by mouse C1q and thereby reduce its availability to the immune system to stimulate antibody formation. Mouse C1q is known to function with human C1s and C1r in the haemolysis of sheep red blood cells (Seino, 1984). While it is not known if human C1q could fill all the functions of C1q in the mouse, such a study would be of interest but falls beyond the scope of this project. Such sequestration would have the potential of lowering the availability of C1q for antigen presentation and the stimulation of C1q-specific B cells.

In an attempt to increase antibody titres, mice were boosted with a larger quantity of C1q, either in its pure native form, or cross-linked with glutaraldehyde. Glutaraldehyde is a homotypic cross-linking agent that reacts with primary amines and the side chains of lysine and arginine (Migneault, 2004). Cross-linking C1q with glutaraldehyde would render C1q incapable of being biologically active in the complement cascade or in efferocytosis, and yet still be suitable for antigen presentation and antibody production. Using cross-linked C1q as coating antigen in ELISA resulted in the complete loss of antibody binding, likely as a result of epitope destruction and/or a decrease in C1q solubility (data not shown). Cross-linked C1q became turbid and a precipitate settled out in the tube, showing visible evidence of decreased solubility.

Antibody titres were assessed in two mice boosted with 5 µg of native C1q (Mouse 2 and 3) and two with 5 µg of cross-linked C1q (Mouse 4 and 5). Comparison of antibody titres in each mouse demonstrated that cross-linked antigen was not superior to native C1q in boosting the immune response (Figure 3.12). The boosting did however increase the serum titre of Mouse 2 to 1:100,000, the desired level for fusion. This indicated that, regardless of C1q potentially being absorbed by the complement system, there was still sufficient antigen processed by antigen-presenting and B cells to stimulate an immune response.
Mouse 2 was the spleen cell donor for BHI fusion #2. The fusion resulted in 904 cultures being plated in 96 well plates and, of these wells, 785 produced growing hybrids for a fusion efficiency of 86.8%. Unfortunately, none of the cultures screened produced antibody specific for C1q. This was a disappointing result; however, fusion events occur randomly and at low frequency, therefore not all fusion experiments can be expected to produce antibody-secreting hybridomas.

3.2.4.4 Generation of anti-C1q hybridomas - BHI fusion #3

The three remaining mice were boosted again to increase antibody titres in anticipation of another fusion. Two mice (Mouse 3 and 4) were boosted with native C1q and one (Mouse 5) received cross-linked C1q. The titres of both mice immunised with native C1q increased to a greater extent than the mouse receiving cross-linked antigen, showing a slight superiority of native protein in improving the immune response in this particular case (Figure 3.12), (Figure 3.13).

Mouse 3 was used as the spleen donor for BHI fusion #3 with a resultant 1,056 cultures plated to 96 well plates. This was the largest fusion of the three performed and larger fusions tend to produce more hybridomas in general and more antigen-specific clones. During PEG-induced fusion, myeloma cells fuse randomly to B cells; therefore, for mice with similar antibody titres, more B cells equate to more fusion events and more antigen-specific hybridomas. In this case, the 1,056 wells plated produced 727 growing hybrids, representing a fusion efficiency of 68.8%. Upon ELISA screening, five C1q antibody-secreting hybridomas were identified and selected for single-cell cloning. Of these 5 candidates, 2 produced stable cultures secreting anti-C1q antibodies and were named BHI3-3F6 and BHI3-8B9.

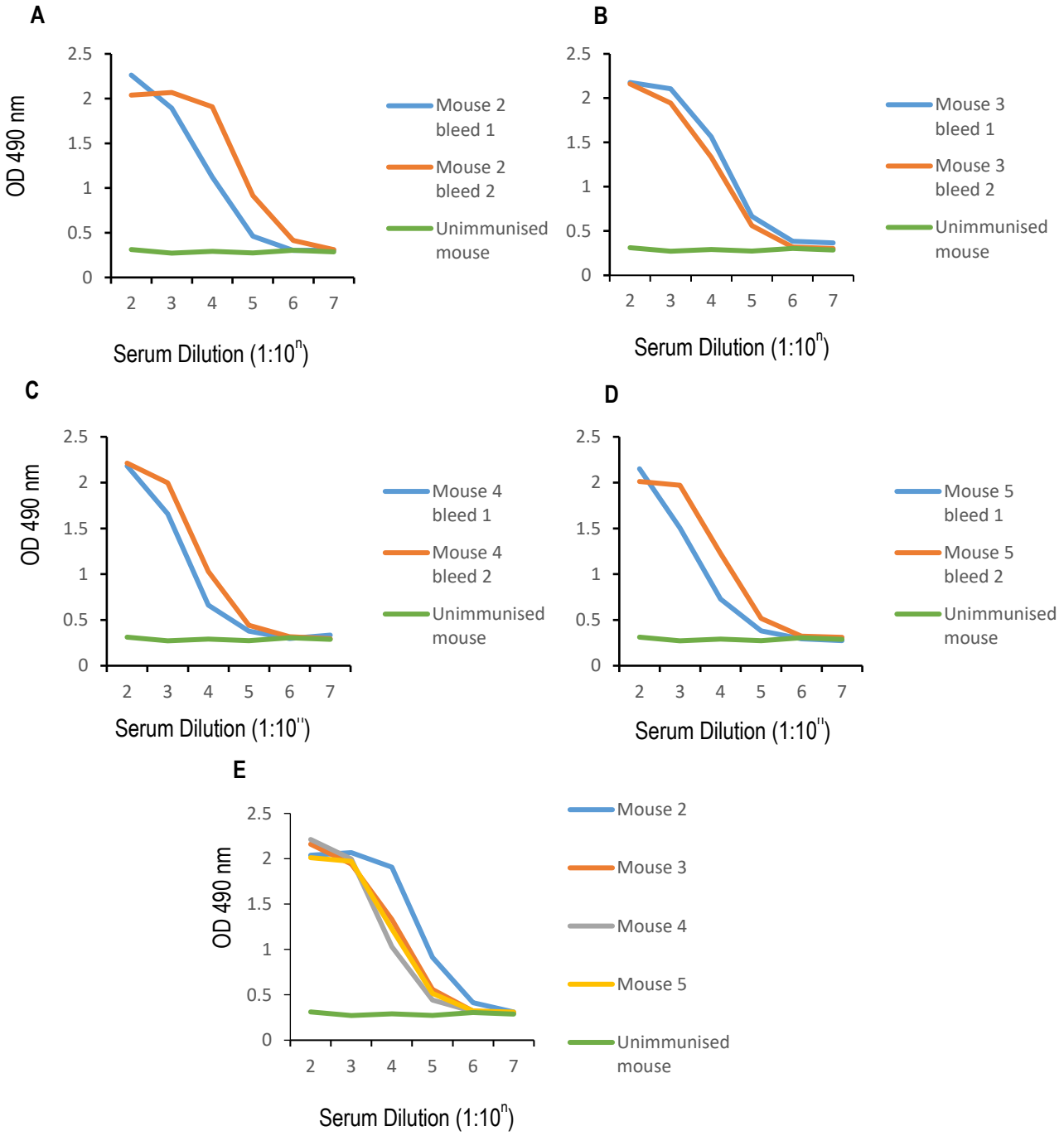

Figure 3.12 Comparison of antibody titres in mice boosted with 5 ug of native or cross-linked C1q

Mice 2 and 3 (A and B) were boosted with 5 µg of native C1q while mice 4 and 5 (C and D) received 5 µg of glutaraldehyde cross-linked C1q. Boosting with cross-linked C1q resulted in a small increase in titre that was not superior to native protein, as shown by overlaying the titration curves (E).

.

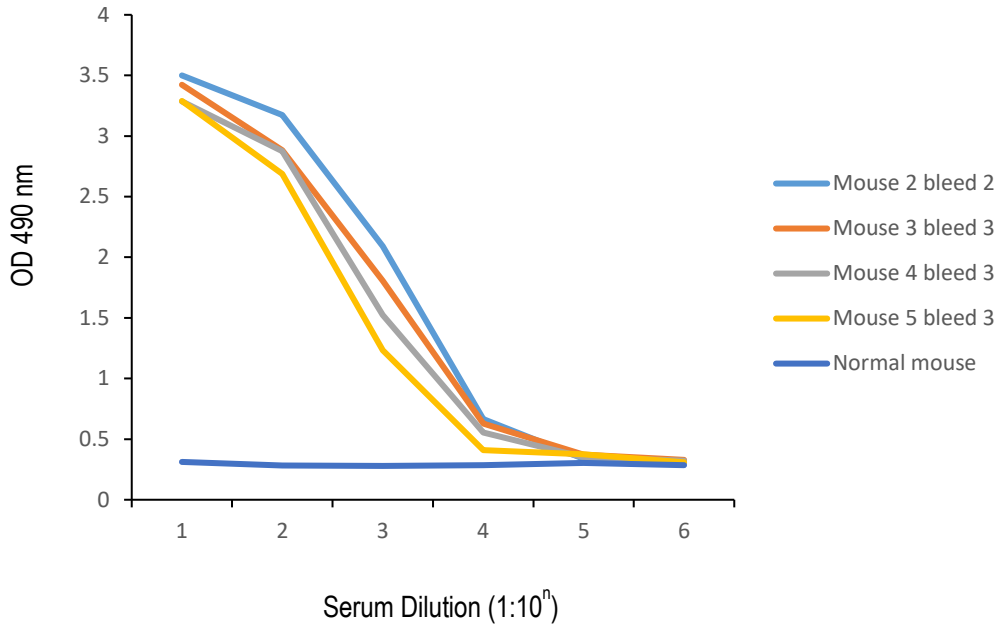

Figure 3.13 Comparison of antibody titres in mice boosted with 5 ug of native or cross-linked C1q for BHI3 fusion

Mice 3 and 4 were boosted with 2.5 µg of native C1q and mouse 5 with 2.5 µg of cross-linked C1q. Serum titres were compared with the serum from mouse 2 which had produced the best titre and was used as the source of splenocytes for fusion BHI2. The serum titres for mice 3 and 4 were higher than mouse 5, leading to the selection of mouse 3 for fusion BHI3.

3.3 DISCUSSION

3.3.1 PURIFICATION OF C1q FROM HUMAN PLASMA

To derive sufficient quantities of C1q for the immunisation of mice and the downstream screening of hybridomas, it was decided to purify C1q from human plasma. As the twentieth most abundant protein in plasma, the relative abundance of C1q was not a major obstacle in the purification scheme (Figure 3.2). Fully half the protein content in human plasma is albumin, a protein with important protein carrier functions as well as for the maintenance of colloid osmotic pressure (Tirumalai, 2003). Removal of albumin would therefore facilitate the further purification of proteins from the remnant plasma fraction. This was accomplished through sequential precipitation with increasing amounts of saturated ammonium sulphate (SAS). Since albumin is an extremely hydrophilic molecule, eighty percent ammonium sulphate saturation was required to effectively precipitate this protein. With C1q precipitating at thirty percent SAS, a large amount of contaminating protein was removed by this technique thereby producing a less complex protein mixture for further purification steps.

Past experience with less complex protein mixtures had demonstrated the efficacy of ion exchange and gel filtration chromatography techniques, particularly for proteins with suitable characteristics. Ion exchange works well for proteins with an isoelectric point (pI) value at either extreme of the pH range, a reflection of the charge carried by the protein at physiological pH (Ó'Fágáin, 2017). C1q fit well into this category of protein, having a pI of 9.3 and therefore carrying a significant positive charge at pH 7.2. Gel filtration is a good option for large proteins as the gel matrix will retard the passage of proteins with molecular weights below the cut-off pore size while larger proteins will simply pass through the column without interacting with the beads (Ó'Fágáin, 2017). This non-interacting fraction passes from the column with the void volume, which is the volume of the mobile phase contained in the column. With a molecular weight of 420 kD, C1q would easily pass through in the void volume of a 200 kD cut-off gel filtration matrix. A combination of high pI and high molecular weight makes for an attractive combination of qualities for C1q in a purification scheme as seen by the breakdown of the pI and molecular weight proteomes (Nanjappa, 2014).

As a source of C1q, plasma is an extremely complex mixture of proteins which fills a multitude of roles in the body. Plasma is the fluid that suspends blood cells; red blood cells that supply oxygen to the tissues and white blood cells that fight foreign organisms, kill cancer cells and remove dying cells. Plasma buffers the blood to resist pH shifts in the presence of higher CO_2 concentrations. Plasma delivers waste products for removal by the kidneys and circulates hormones and growth factors to their target tissues (Anderson, 2002), (Tirumalai, 2003), (Nanjappa, 2014). Due to its multitude of functions, the complexity of plasma is illustrated by the plasma proteome, which contains over 10,500 different protein species (Nanjappa, 2014). This incredible diversity of protein species negatively impacted the selection criteria for purification of C1q from plasma, namely that the highly basic charge and high molecular weight of C1q would be sufficient to isolation from other the plasma proteins. Although the approach to purification diverged from the use of gel filtration to removal of contaminating immunoglobulin with protein A, the Coomassie-stained gel of the final product revealed a significant number of high molecular weight species. This indicates the combination of ion exchange and gel filtration chromatography would have been inadequate to yield a highly pure sample of C1q. Such an impure preparation would compromise the yield of C1q-specific antibodies from immunised mice and therefore the identification of specific monoclonal antibodies from among the hybridomas derived from those mice.

3.3.2 IMMUNISATION OF C1q NULL MICE

Monoclonal antibody production is an unpredictable endeavour, depending on the nature of the protein used for immunisation. From prokaryotic antigen targets to specific protein sequences or proteins with high sequence similarity, the effort required to derive specific monoclonal antibodies varies greatly. For example, mice immunised with the prokaryote *Chlamydia trachomatis* produced specific hybridomas with the first fusion (unpublished work). *Drosophila melanogaster* protein CCNE1 with approximately 60% sequence identity to the mouse protein required several fusions to produce a specific monoclonal (Richardson, 1995). More difficult was the production of antibodies to the histone H2A.Z with greater than 90% sequence identity to mouse protein, using peptides corresponding to the divergent C terminus of the protein (Faast, 2001). This correlation of protein sequence similarity and immunogenicity does not hold universally. Three rows (*thr*), a Drosophila protein of 157 kD involved in cell division (D'Andrea, 1993) consistently produced no immune response, in rabbits, rats, or mice, indicating an interaction between the protein and the immune that blocked antibody formation (unpublished work). Therefore, protein sequence similarity is a good guideline for antigenic immunogenicity, but not an absolute one.

Human C1q bears seventy-one to seventy-nine percent sequence identity to mouse C1q across the A, B and C chains (Blast protein alignment www.uniprot.org), a level that should yield a reasonable antibody response and lead to isolation of anti-C1q monoclonal antibodies. However, the availability of C1qA null mutant mice to our laboratory led to the immunisation C1qA null mice to increase the lack of sequence identity to the immunogen. An antigen injected into its corresponding null mutant mouse would have a sequence identity level of zero percent, but regions in the C1q collagen-like domain retain 4.9 % sequence identity to endogenous Col1A over the length of the collagen sequence (Blast protein alignment www.uniprot.org). This low sequence identity would unlikely to produce anti-collagen antibodies and decrease the possibility of producing monoclonal antibodies that cross-react to collagens. Concerning the neutralisation capacity of monoclonal antibodies, it is possible to inhibit C1q function by binding either the globular region or the collagen-like tail. And given the bulkiness of a 150 kD immunoglobulin, it is not necessary to bind to the specific ligand-binding domain of the globular region or the receptor-binding domain of the tail, but merely close enough to interfere with these binding events.

The immunisation proceeded according to a schedule proven successful in many different target antigens (Fendly, 1987), (Halenbeck, 1989), (Shi, 1995), (Kaur, 1997), (Gajanandana, 1998). The immunising antigen dose was tapered down with each boost in order to stimulate B cells that produce higher affinity antibodies and thereby more useful monoclonal antibodies. The C1q screening ELISA employing TMB substrate led to a overestimate of the immune response. Re-optimisation of the ELISA showed that, despite the low sequence identity, the titre of the mouse used for fusion was 1:10,000 whereas the immunisation schedule employed usually yields titres of 1:100,000 or more. Nevertheless, since the first fusion still produced two hybridomas specific for C1q, two other fusions proceeded to derive more positive clones.

3.3.3 GENERATION OF C1q ANTIBODY-SECRETING HYBRIDOMAS

The immunisations with C1q presented the possibility that C1q could potentially be inhibiting the ability of the immune system to mount an antibody response to antigens, either specifically to C1q or generally. Immunomodulatory proteins interfering with the immune response can inhibit antigen-presentation to lymphocytes of the adaptive immunity. An example of such a protein is three rows (*thr*), a Drosophila protein involved in cell division (D'Andrea, 1993). Three rows protein failed to yield polyclonal antibodies in rats and rabbits and no clones could be recovered from mouse hybridoma fusions. C1q has been shown to modulate the activity of NK, T, and B cells and to inhibit the maturation of dendritic cells, the most

important of antigen-presenting cells (Son, 2012), (Afshar-Khargan, 2017). It could well be that the lower than anticipated antibody titres could be due to a dampening effect of C1q on the adaptive immunity.

It was possible C1qA null mice would present with an impaired immune system since C1q is integral to immune functions. However, most C1q functions involve innate immunity, such as complement-dependent cytotoxicity and antibody dependent cellular cytotoxicity. The interactions of C1q with humoral immunity lead to negative regulation of antibody production, therefore C1qA null mice could be a better system for production of anti-C1q monoclonal than wild type mice.

There was a possibility the injected human C1q was being sequestered into the classical complement cascade or the efferocytic function in the knockout mice. To test this, mice were immunised with a glutaraldehyde cross-linked C1q, anticipated to inactivate C1q in immune functions; as demonstrated by decreased solubility and lack of antibody binding in ELISA. But cross-linking C1q did not raise the antibody titre, suggesting that sequestration of C1q by the innate immune system was not responsible for the less-than-anticipated antibody response, but more likely to be due to a direct effect of the C1q on immune cells. C1q interaction with the LAIR-1 molecule is able to suppress the activation of B and T cells, maturation of dendritic cells and can direct macrophage differentiation towards anti-inflammatory M2 phenotypes (Kouser, 2015), (Son, 2016), (Son, 2017), a possible mechanism of immune suppression. Despite this possible suppression of response, additional boosting with native C1q increased the titre in one of the mice and two more fusions were performed. Screening of these fusions led to the identification of an additional two anti-C1q hybridomas, making a total of four monoclonal antibodies generated over three fusions.

In total, fusions performed on three C1q immunised mice resulted in 2,776 cultures in 96 well plates that yielded 2,017 growing cultures, an overall fusion efficiency (wells growing/wells plated) of 72.6%. From these cultures, four were identified as binding C1q in ELISA, a specific efficiency (wells positive/wells screened) of 0.2%. The anti-C1q monoclonal antibodies generated here will require further testing of C1q binding specificity and their capacity to neutralise C1q activity *in vitro*.

The techniques used to generate these monoclonal antibodies have been used successfully many times and include immunisation schedules and adjuvant use. The immunisation schedule shown in Figure 3.9 is kept invariant and represents the time for an antibody response to peak and subside prior to the next boost. After that initial period of one priming shot followed by two boosts, the schedule is varied with dose adjusted to best attempt to produce the best immune response, as shown in Table 3.1.

The use of Freund's adjuvant is no longer permitted in Australia which narrows the choices to oil-in-water adjuvants. Ribi and Gerbu adjuvants have been used in the past but after supply difficulties, Addavax was selected for use in immunisation. Another factor in trying too many variables is the limit on the number of animals that can be immunised, with an emphasis on reducing numbers.

The choice of animal for immunisation fell to the use of mice. Well-established protocols using mice meant there was no need to optimise a new regimen of immunisation and boosting. Rats require special conditions for fusion and are best done with a rat myeloma which can be difficult to obtain. Regardless of the other options, the choice for the immunisation was decided by the availability of the C1qA null mutant mouse. The lack of sequence identity is useful in producing monoclonal antibodies to C1q since the C1qA chain is essentially a foreign antigen.

CHAPTER FOUR: INVESTIGATION OF C1Q BINDING CAPACITY OF ANTI-HUMAN C1Q MONOCLONAL ANTIBODIES

4.1 INTRODUCTION

Once the panel of antibody-secreting hybridomas had been generated, single cell cloning of these potentially heterogeneous cultures was necessary to establish homogeneous cultures of hybridoma cells secreting an antibody of single specificity. These monoclonal antibodies required further screening to determine the most useful candidates for neutralisation of C1q activity. A monoclonal antibody has binding specificity for a single epitope and can be useful for the investigation of biological systems and in clinical settings for both imaging and therapy (Rosen, 2012), (Sano, 2012), (Li, 2015). However, the high specificity can also limit the utility of a monoclonal antibody. The antibody may only bind the epitope on the antigen under specific conditions, with improper protein folding or protein denaturation having the potential to affect the antibody-epitope interaction. In order to increase the chance of identifying a useful antibody, it is preferable to use a screening regime tailored to match the desired application (Kim, 2017), (Hatano, 2019). However, this is not always possible due to limited resources and/or time. If the intended use is neutralising capacity, screening a panel of potential hybridoma candidates for this application can be laborious, expensive and require more time than is reasonable for the recovery of secreting clones. Therefore, an alternate screening regime may be used to identify candidates for further studies on neutralising capacity.

Prior to analysis of C1q neutralising capacity of the anti-human C1q monoclonal antibodies, the antibody-secreting hybridomas were assessed for capacity to bind C1q under different conditions to determine the best candidates for further investigation. Investigation of the binding potential of an antibody in an assay can be challenging. The interaction of a protein with the surface of an ELISA plate can influence the conformation of the protein and hence the epitopes displayed (Kumar, 2015). Some methods of fixation can destroy certain epitopes while leaving others unaffected (Hunziker, 1993). The challenge presented is to select suitable immunoassays, being mindful that lack of binding in a specific assay may not automatically exclude the antibody from further consideration. Thus, design of the screening assay is essential to detect antibody-antigen binding while not missing useful candidates.

The ELISA immunoassay was chosen for screening of the C1q fusions. ELISA is a rapid high-throughput assay capable of handling large numbers of test samples, performed by a single operator. Despite using human C1q at >/= 96% purity for immunisation and screening on the same protein, a second C1q assay to prove the specificity of the monoclonals was required. Immunoassays fall into two categories: denaturing and non-denaturing that refer to the state of the antigen in the assay. Denaturing assays involve the use of detergents that unwind tertiary structure or reducing agents that break intra- and inter-protein disulphide bonds. Denaturing assays include western blotting, immunohistochemistry, and fixed immunocytochemistry. Non-denaturing assays do not interfere with the native conformation of the antigen and identify antibodies more likely to bind antigens *in vivo.* These assays include ELISA, immunoprecipitation, and sandwich ELISA.

In this chapter, the four antibody-secreting hybridomas (BHI1-1G4 and 4D3, BHI3-3F6 and 8B9) were single cell cloned and C1q binding capacity was assessed by ELISA and immunoprecipitation. The commercially available 9A7 anti-C1q monoclonal antibody was used as a positive control and no primary antibody was a negative control. Further studies on two of the most promising candidates (BHI1-1G4 and 4D3) were conducted to assess cellular binding by immunohistochemistry and immunocytochemistry.

4.2 RESULTS

4.2.1 HYBRIDOMA SINGLE CELL CLONING

Chapter 3 described the successful generation of four anti-C1q secreting hybridoma cultures. During the three BHI fusion procedures, the cells plated onto 96-well cultures settled into individual wells according to a Poisson distribution, in which some wells would contain no cells, a proportion would contain a single hybridoma, and other wells would contain two or more clones. In the case of more than one hybridoma clone within the one culture well, the clones compete for medium nutrients and there exists potential that non-antibody secreting clones could outgrow clones secreting specific antibody. It is essential that hybridoma cultures contain single cell clones, ensuring that all cells within the culture secrete the same antibody and thus can be termed a “monoclonal antibody”.

To ensure each antibody-secreting hybridoma generated in Chapter 3 was a homogeneous culture, each specific culture from the fusion was single-cell cloned. Cultures were diluted 1:2 sequentially until wells with single cells were obtained. Upon screening, the presence of wells containing hybridomas that did not secrete anti-C1q antibody indicated that more than one clone was present in the culture, and an additional sub-cloning was performed (Table 4.1). Of the cloning wells that grew cultures for BHI1-1G4 and BHI3-3F6, 100% were positive for anti-C1q antibody indicating they were already monoclonal at the time of cloning. However, BHI1-4D3 and BHI3-8B9 did not have clonal populations at the time of single-cell cloning and required subcloning. 4D3 required two rounds of subcloning before producing monoclonal cultures. As 8B9 was not successfully single cell cloned after one round of subcloning, this hybridoma would require another round to ensure complete clonality. This highlights the heterogeneity resulting from the plating of splenocyte:myeloma fusion cultures to 96 well cultures.

4.2.2 DETERMINATION OF ANTI-C1Q MONOCLONAL ANTIBODY BINDING TO C1Q BY ELISA

ELISA was the screening assay for the hybridoma fusions. The human C1q used was of high purity (>/= 96%) making the likelihood that the antibodies were not binding to C1q extremely low. ELISA employs non-denatured antigen attached to a plastic plate for antibody capture and while some antigens can be altered by attachment to a plate (Kumar, 2015), most epitopes are displayed in their native conformation.

Generally, assays used to characterise the anti-C1q monoclonals were qualitative and not repeated once the initial result had been obtained and therefore not analysed statistically. A difference to this norm was the screening ELISA, which was used to monitor antibody secretion during expansion form the original 96 well culture and during the cloning procedure.

.

	BHI1-1G4	BHI1-4D3	BHI3-3F6	BHI3-8B9
Cloning: Wells plated	95	95	95	95
Wells growing	34 (35.8%)	44 (46.3%)	8 (8.4%)	42 (44.2%)
Wells positive	34 (100%)	1 (2.3%)	8 (100%)	11 (26.2%)
Clonal status	**Clonal**	**Non-clonal**	**Clonal**	**Non-clonal**
Subcloning: Wells plated		95		95
Wells growing		74 (77.9%)		50 (52.6%)
Wells positive		16 (21.6%)		26 (52%)
Clonal status		**Non-clonal**		**Non-clonal**
Subcloning: Wells plated		95		
Wells growing		43 (45.3%)		
Wells positive		43 (100%)		
Clonal status		**Clonal**		

Table 4.1 Single cell cloning of hybridomas

Antibody-secreting hybridomas BHI1-1G4, BHI1-4D3, BHI3-3F6 and BHI3-8B9 were plated at low density to establish cultures derived from a single cell, also known as monoclonal cell lines. BHI1-1G4 and BHI3-3F6 proved to be clonal cultures as all the wells with growing cultures were positive for anti-C1q antibody. BHI1-4D3 and BHI3-8B9 were not clonal when subjected to single-cell cloning and additional rounds of low density culture were required. 4D3 required two rounds of subcloning to produce monoclonal cultures, while 8B9 still requires further subcloning to ensure its clonal status.

To compare the binding activity of the four newly-generated monoclonal antibodies to each other and commercial 9A7 antibody, an ELISA was performed titrating the antibody supernatant on a constant concentration of plated C1q (Figure 4.1A) and titrating the C1q antigen coating with a constant antibody concentration (Figure 4.1B). While the results indicated that all of the antibodies bound well to C1q, 9A7 exhibited the best binding capacity both as a function of primary antibody concentration and against diminishing C1q concentrations on the assay plate.

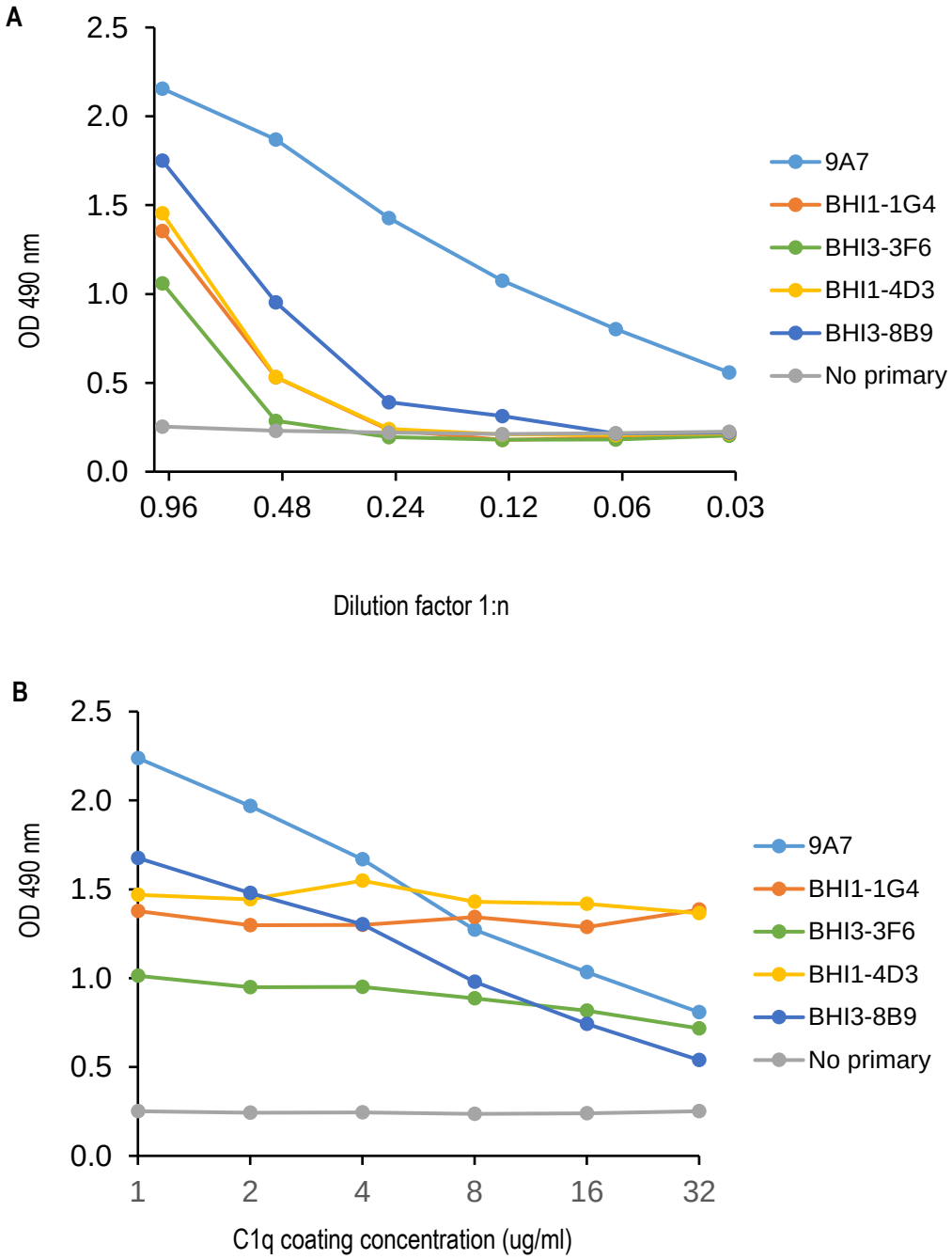

Figure 4.1 ELISA to assess anti-C1q monoclonal antibody binding to C1q

ELISA performed to compare the binding capacity of hybridoma supernatants to C1q. (A) describes the binding profile of the monoclonals as the C1q coating concentration is decreased through a series of doubling dilutions. (B) displays the binding profile of monoclonal supernatants through a series of doubling dilutions with differing kinetics seen for 9A7 and 8B9 vs 1G4, 4D3 and 3F6. Difference in the binding between 9A7 and the BHI monoclonals could be due to a number of different factors including antibody affinity, isotype and/or concentration.

The binding profiles of antibodies in Figure 1B fall into two groups: Group1, 1G4, 4D3 and 3F6; and Group 2, 8B9 and 9A7. Group 1 signal decreases very little while Group 2 has a more pronounced signal decrease. The difference in the behaviour of the two groups is likely due to factors such as antibody concentration, affinity, and/or isotype. The binding of the monoclonals in Figure 4.1A are much more consistent with each other and less like 9A7. The cause of the disparity between Figures 4.1A and 4.1B are not readily apparent.

4.2.3 DETERMINATION OF ANTI-C1Q MONOCLONAL ANTIBODY BINDING TO C1Q BY IMMUNOPRECIPITATION

Immunoprecipitation involves the binding of antigen to native protein in solution, and thus is a method to identify antibodies that recognise conformational epitopes. Antibodies are combined with a protein solution, antibody-antigen complexes are allowed to form, which in turn bind to and are pulled down by protein A conjugated to agarose beads. A significant consideration with this technique is that protein A binds immunoglobulins via the CH2 and CH3 regions, coincidentally overlapping with the region by which C1q binds immunoglobulins (Duncan, 1988), (Wines, 2000). This points to the need for proper controls to ensure the antibody-C1q interaction is occurring through the antibody binding site and not the heavy chain region.

Antigens used in immunoprecipitation are typically labelled with a small tag that will not interfere with antibody-antigen interactions, such as radioactive ^{125}I, biotin, the six-residue polyhistidine (his) or the ten amino acid myc tags. Subsequent to the precipitation step, the agarose beads are washed and run on a PAGE gel. Detection method will depend on the specific tag: autoradiography for ^{125}I tag, incubation with streptavidin HRP for biotin tag, incubation with anti-his antibody for his tag, and incubation with anti-myc antibody for myc tag. The method for detecting precipitated C1q was western staining with the 9A7 antibody, which was the method used in Chapter 3 for C1q purification and antibody characterisation.

The immunoprecipitation assay used 9A7 as a positive control for C1q binding, anti-S100 A8 as a non-specific antibody control, the BHI1 and BHI3 hybridoma supernatants, and a no primary antibody as negative control. Following the precipitation step, the agarose beads were run on a PAGE gel, blotted to a PVDF membrane, and probed with the 9A7 antibody (Figure 4.2). The hybridoma supernatants BHI1-1G4 and 4D3, BHI3-3F6 and 8B9 and the anti-C1q antibody 9A7 all pulled down a band in the area of 30kD, which is consistent with binding to C1qA. The non-specific antibody anti-S100 A8 and the no primary antibody conditions showed a faint band at 30 kD, possibly indicating non-specific C1q binding to protein A (Duncan, 1988). However, there is a possibility that this faint binding in negative controls could indicate that the assay was not effective in identifying specific C1q binding. Further optimisation of the assay is required to confirm this result.

4.2.4 DETERMINATION OF ANTI-C1Q MONOCLONAL ANTIBODY BINDING TO C1Q IN WESTERN BLOTS

Western blotting is a technique to identify monoclonal antibodies with binding capacity to C1q and is similar in some respects to ELISA. Western blot detection involves binding of the antibodies to immobilised protein epitopes, with washes in between followed by detection with an enzyme-modifiable substrate. However, unlike ELISA that can detect conformational and linear epitopes, western blotting can only detect linear epitopes as the treatment of proteins with B-mercaptoethanol as well as sodium dodecyl sulphate (SDS) and heat denaturation reduces all disulphide links and separates C1q into its eighteen component chains. Nonetheless, western blotting can be a good method for confirming the binding of a monoclonal antibody to a C1q component protein through binding to a band at an appropriate molecular weight.

To determine C1q binding in a western blot, denatured C1q at 2, 1, 0.5 and 0.25 µg was loaded onto a PAGE gel and transferred to a PVDF membrane prior to incubation with 9A7 antibody as a positive control and the first anti-C1q hybridoma identified, BHI1-1G4. 9A7 effectively bound C1q at all concentrations; however, BHI-1G4 showed only faint binding to 2 µg of C1q (Figure 4.3).

A follow-up western blot with 2 µg of C1q per lane assessed binding capacity of 9A7, BHI-1G4 and BHI-4D3, as well as a no primary antibody negative control. Again, effective binding was observed for 9A7; however, BHI1-1G4, BHI1-4D3 and the no primary negative control did not show any binding to C1q, (Figure 4.4), not even the minimal binding observed for BHI-1G4 in the previous assay.

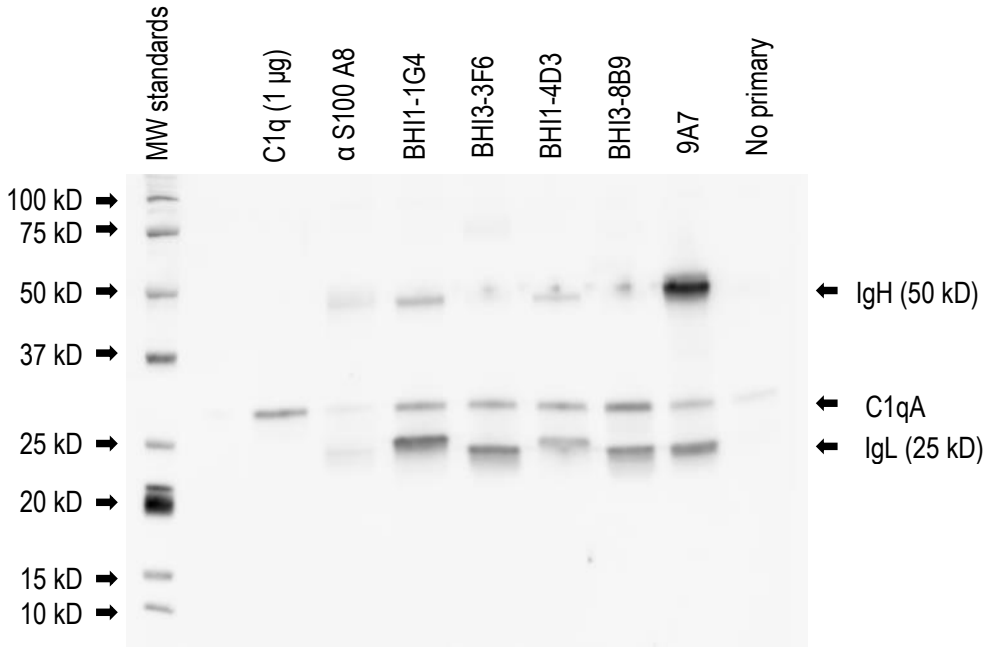

Figure 4.2 Immunoprecipitation to assess anti-C1q monoclonal antibody binding to C1q in solution

C1q was immunoprecipitated by 9A7, BHI1 and BHI3 antibodies followed by western blotting and probing with 9A7 anti-C1qA antibody. Antibody supernatants were mixed with C1q in solution prior to precipitation of the immune complexes with protein A. The first lane contains 1 µg of C1q protein as a control for 9A7 binding. BHI1-1G4, BHI1-4D3, BHI3-3F6, and BHI3-8B9, and the 9A7 antibody all pulled down a band at approximately 30 kD, consistent with the control band for C1qA. The non-specific anti-S100 A8 and the no primary have faint bands at 30 kD that likely represented the background binding of C1q to protein A. The rabbit anti-mouse IgG also detects the heavy (IgH) and light (IgL) chains of the monoclonals present in the samples.

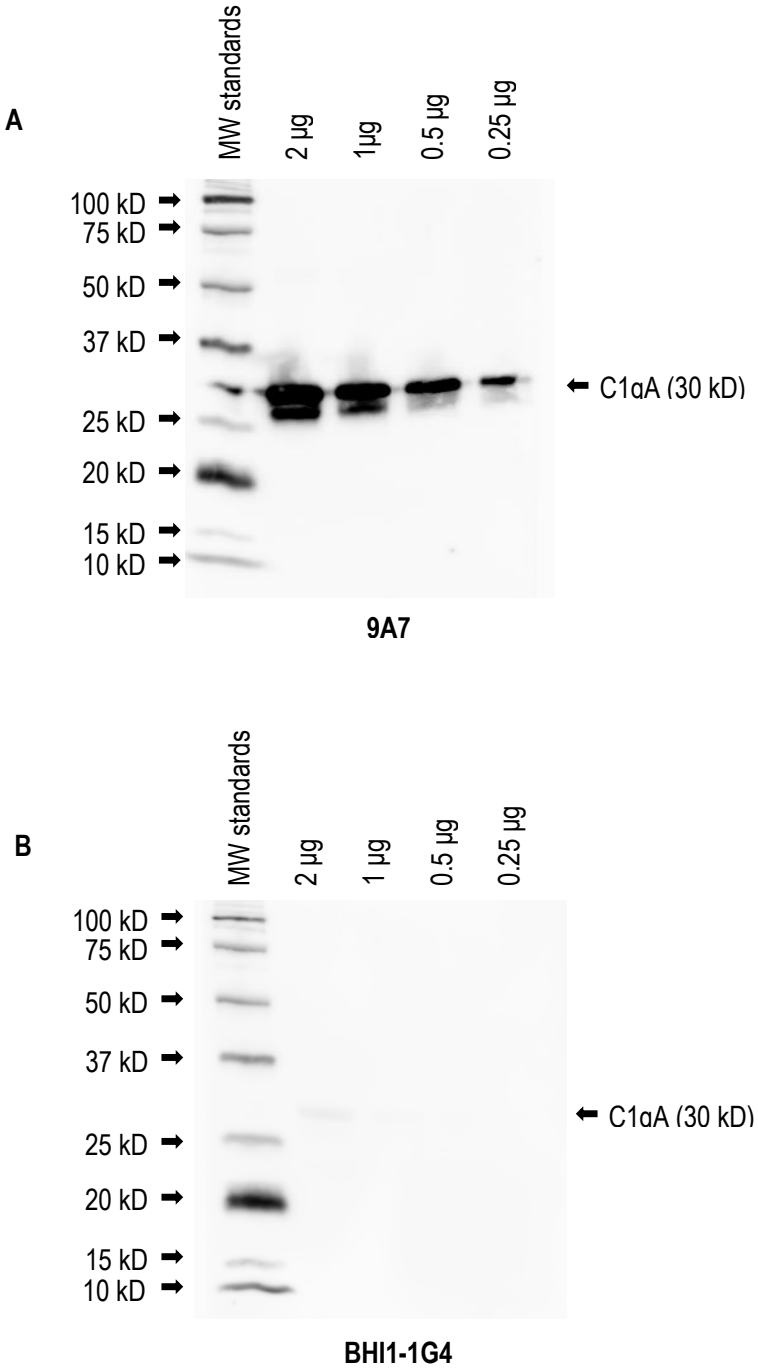

Figure 4.3 Western blot to assess binding capacity of 9A7 and BHI-1G4 antibodies to denatured C1q

A 12% PAGE gel was loaded with C1q at 2, 1, 0.5 and 0,25 µg per lane and blotted onto a PVDF membrane. (A) 9A7 antibody incubated at 1 µg/mL bound C1q in all lanes, detected at the anticipated molecular weight of 30 kD. (B) BHI-1G4 supernatant incubated neat, had little capacity to detect C1q, displaying only a faint band in the lane containing 2 µg.

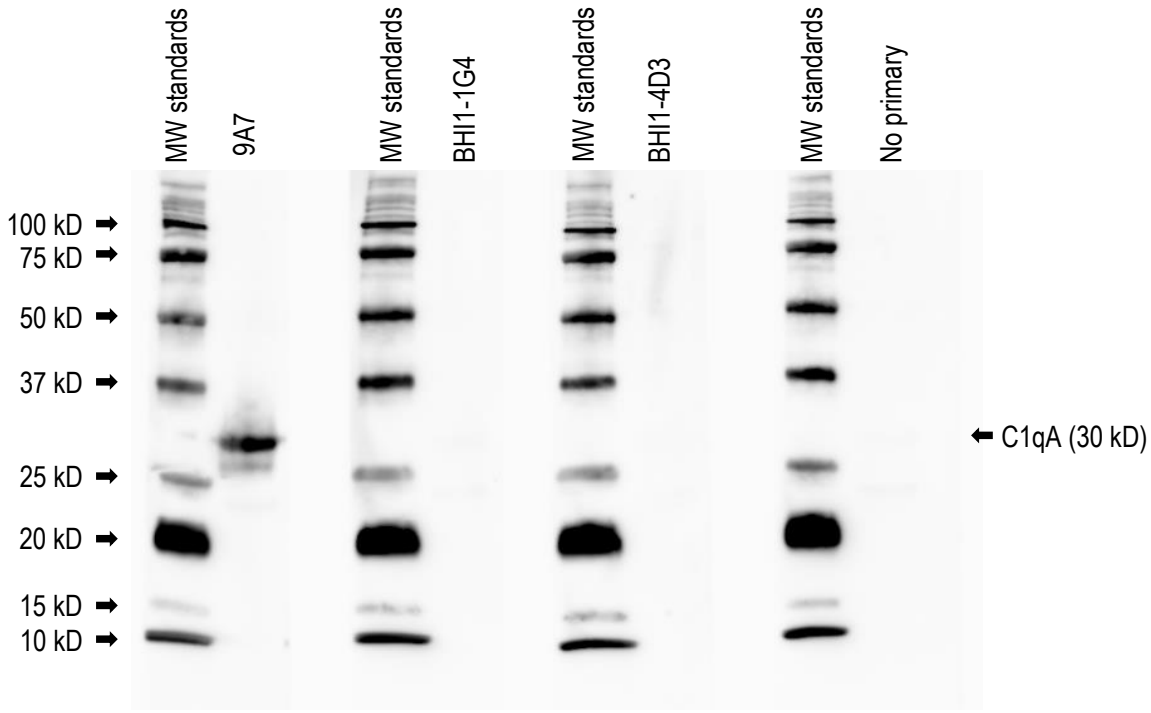

Figure 4.4 Western blot to assess binding capacity of 9A7, BHI-1G4 and BHI1-4D3 antibodies to denatured C1q

A 12% PAGE gel was loaded with C1q at 2 µg per lane and blotted onto a PVDF membrane. 9A7 antibody incubated at 1 µg/mL bound the C1qA band at the anticipated molecular weight of 30 kD. The neat hybridoma supernatants of BHI--1G4 and BHI1-4D3 failed to bind the C1q band as did the no primary antibody negative control.

4.2.5 DETERMINATION OF ANTI-C1q MONOCLONAL ANTIBODY BINDING TO C1q IN FORMALIN-FIXED PARAFFIN-EMBEDDED TISSUE SECTIONS

Immunohistochemistry involves binding antibodies to tissue sections preserved by either formalin fixation or by ultra-cold freezing, and while these protocols are similar, each method has its advantages and drawbacks. Frozen sections require snap freezing of the specimen, ultra-cold storage and a freezing microtome. Frozen tissues preserve the genetic integrity of nucleic acids and the antigenic properties of proteins; therefore, it is the superior method for the investigation of genetic mutations, mRNA expression and protein regulation/localisation. Frozen sectioning relies on cold temperatures to slow the degradation of proteins and nucleic acids through enzymatic and chemical processes. However, despite minimising molecular alterations through freezing, some deterioration of staining is seen in some samples when compared with formaldehyde-fixed paraffin-embedded (FFPE) sections (Argon, 2014).

Alternatively, tissues processed for FFPE sections require fixation in formalin, paraffin embedding, and dewaxing with xylene. Formaldehyde alters protein and nucleic acid structure through chemical cross-linking during the process of fixation. FFPE blocks exhibit better preservation of tissue architecture compared to frozen tissue blocks, and thus make superior starting material for studies that require histochemical staining or tumour grading.

Staining of FFPE blocks to assess antibody binding to C1q carries some of the same caveats as western blotting since proteins in FFPE tissue are, by definition, denatured during the fixation process. An antigen recovery process through heating in pH 9 citrate buffer can increase antigenicity through the breaking of formalin cross-links but does not refold denatured proteins back to their native state. Therefore, antigen recovery is most useful for exposing linear epitopes, much like those displayed in western blotting.

FFPE blocks of normal breast tissue from patients who had undergone breast reduction surgery at The Queen Elizabeth Hospital were accessed from the Breast Biology and Cancer Unit's breast tissue repository. Two different patient samples were deparaffinised, rehydrated and then subjected to antigen retrieval by heating to 95 °C for 20 minutes in pH 9 citrate buffer. Primary antibodies 9A7, BHI1-1G4, and BHI1-4D3 were incubated for 30 minutes followed by incubation with the anti-mouse HRP polymer and development with DAB substrate. Positive staining was observed using the 9A7 positive control antibody. Stained cells exhibiting macrophage-like morphology were detected throughout the ductal and stromal compartments of both patient breast tissue samples. However, no positive staining was detected on tissue samples incubated with either BHI1-1G4 or BHI1-4D3 antibodies (Figure 4.5).

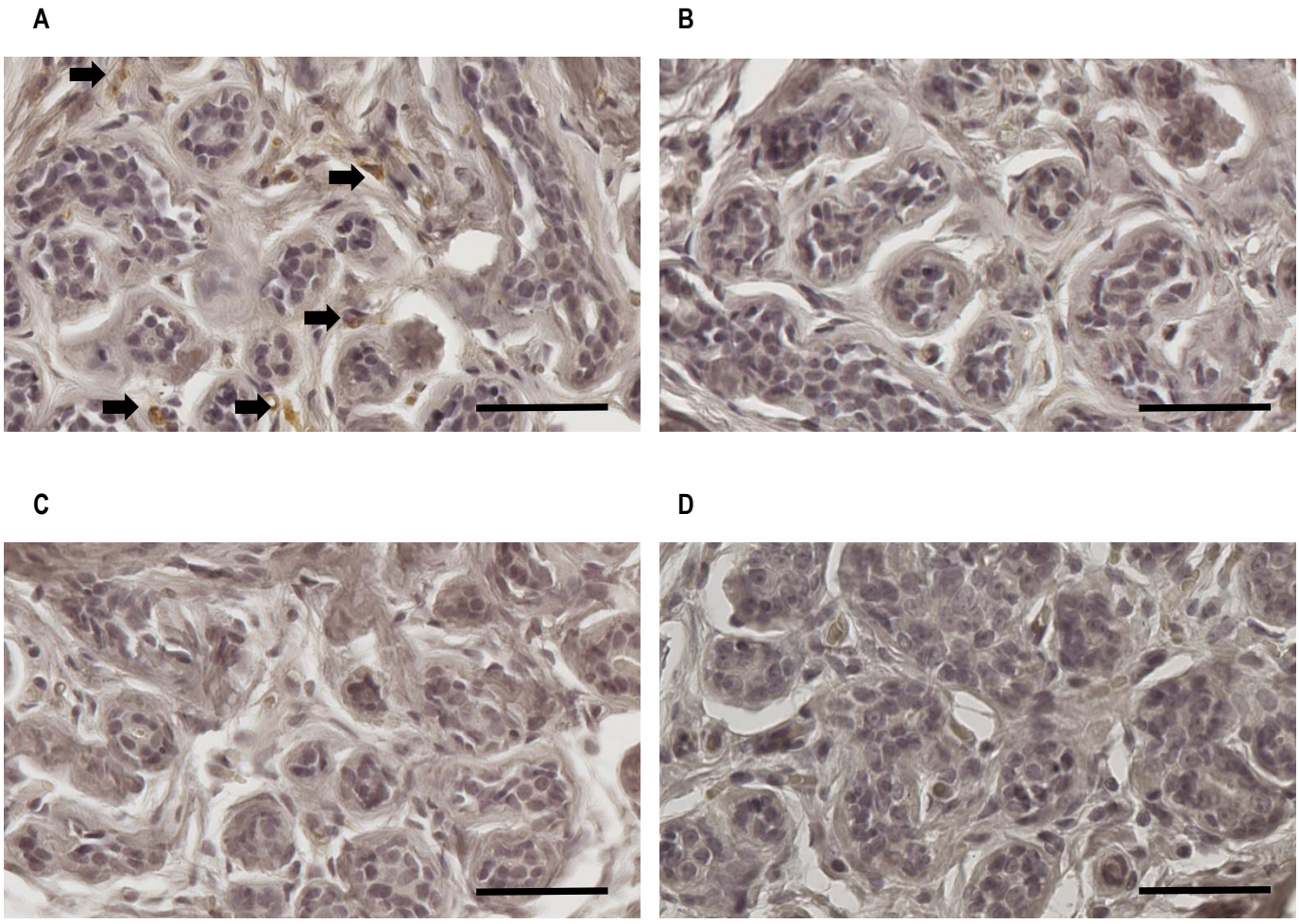

Figure 4.5 Immunohistochemical staining of normal human breast tissue with 9A7 and BHI1 antibodies

Immunohistochemical staining of FFPE sections of normal breast tissue from the Breast Biology and Cancer Unit tissue repository (patient 12). The tissue was deparaffinised, treated for antigen retrieval in pH 9 citrate buffer at 95 °C for 20 minutes, then stained with 9A7 (A), BHI1-1G4 (B), BHI1-4D (C), or no primary antibody (D). Sections were then incubated with rabbit anti-mouse IgG HRP followed by diaminobenzidine (DAB) development and haematoxylin counterstaining. Characteristic brown DAB staining is seen for 9A7 on normal human breast tissue (arrows), representing the presence of macrophages in the mammary ducts and stroma. No staining is detected for BHI1-1G4, BHI1-4D3 or the no primary antibody control. The scale bar is 50 um.

4.2.6 DETERMINATION OF ANTI-C1q MONOCLONAL ANTIBODY BINDING TO C1q IN ALCOHOL-FIXED AND UNFIXED RAW 264.7 CELLS

Immunocytochemistry is a technique similar to immunohistochemistry and can be used to assess antibody binding to specific cells; however, the difference between the two lies in the source of the cells used for immunostaining. While immunohistochemistry is performed on FFPE or fresh frozen tissues, immunocytochemistry can be performed on either a cell suspension or adherent samples of cell culture lines. For the determination of monoclonal antibody binding by immunocytochemistry, RAW 264.7 tissue culture macrophages were grown on cover slips. The use of fresh tissue culture cells removed the requirement for sample deparaffinisation, and antigen retrieval required for immunohistochemistry of FFPE tissue.

Immunocytochemistry can be performed on formalin-fixed cells but it is preferable to use non-polar solvents such as methanol or acetone or acid-methanol to fix the cells, thereby doing less damage to protein epitopes (van Essen, 2010). However, non-polar solvents can denature some proteins and reduce the sensitivity of antibody binding. It is also possible to stain unfixed cells if care is taken not to dislodge the cells from the substratum during wash steps. This is highly dependent on the cell type as some cells, such as fibroblast monolayers, are quite easily dislodged from a culture well or cover slip and therefore not suitable candidates for unfixed assays.

To determine the optimal staining strategy for immunocytochemical staining of C1q, positive control antibody 9A7 was used to stain the mouse macrophage cell line RAW 264.7. RAW cells are highly adherent cells in tissue culture and are known to express C1q (Spivia 2014). Although it is known that C1q modulates macrophage polarisation and function (Benoit, 2012), (Son, 2016), it was of interest to study the effect of macrophage polarisation on C1q expression in macrophages. To assess optimal culture conditions for immunocytochemistry, the RAW cells were grown on glass cover slips and treated with different stimuli for 24 hours to alter the differentiation status of the cells, with IFNG and LPS inducing an M1 phenotype, IL4 producing M2a cells, and TGFB inducing M2c cells (Hamczyk, 2015). Untreated cells were also assessed and considered as unstimulated macrophages.

Following culture, the cells were fixed with 10% acetic acid in methanol prior to incubation with 1 µg/mL 9A7. After incubation with rabbit anti-mouse IgG HRP and the DAB substrate, the cover slips were mounted and observed on a Nikon TE 2000 inverted microscope. 9A7 bound well to all of the RAW cell cultures, with strong cytoplasmic staining particularly in M1 cells that had been stimulated with IFNG and LPS, suggesting the assay was suitable for investigating the binding of the hybridoma antibodies (Figure 4.6).

A subsequent immunocytochemical assay included the BHI1 antibodies 1G4 and 4D3 alongside 9A7 with the RAW 264.7 cells differentiated with IFNG and LPS into M1 macrophages. Despite a much-reduced staining intensity for the 9A7 antibody, staining of the M1 cells was still faintly positive (Figure 4.7). In this assay, staining was not observed for the BHI1-1G4 and BHI1-4D3 monoclonal antibodies. Since these results were consistent with the immunohistochemistry where staining was present with 9A7 but absent with BHI1 antibodies, it was decided to not pursue this assay further but to explore staining in unfixed cells.

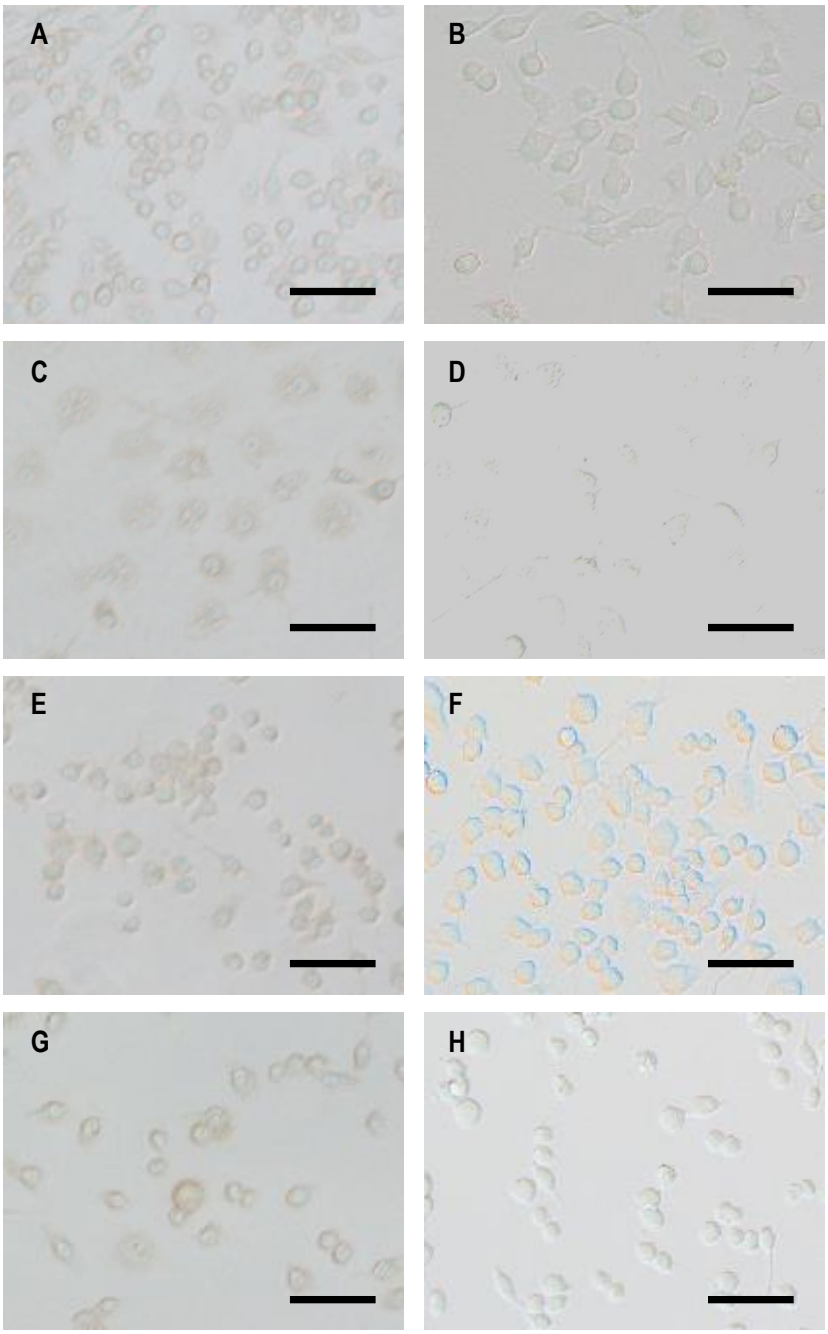

Figure 4.6 Immunocytochemical staining of acid-methanol fixed RAW 264.7 cells with anti-C1q antibody 9A7

Immunocytochemical staining of anti-C1q antibody 9A7 on RAW 264.7 cells either untreated (A), treated with 200 ng/mL LPS and 20 ng/mL IFNG (M1)(C), treated with 20 ng/mLI4 (M2a)(E) or treated with 20 ng/mL TGFB (M2c)(G) along with paired no primary antibody controls (B), (D), (F), and (H). Cytoplasmic staining was seen for all four conditions, particularly for the M1 phenotype, which are flattened and exhibit greater cytoplasmic area relative to the other treatments. Scale bar is 50 um.

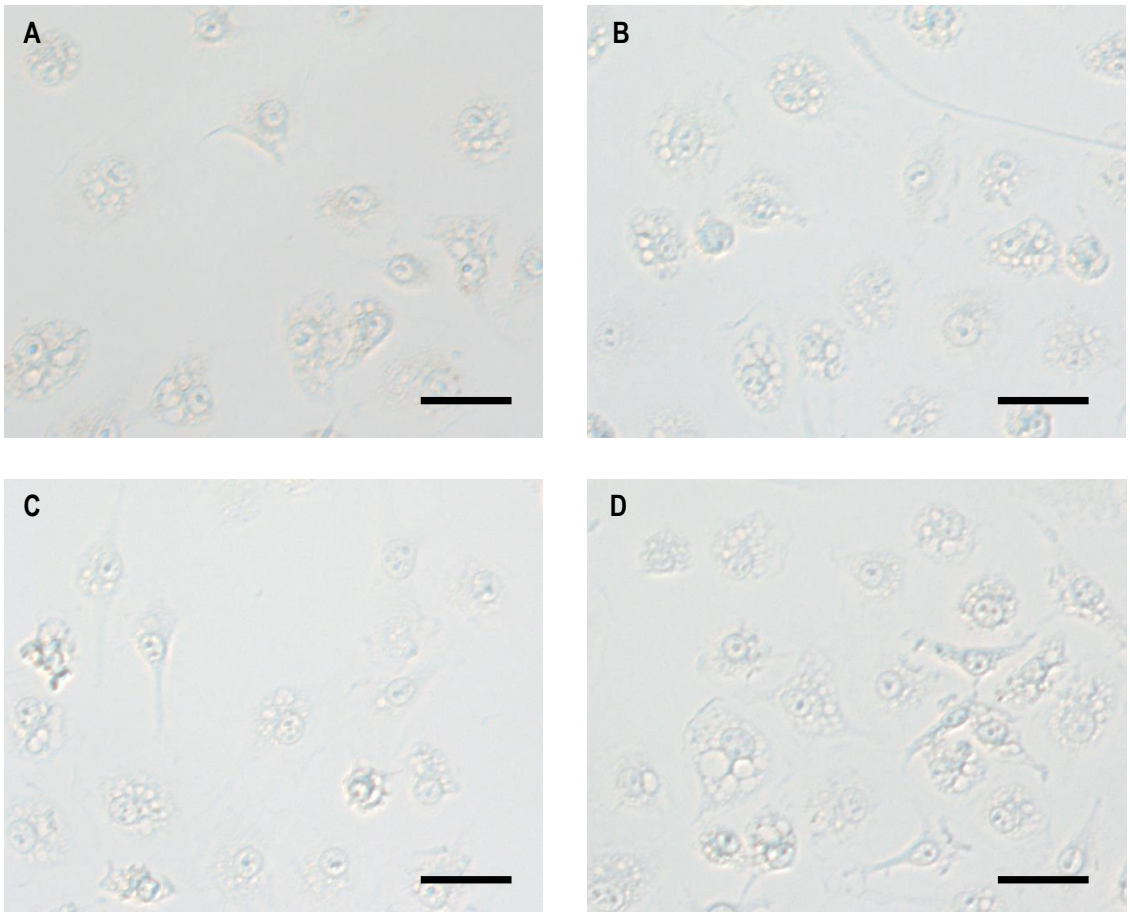

Figure 4.7 Immunocytochemical staining to assess binding capacity of 9A7, BHI1-1G4 and BHI1-4D3 antibodies to M1 RAW 264.7 cells

Staining for C1q on RAW 264.7 cells that had been treated with 200 ng/mL LPS and 20 ng/mL IFNG to stimulate an M1 macrophage phenotype. These cells were fixed with acid-methanol, then stained with 9A7 (A), BHI1-1G4 (B), BHI1-4D3 (C) or no primary antibody (D). Following development with DAB, some faint staining in evident for the 9A7 antibody but not for the BHI1 antibodies or the no primary antibody control. Scale bar is 25 um.

Evidence from assays performed on fixed tissue or cells suggested any assay that featured the denaturation of C1q would result in antibody staining by 9A7 but not BHI1-1G4 or BHI1-4D3. Therefore, an immunocytochemistry assay was performed on unfixed M1 phenotype RAW 264.7 cells to look for binding to native C1q. The RAW 264.7 cells were treated with LPS and IFNG and then stained with 9A7 and the BHI1 antibodies 1G4 and 4D3, none showed any detectable binding to C1q on the cells (Figure 4.8).

This result would appear to be at odds with the previous results from the assays with fixed RAW 264.7; however, there was a distinction between the assays of fixed and unfixed cells that could explain this disparity. C1q acts as a bridge between phagocytic cells and cells undergoing apoptosis and does not at any time exist as a membrane-inserted protein (Lauber, 2004), (Barth, 2017). Therefore, it is possible secreted C1q engages apoptotic markers on dying cells prior to binding phagocytes via the collagen-like tail and never exists as a cell-surface protein in the absence of apoptotic cells. Although cell surface expression of C1q on macrophages has been reported, (Kaul, 1997), (Ghebrehiwet, 2017), this was not seen for this assay. The immunocytochemical staining seen in fixed cells was cytoplasmic where the permeabilisation of the cells by the methanol fixation allowed the 9A7 antibody access to C1q. The unfixed cells retained intact cell membranes and therefore offered no access for antibodies to cytoplasmic C1q.

4.2.7 DETERMINATION OF MONOCLONAL ANTIBODY ISOTYPES

Monoclonal antibody isotypes were identified using the IsoStrip kit from Roche and are detailed in Table 4.2. Isotypes are important for immune function with different isotypes fulfilling distinct roles. IgM antibodies predominate in the primary humoral response and is also important for immunity to bacterial pathogens and virally-infected cells (Janeway, 2001). IgG antibodies perform different functions in humoral immunity that are dictated by their ability to interact with the various Fc receptors on immune effector cells (Michaelsen, 2004). Mouse IgG1 antibodies do not interact with C1q, which renders them less effective at complement-mediated bactericidal activity and implicates them in regulation of the humoral response (Michaelsen, 2004), (Lilienthal, 2018). However, the significance of mouse monoclonal antibody isotype becomes moot since antibodies selected for clinical applications are invariably humanised, which allows for tailored optimisation of *in vivo* function (Dondelinger, 2018).

From the results obtained from western blotting, acid-alcohol fixed RAW 264.7 cells and FFPE breast tissue, it would appear the derived monoclonal antibodies do not bind to linear epitopes as presented by these assays. The monoclonals do show good binding to C1q in ELISA and may be pulling down native C1q in immunoprecipitation, results consistent with recognition of conformational epitopes. The unfixed RAW cells did not represent a good source of C1q for antibody binding since C1q is a cytoplasmic protein until stimulated to bind the cell surface. All of these assays performed could benefit from additional trials and optimisation of conditions, especially the quantification of antibody content in solution. These assays were all performed on an exploratory basis and therefore lacked the replicate numbers required for rigorous statistical analysis, another feature that would enhance the finding of these monoclonal antibodies.

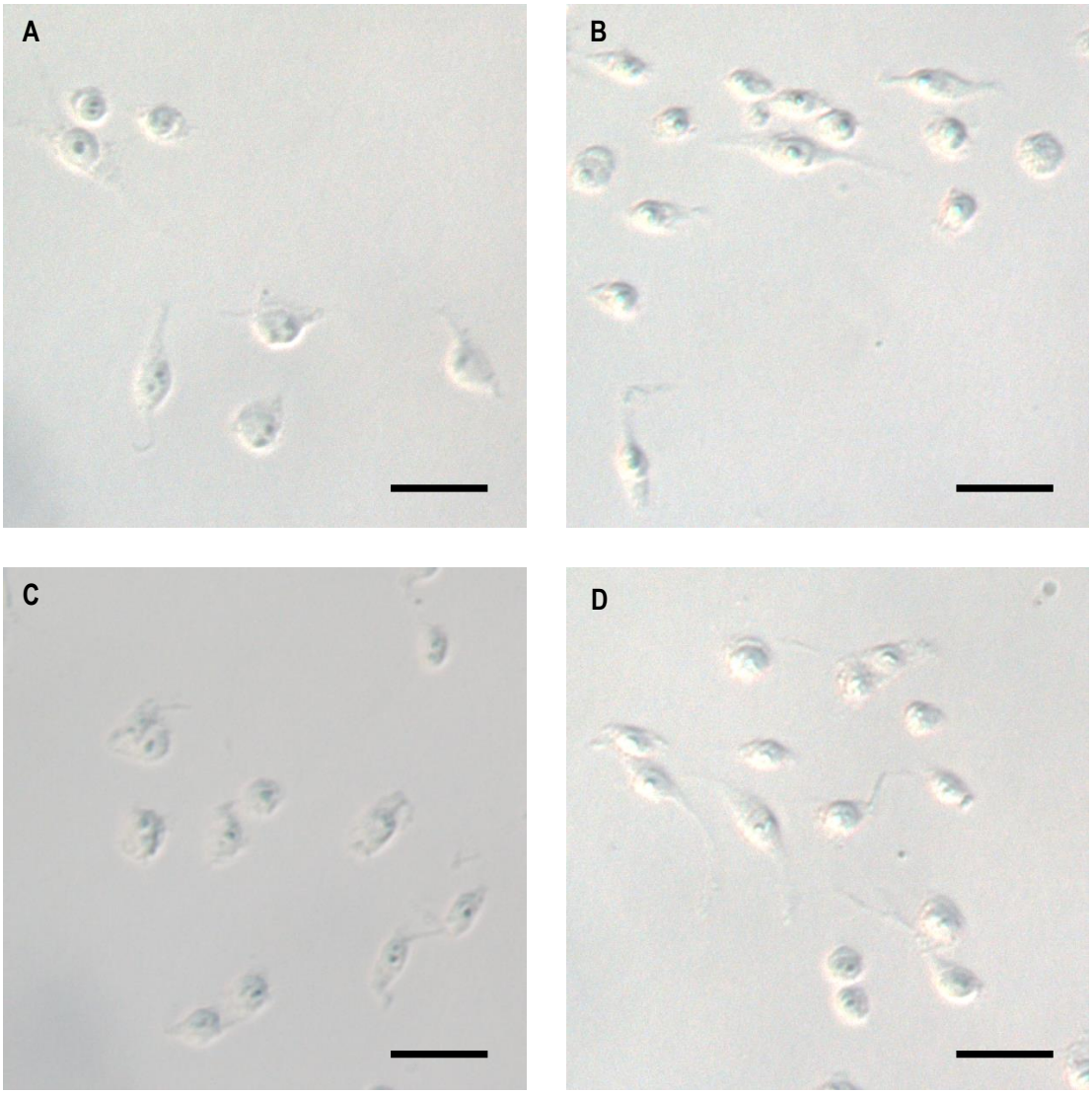

Figure 4.8 Immunocytochemical staining to assess binding capacity of 9A7, BHI1-1G4 and BHI1-4D3 antibodies to unfixed RAW 264.7 cells

Staining for C1q in untreated live RAW 264.7 cells with monoclonal antibodies 9A7 (A), BHI1-1G4 (B), BHI1-4D3 (C), and a no primary antibody control (D). The assay required careful washing between incubations to avoid detaching the unfixed cells. Unlike the acid-alcohol fixed assay, none of the monoclonal antibodies showed any staining of C1q protein. Scale bar is 25 um.

Monoclonal antibody	Isotype
BHI1-1G4	IgG1 κ
BHI1-4D3	IgG1 κ
BHI3-3F6	IgM κ
BHI3-8B9	IgM κ

Table 4.2 Monoclonal antibody isotypes

Isotypes for the monoclonal antibodies generated within this project, as determined by the IsoStrip kit from Roche, expressed as heavy chain type followed by the light chain type.

4.3 Discussion

4.3.1 IMMUNISATION STRATEGY FOR THE PRODUCTION OF ANTI-C1q MONOCLONAL ANTIBODIES

When commencing a project to produce hybridomas to an antigen, it is not possible to know the quality of the immune response that can be produced in mice. In silico models have been devised to predict amino acid sequence elements that will prove to be immunogenic. Particularly useful for peptide-based approaches to immunisation, these models include features such as beta turns hydrophilicity (Chou, 1979), (Hopp, 1981), (Parker, 1986), surface accessibility (Emini, 1985), flexibility (Karplus, 1985), hydropathy (Kyte, 1982) and general antigenicity (Welling, 1985), (Jameson, 1988). Although these methods are at least thirty years old, there are still programs available that use these methods, which are attractive due to their simplicity (http://tools.immuneepitope.org/bcell/). Methods today have the sophistication of biophysics (De Groot, 2020), logistic regression (Lee, 2020), immunoinformatics (Marchan, 2019), and reverse and structural vaccinology (Kulp, 2013), bringing the power of bioinformatics to the tasks of antigenicity and epitope design.

These predictive methods can be of most use when designing immunising peptides to proteins that are highly homologous to the species immunised (Katoh, 1996), (Abbott, 2001) or to direct the immune response to extracellular portions of a protein (Jasinska, 2003). Peptide immunisation can be problematic, depending upon the intended application for the monoclonal. Linear epitopes work well for applications defined by denatured protein but can be poorly cross-reactive to native protein. A useful alternative to peptides for producing monoclonals that react to extracellular protein domains is to inject mice with a syngeneic cell line transfected with the protein of interest, then screen the transfected and host cell lines to find specific monoclonals (Shi, 1995).

Some protein antigens carry a high degree of post-translational modification by way of n- or o-linked glycosylation that can decrease the immunogenicity of protein; thus, removing carbohydrates from immunogens can increase their immunogenicity of protein epitopes (Dowling, 2007). An additional advantage to removing repetitive carbohydrate side chains is to decrease the number of IgM antibodies produced in the immune response. These antibodies are generally of lower affinity and, as such, not as useful as monoclonal reagents (Ragupathi, 1996).

If the constraints of high sequence identity or extracellular localisation are not an issue, the simplest approach is to inject the protein into mice and observe the immune response. Even with this simplistic approach, sequence identity between the immunogen and mouse homologs will impact on the immune response. A protein with ten percent sequence identity to the immunised host will yield a better response than one with ninety percent. The ideal situation would involve immunisation with a protein having no sequence identity to the host animal. This is problematic since, outside of prokaryotic organisms, there are few proteins without homologs as one descends the phylogenetic scale (Taylor, 2004), (Koonin, 2005). However, genetic engineering has allowed scientists to produce mice null for specific protein expression via gene knockout (Zijlstra, 1990) and, more recently, CRIPSR Cas9 technology (Mali, 2013). These mice can be useful for monoclonal antibody production as long as the engineered gene is not essential for development or normal functioning resulting in embryonic or perinatal lethality (Yuan, 2012).

This project was able to take advantage of access to a C1qA null mutant mouse line for use in immunisation. This endeavour was not without its drawbacks, as became obvious as the immunisations progressed. C1q is a pleiotropic protein that is intimately associated with immune function. C1q is vital for the initiation of the classical complement cascade and plays an important role in the removal of dying cells undergoing apoptosis (Lu, 2007), (Galvan, 2012), (Son, 2015). In addition, C1q has immunosuppressive

capacity through direct interaction with T and B lymphocytes as well as dendritic cells (Hosszu, 2012), (Son, 2017). These complex interactions raised some interesting questions. Would C1q injected into C1q knockout mice be sequestered by complement cascade and efferocytosis functions? Would C1q interfere with antigen presentation by dendritic cells? Would C1q suppress the activation of B and T cells during the activation of adaptive immunity?

An attempt was made to explore the sequestration of C1q by c1qA null mice by cross-linking the immunogen with glutaraldehyde. Glutaraldehyde cross-links proteins through primary amines and renders them into a non-native confirmation, a process that eliminates mature function. The glutaraldehyde treatment eliminated the antigenicity of C1q in ELISA and caused the C1q to become turbid in solution with eventual precipitation. Despite the loss of activity, cross-linking did not affect the immunogenicity of C1q (Figure 3.13) adding evidence to the supposition that C1q is not sequestered into innate immune niches in the C1qA mice.

It would not be possible to answer these questions without specifically studying these phenomena; however, the results of the immunisations did shed some light on these points. Many years of experience by the PhD candidate in producing monoclonal antibodies has generated an appreciation of the dynamics of antibody response to immunogens. The immunisation schedule employed had been used many times and typically generated antibody titres to the immunogen in the area of 1:100,000 to 1:1,000,000. Only in one case had this schedule failed to produce an antibody response, which led to the supposition that the immunogen had a strong immunomodulatory effect and suppressed antigen processing and/or antibody production. The immunisations with C1q produced a titre of 1:10,000 with one mouse achieving a titre of 1:100,000. This implied a degree of interference in the formation of an adaptive immune response and in an active manner rather than passively. In other words, it would appear C1q interferes with immune cells directly and is not simply sequestered into its innate immune functions. This suppression of antibody response was not complete; antibodies were stimulated and upon hybridoma fusion, antigen specific clones were identified.

Consistent with the concept of C1q-mediated immune suppression are the isotypes of the antibodies derived from fusion BHI3. The mouse that was the source of the splenocytes for fusion BHI3 had been immunised nine times and yet only yielded specific antibodies of the IgM isotype. IgM antibodies can be specific for antigens with repeating epitopes, such as polysaccharides, but tend to be the product of a primary humoral response (Janeway, 2001). Since C1q does not contain repeating epitopes suitable for binding of pentameric IgM it is more likely the reflection of a primary humoral response. C1q does contain repetitive sequences in the collagen-like tail but the linear arrangement of these potential epitopes would not be conducive to binding by pentameric IgM. IgM can bind protein epitopes but these tend to be restricted to repetitively expressed proteins such as those displayed by virally-infected cells (Gong, 2020). For a mouse boosted with antigen multiple times, this primary response would be consistent with suppression of B cell response or the isotype switching that occurs with subsequent antigenic stimulation.

Also, with regard to isotype, it is interesting to note the relative lack of heavy chain binding by the secondary antibody for BHI3-3F9 and BHI3-8B9 in the immunoprecipitation assay (Figure 4.2) These two antibodies are both IgM isotype and the secondary antibody used for detection was a rabbit anti mouse IgG HRP. This implies during the screening ELISA these two antibodies were detected through their light chains and that an anti-mouse IgG, A and M HRP would have been a better choice for the screening ELISA.

4.3.2 CHARACTERISATION OF THE NATURE OF ANTI-C1q MONOCLONAL ANTIBODY BINDING

Characterisation of monoclonal antibody binding involves the range of assays the antibody will bind in and the nature of the binding relative to the positive control antibody 9A7. The assay depicted in figure 4.1 assessed antibody binding when either antibody or antigen was titrated in the ELISA. Figure 4.1A shows an unremarkable decline in binding for three of the antibodies but did divide the antibodies into two groups based on their decline in binding during titration. On the other hand, Figure 4.1B a regular decline in binding with titration for all of the antibodies. While 4.1A is quite unremarkable, 4.1B clearly shows a titratable binding of the monoclonals to C1q.

Having derived four monoclonal antibodies that bound C1q in ELISA, it was important to confirm the binding of C1q with a different assay. Since pure C1q was used as both immunogen and screening antigen, there was little chance the antibodies did not bind C1q; however, characterisation with a second assay not only confirms binding to the immunogen but also elucidates the types of assays in which the antibodies will likely bind, providing important information regarding the nature of the antigenic epitope recognised.

Basically, the epitope bound by a monoclonal can be separated into one of two categories: linear epitopes or conformational isotopes (Forsström, 2015). Linear epitopes are represented by a contiguous stretch of amino acids, typically eight to eleven residues (Berger, 2016), (Yao, 2020). Assays employing denaturing conditions eliminate conformational epitopes and the binding of antibodies specific for those epitopes (van Essen, 2010), (Hoffman, 2015), (Hobro, 2017). Denaturing assays include the reducing PAGE conditions used for western blotting, and fixation by formalin or alcohols in immunohistochemistry or immunocytochemistry.

The denaturation associated with western blotting ablates antibody activity to conformational epitopes, leaving this as a technique for identifying linear epitopes (Ando, 2004), (Chang, 2019). Inter-chain epitopes are eliminated by definition during reducing PAGE since all disulphide bonds are reduced, the proteins unwound and associated with SDS, necessary for migration towards the electrophoresis anode, followed by transfer to a PVDF membrane. Western blot positive monoclonals are almost always binding linear epitopes.

Immunohistochemistry is not an ideal assay for antibodies binding conformational epitopes. While it is possible for some conformational monoclonal antibodies to bind in immunohistochemistry for ethanol-fixed tissues (Gibbons, 2018), fixation with formalin prior to paraffin embedding is more the standard protocol for this technique. Formalin forms cross-links between the amine groups of proteins, with N-terminal amines and the side chains of cysteine, histidine, lysine, tryptophan, and arginine (Hoffman, 2015). These cross-links distort the conformation of proteins and thereby eliminate conformational epitopes. Even with antigen retrieval breaking of cross-links, binding activity of monoclonal antibodies to conformational epitopes is abrogated (Bogen, 2009).

To avoid the effects of protein cross-linking during fixation, immunocytochemistry was performed on acid-methanol fixed RAW 264.7 cells. Generally, organic solvent fixation denatures protein epitopes, although this can be less severe for antibody binding compared to FFPE with antigen retrieval steps (van Essen, 2010), (Hobro, 2017). In the case of C1q detection, acid-methanol fixation allowed for strong staining by the 9A7 antibody with M1/M2 macrophage phenotype not affecting the intensity of staining. However, there was no detectable staining observed for the BHI monoclonal antibodies, consistent with the premise that solvent fixation had denatured the conformational epitopes the hybridomas presumably bound.

It was then decided to circumvent fixation altogether and stain live cells. Live cell assays work well in ELISA format and immunocytochemistry is essentially an ELISA employing a different substrate. It was therefore disappointing to find that none of the antibodies, not even 9A7, bound in these conditions. This result is fairly easily explained by the fact that C1q was not found to be a membrane bound protein, despite reports of C1q membrane expression (Kaul, 1997), (Ghebrehiwet, 2017). It is found expressed in the cytoplasm, as seen in the fixed immunocytochemistry, and of course is secreted. An alternative method to confirm this observation would be staining frozen tissue embedded in optimal cutting temperature (OCT) compound.

C1q could be secreted and then bind the receptors of its collagen-like tail C91, CD93, calreticulin, or SCARF1 on the macrophage and be available for antibody detection. That this does not appear to be the case suggests C1q does not bind to macrophages until the globular domain has engaged a target molecule. This premise would suggest a model for C1q activity in which soluble C1q binds to target molecules of apoptotic cells while the macrophage responds to the gradient of “find me“ molecules, seeking out the dying cell, engaging the bound C1q and initiating efferocytosis (Arandjelovic, 2017). At this point, the screening ELISA had demonstrated C1q binding activity by the hybridomas. Since the ELISA used pure C1q, there could be little doubt the monoclonals were indeed binding C1q and with each new assay used for characterisation, the evidence was building that the antibodies bound conformational epitopes.

Conformational epitopes can either be a contiguous sequence of amino acids folded into a specific three-dimensional shape, or non-contiguous portions folded into proximity by the tertiary or quaternary structure of the protein (Ando, 2004), (Forsström, 2015), (Ferdous, 2019). Thus, only assays that utilise native protein will be bound by antibodies recognising conformational epitopes, assays such as immunoprecipitation, ELISA or immunoassays on live cells (Keck, 2008). One subset of conformational epitopes is the functional epitope. Binding of antibody to functional epitopes can have the capacity to disrupt the function of the protein *in vitro* and/or *in vivo*. These interactions can further be divided into interactions that disrupt receptor ligand interactions by steric hindrance (Fendly, 1987) and those that disrupt or activate mature function by inducing conformational change in the protein (Goldenberg, 1999), (Vonderheide, 2020). Inhibitory monoclonals are highly prevalent in clinical practice and include antibodies such as Trastuzumab and Pertuzumab that disrupt EGF family signalling through the Her2 protein in breast cancer (Nahta, 2004). An agonist antibody trialled in the clinic is Drozitumab, which activates the TRAIL 2 receptor to induce apoptosis in the target cell (Camidge, 2010).

Since unfixed macrophages were not suitable as a target for C1q binding, another assay had to be found for native C1q. And since an assay using pure C1q would be ideal, immunoprecipitation was selected as the assay to confirm C1q binding by the monoclonal antibodies. The immunoprecipitation used antibody binding of C1q in solution, followed by protein A precipitation, PAGE and western blotting. Since C1q can bind immunoglobulin via the heavy chain, it was necessary to have adequate controls to ensure any C1q precipitated by protein A was bound by the antigen binding site of the antibody and not heavy chain binding through the CH2 domain.

Results showed all four monoclonals and 9A7 pulled down a specific band at 30kD, corresponding to the lane loaded with pure C1q. Also evident were bands at 25 and 50 kD that have been seen before in western blots of C1q. In this instance, the only proteins present in the assay were C1q, immunoglobulin and protein A, thereby confirming that the bands bound by the rabbit anti-mouse IgG HRP secondary antibody were indeed heavy and light chain from IgG. The non-specific control antibody, anti-S100 A8, had the heavy and light chain bands and a faint band at 30kD. The faint band could be either C1q binding antibody heavy chain or C1q binding protein A non-specifically. The no primary antibody lane had a comparable faint band at 30 kD showing that this band is likely non-specific binding of C1q to protein A.

This is also consistent with the fact that C1q binding to IgG heavy chain would likely sterically hinder access of protein A to the same region of the antibody.

In the immunoprecipitation assay, all four monoclonals bound to a 30 kD band indistinguishable from the band detected by 9A7. This brought up the interesting point that Cq1 is composed of A, B and C chains with molecular weights of 29, 27, and 23 kD respectively (Thielens, 2017). These three different bands are distinguishable on western blots, implying the four derived monoclonals, like 9A7, were all binding the C1qA chain. This suggested the immune response may not be equally distributed among the three chains, rather the C1qA chain may be the immunodominant protein driving the antibody response in B cells. Some credibility for this argument could be found in the sequence sequence identity between human and mouse C1q with C1qA having the lowest sequence identity : A chain = 70.6%, B chain = 78.8%, and C chain = 73.6% (Blast protein alignment at www.uniprot.org). However, the antibodies were produced in C1qA null mice, which would skew the immune response towards the C1qA chain. The anti-C1q antibody 9A7 used extensively in these studies as a positive control antibody binds C1qA, which could indicate C1qA is more immunogenic in whole C1q immunisation, but without information concerning the derivation of this antibody no definitive conclusions can be drawn. To determine if C1qA epitopes in intact C1q are more immunogenic would require extensive study through antigenicity modelling and immunisation. Epitope mapping of antibody binding sites and three-dimensional modelling of native C1q could be helpful in clarifying this observation.

Another essential characteristic affecting the function of the antibodies is the isotype. Most monoclonal antibodies are IgG isotypes with IgM isotypes being uncommon and IgAs unheard of (personal observation). IgM antibodies tend to have lower affinity than IgGs and more commonly directed against repetitive sequences such as carbohydrates which pentameric IgMs bind with high avidity. IgA-secreting B cells are associated with immunity in mucosal tissues and their distribution is limited to the mucosal and gut-associated lymphoid tissue (MALT and GALT) and therefore do not traffic to the spleen (Janeway, 2001).

IgG isotypes direct various functions *in vivo* based on their binding to different Fc receptors; however, the capacity for neutralisation is more reliant on affinity since Fc binding is not required to block protein function. For *in vitro* assays, isotype is most relevant for the selection of an isotype control antibody for the accurate determination of neutralisation capacity. Prediction of the efficacy of IgM antibodies in blocking efferocytosis is difficult. IgMs could be less useful since their affinities tend to be low, making their antigen binding less stable. Alternatively, IgMs could employ their multiple antigen binding sites to attach to C1q immobilised to a target cell in the manner of high avidity binding to bacterial targets. IgM binding would be subject to steric hinderance by other monoclonals competing for C1q binding as well as the distribution of C1q bound to the cells surface. These factors are applicable only to the assessment of *in vitro* binding since, as mentioned in section 4.2.6, antibodies selected for clinical application are invariably humanised.

CHAPTER FIVE: DEVELOPMENT OF AN *IN VITRO* EFFEROCYTOSIS ASSAY

5.1 INTRODUCTION

Apoptosis is an essential mechanism for removing cells that are senescent, damaged, or no longer required in the body (Elmore, 2007), (Erwig, 2007). The phagocytic uptake of dying cells, a process called efferocytosis, is a vital function in the body. Efficient efferocytosis prevents apoptotic cells progressing to necrosis with the resultant release of pro-inflammatory factors that can provoke undue and potentially harmful inflammation(Ortega-Gómez, 2013), (Liang, 2014). This is particularly important since persistent self-antigens from dead cells can be taken up by antigen presenting cells in the presence of inflammatory leukocytes, leading to inappropriate stimulation of self-reactive B and T cells (Walport, 1998). Depending on the tissue involved, anti-self immune activity can lead to an array of chronic autoimmune diseases that are difficult to treat (Katsumata, 2011).

Thus, the efficient engulfment of dying cells is important for the maintenance of an appropriate immune response solely directed at foreign antigens. Professional phagocytes, primarily myeloid lineage monocytes, macrophages, and neutrophils, are able to bring about rapid and efficient efferocytic uptake of dying cells (Han, 2016). Of these cells the predominant phagocyte is the macrophage, whether as resident macrophages or macrophages derived from monocytes recruited from the circulation (Ingersoll, 2011), (Crane, 2014), (Das, 2015). Other cell types such as epithelial cells and fibroblasts can act as non-professional phagocytes; however, these cells are much less efficient and have a greater lag time for uptake of apoptotic cells compared to professional phagocytes (Atabai, 2007), (Arandjelovic, 2015), (Han, 2016).

The most important element responsible for this difference in the kinetics of efferocytosis is the array of receptors displayed on the phagocyte. Efferocytic receptors known to be important on macrophages include CD91 (Duus, 2010), (Basu, 2001), calreticulin (Duus, 2010), (Vandivier, 2002), (Basu, 2001), (Ogden, 2001), CD93 (Norsworthy, 2004), (Lu, 2008), and SCARF1 (Murshid, 2016), (PrabhuDas, 2017), (Patten, 2018), (Ramirez-Ortiz, 2017), all of which are capable of binding complement protein C1q. Other molecules are also able to bind apoptotic cells, such as MerTK (Seotz, 2007), (Crane, 2014) TIM4, BAI1, and stabilin-2 (Ravichandran, 2011) and RAGE (He, 2011). However, C1q appears to be an essential component for efferocytosis. Depleting macrophages during mammary regression results in a net build-up of apoptotic cells in the senescent mammary gland (Chua, 2010). Similarly, mice null for C1q expression also accumulate apoptotic cells in regressing mammary tissue (Noor Din, 2017). Deletion of MerTK will also lead to accumulation of dying cells, however expression of MerTK is not sufficient to rescue efferocytic function in mice lacking C1q (Santulli-Marotto, 2015).

Efferocytosis limits inflammation in cycling mammary tissue through two mechanisms. First, by removing dying cells before they can become necrotic and attract inflammatory leukocytes; and second, by secretion of anti-inflammatory cytokines such as IL10 and TGFB by phagocytes (Ortega-Gómez, 2013), (Brady, 2016). In addition, C1q can modulate immune function through binding to LAIR1, thereby inhibiting the maturation of dendritic cells, disrupting antigen presentation, and inhibiting Th1 T cell activation (Son, 2012), (Son, 2017), (Kouser, 2015). This anti-inflammatory environment during mammary regression is transitory and resolves as the mammary gland remodels back to its basal architecture (Chua, 2010), (Hodson, 2013).

Although C1q-mediated protection of the mammary gland from inflammation during regression can be beneficial, there is also a downside to this anti-inflammatory microenvironment. Carcinogens injected during proestrus provoke more tumours than injection during diestrus, with the implication that the regression phase is more susceptible to the early events of tumour formation than the proliferation phase (Nagasawa, 1976), (Ratko, 1985). Further studies in mice suggest the anti-inflammatory environment of the regressing mammary gland suppresses the ability of the immune system to detect and eliminate nascent neoplastic cells (Hodson, 2013).

Tying the role of C1q-mediated efferocytosis to the process of onconeogenesis, it has been shown the incidence of DMBA carcinogen-induced mammary tumours in C1qA null mice was seven-fold less than in C1q replete mice (Noor Din, 2017). Similarly, in a mouse model of mammary cancer employing the mammary-specific MMTV promoter driving the polyoma middle T oncogene, C1qA null mice developed half the tumour burden and one third the advanced carcinoma stage seen in C1q replete mice (Noor Din, 2017). These observations support the hypothesis that abrogation of C1q activity can inhibit the establishment of cancers during ovarian cycling. In turn, this could represent the basis for a novel treatment for breast cancer, especially in triple negative breast cancers that lack the receptors that are the basis for targeted therapeutic intervention.

Small molecule inhibitors are potential therapeutic agents capable of interrupting the activity of a variety of disease-mediating molecules, and some have been directed to C1q (Roos, 2001). However, when choosing an approach for the generation of a C1q inhibitor, production of monoclonal antibodies represented a more accessible option and one that has produced numerous therapeutic agents present in the clinic today (Goldenberg, 1999), (Hatano, 2019), (Wang, 2018), (Nahta, 2004). Monoclonal antibody generation entails the immunisation of mice followed by fusion of immune splenocytes with a mouse myeloma cell line (Köhler, 1975), (Fendly, 1987). The resultant hybridomas can be screened against the immunogen by a variety of assays, but typically ELISA represents the most practical option.

Having performed hybridoma fusions and identified monoclonal antibodies that recognised the C1q immunogen, a bioassay was required to measure its capacity to neutralise C1q function. While the DMBA-treated and PyMT mouse models have been used to study function of C1q during mammary carcinogenesis, *in vivo* modelling would be an impractical system for the assessment of candidate monoclonal antibody inhibitors. Ideally, an *in vitro* assay with a quick turn-around time would be best suited for assessing C1q neutralisation. Assays developed to study the classical complement cascade function of C1q utilise IgG-opsonised sheep red blood cells with red cell lysis as the positive readout for C1q function (Roos, 2001). However, an assay measuring inhibition of C1q in efferocytosis is more relevant for assessing the ability of monoclonal antibodies to interrupt this function-specific role of C1q.

The aim of this chapter was to develop a bioassay to assess the capacity of novel monoclonal antibodies to neutralise C1q-mediated efferocytosis of dying cells. Bone marrow-derived macrophages and the macrophage cell line RAW 264.7 were explored as phagocytes for the bioassay. Methods of induction of apoptosis were investigated in two different breast cancer cell lines. In macrophage-cancer cell co-cultures, macrophages were tagged with a green fluorescent dye while the cancer cells carried a red fluorescent marker. Efferocytic activity was quantified through measurement of the overlap of the red and green signals as assessed by the image processing package FIJI.

5.2 RESULTS

5.2.1 ANALYSIS OF APOPTOSIS IN BREAST CANCER CELL LINES T47D AND MDA-MB-231

The first step in development of the *in vitro* efferocytosis assay was to investigate a method of reliably inducing apoptosis in a breast cancer cell line. T47D is a hypotriploid ductal breast carcinoma line derived from a metastatic pleural effusion and bears receptors for estrogen and progesterone (ATCC: www.atcc.org). Protocols for induction of apoptosis that were investigated included two methods for activation of intrinsic apoptotic pathways – ultraviolet (UV) irradiation and doxorubicin treatment, and one method for inducing extrinsic apoptosis – hormone withdrawal followed by tamoxifen treatment.

UV radiation damages DNA through the formation of purine:purine dimers (Rastogi, 2010). These dimers interrupt the DNA replication machinery during mitotic S phase, such that apoptosis is initiated during the G1/S phase transition. Doxorubicin, an anthracycline chemotherapeutic agent, intercalates into DNA and interferes with topoisomerase II ligation of DNA strand breaks and chromatid segregation during S phase, leading to apoptotic cell death (Thorn, 2011). T47D is an estradiol-dependant cell line and thus can be induced to undergo apoptosis by treatment with tamoxifen, a selective estrogen receptor modulator (SERM) that antagonises signalling through the estrogen receptor (Zheng 2007).

Cell death was assessed by flow cytometry. Following induction of apoptosis, the cells were stained with Annexin V (AnV) FITC, which binds the early apoptosis marker phosphatidylserine on the outer membrane envelope, and/or propidium iodide (PI), which binds DNA in cells with non-intact cell membranes. Apoptotic cells were AnV positive but PI negative, while necrotic cells were both AnV and PI positive. To detect late apoptosis, end-labelling of DNA with BrDU was used to detect DNA breaks occurring in cells undergoing apoptotic chromatin fragmentation. UV and doxorubicin-treated cells were serum starved to synchronise the cells in G1 phase of the cell cycle. This approach was not successful in generating reliable apoptosis as inter-assay variability was high. Each experiment exhibited a different pattern of early and late apoptosis over a different time course which might have been dependent on the confluence of the cell culture (data not shown). In addition, the T47D cells tended to detach from the plate as they underwent apoptosis which would make it difficult to assess efferocytosis by macrophages.

Analysis of apoptosis next focussed on the cell line MDA-MB-231 TXSA-S, an aneuploidy/near triploid breast cancer line from a metastatic pleural effusion, which is negative for estrogen, progesterone, and HER-2 receptors (i.e., triple negative phenotype). MDA-MB-231 carries the Death Receptor 5 (DR5) that, upon binding TRAIL, assembles the death-inducing signalling complex and induces extrinsic apoptosis in the target cell (Elmore, 2007). Drozitumab, a monoclonal antibody to DR5 mimics the binding of TRAIL and acts as a reproducible trigger for apoptosis (Zinonos, 2009). Drozitumab induced apoptotic membrane blebbing within one hour of treatment in MDA-MB-231 cells with the cells remaining attached to the plate (Figure 5.1). This result was far more reproducible than studies using T47D breast cancer cells. In addition, Drozitumab treatment did not produce membrane blebbing in T47D cells that lack the DR5 receptor (data not shown).

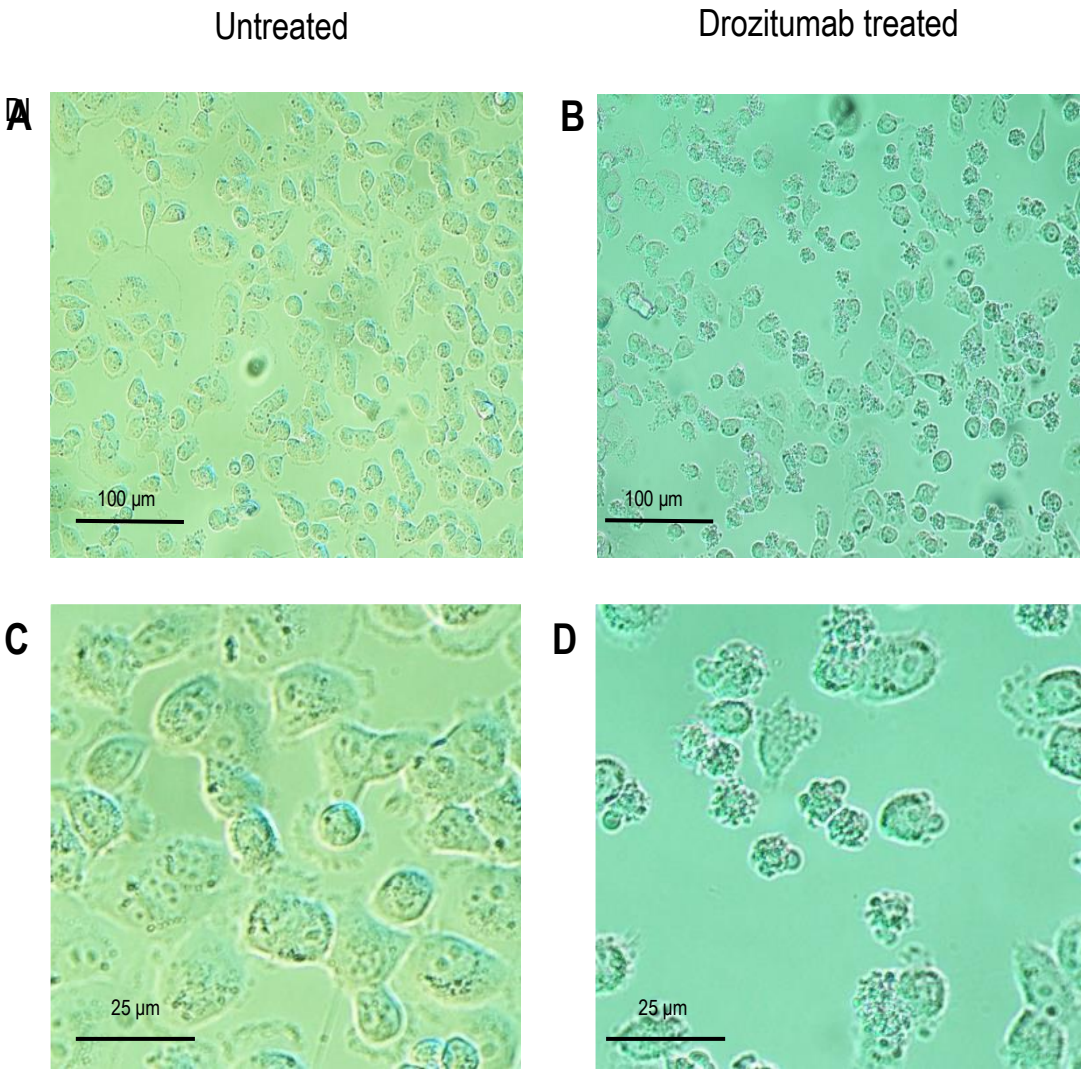

Figure 5.1 Induction of apoptosis with Drozitumab

Confluent MDA-MB-231 cells were treated with varying concentrations of Drozitumab cross-linked with goat anti-human Fc receptor. (A) and (C) show untreated MDA-MB-231 cells. (B) and (D) show MDA-MB-231 cells treated with 40 ng/ml of Fc cross-linked Drozitumab, all after two hours. (D) shows the characteristic membrane blebbing seen in apoptosis. (A) and (B) were taken on a Nikon TE 2000 with a 20x objective, images (C) and (D) with a 40x objective. All four images employed differential interference contrast (DIC) optics.

5.2.2 INVESTIGATION OF AN EFFEROCYTOSIS ASSAY USING THE MDA-MB-231 BREAST CANCER CELL LINE AND MOUSE BONE MARROW MACROPHAGES BY CONFOCAL MICROSCOPY

Bone marrow isolated from MacGreen mice was treated with CSF1 to differentiate macrophage/dendritic progenitor cells into macrophages, a process requiring seven days. MacGreen mice express green fluorescent protein (GFP) driven by the myeloid cell-specific c-fms (CSF-1 receptor) promoter in macrophages. The breast cancer cell line MDA-MB-231 expressing red fluorescent protein (RFP) was added to the macrophage cultures and co-cultured overnight. The following day, the co-culture was treated with 100 ng/mL cross-linked Drozitumab to induce apoptosis in the cancer cells. Images were then taken on a Zeiss LSM700 confocal microscope over a course of six hours (Figure 5.2). Prior to Drozitumab treatment (0 hours), macrophages exhibited a dendritic morphology. Following 6 hours of treatment, the macrophages appeared rounded and the cancer cells exhibited membrane blebbing. There was also evidence of efferocytosis of cancer cells by macrophages, shown by colocalisation of green and red fluorescence.

In order to develop a method of quantifying the impact of C1q inhibition on the rate of efferocytosis, bone marrow-derived macrophages from wild type C57Bl/6 mice and C1q null mutant mice on a C57Bl/6 background were compared for their ability to efferocytose apoptotic MDA-MB-231 cells. Mouse macrophages were labelled with green fluorescent cell tracker and apoptosis was induced with Drozitumab treatment of RFP-labelled MDA-MB-231 cells. The two co-cultures were observed by confocal microscopy and appeared similar prior to Drozitumab treatment (0 hour; Figure 5.3). However, following 6 hours of treatment, co-cultures that contained macrophages derived from C1q replete mice exhibited colocalisation of red and green fluorescence indicative of efferocytosis, while C1q null macrophage co-cultures developed a build-up of apoptotic red fluorescent breast cancer cell fragments with little colocalisation of red and green fluorescence (6 hours; Figure 5.3). This result suggested the co-culture experimental approach was effective in demonstrating a difference in C1q-mediated efferocytosis and thus could be used to investigate quantification approaches that measure the rate of efferocytosis.

Co-cultures using macrophages derived from either C1q replete or null mice labelled with green fluorescent cell tracker, together with RFP-labelled MDA-MB-231 cells induced to undergo apoptosis with Drozitumab treatment were imaged over a period of 6 hours. The confocal microscope was programmed to image eight defined areas in each co-culture well every 20 minutes. Colocalisation of green and red signal as a measure of efferocytosis utilised FIJI software that analysed digital images, using masks and Boolean logic. Boolean logic is derived from operations in algebra to compare two sets of data, frequently expressed as Venn diagrams. Boolean logic allows the comparison of two data sets through the commands ADD (include all data from both sets), NOT (exclude all areas of data overlap) or AND (determine areas of overlap between the sets). The two-colour image was split into green and red channels and a threshold algorithm was applied to each channel to digitise the signal and a digital mask of the channels was created (Figures 5.4 and 5.5). The masks were compared using the Boolean operator AND to find the areas of overlap. The efferocytic index is the ratio of the area of overlap over the area of the macrophages. The average efferocytic index of the eight fields of view for each time point was calculated.

Analysis of efferocytosis in 20 minute intervals over the 6 hour time period demonstrated a high level of variability, with peaks and troughs observed from one time point to the next (Figure 5.6). Through observation of the confocal images, it was clear that the images varied in fluorescence intensity due to a shifting focal plane, background fluorescence, and some regions of the culture exhibiting higher density of cells than others. To minimise this variability, the four fields showing the highest density of cells for each time point were selected from the eight fields of view and the green macrophage images from three adjacent time points were processed with the Boolean operator ADD to merge the images taken over 60 minutes into one. The signals from the MDA-MB-231 cancer cells were processed to minimise the impact of the higher background fluorescence in the images. Three adjacent time points were processed with the Boolean operator AND that subtracts fluorescence not common to the images, thereby leading to a truer signal of the cellular fluorescence. The optimised macrophage and cancer cell images were then processed with the operator AND to determine the area of signal overlap to quantify colocalisation as a

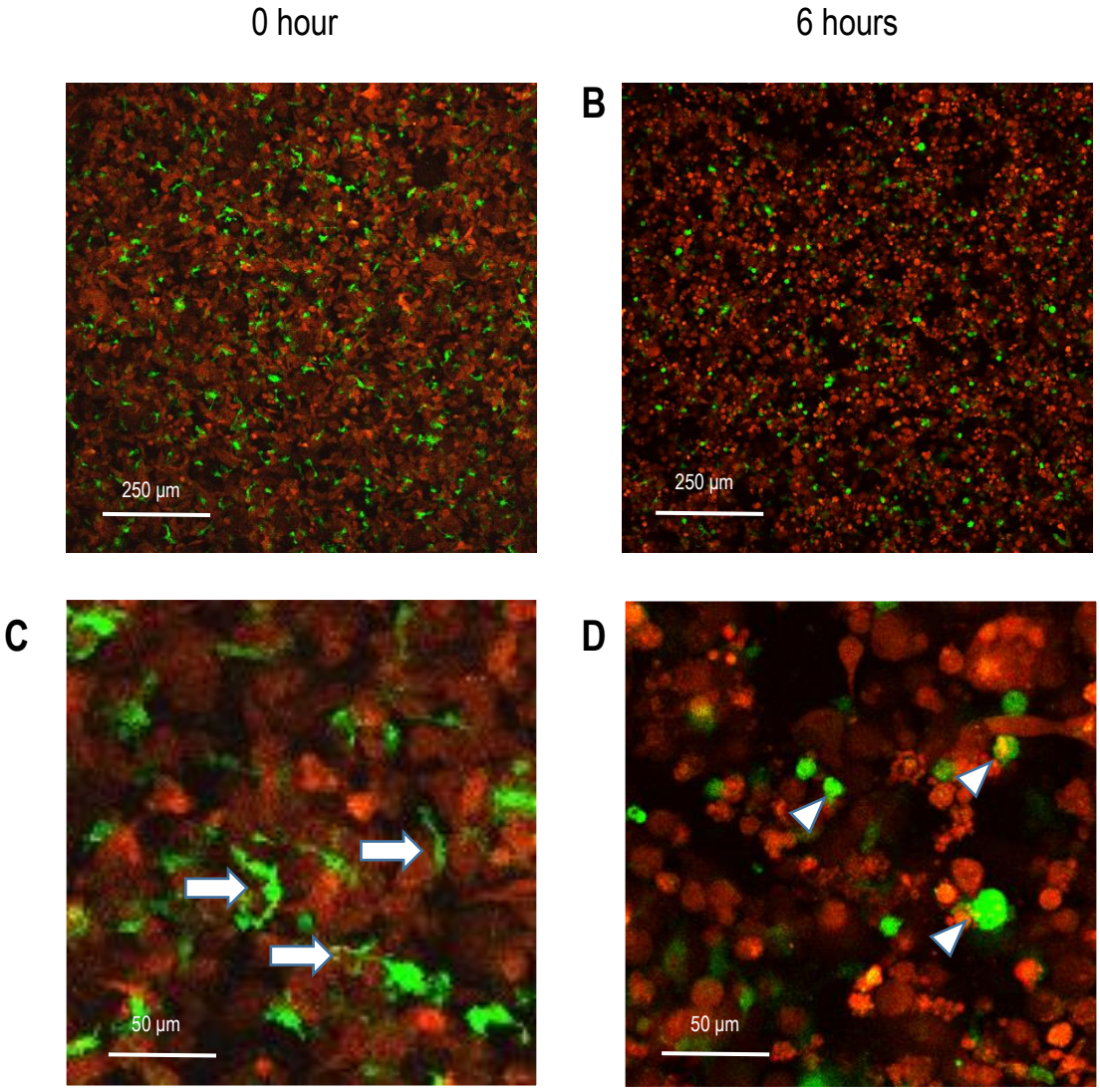

Figure 5.2 Efferocytosis assay image on the Zeiss LSM700 confocal

A confocal image showing the set-up of an efferocytosis assay. GFP-expressing MacGreen bone marrow-derived macrophages were co-cultured overnight with the RFP-expressing human breast cancer cell line MDA-MB-231. Treatment of the co-culture with cross-linked Drozitumab induced apoptosis in the cancer cells and images were taken at 0 hour ((A) and (C)) and 6 hours.((B) and (D)). Image (C) shows the dendritic morphology of the green macrophages at 0 hour (arrows). Image (D) shows the rounding of the green macrophages at 6 hours (arrowheads). Image (D) illustrates the rounding and blebbing of cancer cells undergoing apoptosis at 6 hours. (A) and (B) were taken on a Zeiss LSM700 confocal microscope at 10x power, (C) and (D) are a digital zoom of 10x images.

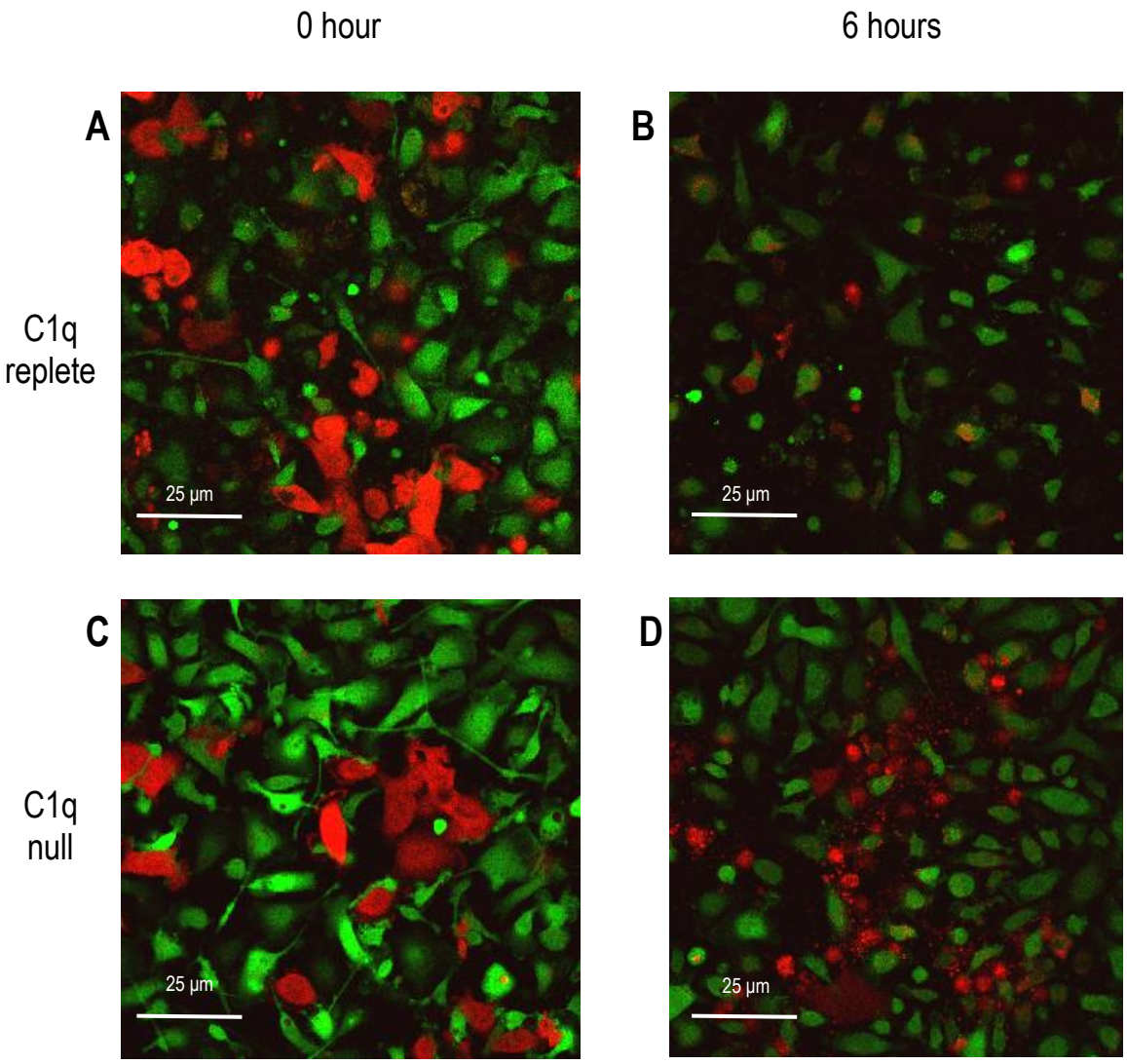

Figure 5.3 Contrasting the efferocytosis by C57Bl/6 and C1q null macrophages

Bone marrow-derived macrophages from C57Bl/6 and C1q null mice labelled green with CellTracker, co-cultured with MDA-MB-231 RFP cells and treated with Fc cross-linked Drozitumab to induce apoptosis. At zero hour, macrophages from C57Bl/6 (A) and C1q null mice (C) do not differ appreciably in appearance. However, at six hours the C57Bl/6 macrophages (B) appear to have efficiently engulfed dying cancer cells in contrast to the C1q null macrophages (D) surrounded by fragments of dead cancer cells that have not been phagocytosed.

- File: open
- Image: colour: split channels
- Select green channel
- Image: adjust: threshold: Li
- Analyse: measure
- Select red channel
- Image: adjust: threshold: triangle
- Process: image calculator
- Select c1 and c2
- Select operator: AND
- Tick create new window box and hit OK
- Analyse: measure
- Efferocytic index = area of overlap/area of green mask

Figure 5.4 FIJI commands for co-localisation analysis

The series of FIJI commands used for the calculation of co-localisation. The commands are found in various drop-down menus found on the FIJI tool bar, along with pop-up boxes. Final calculation of efferocytic index (Co-localised area/macrophage area) was performed in Microsoft Excel.

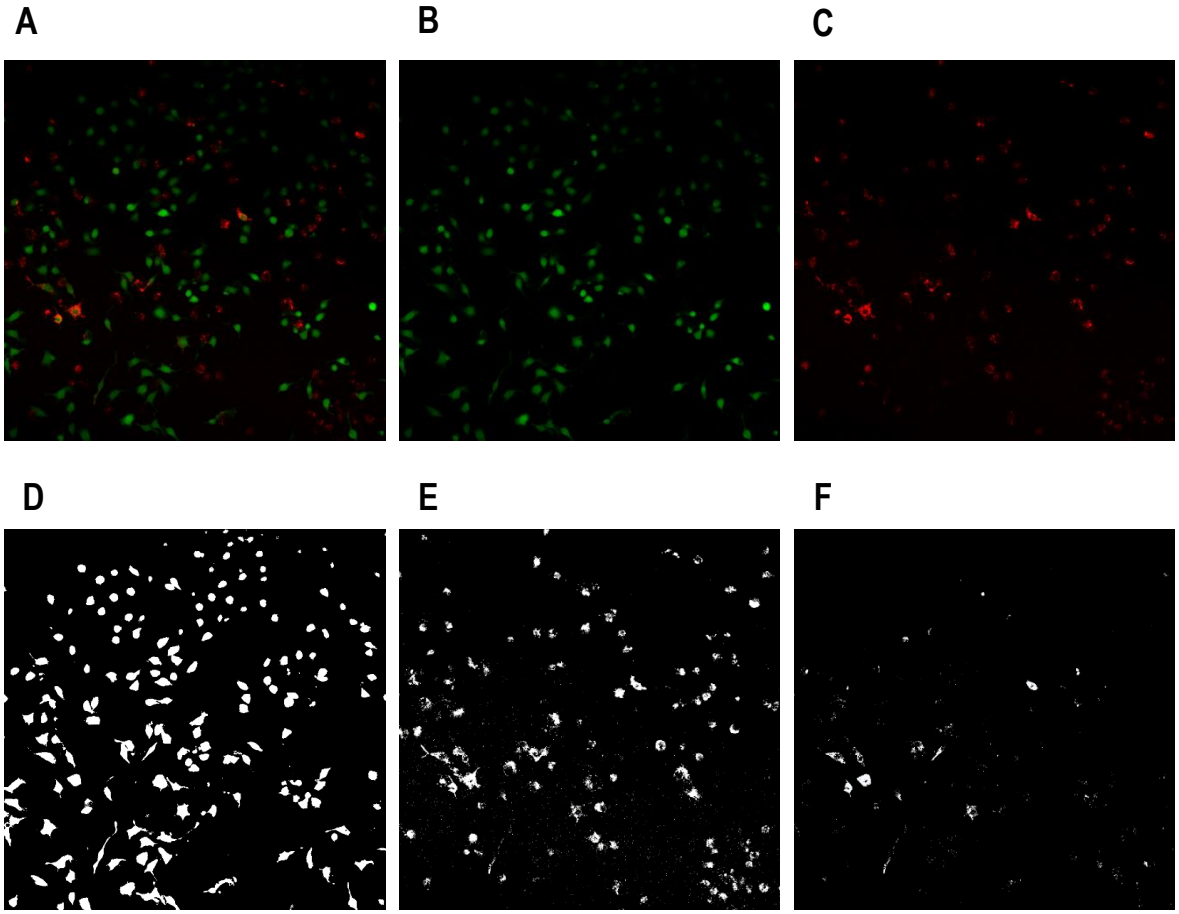

Figure 5.5 Boolean logic in efferocytosis analysis

An illustration of the FIJI image processing described in Figure 5.4. A two-colour image (A) of green macrophages and red breast cancer cells is split into individual green (B) and red channels (C). FIJI thresholds are applied to produce a digital mask for each channel (D) and (E). The masks are processed by the Boolean operator AND to derive the area of overlap for the two channels (F). The area of the overlap is expressed as a proportion of the total macrophage area to derive the efferocytic index.

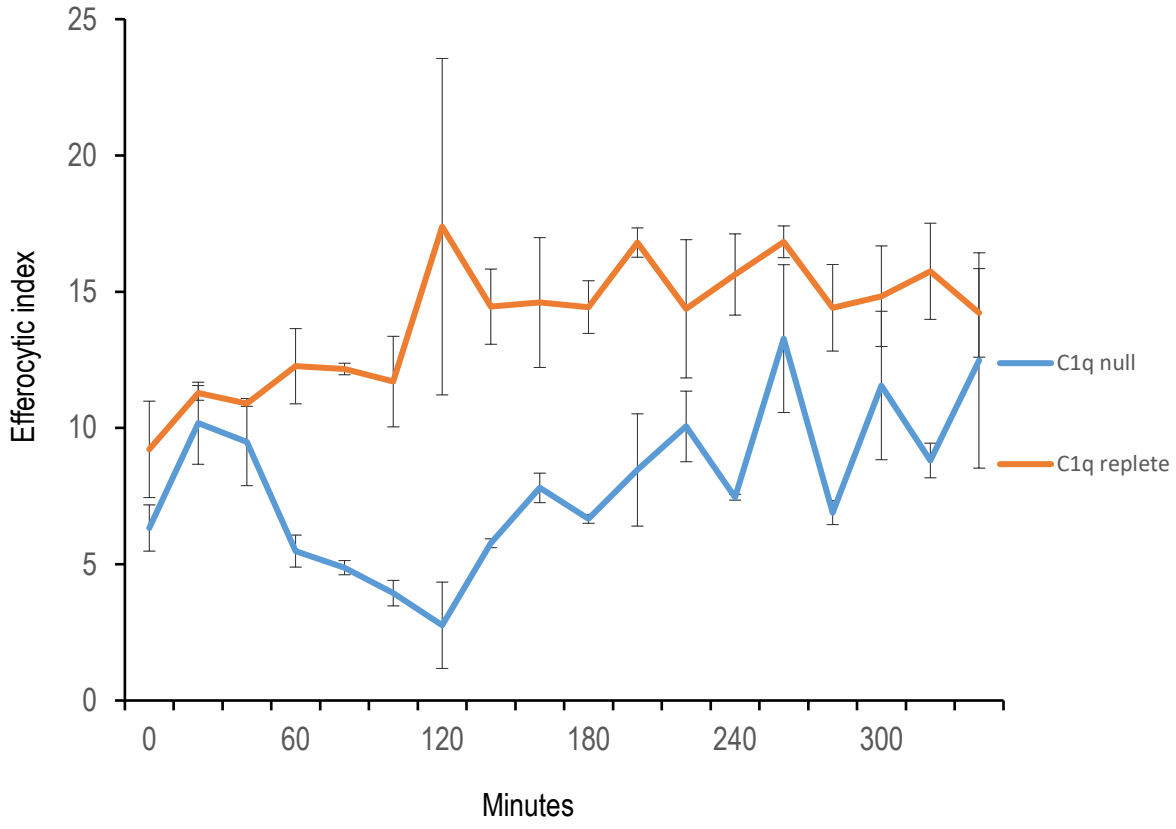

Figure 5.6 Comparison of efferocytic activity of C57Bl/6 C1q replete and C1qA null macrophages

Plots of fluorescence signal colocalisation representing efferocytic activity for both C1q replete and C1q null mutant macrophages showed a high degree of variability. Averaging of two adjacent time points dampened the amplitude of the variation and produced a plot of enhanced apoptotic uptake by the C1q wild type macrophages. The high degree of error seen in the C1q replete culture at 120 minutes is due to an obvious outlier value that was included for consistency.

proportion of macrophage area over 60 minute time intervals. This approach overcame the inherent noise and variability in the confocal imaging and produced a result that showed a clear difference in rate of efferocytosis between macrophages derived from C1q replete and C1q null mice (Figure 5.7). This method of quantification demonstrated increased rate of uptake of apoptotic cancer cells by macrophages derived from C1q replete mice compared to those derived from C1q null mice, consistent with the visual assessment of the two-colour images (Figure 5.3).

5.2.3 INVESTIGATION OF AN EFFEROCYTOSIS ASSAY USING THE MDA-MB-231 BREAST CANCER CELL LINE AND RAW 264.7 MACROPHAGE CELL LINE BY CONFOCAL MICROSCOPY

5.2.3.1 Activation of RAW 264.7 macrophages to M1, M2a, and M2c phenotypes

Having developed a quantifiable means of assessing the rate of efferocytosis using RFP-labelled MDA-MB-231 breast cancer cells induced to undergo apoptosis with Drozitumab, a different source of macrophages for the bioassay was sought. While bone marrow-derived mouse macrophages were useful in development of the quantification approach, the generation of the macrophages relied upon availability of mice and a seven day procedure using L-cell supernatant as a source of cytokines for macrophage differentiation. The mouse cell line RAW 624.7 is a monocyte/macrophage cell line transformed by the Abelson murine leukaemia virus. RAW 264.7 has been shown to express fewer Fc receptors than the mouse macrophage line J774A.1 (Verma, 2009), which would minimise the role of Fc -mediated effects in the assay. RAW 264.7 was anticipated to be a better source of macrophages to mediate efferocytosis in the bioassay than bone marrow-derived mouse macrophages.

At this time, the red dye for labelling the MDA-MB-231 cells was changed to pHrodo. pHrodo becomes more brightly fluorescent when in acidic conditions. Since phagocytosed apoptotic cells are processed through acidic lysosomes, it was considered that this would better reflect engulfed cells and lower non-specific red background.

To investigate RAW 264.7 cells for the bioassay, the impact of macrophage differentiation into different macrophage phenotypes on efferocytosis was first assessed. Alternatively activated or M2 macrophages are the primary cells involved in efferocytic uptake of dying cells and these cells were compared to classically activated or M1 macrophages and resting macrophages (Das, 2015). Overnight stimulation with cytokines mimicked the different phenotypic states macrophages express *in vivo*. Cytokine treatments to induce phenotypic modulation included: M0 (untreated), M1 (LPS + IFN-G), M2a (IL-4) and M2c (TGF-B). Untreated RAW cells were ostensibly considered to be M0, but as a virally transformed cell this may well not be the case. The untreated, M2a, and M2c cells did not differ appreciably in morphology; however, the M1 cells differed markedly from the other conditions. M1 cells adopted a flattened morphology with numerous vacuoles throughout the cytoplasm, which resembled small pits under differential interference contrast microscopy (Figure 5.8). The rate of efferocytosis of apoptotic MDA-MB-231 cells was investigated in treated and untreated RAW macrophages. The confocal images were captured at two hour intervals for the first eight hours and again at 24 hours, to observe any residual efferocytosis. The efferocytic index peaked at 4 hours for all co-cultures, with the highest rate of efferocytosis occurring in untreated cells (Figure 5.9). Untreated cells were subsequently used to assess inhibition of efferocytosis by the monoclonal antibodies.

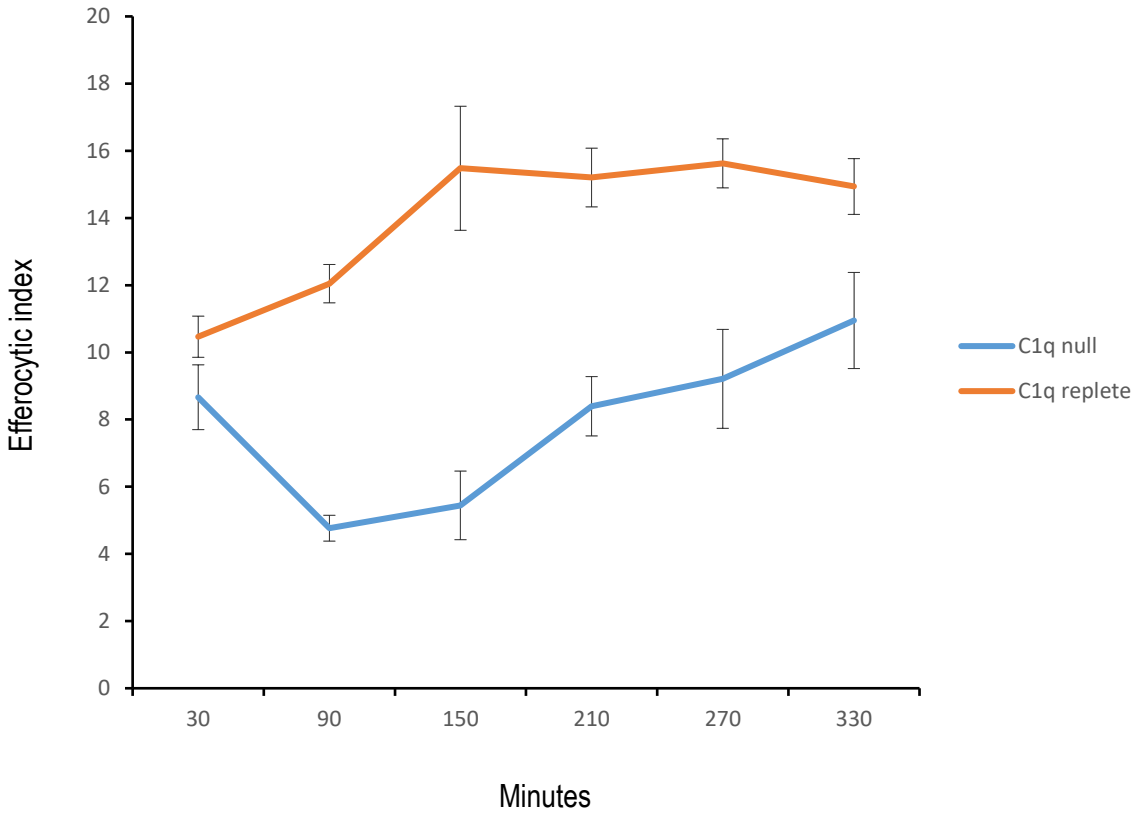

Figure 5.7 Smoothing C1q replete vs C1q null data into sixty minute blocks

Green macrophage images were processed by the Boolean ADD to merge three images taken over sixty minutes into one. The signals from the red cancer cells were processed by the Boolean AND to minimise background fluorescence. The green and red images were then processed by the operator AND to determine the red/green signal overlap. This analysis demonstrated an increased rate of efferocytic uptake by macrophages from C1q replete mice compared to C1q null mice, consistent with the visual assessment of the two-colour images (Figure 5.3).

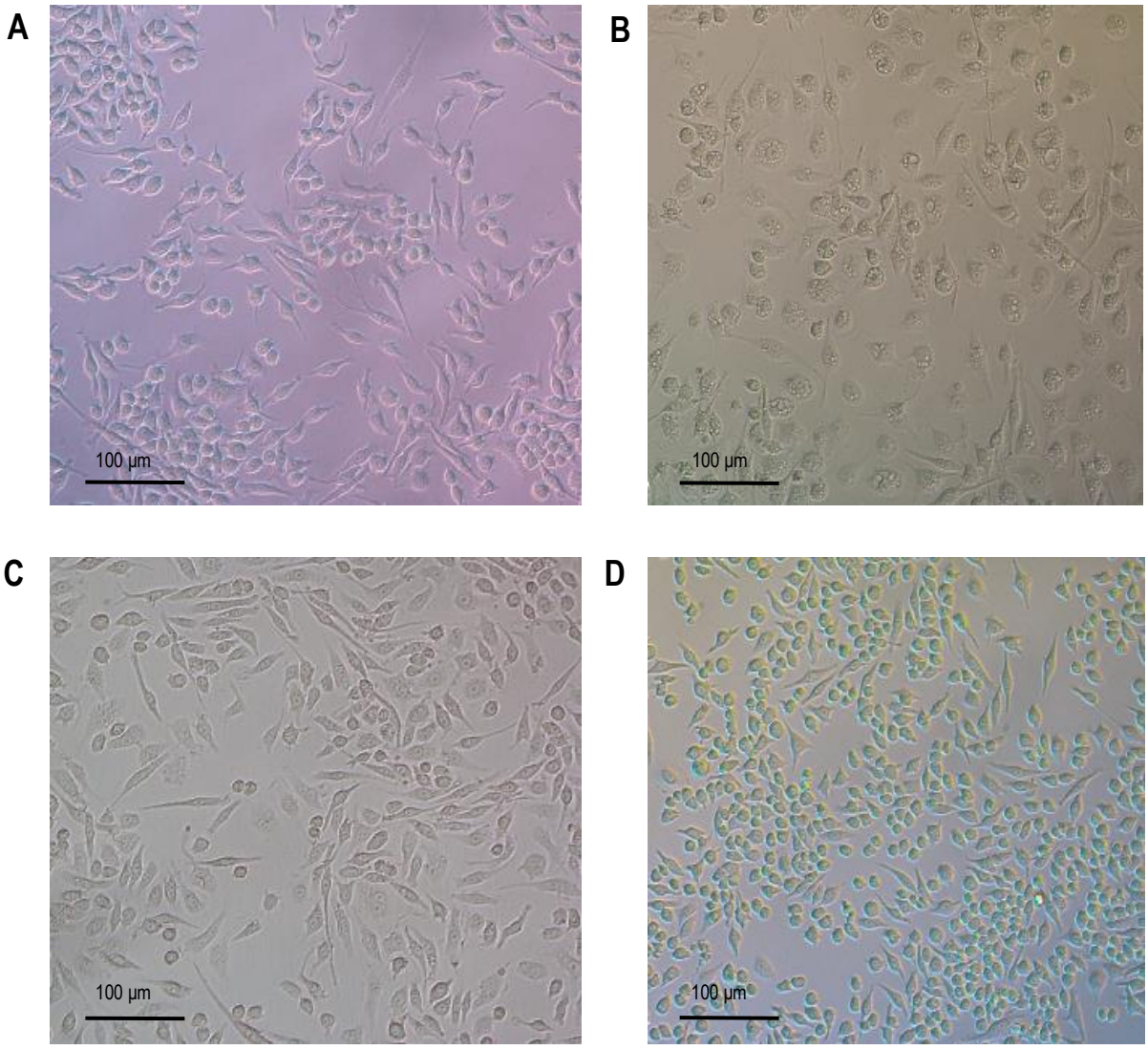

Figure 5.8 Morphology of different RAW 264.7 phenotypes

Different phenotypes produced with cytokine treatment overnight: (A) M0 with no treatment, (B) M1 with 200 ng/ml LPS + 20 ng/ml IFN-G, (C) M2a with 20 ng/ml IL-4, and (D) M2c with 40 ng/ml TGF-B. The appearance of M0, M2a and M2c cells was indistinguishable; however, the M1 cells adopted a more rounded and flattened phenotype. In addition, M1 cells contained multiple vacuoles or inclusions that gave them a pitted appearance. Images taken on a Nikon TE2000 at 10x power with

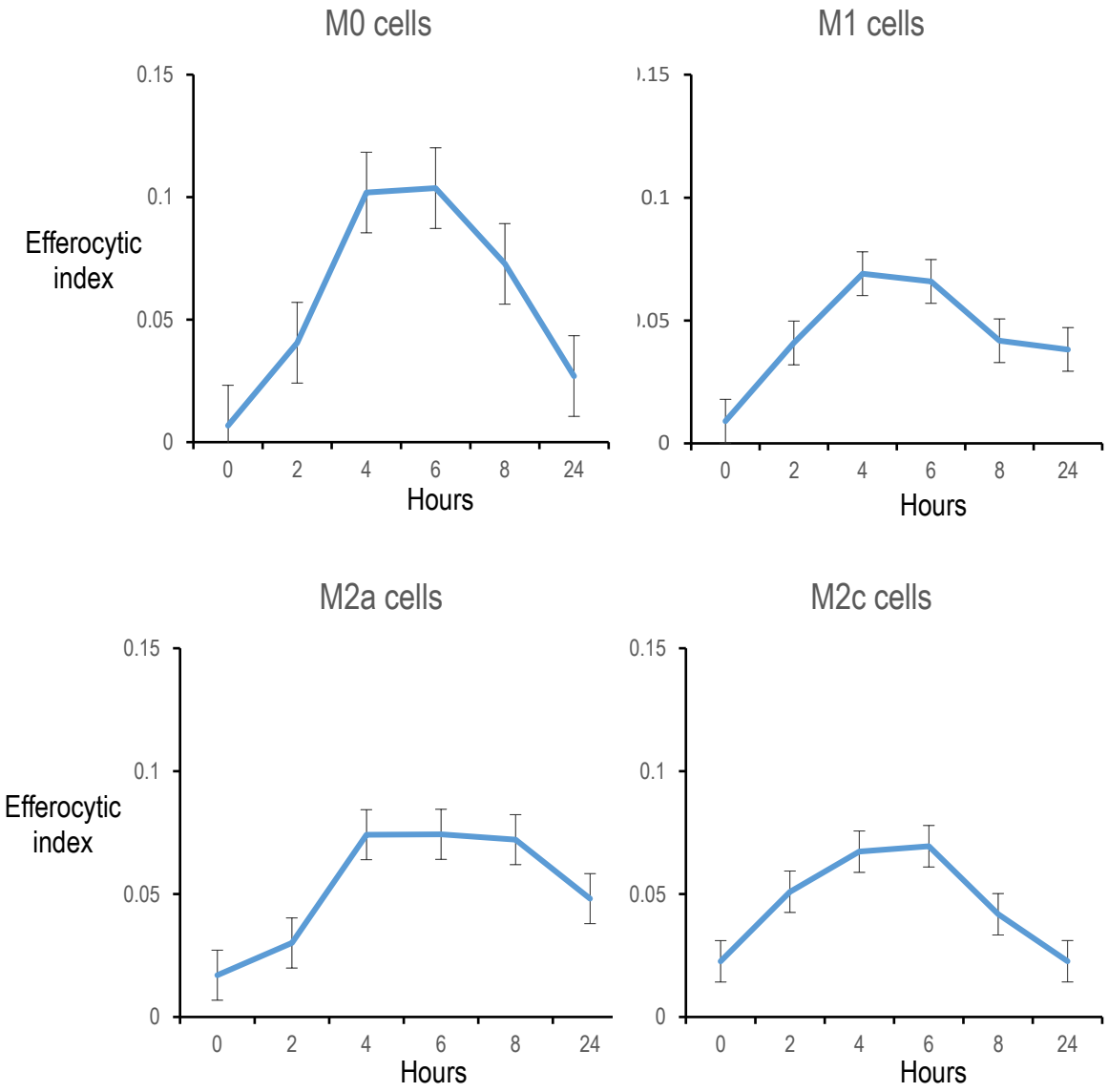

Figure 5.9 Addition of MDA-MB-231 cells on day two of the efferocytosis assay

Efferocytic uptake by RAW 264.7 cells of Drozitumab-treated MDA-MB-231cells over a 24 hour time course. RAW 264.7 cells were untreated (A), treated with 200 ng/ml LPS + 20 ng/ml IFNG (B), 20 ng/ml IL4 (C) or 20 ng/ml TGFB (D). MDA-MB-213 cells were not added until just prior to assay in an effort to lower the time zero background. Peak uptake occurred at the four to six hour time points and tapered back down by twenty-four hours. Activation state did not make a major difference to the extent of apoptotic cell engulfment. (n=8).

5.2.4 ASSESSMENT OF INHIBITION OF C1Q-MEDIATED EFFEROCYTOSIS BY MONOCLONAL ANTIBODIES

Hybridoma supernatants from monoclonal hybridoma cultures were added to the bioassay incorporating untreated CellTracker green labelled RAW 624.7 macrophages and pHrodo red labelled MDA-MB-231 cells induced to undergo apoptosis with Drozitumab. The supernatants were diluted 1:2 into the assay wells. BHI1-1G4 and BHI1-4D3 are hybridomas that secrete C1q monoclonal antibodies as shown in Chapter 4. A non-C1q binding control antibody (BHI3-2C12) was used as a negative control. 9A7 is a commercially available mouse monoclonal anti-human C1q antibody and was applied to the bioassay at a concentration of 10 µg/mL. 9A7 has not been previously investigated for inhibition of C1q-mediated phagocytosis however it has been shown to bind C1q using methods including western blot and immunohistochemistry. None of the antibodies assessed were shown to be effective in inhibiting efferocytosis in the bioassay (Figure 5.10).

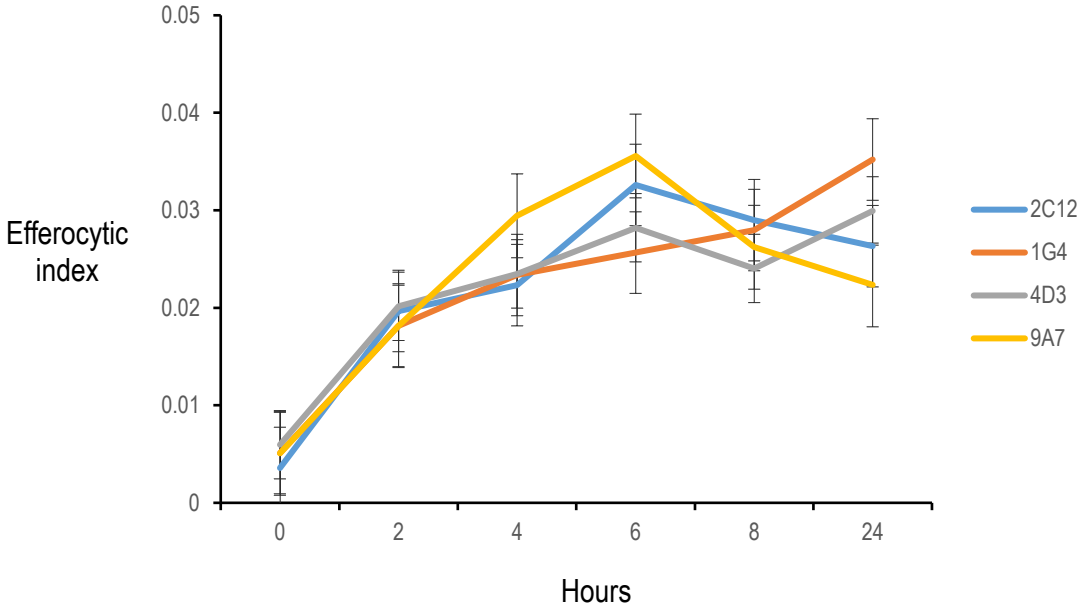

Figure 5.10 *In vitro* efferocytosis assay time points for anti-C1q monoclonal antibodies

Time points for the efferocytosis assay at 0, 2, 4, 6, 8, and 24 hours to assess potential inhibition of apoptotic cell uptake. BHI3-2C12 is non-C1q binding control antibody, BHI1-1G4 and BHI1-4D3 are C1q binding monoclonals and 9A7 is a commercial anti-C1qA monoclonal antibody. None of the antibodies inhibited efferocytosis over the time points tested.

5.3 DISCUSSION

Macrophage engulfment of dying cells, also known as efferocytosis, is a complex process mediated by immune cells and modulated through interactions with stroma and extracellular matrix (Atkin-Smith, 2015), (Santulli-Marotto, 2015), (Ortega-Gómez, 2013). While *in vivo* studies have highlighted the role of C1q in this process (Noor Din, 2017), (Hodson, 2013), identification of a C1q-binding antibody capable of inhibiting efferocytosis required the development of a reliable *in vitro* bioassay. *In vitro* simulation of efferocytosis is an over-simplification of the complex process that occurs *in vivo*; however, even a simple *in vitro* assay involving phagocytes and apoptotic cells can be quite complex with multiple facets requiring optimisation. Parameters investigated included different culture conditions for cancer cells and macrophages, methods of apoptosis induction, bone marrow-derived macrophages vs the macrophage cell line RAW 264.7, use of different fluorescent tags, and phagocyte phenotype (M1 vs M2a vs M2c). Quantification of the apoptotic cell uptake also proved challenging. There were issues of shifting focal plane on the confocal microscope, background fluorescence and variable cell density within the well. In addition, designing the series of commands to quantify apoptotic uptake without subjective bias required considerable work.

Most studies investigating the uptake of dying cells by phagocytes employ leukocytes as the target of apoptosis, particularly thymocytes or leukocyte cell lines that exist as suspension cultures (Atkin-Smith, 2015), (Stöhr, 2018). Breast cancer cells were used in the development of this bioassay to best mimic the interaction between macrophages and senescent breast cells *in vivo*. T47D cells were determined to not be appropriate for this assay as the methods trialled for the induction of apoptosis resulted in the cells detaching from the plate as well as a high degree of variability in the timing of apoptosis. Use of MDA-MB-231 cells induced to undergo apoptosis by treatment with the monoclonal antibody Drozitumab was an effective alternative. Drozitumab recognises DR5 and induces rapid apoptosis evident as cell membrane blebbing as early as one hour post-treatment. MDA-MB-231 TXSA-S expresses DR5 and undergoes rapid apoptosis following Drozitumab treatment, which made these cells an ideal target cell line (Zinonos,2009).

Drozitumab experiments were imaged on the Zeiss LSM 700 confocal microscope. GFP-expressing MacGreen mouse (Sasmono, 2012) bone marrow was induced to mature into macrophages with conditioned media from CSF1 expressing L cells. These macrophages were mixed with MDA-MB-231 cells expressing RFP, treated with Drozitumab and imaged at intervals for six to twenty-four hours. Problems with the confocal microscope image acquisition including shifting focal plane, background fluorescence and variable cell density made interpretation of the results difficult. However, this was adjusted for in the image analysis and generation of the efferocytosis index. With this approach, the rate of efferocytosis was shown to be regulated by C1q, with macrophages derived from C1q null mice exhibiting slower uptake of apoptotic breast cancer cells than macrophages derived from C1q replete mice.

It was necessary to switch from bone marrow-derived macrophages to a macrophage cell line for further development of the bioassay due to the long lead time required for macrophage differentiation. Efferocytosis by RAW 264.7 macrophages was not affected by cytokine-induced activation state and so untreated cells were used in the bioassay. While efferocytosis occurred over a similar time frame of approximately 2-6 hours in bone marrow-derived and RAW cell macrophages, it was not possible to directly compare the two assays. The bone marrow assay used GFP-expressing macrophages and RFP positive cancer cells. The RAW assay used CellTracker stained macrophages and pHrodo stained cancer cells. In addition, the measure of efferocytic index was far higher for the bone marrow assay, due to the larger number of macrophages on the plate leading to a greater incidence of macrophage-cancer cell overlap and dye uptake during efferocytosis; while in the RAW cell assay, engulfed cells only fluoresced when present within the acidified phagosome. Despite these differences, the efferocytosis was

quantifiable and the bioassay assessed whether anti-C1q antibodies could inhibit efferocytosis. No difference in efferocytosis was observed when the co-culture was treated with the two experimental monoclonal antibodies BHI1-1G4 and BHI1-4D3, or with the commercially available 9A7 antibody.
Despite making step-wise improvements to the assay, it was not possible to prove any efficacy for neutralisation of C1q by the antibodies. There could be a number of reasons for this, none of which necessitate that the antibodies are not neutralising C1q activity. The studies with the antibodies blocking efferocytosis were preliminary and could be improved. The most obvious deficiency was the lack of knowledge concerning the antibody concentration in the supernatant. Antibody content in hybridoma supernatants vary widely with concentrations ranging from five to seventy-five µg/mL (personal observation). Titrating known quantities of antibody in an efferocytosis assay would give a more definitive answer of the C1q neutralising capacity.

A point of concern with the RAW cell assay is the appropriateness of these cells for efferocytosis. RAW cells have been shown to phagocytose antibody-opsonised sheep red blood cells (Montaño, 2018) as well as apoptotic cells (Selvarajan, 2017). RAW cells express fewer Fc receptors than the J774A.1 cell line (Verma, 2009), which could make them a better candidate for demonstrating inhibition of efferocytosis through the reduction of Fc meditated phagocytosis. However, the relative rate of efferocytosis by RAW cells compared to bone marrow macrophages is unknown. Use of the J774A.1 cell line in parallel with RAW cells and bone marrow macrophages could elucidate the extent of this potential drawback.

Future work with the *in vitro* efferocytosis assay could involve the optimisation of cell numbers, both phagocyte and cancer cells. Too many apoptotic cancer cells may have the potential of saturating phagocytic uptake with potential feedback inhibition. Macrophage cultures at high density may not be as phagocytically active whereas a low density culture might lack a critical level of paracrine signalling required for efficient efferocytosis. An experiment with a chequerboard design to match differing cell numbers could be useful in optimising the *in vitro* assay. Experiments with activation of macrophages surprisingly showed no difference in efferocytosis; however, one study employed CSF-2 activation of RAW 264.7 cells (Selvarajan, 2017) and this could be of value for the assay. Cytokine activation of bone marrow- derived macrophages represents another avenue of enquiry.

Investigation of *in vitro* efferocytosis was chosen as the most relevant assay, interrupting the uptake of dead and dying cells by phagocytes. However, another assay of complement function involves the lysis of sheep red blood cells by C1q binding and complement cascade activation (Bonaparte, 2008). In this assay C1q binds to immunoglobulin-sensitised sheep red blood cells and initiates the classical complement cascade. As such, antibodies binding the globular domains of C1q could inhibit this process but antibodies directed to the collagen-like tail might not inhibit C1 assembly that occurs in proximity to the globular regions.

Location of the epitope on the target protein recognised by the antibody can be important for the ability to bind the antigen in different assays. For example, the mouse monoclonals generated for this project were able to bind C1q presented by ELISA and in immunoprecipitation but not able to recognise C1q in western blotting or immunohistochemistry. The commercial 9A7 antibody bound C1q in the above assays but was not able to inhibit efferocytosis in the *in vitro* assay. This could be due to 9A7 binding to a region of C1q not engaged in the efferocytic process; however, since none of the antibodies tested inhibited efferocytosis, it is more likely the assay was not appropriate to demonstrate inhibition and required more optimisation for this purpose.

Monoclonal antibodies would have two means of neutralising C1q activity. First, steric hindrance can block C1q binding to its receptor, either to the apoptotic cell via the globular domain or to the phagocyte via the collagen-like tail. Second, certain monoclonals can block binding by inducing a conformational change in the target protein. Since the collagen-like tail is rigidly disulphide cross-liked and wrapped in a triple helix

of triple helices, conformational change would more likely occur in the globular domain. This less common type of interaction usually involves either hydrophilic sequences, particularly the sequence loops connecting beta sheets of globular domains, or hydrophobic patches deeper within the protein (Gaboriaud, 2012), (Shapiro, 1998). Determining the binding specificity of a monoclonal to a C1q domain could be possible by isolating C1q globular domains following collagenase treatment or collagen-like tails isolated after pepsin treatment (Kojouharova, 2014).

Throughout the development of the *in vitro* assay, the timing of peak uptake of dying cells proved to be quite variable. Early experiments determined that maximal uptake occurred quite late, peaking at around forty-eight hours. Obviously, this had little relation to the efferocytosis process in the mouse mammary gland where the time course for the complete removal of dying epithelial cells occurs in approximately forty-eight hours (Noor Din, 2017). The process of extrinsic apoptosis is initiated by extracellular signals that lead to rapid caspase activation and onset of apoptosis, generally within three hours (Elmore, 2007). This concept was confirmed by this project's experiments in the induction of extrinsic apoptosis by Drozitumab treatment of DR5-positive MDA-MB-231 breast cancer cells. Like extrinsic apoptosis, intrinsic apoptosis may have variable time to onset, yet once Bcl-2 oligomer disruption occurs, caspase activation follows a rapid time course of approximately four hours (McComb, 2019).

As refinements were made in the *in vitro* efferocytosis assay, the peak uptake moved to a window of four to six hours; however, for the last experiments peak uptake again shifted to twenty-four hours. Regardless of whether apoptotic cell uptake peaks at four, six, or twenty-four hours *in vivo* was not at issue, the lack of consistency in the *in vitro* uptake complicated the identification of monoclonal antibody inhibition of C1q efferocytic activity. However, any point with vigorous apoptotic uptake should allow for demonstration of C1q inhibition by monoclonal antibodies with a resultant decrease in dying cell uptake.

Another aspect of the *in vitro* efferocytosis assay that yielded unanticipated results was cytokine-driven macrophage phenotype modulation. Untreated cells were taken as the default M0 or resting phenotype, but even resting bone marrow-derived macrophages are polarized towards the M2 phenotype (Zhao, 2017) and this could well be the case for RAW 264.7 cells as well. Results of a thirty day culture showed untreated RAW 264.7 cells behaved in the same manner as IL4-treated M2a cells (data not shown). Analysis of cell surface markers typical for macrophages of M1 and M2 phenotypes could clarify the activation state induced by the cytokine in question (Hodson, 2013); but as the purpose of the activation was to find the phenotype with the best efferocytic capacity, this was not pursued.

Regardless of the phenotype of cells in the resting state, it is generally accepted that M2 phenotype macrophages are superior phagocytes (Hesketh, 2017), (Mantovani, 2013). Yet, in the *in vitro* efferocytosis assay, activation towards the M1, M2a or M2c phenotype had essentially no impact on the ability of the macrophages to phagocytose dying cells. This could be taken as an indication that macrophages of differing phenotypes are equally capable of efferocytic uptake. At variance with this view of phenotypic equivalence is the marked differences between the M1 and M2 phenotypes. The LPS/IFNG-treated M1 macrophages at forty-eight hours yielded fewer cells and RNA compared to untreated, IL4, or TGFB-treated cells (data not shown). In addition, M1 cells had a strikingly different appearance, spread out on the culture flask surface and containing multiple cytoplasmic vacuoles. The M2 cells occupied a smaller footprint on the culture substrate and adopted either a round refractile appearance or a flatter spindle-shaped phenotype. That the macrophage phenotypic differences did not impact the uptake of dying cancer cells is likely to be inherent to the *in vitro* assay and no doubt phenotype would be more relevant in the *in vivo* mammary gland microenvironment.

Despite the inconsistencies in the assay, a window of maximum uptake inevitably appeared that theoretically could have been inhibited if an antibody introduced into the assay was capable of blocking C1q binding to either the phagocyte or the dying cell. Some experiments showing lower uptake for C1q

monoclonals compared to controls were in fact an artefact of red pHrodo dye bleaching during frame acquisition. By imaging each condition on a separate slide, no differences could be seen for the BHI monoclonals, 9A7 or unrelated control antibody. While this result was disappointing, it does not mean the antibodies are not able to inhibit C1q activity, rather that they did not inhibit apoptotic cell uptake in the context of this assay and its conditions. And given the difficulties encountered during the assay development, it is quite possible this assay was not adequate for assessing the C1q-inhibitory capacity of the monoclonal antibodies.

5.4 CONCLUSION

The development of the *in vitro* efferocytosis assay was a simulation of the *in vivo* process of phagocyte uptake of dying epithelial cells in the mammary gland. Two of the main elements in this process, macrophages and C1q, have been studied previously in this lab and shown to have vital roles in the timely uptake of apoptotic mammary epithelium during regression. Despite the important roles of macrophages and C1q in efferocytosis, the environment of the mammary gland is quite complex and undoubtedly leukocytes, fibroblasts, adipose tissue, and extracellular matrix in an ever-changing milieu of hormones, cytokines, and chemokines play a vital role in this process.

However, even the simplified approach of the *in vitro* efferocytosis assay for the study of this vital *in vivo* process had its challenges. Attempts to standardise a protocol for the assay were complicated by the need to optimise numerous parameters, including the conditions for the two cell types, the use of different marker dyes, and the timing and coordination of the various conditions. It was important for each element of the assay to operate in an optimal manner simultaneously with every other, making it difficult to determine which variable required adjustment from one assay to the next. Even such factors as user traffic through the CO_2 incubator used for the cell cultures, the water levels in the incubator and the communal use of the confocal microscope had the potential to introduce variability in the set-up and imaging of the assay, irrespective of assay set-up. In the end, it was not possible to observe inhibition of efferocytosis by any of the monoclonal antibodies tested. This could be because the antibodies were not capable of blocking C1q-mediated efferocytosis or that the assay was not adequate to show this. Furter development of the *in vitro* assay would be useful as would the possible use of pre-clinical mouse models.

The only remedy for these more-or-less hidden influences in the assay was repetition and looking for consistent trends amid the assay variation. Even with variation in assay read-outs, solid trends showing effectiveness of changes to the protocol was the best way to be assured that the conclusions drawn were in fact correct and, indeed, reproducible.

CHAPTER 6: GENERAL DISCUSSION

6.1 INTRODUCTION

The observations of Hodson establishing a connection between the absence of C1q and decreased mammary cancer incidence placed the focus of this research on the role of C1q in mammary gland function (Hodson, 2013). Noor Din investigated the mechanism of this effect and explored how C1q deficiency led to increased abundance of apoptotic cells in the mammary gland specifically during the regression phase of the ovarian cycle (Noor Din, 2017). This finding implicates the normal function of C1q in efferocytosis to the process of carcinogenesis in the mammary gland. This project was inspired by the observations of Hodson and Noor Din with the goal of developing an inhibitor of C1q-mediated effercytosis, to enable further research and potential therapeutic applications.

The mammary gland is an organ with hormone-driven epithelial cell proliferation and regression during the ovarian cycle that occurs throughout the reproductive lifetime. In response to rising estrogen and progesterone levels, mammary epithelial cells proliferate to form alveolar buds, the forerunners of milk-producing lobules (Hodson, 2013), (Chua, 2010). If no pregnancy occurs, the alveolar buds regress by undergoing apoptosis and are removed by phagocytes. C1q facilitates the removal of the dying epithelium and through this process inhibits inflammation, thereby maintaining self-tolerance during mammary gland regression (Elliott, 2017), (Ortega-Gómez, 2013), (Barth, 2017). The anti-inflammatory environment created by efferocytosis is maintained by secretion of the cytokines IL10 and TGFB that are able to suppress lymphocyte-associated inflammation by directing macrophages to a M2 phenotype (Hesketh, 2017).

Since C1q is central to the timely elimination of dying cells through efferocytosis and this process is intimately associated with increased incidence of mammary tumours, inhibition of C1q activity could represent a viable therapeutic approach to suppressing the development and progression of mammary cancers. In line with current therapeutic practice, a monoclonal antibody approach was selected as a suitable candidate for a C1q inhibitor. The test of the usefulness of these monoclonals was their capacity to inhibit efferocytosis, hence the need for the development an *in vitro* efferocytosis assay to demonstrate the ability of antibodies to block this crucial C1q function.

Efferocytosis is a complex biological process. It is mediated primarily by macrophages that are attracted to dying cells through “find me” signals. The recognition of specific cell-surface molecules on the apoptotic cell (“eat me” signals) leads to the engagement of phagocytic signalling pathways and engulfment of the dying cell (Arandjelovic, 2015). But far from occurring in isolation, this process takes place in the presence a complex environment containing leukocytes, stroma, extracellular matrix, and adipose tissue. Therefore, attempts to model efferocytosis would of necessity be overly simplistic; but in the absence of a better alternative, an attempt was made to produce an assay based solely on breast cancer cells in the presence of macrophages. The studies reported in Chapter 5 failed to demonstrate inhibition of efferocytosis by the monoclonal antibodies generated during this project; however, this does not preclude the potential usefulness of the antibodies for preclinical and potentially clinical applications. Further studies will be required to characterise the monoclonal antibodies prior to any application to *in vivo* research. For clinical applications, the monoclonal antibody would require considerable modification. This chapter discusses future research directed at development of new approaches to treating and preventing breast cancer through inhibition of C1q-mediated efferocytosis.

6.2 ANTIBODY DERIVATION, MODIFICATION AND SCALE-UP

6.2.1 ANTIBODY DERIVATION AND SCALE-UP

The monoclonal antiboides isolated in this project were derived using a modification of the method described by Köhler in 1975 (Köhler, 1975). Köhler and Milstein fused splenocyte B cells from sheep red blood cell (SRBC) with the myeloma line P3-X67Ag8 to produce the hybridomas SP1 and SP2 that secreted anti-SRBC monoclonal antibodies. The Sp2 hybridoma was selected to yield a variant that did not contain or secrete endogenous immunoglobulin (Ig), named SP2/0-Ag14 (Shulman, 1978). Hybridomas derived from fusion of B cells with SP2/0 secrete only the Ig expressed by the B cell and represented an early innovation to hybridoma technology. Shulman also demonstrated the superiority of polyethylene glycol (PEG) for inducing fusion and the use of feeder cells to support the nascent hybridomas. The only other innovations introduced for the fusions of this project were the use of azaserine rather than aminopterin during hybridoma selection and the use of an oil-in-water emulsion for immunisation. This method for hybridoma production is simple and effective with the main challenge being the means of screening for specific antibodies.

Various innovations to monoclonal antibody production have been devised by different labs. Many of these alternatives require specialist skills and high-end equipment, particularly molecular biology techniques. As such, these alternatives are not accessible to all labs, but descriptions of a few of these methods follow.

One method to simplify the identification and isolation of hybridomas secreting specific antibodies is to screen the fusion by fluorescence-activated cell sorting (FACS). Fluorescently-labelled antigen is allowed to bind to the antibody on the hybridoma surface and the antigen-binding cells are sorted into microtitre plates by FACS. This not only identifies specific antibody-secreting hybridomas before they can be overgrown by non-secreting hybrids but simultaneously single-cell clones them as well (Akagi, 2018). FACS screening can also be done with fluorescently-labelled whole cells as well to identify antibodies that bind to surface antigens (Greenfield, 2022).

An alternative to immunising with a protein antigen is immunisation with nucleic acid, DNA or RNA. Purification of protein antigen can be a limiting step in hybridoma production, requiring molecular biology or protein chemistry experience. Nucleic acid immunisation represents an alternative to traditional protein purification. After constructing a plasmid coding for the protein of interest, the nucleic acid is then injected into the skin of a mouse using a biolistic system with nucleic acid-coated gold spheres (Tang, 1992), although it is also possible to inject the animals intramuscularly (Leitner, 1999). Cells taking up the DNA/RNA are able to transcribe the nucleic acid and present the resultant protein via MHC class I and II, producing both antibody and cytotoxic cell responses (Leitner, 1999). DNA immunisation does not always induce a strong immune response but additional factors such as addition of CpG sequences, cytokine adjuvants, and self-replicating constructs can boost the response into a more therapeutic range.

Another variation involves the use of human peripheral blood leukocytes cultured with cytokines and antigen to immunise B cells *in vitro.* These cells are then fused to myeloma cells to produce hybridomas that then can be screened for specific antibody (Li, 2006). This technique bypasses the use of rodents for immunisation and antibody production, saving the effort required for humanising the monoclonal prior to clinical trials.

A more technically challenging method is production of phage display antibodies. The phage display technique was innovated by McCafferty et al and involved cloning the single chain variable fragment (scFv) of an anti-ovalbumin antibody into the III gene of the filamentous fd phage. Phage displaying the anti-ovalbumin scFv on their protein coat bound to ovalbumin in ELISA and were termed phage antibodies

(McCafferty, 1990). A further development of phage antibodies allows for development of immunisation-free antibodies. A library of scFv fragments composed of heavy and light antibody variable regions is cloned into the filamentous phage coat protein and scFv-bearing phage are then selected by panning on the antigen of choice (Marks, 1991), (Alfaleh. 2020) The phage are then single-cell cloned and subjected to restriction-length length polymorphism (RFLP) analysis prior to infecting bacteria to scale-up antibody production (Jones, 2010).

Whatever the manner of monoclonal antibody derivation is selected, the next consideration is the scaling up of antibody production to produce quantities suitable for preclinical models. In the past, the best method for scaling up the quantity of monoclonal antibodies for purification had been the use of ascitic fluid production in mice. Using a host mice syngeneic with the hybridoma, a single run of five mice could yield tens to hundreds of milligrams of monoclonal antibody. However, animal ethics no longer allows ascites production, leaving the use of CELLine bioreactors (Sigma Z688029) as the best alternative for medium-scale antibody production. These bioreactors yield milligram quantities but in a small volume, with production of larger quantities of antibody necessitating longer culture times. Individual lots of bioreactor supernatants require assessment of antibody content to ensure secretion is not lost due to the high cell densities within the reactor vessel. This is a relatively cheap method that can be adapted to serum-free conditions to minimise serum protein impurities.

Producing larger amounts of antibody requires transient transfection of DNA encoding antibody constructs into mammalian cell lines followed by bioreactor culture (Frenzel, 2013) (Vazquez-Lombardi, 2018). Originally, antibody expression in mammalian cells involved transfection of two constructs, one for light chain and one for heavy chain, into either human embryonic kidney cells (HEK) or Chinese hamster ovary (CHO) cells; however, techniques have been developed to allow for the transfection of a single construct for antibody expression (Gion, 2013), (Carrarra, 2021). Transfected cells are then cultured at high density to maximise the yield of the antibody product. This can involve culture of cells on microsphere carriers of various different materials in a spinner culture to produce a very high cell density and product yield (Huang, 2020). Post-production, antibody can be purified with protein G or L using standard techniques. The whole procedure should be carried out with an effort to minimise introduction of endotoxin that may impact the results obtained from the chosen preclinical model.

What is of interest in this project is the possible effect of C1q on immunisation. The author has performed and screened over five hundred hybridoma fusions and has a good appreciation of the antibody response to be expected from a target protein. Immunisation with C1q only produced a titre of $1:10^6$ for one mouse after one particular boost with all other mice producing titres of $1:10^5$. This can be partially explained by the degree of sequence identity between the host mouse protein and the human immunogen but antigens with far less sequence identity can produce a vigorous immune response. This lower than anticipated response led to a speculation that the C1q used as antigen was sequestered into its innate immune niche in the C1qA null host mouse. To test this theory, C1q was reacted with glutaraldehyde via amine groups to produce an imine cross-linked product, rendering C1q unable to function *in vivo* or as a native antigen *in vitro*. This loss of functionality was demonstrated by the elimination of antibody binding in ELISA, producing a reasonable expectation of this C1q would be unable to function as complement in the immunised mice. Mice boosted with cross-linked C1q showed no appreciable difference in titre to mice boosted with native C1q. This implied C1q was not becoming sequestered into the innate immune system of the host mouse and becoming less available for antigen presentation. The lower than anticipated antibody titre obtained from immunisation could be due to immune suppression by C1q immunogen, through inhibition of dendritic cell maturation, as well as B and T cell function through binding to LAIR and CD33 cell surface proteins. Alternatively, the immunisation might not have performed as well as expected due to another factor or factors, but not antigen dose, injection schedule, adjuvant or injection site since these had all been optimised by numerous immunisations performed before this project had commenced.

Another interesting finding was the derivation of two IgM monoclonals in fusion 3. The mouse used for fusion 3 had been immunised nine times by the time of fusion, a situation highly conducive to class switching and the production of IgG isotypes. Production of IgM antibodies after repeated boosting suggests a lack of T cell cytokine stimulation, which drives class switching. The *de novo* stimulation of naïve B cells is not a likely scenario after so much previous antigenic stimulation. For class switching to not occur implies a deficit in t cell cytokine secretion necessary for IgM class switching. Presumably this does not involve a total blockade of T cell function since two specific monoclonal-secreting hybridomas were derived from fusion 1 which were IgG1 isotype.

Derivation of IgM isotype monoclonals is unusual, mainly because immunised mice have received a priming shot and at least three boosts before they are used for fusion. IgM antibodies feature in anti-bacterial and anti-parasite immunity, pathogens that feature repetitive antigens on their surface that are bound with high avidity by pentameric IgM. The decreased antibody titres and generation of IgM monoclonals after multiple boosts provides an interesting area for research of immune regulation. It is not surprising a protein already characterised for its involvement in immunity and autoimmunity may have additional roles in humoral immunity. This area presents another research opportunity for the elucidation of C1q's role in immune regulation, beyond its role in carcinogenesis, tumour inhibition and promotion.

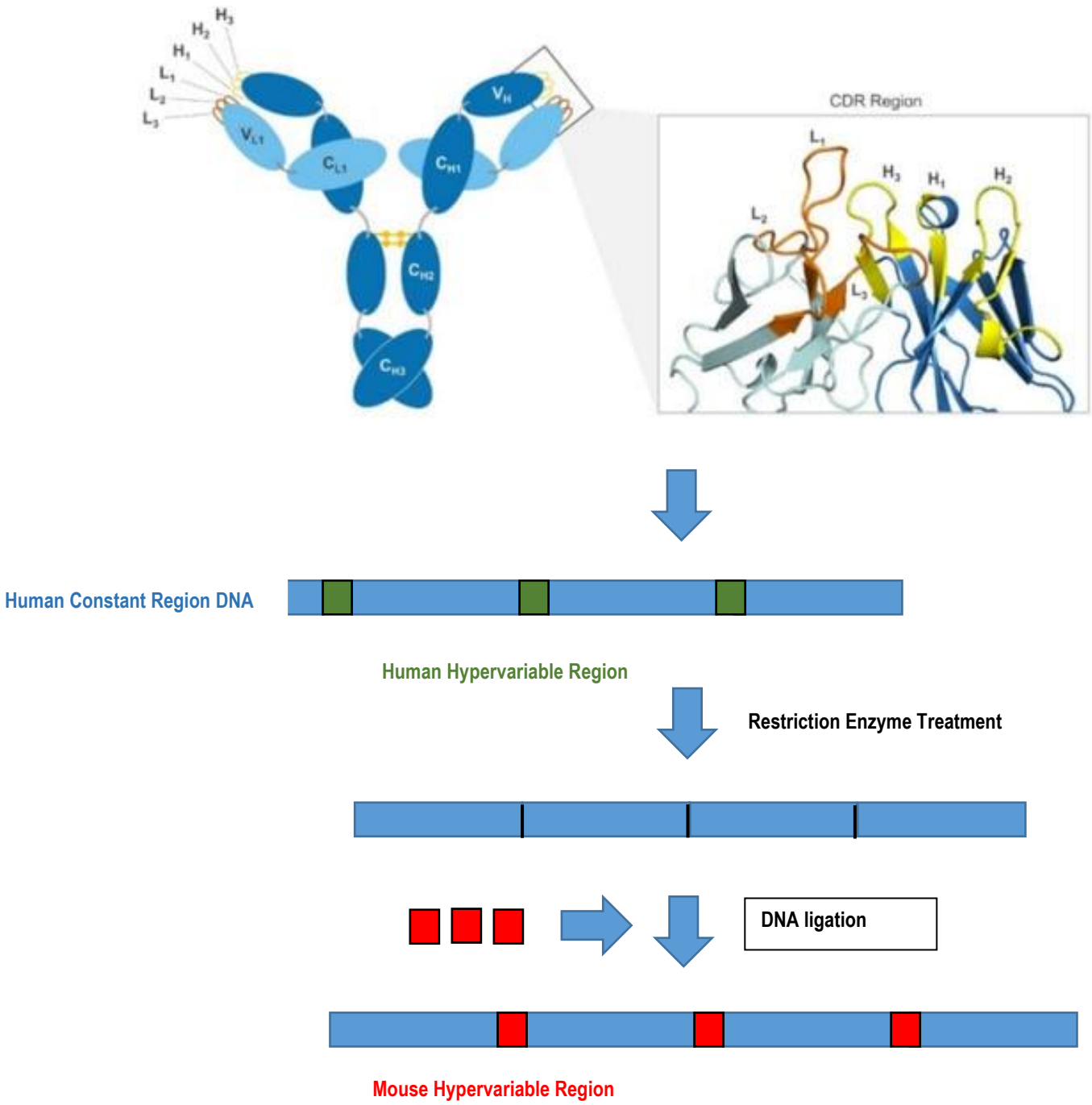

Figure 6.1 Structure of the antibody complementarity determining region

The antigen recognition site of an antibody, also known as the complementarity determining region (CDR), is composed of regions from both the heavy and light chain in proximity. (A) shows the entire immunoglobulin including the juxtaposition of heavy and light chains. Each Ig chain contains three hypervariable regions that contribute to the CDR: L1, L2, and L3 on the light chain and H1, H2, and H3 on the heavy chain (B). The framework regions of the variable regions (VL and VH) fix the six loops of the CDR into place to form the antigen binding site. Figure drawn from Graves et al, Antibodies (2020), 9, 12.

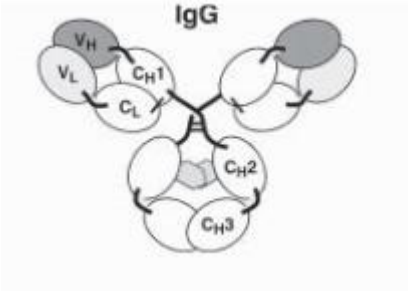

Function		
Ligand/receptor antagonist	+	+
Receptor agonist	+	+
Drug/radionuclide/toxin conjugate	+	+
Half-life in circulation	++	+
Mammallan expression	+	+
Bacterial expression	-	+
Immune effector activity (ADCC, CDC)	+	-

Figure 6.2 Antibody production and therapeutic utility

Intact immunoglobulin requires a mammalian expression system to ensure proper glycosylation and folding. ScFv can also be expressed by mammalian cells and also by bacteria, however bacterial system can produce improperly folded product. Both antibody types share agonist/antagonist activity as well as the ability to deliver conjugated agents to target cells. ScFv antibodies have a lower residence in circulation and lack the ability to participate in immune effector cell function, such as antibody-dependent cellular cytotoxicity (ADCC) or complement-dependant cytotoxicity (CDC).

6.2.2 ANTIBODY MODIFICATION

Monoclonal antibodies are an important class of therapeutics for the treatment of cancer, rheumatic disease, and other conditions. Since the introduction of the first therapeutic monoclonal antibody in 1986 (Hooks, 1991), inhibitor and agonist monoclonal antibodies have become familiar components of the modern medical toolbox. Generally, these antibodies are produced in mice and therefore represent foreign proteins in humans that inevitably provoke an anti-mouse immunoglobulin immune response, thereby limiting their usefulness. Anti-mouse immunoglobulins would clear the monoclonal antibody from a patient's system thereby nullifying its therapeutic effect; however the antigenicity of monoclonals can be circumvented through the process of humanisation.

At the genetic level, antibody diversity is generated through the recombination of DNA domains in the variable region of the antibody gene: the V, D, and J regions for heavy chain, and the V and J regions for the light chain (Giraud, 2014). The heavy chain locus contains forty-four V regions, twenty-seven D regions and six J regions that recombine to produce a great diversity of unique sequences that make up the complementarity determining region (CDR) (Figure 6.1). The recombined heavy chain variable regions in association with recombined light chain variable regions make up the antigen recognition site of the antibody. Adding to the already large diversity of binding sites is the inexact nature of the recombination events that join the regions, allowing for bases to be deleted from or added onto the ends of the recombining regions. These alterations of bases produce frameshifts in the sequence of the antibody CDR, resulting in changes to amino acid sequence (Roth, 2015).

The CDR itself is formed by folding the three loops of the hypervariable regions from each chain into proximity with each other to form the antigen binding domain (Dondelinger, 2018). The remainder of the antibody variable region outside the CDR functions as a framework to bring these six loops together and hold the CDR in place (Graves, 2020). Using genetic engineering techniques, the mouse CDR sequences can be excised and spliced into a human variable region framework sequence, rendering the final antibody product that is completely human but for the CDRs (Clavero-Álvarez, 2018), (Figure 6.1).

CDRs are unique and are not recognised as an antigen with the exception of the anti-idiotypic response (Kohler, 2019). Humanised antibodies can be introduced into patients without provoking an immune response and therefore can continue to bind their target antigen to deliver a therapeutic effect after repeated dosing. An alternative approach to producing humanised antibodies is to immunise mice that have been genetically engineered to express a human humoral response, resulting in the production of human antibodies (Laffleur, 2012).

One of the limitations for monoclonal antibodies, particularly for cancer therapeutics, is the size of the molecule (150 kD) that restricts its ability to reach its target tissue, particularly for solid tumours with poor vascular perfusion. One means of increasing antibody availability is to diminish the size of the antibody to increase its permeability into tissues while retaining its binding characteristics. The scFv contains the heavy and light chain CDRs from the monoclonal antibody held together by a linker peptide of ten to twenty-five amino acids (Unverdorben, 2016). Removing the heavy and light chain constant regions reduces the molecular weight of the antibody from 150 kD to about 27 kD, thereby enhancing the ability of the antibody to access target tissues. The downside of the smaller chain is a shorter half-life in circulation, an effect that can be mitigated by adding portions of the heavy chain to increase circulatory residence (Unverdorben, 2016). Antibody circulatory half-life is likely to be highly dependent on each individual scFv chain and optimisation of fragment size would be required to determine the optimal therapeutic effect. Figure 6.2 summarises the advantages and disadvantages of full-length antibodies vs scFvs in antibody therapy.

An alternative approach to the use of antibodies as therapeutics is the development of an antigen-binding mimetic as an inhibitor of C1q . In silico modelling of the antibody CDR can be used to design small

molecule inhibitors that mimic the binding surface of the antibody CDR (Lawson, 2017), (Wang, 2018). The advantage of this approach is the reduction of the cost associated with the genetic engineering and scale-up production of a monoclonal antibody for therapeutic application. Small molecule inhibitors have superior penetrance into tissues and the reduced cost lends itself to more frequent dosing with potentially better efficacy. Small molecule mimetics can be produced directly to the target molecule if it is adequately characterised (Yannakakis, 2017), but using a neutralising antibody can be useful if neutralising epitopes on the target are not yet known. This emerging technology represents an exciting opportunity in the field of monoclonal antibody-based therapeutics.

6.2.3 THERAPEUTIC APPLICATIONS IN BREAST CANCER PREVENTION AND TREATMENT

The anti-cancer effects of C1q deficiency observed null mutant mouse models point to the potential usefulness of an anti-C1q monoclonal antibody in the prevention of breast cancer (Noor Din, 2017). There are currently very few options for breast cancer prevention. For women with very high risk of breast cancer, such as those carrying a genetic mutation in Brca1 or 2, prophylactic mastecomy and tamoxifen therapy are available, but come with significant side effects. For women with low or moderate risk, the options available are lifestyle interventions such as maintaining a healthy body weight, limiting alcohol consumation, and breastfeeding if possible. Given the high rate of breast cancer, even in women with no family history of the disease, a preventative therapy would be of interest.

While mouse model studies suggest that C1q inhibition could reduce breast cancer risk, consideration must be made to the potential harm of the therapy in relation to its benefit to breast cancer outcomes. Most importantly, preventative therapies need to be safe, and for this reason, inhibition of C1q as a breast cancer preventation therapy on a permanent basis would not be desirable for at least two reasons. First, C1q inhibition would affect activation of the classical complement cascade and potentially render the individual more susceptible to bacterial and viral infections. Second, and more importantly, inhibition of the efferocytosis function of C1q could eventually lead to the loss of self-tolerance leading to the formation of antibodies to self-antigens such as anti-nuclear antibodies (ANA), and the development of the autoimmune disease systemic lupus erythematosus (SLE). Mouse model studies suggest that inhibition of C1q activity is most effective in the mammary gland during regression phase of the ovarian cycle, a biological function that stretches over the reproductive life of women, typically thirty to forty years. There is potential to administer a therapy that inhibits C1q activity specifcally during the regression phase of the menstrual cycle. This stage occurs at the time a woman has her period, so it would be easy to identify.

Another hurdle in development of a breast cancer prevention therapy is the timeframe in which research can be done to meaningfully assess breast cancer incidence in a randomised controlled trial. Assessing the efficacy of a monoclonal directed towards a cancer is relatively simple since monitoring the progress of tumour growth or regression is established clinical practice (Schwartz, 2016). However, breast cancers can arise over a span of many years, and a therapy given to premenopausal women could require decades to demonstrate clinical benefit. Given that ninety-three percent of breast cancers develop in women over thirty (Anders, 2009), focussing on this older population still leaves a time span of approximately twenty years over which a woman would require treatment at monthly intervals. With the expense of a monoclonal antibody treatment, a preventative treatment would likely only be feasible for a small molecule inhibitor capable of blocking C1q activity during mammary regression. It is possible that women with high risk genetic disorder such as BRCA mutations (King, 2003) might be candidates for

monoclonal antibody treatment but unless the cost was considerably lower than monoclonal antibody therapeutics currently on the market, the cost would be prohibitive. Either way, a small molecule inhibitor would be a preferable option to limit the cost. Most patients are only willing to pay for expensive cancer treatments because the consequences of untreated cancer are dire and the treatment window relatively short.

However, a C1q inhibitor could also be useful in a cancer treatment setting, particularly for premenopausal women or women with triple negative breast cancer. Unlike the ER/PR/HER2 receptor positive cancers, triple negative breast cancers have no targeted therapies and are treated with chemotherapy alone. Premenopausal women undergoing chemotherapy may or may not continue menstrual cycling (Blumenfeld, 2012), meaning some benefit could accrue from the inhibition of efferocytic activity by a C1q monoclonal. But C1q can also contribute to cancer growth through a low-level, smouldering classical complement cascade activation that feeds the cancer with C3a and C5a, factors known to promote cancer progression (Markiewski, 2007), (Afshar-Khargan, 2017). Anti-C1q activity of a monoclonal antibody could be tested in preclinical models to assess treatment efficacy against a triple negative breast cancer, both with and without chemotherapy treatment. Any anti-cancer activity seen in this setting would open the possibility for treatment of women with breast cancer, especially triple-negative cancers with their lack of targeted treatment and poorer prognosis (Geyer, 2017).

Another potential clinical application for C1q monoclonal antibodies would be in promoting immune attack on breast cancers during neoadjuvant chemotherapy treatment. Neoadjuvant chemotherapy is a treatment option for locally-advanced breast cancers that are challenging or impossible to remove surgically (Thompson, 2012). The patient is treated with several cycles of chemotherapy to shrink the tumour prior to resection. In some cases, neoadjuvant chemotherapy will induce a pathological Complete Response (pCR) (Spring, 2020), (Sidaway, 2020). The definition of pCR is still being debated as to whether absence of in situ cancer should also be included (Kuroi, 2015). At The Queen Elizabeth Hospital, pathologists define pCR as the absence of invasive cancer in all excised tissue. We are now seeing neoadjuvant chemotherapy inducing pCR in primary breast cancer which is confirmed post-surgically. What factors cause pCR in some patients and not others is not known, but is likely to be associated with the type of immune response generated against the cancer cells (Ladoire, 2008), (Varadan, 2016). pCR is associated with excellent long-term, cancer-free, survival in women diagnosed with triple negative breast cancer or trastuzumab-treated HER2+ breast cancer (Cortazar, 2014). Inhibition of C1q-mediated efferocytosis could help to promote a cytotoxic immune response and assist attainment of pCR during neoadjuvant chemotherapy and improve the long term outlook of the patient.

6.3 CONCLUSION

This project aimed to generate monoclonal antibodies against human C1q in order to develop new approaches to treating and preventing breast cancer. The project was successful in generating four antibodies with potential for further analysis. However, there are a number of limitations to what was achieved. The lack of a stronger immune response limited the number of monoclonal antibodies obtained and the opportunity to identify C1q inhibition. The antibody characterising assays were capable of being performed with larger number of samples; however the *in vitro* efferocytosis assay was labour intensive and limited the number of samples able to be tested to two test antibodies. This slowed progress as the efferocytosis assay was optimised while testing antibody samples.

The initial aim of this project was the production of C1q-binding monoclonal antibodies capable of inhibiting efferocytosis. This was to be accomplished in three steps: 1) immunisation of mice and production of monoclonal antibodies, 2) development of an *in vitro* efferocytosis assay using macrophages and apoptotic breast cancer cells, and 3) testing the ability of the newly-generated monoclonal antibodies to block efferocytosis in the assay. The efferocytosis assay lacked reproducibility, which made it more difficult to interpret results; however, the assay consistently produced a window of apoptotic cell uptake by macrophages able to highlight inhibition of efferocytosis if it were taking place. When monoclonal antibodies were tested in the efferocytosis assay though, no inhibition was seen for either the derived monoclonals or the commercial anti-C1q antibody.

The lack of inhibition of efferocytosis in the *in vitro* assay poses the question of why the antibodies failed to block dying cell uptake. The simplest explanation is the assay did not work as anticipated, i.e., the uptake of apoptotic cells did not depend on C1q-mediated efferocytosis. An alternative explanation is that the assay was employing C1q-mediated efferocytosis but none of the antibodies tested blocked C1q-mediated efferocytosis of dying cells. Although the antibodies had been shown to bind C1q by ELISA and possibly immunoprecipitation, the conditions of the efferocytosis assay might have been suboptimal for the antibodies, most likely relating to antibody concentration. The commercial 9A7 antibody might recognise a linear epitope in either the beta sheets of the globular region or possibly the collagen-like region of the tail. Due to its length, sequences in the tail offer the possibility of an antibody that binds but will not block efferocytosis. Without a blocking antibody as a control, the reason(s) for the lack of neutralisation in the efferocytosis assay remain unclear.

What the project did accomplish was the derivation of four monoclonal antibodies that bound C1q in ELISA and possibly in immunoprecipitation. And in the process of deriving these antibodies, several aspects of interest regarding C1q immunisation and immunogenicity were noted. The lower than anticipated antibody titre highlighted the possible role of C1q in supressing the immune response, through interaction with dendritic cells, B and T lymphocytes. The possibility that C1q was becoming sequestered into innate immune functions in mice lacking the C1qA chain was examined using glutaraldehyde cross-linking. The cross-linked protein did not alter the antibody titres obtained during immunisation making it unlikely C1q was fulfilling immune functions in the C1qA null mice.

Another aspect of interest was the isolation of IgM-secreting hybridomas after repeated immunisation. Primed B cells found in lymph node germinal centres interact with T cells to bring about immunoglobulin class-switching. IgM antibodies are fit to purpose binding to repetitive epitopes on pathogens. IgMs may bind to the collagen-like tail of C1q which contains repetitive motifs folded into a triple helix, but this would require epitope mapping of the monoclonal antibodies to determine their binding site(s).

The development of the *in vitro* efferocytosis assay was not able to demonstrate inhibition of C1q-mediated efferocytosis but an interesting and potentially useful assay did result. Introduction of the pHrodo dye for labelling the cancer cells produced a reliable intracellular fluorescence in the phagocyte that eliminated the scoring of cancer cells overlapping the phagocytes while not actually having been

efferocytosed. The assay featured a window of peak uptake of apoptotic cells that should be capable of highlighting any inhibition of efferocytosis taking place.

6.4 FUTURE DIRECTIONS

Future directions for this project revolve around assessing the monoclonal antibodies for their capacity to neutralise C1q activity, or more specifically, neutralisation of efferocytosis. The *in vitro* efferocytosis assay developed in this project could well be sufficient for this task, but some basic characterisation of the monoclonal antibodies would be useful in the optimisation of the assay. In other words, the antibodies may not have more clearly blocked C1q-mediated efferocytosis because the assay conditions were sub-optimal.

Hybridoma cell lines produce differing concentrations of antibody, ranging between five and seventy-five µg/mL (personal observation). Optimising antibody concentration is important when assaying for neutralisation capacity, with at least equimolar quantities of antibody required to neutralise the target antigen or, in the case of lower affinity antibodies, even greater (Grossberg, 2009). Since none of the antibodies neutralised C1q in the efferocytosis assay, the likely explanations are either that the antibodies lack the capacity to fully neutralise C1q, or the concentration of the antibodies was insufficient to mediate neutralisation. To improve the efferocytosis neutralisation assay, purification and quantification of the monoclonal antibodies would be required in order to standardise the input concentration of antibody and enable direct comparison of the different antibodies.

Following production of large quantities of hybridoma supernatant, purification of the antibody from the culture medium is required. This is a straightforward process involving binding the antibody to either protein A, protein G or protein L followed by elution with a low pH buffer, typically citrate or glycine at pH 3 (Chahar, 2020). This quick simple purification yields monoclonal antibodies of good purity and concentration, such that a protein determination assay can be used to quantify the antibody concentration. Alternatively, a sandwich ELISA with an antibody of known concentration can be employed to precisely quantify antibody concentration.

Determination of the affinity of monoclonal antibodies is not necessary in the early stages of assessing the functionality of an antibody, but it is a feature of great importance for downstream preclinical studies. Higher affinity antibodies drive better neutralisation activity and determining antibody affinity is useful when developing preclinical models prior to moving into clinical studies.

Regardless of whether further optimisation of the *in vitro* assay would demonstrate C1q neutralisation by the monoclonal antibodies derived by this project, it would be expedient to test the antibodies in at least one mouse model for an indication of their usefulness *in vivo*. As monoclonal antibodies are extremely useful therapeutics in the clinic, testing conditions for preclinical studies are well established, which facilitates the assessment of the neutralisation capacity of candidate antibodies (Kim, 2017), (Zeitelhofer, 2018). Both the DMBA carcinogen model and the MMTV-PyMT model were employed on a C1q null background to show the role of C1q in carcinogenesis and cancer progression (Hodson, 2013), (NoorDin, 2017). Alternatively, the MMTV-neuT mouse model of mammary cancer, in which the mammary-specific MMTV promotor drives expression of a mutant neu (HER2) protein, could also be useful (Muller, 1988). Indications that one or more antibodies are able to inhibit C1q activity during cancer initiation and/or progression could open the door for modification of the antibody structure in order to render it more suitable for use in the clinic.

Translation of basic scientific findings into clinical applications is a long process. Previous studies in C1q null mutant mice showed potential for development of a new approach to treating and preventing breast cancer through inhibition of C1q. The ability to pharmacologically inhibit C1q is required in order to take the first step into pre-clinical studies. This thesis describes the successful generation of four candidate monoclonal antibodies with C1q binding affinity that may have potential to neutralise C1q-mediated efferocytosis *in vitro*. Further work is now required to determine the extent to which these monoclonal antibodies can be developed to assist breast cancer prevention and treatment strategies in the clinic.

REFERENCES

Abbott, D.W., Ivanova, V.S., Wang, X., Bonner, W.M. and Ausió, J., 2001. Characterization of the stability and folding of H2A. Z chromatin particles: implications for transcriptional activation. Journal of Biological Chemistry, 276(45), pp.41945-41949.

Afshar-Kharghan, V., 2017. The role of the complement system in cancer. The Journal of Clinical Investigation, 127(3), pp.780-789.

Ahmed, M. and Rahman, N., 2006. ATM and breast cancer susceptibility. Oncogene, 25(43), pp.5906-5911.

Akagi, S., Nakajima, C., Tanaka, Y. and Kurihara, Y., 2018. Flow cytometry-based method for rapid and high-throughput screening of hybridoma cells secreting monoclonal antibody. Journal of Bioscience and Bioengineering, 125(4), pp.464-469.

Alabdulkareem, H., Pinchinat, T., Khan, S., Landers, A., Christos, P., Simmons, R. and Moo, T.A., 2018. The impact of molecular subtype on breast cancer recurrence in young women treated with contemporary adjuvant therapy. The Breast Journal, 24(2), pp.148-153.

Alfaleh, M.A., Alsaab, H.O., Mahmoud, A.B., Alkayyal, A.A., Jones, M.L., Mahler, S.M. and Hashem, A.M., 2020. Phage display derived monoclonal antibodies: from bench to bedside. Frontiers in Immunology, 11, p.1986.

Anders, C.K., Johnson, R., Litton, J., Phillips, M. and Bleyer, A., 2009, June. Breast cancer before age 40 years. In Seminars in Oncology (Vol. 36, No. 3, pp. 237-249). WB Saunders.

Anderson, N.L. and Anderson, N.G., 2002. The human plasma proteome: history, character, and diagnostic prospects. Molecular & Cellular Proteomics, 1(11), pp.845-867.

Ando, T., Latif, R., Daniel, S., Eguchi, K. and Davies, T.F., 2004. Dissecting linear and conformational epitopes on the native thyrotropin receptor. Endocrinology, 145(11), pp.5185-5193.

Arandjelovic, S. and Ravichandran, K.S., 2015. Phagocytosis of apoptotic cells in homeostasis. Nature Immunology, 16(9), pp.907-917.

Arendt, L.M. and Kuperwasser, C., 2015. Form and function: how estrogen and progesterone regulate the mammary epithelial hierarchy. Journal of Mammary Gland Biology and Neoplasia, 20(1), pp.9-25.

Argon, A., Şener, A., Zekioğlu, O., Özdemir, N. and Kapkaç, M., 2014. The Effect of Freezing on the Immunoprofile of Breast Carcinoma Cells. Balkan Medical Journal, 31(4), pp.335-339.

Armstrong, A. and Ravichandran, K.S., 2011. Phosphatidylserine receptors: what is the new RAGE?. EMBO Reports, 12(4), pp.287-28874.

Atabai, K., Sheppard, D. and Werb, Z., 2007. Roles of the innate immune system in mammary gland remodeling during involution. Journal of Mammary Gland Biology and Neoplasia, 12(1), pp.37-45.

Atkin-Smith, G.K., Tixeira, R., Paone, S., Mathivanan, S., Collins, C., Liem, M., Goodall, K.J., Ravichandran, K.S., Hulett, M.D. and Poon, I.K., 2015. A novel mechanism of generating extracellular vesicles during apoptosis via a beads-on-a-string membrane structure. Nature Communications, 6(1), pp.1-10.

Barth, N.D., Marwick, J.A., Vendrell, M., Rossi, A.G. and Dransfield, I., 2017. The "phagocytic synapse" and clearance of apoptotic cells. Frontiers in Immunology, 8, p.1708.

Basu, S., Binder, R.J., Ramalingam, T. and Srivastava, P.K., 2001. CD91 is a common receptor for heat shock proteins gp96, hsp90, hsp70, and calreticulin. Immunity, 14(3), pp.303-313.

Beleut, M., Rajaram, R.D., Caikovski, M., Ayyanan, A., Germano, D., Choi, Y., Schneider, P. and Brisken, C., 2010. Two distinct mechanisms underlie progesterone-induced proliferation in the mammary gland. Proceedings of the National Academy of Sciences, 107(7), pp.2989-2994.

Benoit, M.E., Clarke, E.V., Morgado, P., Fraser, D.A. and Tenner, A.J., 2012. Complement protein C1q directs macrophage polarization and limits inflammasome activity during the uptake of apoptotic cells. The Journal of Immunology, 188(11), pp.5682-5693.

Berger, P. and Lapthorn, A.J., 2016. The molecular relationship between antigenic domains and epitopes on hCG. Molecular Immunology, 76, pp.134-145.

Bernatsky, S., Ramsey-Goldman, R., Labrecque, J., Joseph, L., Boivin, J.F., Petri, M., Zoma, A., Manzi, S., Urowitz, M.B., Gladman, D. and Fortin, P.R., 2013. Cancer risk in systemic lupus: an updated international multi-centre cohort study. Journal of Autoimmunity, 42, pp.130-135.

Berwin, B., Delneste, Y., Lovingood, R.V., Post, S.R. and Pizzo, S.V., 2004. SREC-I, a type F scavenger receptor, is an endocytic receptor for calreticulin. Journal of Biological Chemistry, 279(49), pp.51250-51257.

Bissell, M.J. and Hines, W'C., 2011. Why don't we get more cancer? A proposed role of the microenvironment in restraining cancer progression. Nature Medicine, 17(3), pp.320-329.

Blumenfeld, Z., 2012. Chemotherapy and fertility. Best practice & research Clinical Obstetrics & Gynaecology, 26(3), pp.379-390.

Bogen, S.A., Vani, K. and Sompuram, S.R., 2009. Molecular mechanisms of antigen retrieval: antigen retrieval reverses steric interference caused by formalin-induced cross-links. Biotechnic & Histochemistry, 84(5), pp.207-215.

Bonaparte, R.S., Hair, P.S., Banthia, D., Marshall, D.M., Cunnion, K.M. and Krishna, N.K., 2008. Human astrovirus coat protein inhibits serum complement activation via C1, the first component of the classical pathway. Journal of Virology, 82(2), pp.817-827.

Botto, M., Dell'Agnola, C., Bygrave, A.E., Thompson, E.M., Cook, H.T., Petry, F., Loos, M., Pandolfi, P.P. and Walport, M.J., 1998. Homozygous C1q deficiency causes glomerulonephritis associated with multiple apoptotic bodies. Nature Genetics, 19(1), pp.56-59.

Bouchardy, C., Fioretta, G., Verkooijen, H.M., Vlastos, G., Schaefer, P., Delaloye, J.F., Neyroud-Caspar, I., Majno, S.B., Wespi, Y., Forni, M. and Chappuis, P., 2007. Recent increase of breast cancer incidence among women under the age of forty. British Journal of Cancer, 96(11), pp.1743-1746.

Brady, N.J., Chuntova, P. and Schwertfeger, K.L., 2016. Macrophages: regulators of the inflammatory microenvironment during mammary gland development and breast cancer. Mediators of inflammation, 2016.

Bulla, R., Tripodo, C., Rami, D., Ling, G.S., Agostinis, C., Guarnotta, C., Zorzet, S., Durigutto, P., Botto, M. and Tedesco, F., 2016. C1q acts in the tumour microenvironment as a cancer-promoting factor independently of complement activation. Nature Communications, 7(1), pp.1-11.

Byrne, J.C., Gabhann, J.N., Stacey, K.B., Coffey, B.M., McCarthy, E., Thomas, W. and Jefferies, C.A', 2013. Bruton's tyrosine kinase is required for apoptotic cell uptake via regulating the phosphorylation and localization of calreticulin. The Journal of Immunology, 190(10), pp.5207-5215.

Calabro, S., Tritto, E., Pezzotti, A., Taccone, M., Muzzi, A., Bertholet, S., De Gregorio, E., O'Hagan, D.T., Baudner, B. and Seubert, A., 2013. The adjuvant effect of MF59 is due to the oil-in-water emulsion formulation, none of the individual components induce a comparable adjuvant effect. Vaccine, 31(33), pp.3363-3369.

Camidge, D.R., Herbst, R.S., Gordon, M.S., Eckhardt, S.G., Kurzrock, R., Durbin, B., Ing, J., Tohnya, T.M., Sager, J., Ashkenazi, A. and Bray, G., 2010. A phase I safety and pharmacokinetic study of the death receptor 5 agonistic antibody PRO95780 in patients with advanced malignancies. Clinical Cancer Research, 16(4), pp.1256-1263.

Canton, J., Neculai, D. and Grinstein, S., 2013. Scavenger receptors in homeostasis and immunity. Nature Reviews Immunology, 13(9), pp.621-634.

Carrara, S.C., Fiebig, D., Bogen, J.P., Grzeschik, J., Hock, B. and Kolmar, H., 2021. Recombinant antibody production using a dual-promoter single plasmid system. Antibodies, 10(2), p.18.

Chahar, D.S., Ravindran, S. and Pisal, S.S., 2020. Monoclonal antibody purification and its progression to commercial scale. Biologicals, 63, pp.1-13.

Chang, C.Y., Cheng, I.C., Chang, Y.C., Tsai, P.S., Lai, S.Y., Huang, Y.L., Jeng, C.R., Pang, V.F. and Chang, H.W., 2019. Identification of neutralizing monoclonal antibodies targeting novel conformational epitopes of the porcine epidemic diarrhoea virus spike protein. Scientific Reports, 9(1), pp.1-11.

Chavez-MacGregor, M., Elias, S.G., Onland-Moret, N.C., Van Der Schouw, Y.T., Van Gils, C.H., Monninkhof, E., Grobbee, D.E. and Peeters, P.H., 2005. Postmenopausal breast cancer risk and cumulative number of menstrual cycles. Cancer Epidemiology and Prevention Biomarkers, 14(4), pp.799-804.

Chou, P.Y. and Fasman, G.D., 1979. Prediction of beta-turns. Biophysical Journal, 26(3), pp.367-383.

Chua, A.C., Hodson, L.J., Moldenhauer, L.M., Robertson, S.A. and Ingman, W.V., 2010. Dual roles for macrophages in ovarian cycle-associated development and remodelling of the mammary gland epithelium. Development, 137(24), pp.4229-4238.

Clarke, R.B., 2004. Human breast cell proliferation and its relationship to steroid receptor expression. Climacteric, 7(2), pp.129-137.

Clavero-Álvarez, A., Di Mambro, T., Perez-Gaviro, S., Magnani, M. and Bruscolini, P., 2018. Humanization of antibodies using a statistical inference approach. Scientific Reports, 8(1), pp.1-11.

Cloutier, B.T., Clarke, A.E., Ramsey-Goldman, R., Wang, Y., Foulkes, W., Gordon, C., Hansen, J.E., Yelin, E., Urowitz, M.B., Gladman, D. and Fortin, P.R., 2013. Breast cancer in systemic lupus erythematosus. Oncology, 85(2), pp.117-121.

Collaborative Group on Hormonal Factors in Breast Cancer. 2012. Menarche, menopause, and breast cancer risk: individual participant meta-analysis, including 118 964 women with breast cancer from 117 epidemiological studies. Lancet Oncology. Nov;13(11):1141-51.

Cortazar, P., Zhang, L., Untch, M., Mehta, K., Costantino, J.P., Wolmark, N., Bonnefoi, H., Cameron, D., Gianni, L., Valagussa, P. and Swain, S.M., 2014. Pathological complete response and long-term clinical benefit in breast cancer: the CTNeoBC pooled analysis. The Lancet, 384(9938), pp.164-172.

Crane, M.J., Daley, J.M., van Houtte, O., Brancato, S.K., Henry Jr, W.L. and Albina, J.E., 2014. The monocyte to macrophage transition in the murine sterile wound. PloS One, 9(1), p.e86660.

Csorba, K., Schirmbeck, L.A., Tuncer, E., Ribi, C., Roux-Lombard, P., Chizzolini, C., Huynh-Do, U., Vanhecke, D. and Trendelenburg, M., 2019. Anti-C1q antibodies as occurring in systemic lupus erythematosus could be induced by an epstein-barr virus-derived antigenic site. Frontiers in Immunology, 10, p.2619.

Dahlbäck, B., 2000. Blood coagulation. The Lancet, 355(9215), pp.1627-1632.

D'Andrea, R.J., Stratmann, R., Lehner, C.F., John, U.P. and Saint, R., 1993. The three rows gene of Drosophila melanogaster encodes a novel protein that is required for chromosome disjunction during mitosis. Molecular Biology of the Cell, 4(11), pp.1161-1174.

Das, A., Sinha, M., Datta, S., Abas, M., Chaffee, S., Sen, C.K. and Roy, S., 2015. Monocyte and macrophage plasticity in tissue repair and regeneration. The American Journal of Pathology, 185(10), pp.2596-2606.

Dasari, P., Sharkey, D.J., Noordin, E., Glynn, D.J., Hodson, L.J., Chin, P.Y., Evdokiou, A., Robertson, S.A. and Ingman, W.V., 2014. Hormonal regulation of the cytokine microenvironment in the mammary gland. Journal of Reproductive Immunology, 106, pp.58-66.

De Groot, A.S., Moise, L., Terry, F., Gutierrez, A.H., Hindocha, P., Richard, G., Hoft, D.F., Ross, T.M., Noe, A.R., Takahashi, Y. and Kotraiah, V., 2020. Better epitope discovery, precision immune engineering, and accelerated vaccine design using immunoinformatics tools. Frontiers in Immunology, 11, p.442.

Dondelinger, M., Filée, P., Sauvage, E., Quinting, B., Muyldermans, S., Galleni, M. and Vandevenne, M.S., 2018. Understanding the significance and implications of antibody numbering and antigen-binding surface/residue definition. Frontiers in Immunology, 9, p.2278.

Dowling, W., Thompson, E., Badger, C., Mellquist, J.L., Garrison, A.R., Smith, J.M., Paragas, J., Hogan, R.J. and Schmaljohn, C., 2007. Influences of glycosylation on antigenicity, immunogenicity, and protective efficacy of ebola virus GP DNA vaccines. Journal of Virology, 81(4), pp.1821-1837.

Duncan, A.R. and Winter, G., 1988. The binding site for C1q on IgG. Nature, 332(6166), pp.738-740.

Duus, K., Hansen, E.W., Tacnet, P., Frachet, P., Arlaud, G.J., Thielens, N.M. and Houen, G., 2010. Direct interaction between CD91 and C1q. The FEBS Journal, 277(17), pp.3526-3537.

El-Hewala, A., Nageeb, G.S., El-shahawy, E.E., Sharaf, D.M., Omran, A.A., El-Messallamy, F.A. and Eassa, S., 2011. Anti-C1q and anti-dsDNA antibodies in systemic lupus erythematosus: Relationship with disease activity and renal involvement in Sharkia governorate, Egypt. The Egyptian Rheumatologist, 33(4), pp.203-208.

Elliott, M.R., Koster, K.M. and Murphy, P.S., 2017. Efferocytosis signaling in the regulation of macrophage inflammatory responses. The Journal of Immunology, 198(4), pp.1387-1394.

Elmore, S., 2007. Apoptosis: a review of programmed cell death. Toxicologic Pathology, 35(4), pp.495-516.

Emini, E.A., Hughes, J.V., Perlow, D. and Boger, J., 1985. Induction of hepatitis A virus-neutralizing antibody by a virus-specific synthetic peptide. Journal of Virology, 55(3), pp.836-839.

Erwig, L.P. and Henson, P.M., 2007. Immunological consequences of apoptotic cell phagocytosis. The American Journal of Pathology, 171(1), pp.2-8.

Faast, R., Thonglairoam, V., Schulz, T.C., Beall, J., Wells, J.R., Taylor, H., Matthaei, K., Rathjen, P.D., Tremethick, D.J. and Lyons, I., 2001. Histone variant H2A. Z is required for early mammalian development. Current Biology, 11(15), pp.1183-1187.

Fata, J.E., Chaudhary, V. and Khokha, R., 2001. Cellular turnover in the mammary gland is correlated with systemic levels of progesterone and not 17β-estradiol during the estrous cycle. Biology of Reproduction, 65(3), pp.680-688.

Fendly, B.M., Toy, K.J., Creasey, A.A., Vitt, C.R., Larrick, J.W., Yamamoto, R., and Lin, L.S., 1987. Murine monoclonal antibodies defining neutralizing epitopes on tumor necrosis factor. Hybridoma, 6(4), pp.359-370.

Ferdous, S., Kelm, S., Baker, T.S., Shi, J. and Martin, A.C., 2019. B-cell epitopes: discontinuity and conformational analysis. Molecular Immunology, 114, pp.643-650.

Flanders, K.C. and Wakefield, L.M., 2009. Transforming growth factor-βs and mammary gland involution; functional roles and implications for cancer progression. Journal of Mammary Gland Biology and Neoplasia, 14(2), pp.131-144.

Forsström, B., Bisławska Axnäs, B., Rockberg, J., Danielsson, H., Bohlin, A. and Uhlen, M., 2015. Dissecting antibodies with regards to linear and conformational epitopes. PloS One, 10(3), p.e0121673.

Frachet, P., Tacnet-Delorme, P., Gaboriaud, C. and Thielens, N.M., 2015. Role of C1q in efferocytosis and self-tolerance–links with autoimmunity. Autoimmunity–Pathogenesis, Clinical Aspects and Therapy of Specific Autoimmune Diseases. Croatia: InTech, pp.21-51.

Frenzel, A., Hust, M. and Schirrmann, T., 2013. Expression of recombinant antibodies. Frontiers in Immunology, 4, p.217.

Gaboriaud, C., Frachet, P., Thielens, N. and Arlaud, G., 2012. The human c1q globular domain: structure and recognition of non-immune self ligands. Frontiers in Immunology, 2, p.92.

Gajanandana, O., Irvine, K., Grant, P.A., Francis, G.L., Knowles, S.E., Wrin, J., Wallace, J.C. and Owens, P.C., 1998. Measurement of an analog of insulin-like growth factor-I in blood plasma using a novel enzyme-linked immunosorbent assay. Journal of Endocrinology, 156(3), pp.407-414.

Gajewska, M., Sobolewska, A., Kozlowski, M. and Motyl, T., 2008. Role of autophagy in mammary gland development. Journal of Physiology and Pharmacology, 59(Suppl 9), pp.237-249.

Galvan, M.D., Greenlee-Wacker, M.C. and Bohlson, S.S., 2012. C1q and phagocytosis: the perfect complement to a good meal. Journal of Leukocyte Biology, 92(3), pp.489-497.

Gardai, S.J., McPhillips, K.A., Frasch, S.C., Janssen, W.J., Starefeldt, A., Murphy-Ullrich, J.E., Bratton, D.L., Oldenborg, P.A., Michalak, M. and Henson, P.M., 2005. Cell-surface calreticulin initiates clearance of viable or apoptotic cells through trans-activation of LRP on the phagocyte. Cell, 123(2), pp.321-334.

Gelebart, P., Opas, M. and Michalak, M., 2005. Calreticulin, a Ca2+-binding chaperone of the endoplasmic reticulum. The International Journal of Biochemistry & Cell Biology, 37(2), pp.260-266.

Geyer, F.C., Pareja, F., Weigelt, B., Rakha, E., Ellis, I.O., Schnitt, S.J. and Reis-Filho, J.S., 2017. The spectrum of triple-negative breast disease: high-and low-grade lesions. The American Journal of Pathology, 187(10), pp.2139-2151.

Ghebrehiwet, B., Hosszu, K.H. and Peerschke, E.I., 2017. C1q as an autocrine and paracrine regulator of cellular functions. Molecular Immunology, 84, pp.26-33.

Gibbons, G.S., Banks, R.A., Kim, B., Changolkar, L., Riddle, D.M., Leight, S.N., Irwin, D.J., Trojanowski, J.Q. and Lee, V.M., 2018. Detection of Alzheimer disease (AD)-specific tau pathology in AD and nonAD tauopathies by immunohistochemistry with novel conformation-selective tau antibodies. Journal of Neuropathology & Experimental Neurology, 77(3), pp.216-228.

Gieniec, K.A., Butler, L.M., Worthley, D.L. and Woods, S.L., 2019. Cancer-associated fibroblasts—heroes or villains?. British Journal of Cancer, 121(4), pp.293-302.

Gion, W.R., Davis-Taber, R.A., Regier, D.A., Fung, E., Medina, L., Santora, L.C., Bose, S., Ivanov, A.V., Perilli-Palmer, B.A., Chumsae, C.M. and Matuck, J.G., 2013, July. Expression of antibodies using single open reading frame (sORF) vector design: demonstration of manufacturing feasibility. In MAbs (Vol. 5, No. 4, pp. 595-607). Taylor & Francis.

Giraud, M., Salson, M., Duez, M., Villenet, C., Quief, S., Caillault, A., Grardel, N., Roumier, C., Preudhomme, C. and Figeac, M., 2014. Fast multiclonal clusterization of V (D) J recombinations from high-throughput sequencing. BMC Genomics, 15(1), pp.1-12.

Glick, D., Barth, S. and Macleod, K.F., 2010. Autophagy: cellular and molecular mechanisms. The Journal of Pathology, 221(1), pp.3-12.

Goldenberg, M.M., 1999. Trastuzumab, a recombinant DNA-derived humanized monoclonal antibody, a novel agent for the treatment of metastatic breast cancer. Clinical Therapeutics, 21(2), pp.309-318.

Gong, S. and Ruprecht, R.M., 2020. Immunoglobulin M: An Ancient Antiviral Weapon–Rediscovered. Frontiers in Immunology, 11, p.1943.

Gouon-Evans, V., Rothenberg, M.E. and Pollard, J.W., 2000. Postnatal mammary gland development requires macrophages and eosinophils. Development, 127(11), pp.2269-2282.

Graham, J.D. and Clarke, C.L., 1997. Physiological action of progesterone in target tissues. Endocrine Reviews, 18(4), pp.502-519.

Graves, J., Byerly, J., Priego, E., Makkapati, N., Parish, S.V., Medellin, B. and Berrondo, M., 2020. A review of deep learning methods for antibodies. Antibodies, 9(2), p.12.

Greenfield, E.A., 2022. Hybridoma screening by antibody capture: Flow cytometry/FACS with whole cells to detect cell-surface binding. Cold Spring Harbor Protocols, 2022(6), pp.pdb-prot103077.

Groenendyk, J., Lynch, J. and Michalak, M., 2004. Calreticulin, Ca 2+, and calcineurin-signaling from the endoplasmic reticulum. Molecules & Cells (Springer Science & Business Media BV), 17(3).

Grossberg, S.E., Casey, M. and Grossberg, L.D., 2009. Quantification of the neutralization of cytokine biological activity by antibody: the ten-fold reduction bioassay of interleukin-6 as growth factor. Journal of Interferon & Cytokine Research, 29(8), pp.421-426.

Guy, C.T., Cardiff, R.D. and Muller, W.J., 1992. Induction of mammary tumors by expression of polyomavirus middle T oncogene: a transgenic mouse model for metastatic disease. Molecular and Cellular Biology, 12(3), pp.954-961.

Gyorki, D.E., Asselin-Labat, M.L., van Rooijen, N., Lindeman, G.J. and Visvader, J.E., 2009. Resident macrophages influence stem cell activity in the mammary gland. Breast Cancer Research, 11(4), pp.1-6.

Halenbeck, R., Kawasaki, E., Wrin, J. and Koths, K., 1989. Renaturation and purification of biologically active recombinant human macrophage colony-stimulating factor expressed in E. coli. Bio/technology, 7(7), pp.710-715.

Hamczyk, M.R., Villa-Bellosta, R. and Andrés, V., 2015. *In vitro* macrophage phagocytosis assay. In Methods in Mouse Atherosclerosis (pp. 235-246). Humana Press, New York, NY.

Han, W., Chen, S., Yuan, W., Fan, Q., Tian, J., Wang, X., Chen, L., Zhang, X., Wei, W., Liu, R. and Qu, J., 2016. Oriented collagen fibers direct tumor cell intravasation. Proceedings of the National Academy of Sciences, 113(40), pp.11208-11213.

Hatano, R., Itoh, T., Otsuka, H., Okamoto, S., Komiya, E., Iwata, S., Aune, T.M., Dang, N.H., Kuwahara-Arai, K., Ohnuma, K. and Morimoto, C., 2019, November. Characterization of novel anti-IL-26 neutralizing monoclonal antibodies for the treatment of inflammatory diseases including psoriasis. In MAbs (Vol. 11, No. 8, pp. 1428-1442). Taylor & Francis.

He, M., Kubo, H., Morimoto, K., Fujino, N., Suzuki, T., Takahasi, T., Yamada, M., Yamaya, M., Maekawa, T., Yamamoto, Y. and Yamamoto, H., 2011. Receptor for advanced glycation end products binds to phosphatidylserine and assists in the clearance of apoptotic cells. EMBO Reports, 12(4), pp.358-364.

Hershfield, M.S. and Seegmiller, J.E., 1976. Regulation of de novo purine biosynthesis in human lymphoblasts. Coordinate control of proximal (rate-determining) steps and the inosinic acid branch point. Journal of Biological Chemistry, 251(23), pp.7348-7354.

Hesketh, M., Sahin, K.B., West, Z.E. and Murray, R.Z., 2017. Macrophage phenotypes regulate scar formation and chronic wound healing. International Journal of Molecular Sciences, 18(7), p.1545.

Hobro, A.J. and Smith, N.I., 2017. An evaluation of fixation methods: Spatial and compositional cellular changes observed by Raman imaging. Vibrational Spectroscopy, 91, pp.31-45.

Hodson, L.J., Chua, A.C., Evdokiou, A., Robertson, S.A. and Ingman, W.V., 2013. Macrophage phenotype in the mammary gland fluctuates over the course of the estrous cycle and is regulated by ovarian steroid hormones. Biology of Reproduction, 89(3), pp.65-1.

Hoffman, E.A., Frey, B.L., Smith, L.M. and Auble, D.T., 2015. Formaldehyde crosslinking: a tool for the study of chromatin complexes. Journal of Biological Chemistry, 290(44), pp.26404-26411.

Hong, Q., Sze, C.I., Lin, S.R., Lee, M.H., He, R.Y., Schultz, L., Chang, J.Y., Chen, S.J., Boackle, R.J., Hsu, L.J. and Chang, N.S., 2009. Complement C1q activates tumor suppressor WWOX to induce apoptosis in prostate cancer cells. PloS one, 4(6), p.e5755.

Hooks, M.A., Wade, C.S. and Millikan Jr, W.J., 1991. Muromonab CD-3: a review of its pharmacology, pharmacokinetics, and clinical use in transplantation. Pharmacotherapy: The Journal of Human Pharmacology and Drug Therapy, 11(1), pp.26-37.

Hopp, T.P. and Woods, K.R., 1981. Prediction of protein antigenic determinants from amino acid sequences. Proceedings of the National Academy of Sciences, 78(6), pp.3824-3828.

Hosszu, K.K., Valentino, A., Vinayagasundaram, U., Vinayagasundaram, R., Joyce, M.G., Ji, Y., Peerschke, E.I. and Ghebrehiwet, B., 2012. DC-SIGN, C1q, and gC1qR form a trimolecular receptor complex on the surface of monocyte-derived immature dendritic cells. Blood, The Journal of the American Society of Hematology, 120(6), pp.1228-1236.

Huang, L., Abdalla, A.M., Xiao, L. and Yang, G., 2020. Biopolymer-based microcarriers for three-dimensional cell culture and engineered tissue formation. International Journal of Molecular Sciences, 21(5), p.1895.

Hunziker, E.B., 1993. Application of cryotechniques in cartilage tissue preservation an immunoelectron microscopy: Potentials and problems. Microscopy Research and Technique, 24(6), pp.457-464.

Ingersoll, M.A., Platt, A.M., Potteaux, S. and Randolph, G.J., 2011. Monocyte trafficking in acute and chronic inflammation. Trends in Immunology, 32(10), pp.470-477.

Italiani, P. and Boraschi, D., 2014. From monocytes to M1/M2 macrophages: phenotypical vs. functional differentiation. Frontiers in Immunology, 5, p.514.

Iyer, S.S., Pulskens, W.P., Sadler, J.J., Butter, L.M., Teske, G.J., Ulland, T.K., Eisenbarth, S.C., Florquin, S., Flavell, R.A., Leemans, J.C. and Sutterwala, F.S., 2009. Necrotic cells trigger a sterile inflammatory response through the Nlrp3 inflammasome. Proceedings of the National Academy of Sciences, 106(48), pp.20388-20393.

Jameson, B.A. and Wolf, H., 1988. The antigenic index: a novel algorithm for predicting antigenic determinants. Bioinformatics, 4(1), pp.181-186.

Janeway, C.A., Travers, P., Walport, M. and Capra, D.J., 2001. Immunobiology (p. 600). UK: Garland Science: Taylor & Francis Group.

Jasinska, J., Wagner, S., Radauer, C., Sedivy, R., Brodowicz, T., Wiltschke, C., Breiteneder, H., Pehamberger, H., Scheiner, O., Wiedermann, U. and Zielinski, C.C., 2003. Inhibition of tumor cell growth by antibodies induced after vaccination with peptides derived from the extracellular domain of Her-2/neu. International Journal of Cancer, 107(6), pp.976-983.

Jlajla, H., Sellami, M.K., Sfar, I., Laadhar, L., Zerzeri, Y., Abdelmoula, M.S., Gorgi, Y., Dridi, M.F. and Makni, S., 2014. New C1q mutation in a Tunisian family. Immunobiology, 219(3), pp.241-246.

Jones, M.L., Seldon, T., Smede, M., Linville, A., Chin, D.Y., Barnard, R., Mahler, S.M., Munster, D., Hart, D., Gray, P.P. and Munro, T.P., 2010. A method for rapid, ligation-independent reformatting of recombinant monoclonal antibodies. Journal of Immunological Methods, 354(1-2), pp.85-90.

Joshi, P.A., Jackson, H.W., Beristain, A.G., Di Grappa, M.A., Mote, P.A., Clarke, C.L., Stingl, J., Waterhouse, P.D. and Khokha, R., 2010. Progesterone induces adult mammary stem cell expansion. Nature, 465(7299), pp.803-807.

Kang, R., Zeh, H.J., Lotze, M.T. and Tang, D.J.C.D., 2011. The Beclin 1 network regulates autophagy and apoptosis. Cell Death & Differentiation, 18(4), pp.571-580.

Karplus, P.A. and Schulz, G.E., 1985. Prediction of chain flexibility in proteins. Naturwissenschaften, 72(4), pp.212-213.

Katoh, S., Terashima, M., Tomioka, K. and Hikida, N., 1996. Use of peptide immunization for porcine insulin of a very high homology with a host protein. Journal of Immunological Methods, 191(1), pp.33-38. 194.

Katsumata, Y., Miyake, K., Kawaguchi, Y., Okamoto, Y., Kawamoto, M., Gono, T., Baba, S., Hara, M. and Yamanaka, H., 2011. Anti-C1q antibodies are associated with systemic lupus erythematosus global activity but not specifically with nephritis: A controlled study of 126 consecutive patients. Arthritis & Rheumatism, 63(8), pp.2436-2444.

Kaul, M. and Loos, M., 1997. Dissection of C1q capability of interacting with IgG: time-dependent formation of a tight and only partly reversible association. Journal of Biological Chemistry, 272(52), pp.33234-33244.

Kaur, P., Paton, S., Furze, J., Wrin, J., Olsen, S., Danks, J. and Scurry, J., 1997. Identification of a cell surface protein with a role in stimulating human keratinocyte proliferation, expressed during development and carcinogenesis. Journal of Investigative Dermatology, 109(2), pp.194-199.

Keener, A.B., Thurlow, L.T., Kang, S., Spidale, N.A., Clarke, S.H., Cunnion, K.M., Tisch, R., Richardson, A.R. and Vilen, B.J., 2017. Staphylococcus aureus protein A disrupts immunity mediated by long-lived plasma cells. The Journal of Immunology, 198(3), pp.1263-1273.

Kerdelhué, B., Forest, C. and Coumoul, X., 2016. Dimethyl-Benz (a) anthracene: A mammary carcinogen and a neuroendocrine disruptor. Biochimie Open, 3, pp.49-55.

Keydar, I., Chen, L., Karby, S., Weiss, F.R., Delarea, J., Radu, M., Chaitcik, S. and Brenner, H.J., 1979. Establishment and characterization of a cell line of human breast carcinoma origin. European Journal of Cancer (1965), 15(5), pp.659-670.

Kim, S.Y., Kim, S., Bae, D.J., Park, S.Y., Lee, G.Y., Park, G.M. and Kim, I.S., 2017. Coordinated balance of Rac1 and RhoA plays key roles in determining phagocytic appetite. PLoS One, 12(4), p.e0174603.

King, M.C., Marks, J.H. and Mandell, J.B., 2003. Breast and ovarian cancer risks due to inherited mutations in BRCA1 and BRCA2. Science, 302(5645), pp.643-646.

Kishore, U. and Reid, K.B., 2000. C1q: structure, function, and receptors. Immunopharmacology, 49(1-2), pp.159-170.

Köhler, G. and Milstein, C., 1975. Continuous cultures of fused cells secreting antibody of predefined specificity. Nature, 256(5517), pp.495-497.

Kohler, H., Pashov, A. and Kieber-Emmons, T., 2019. The promise of anti-idiotype revisited. Frontiers in Immunology, 10, p.808.

Kojouharova, M., 2014. Classical Complement Pathway Component C1q: Purification of Human C1q, Isolation of C1q Collagen-Like and Globular Head Fragments and Production of Recombinant C1q—Derivatives. Functional Characterization. In The Complement System (pp. 25-42). Humana Press, Totowa, NJ.

Koonin, E.V., 2005. Orthologs, paralogs, and evolutionary genomics. Annual Review of Genetics, 39, pp.309-338.

Kouser, L., Madhukaran, S.P., Shastri, A., Saraon, A., Ferluga, J., Al-Mozaini, M. and Kishore, U., 2015. Emerging and novel functions of complement protein C1q. Frontiers in Immunology, 6, p.317.

Kozlowski, L.P., 2017. Proteome-pI: proteome isoelectric point database. Nucleic Acids Research, 45(D1), pp.D1112-D1116.

Kreuzaler, P.A., Staniszewska, A.D., Li, W., Omidvar, N., Kedjouar, B., Turkson, J., Poli, V., Flavell, R.A., Clarkson, R.W. and Watson, C.J., 2011. Stat3 controls lysosomal-mediated cell death *in vivo*. Nature Cell Biology, 13(3), pp.303-309.

Kulp, D.W. and Schief, W.R., 2013. Advances in structure-based vaccine design. Current Opinion in Virology, 3(3), pp.322-331.

Kumar, M., Khan, I. and Sinha, S., 2015. Nature of immobilization surface affects antibody specificity to placental alkaline phosphatase. Journal of Immunoassay and Immunochemistry, 36(4), pp.405-413.

Kuroi, K., Toi, M., Ohno, S., Nakamura, S., Iwata, H., Masuda, N., Sato, N., Tsuda, H., Kurosumi, M. and Akiyama, F., 2015. Comparison of different definitions of pathologic complete response in operable breast cancer: a pooled analysis of three prospective neoadjuvant studies of JBCRG. Breast Cancer, 22(6), pp.586-595.

Kyte, J. and Doolittle, R.F., 1982. A simple method for displaying the hydropathic character of a protein. Journal of Molecular Biology, 157(1), pp.105-132.

Ladoire, S., Arnould, L., Apetoh, L., Coudert, B., Martin, F., Chauffert, B., Fumoleau, P. and Ghiringhelli, F., 2008. Pathologic complete response to neoadjuvant chemotherapy of breast carcinoma is associated with the disappearance of tumor-infiltrating foxp3+ regulatory T cells. Clinical Cancer Research, 14(8), pp.2413-2420.

Laffleur, B., Pascal, V., Sirac, C. and Cogné, M., 2012. Production of human or humanized antibodies in mice. In Antibody Methods and Protocols (pp. 149-159). Humana Press, Totowa, NJ.

Lauber, K., Blumenthal, S.G., Waibel, M. and Wesselborg, S., 2004. Clearance of apoptotic cells: getting rid of the corpses. Molecular Cell, 14(3), pp.277-287.

Lauvrak, V., Brekke, O.H., Ihle, Ø. and Lindqvist, B.H., 1997. Identification and characterisation of C1q-binding phage displayed peptides. Biological Chemistry, 378(12), pp.1509-1520.

Lawson, A.D., MacCoss, M. and Heer, J.P., 2017. Importance of Rigidity in Designing Small Molecule Drugs To Tackle Protein–Protein Interactions (PPIs) through Stabilization of Desired Conformers: Miniperspective. Journal of Medicinal Chemistry, 61(10), pp.4283-4289.

Lee, E.K., Tian, H. and Nakaya, H.I., 2020. Antigenicity prediction and vaccine recommendation of human influenza virus A (H3N2) using convolutional neural networks. Human Vaccines & Immunotherapeutics, 16(11), pp.2690-2708.

Leitner, W.W., Ying, H. and Restifo, N.P., 1999. DNA and RNA-based vaccines: principles, progress and prospects. Vaccine, 18(9-10), pp.765-777.

Li, J., Sai, T., Berger, M., Chao, Q., Davidson, D., Deshmukh, G., Drozdowski, B., Ebel, W., Harley, S., Henry, M. and Jacob, S., 2006. Human antibodies for immunotherapy development generated via a human B cell hybridoma technology. Proceedings of the National Academy of Sciences, 103(10), pp.3557-3562.

Li, X., Miao, X., Wang, H., Xu, Z. and Li, B., 2015. The tissue dependent interactions between p53 and Bcl-2 *in vivo*. Oncotarget, 6(34), p.35699.

Lian, W., Fu, F., Lin, Y., Lu, M., Chen, B., Yang, P., Zeng, B., Huang, M. and Wang, C., 2017. The impact of young age for prognosis by subtype in women with early breast cancer. Scientific Reports, 7(1), pp.1-8.

Liang, Y.Y., Arnold, T., Michlmayr, A., Rainprecht, D., Perticevic, B., Spittler, A. and Oehler, R., 2014. Serum-dependent processing of late apoptotic cells for enhanced efferocytosis. Cell Death & Disease, 5(5), pp.e1264-e1264.

Lilienthal, G.M., Rahmöller, J., Petry, J., Bartsch, Y.C., Leliavski, A. and Ehlers, M., 2018. Potential of murine IgG1 and human IgG4 to inhibit the classical complement and Fcγ receptor activation pathways. Frontiers in Immunology, 9, p.958.

Lillis, A.P., Greenlee, M.C., Mikhailenko, I., Pizzo, S.V., Tenner, A.J., Strickland, D.K. and Bohlson, S.S., 2008. Murine low-density lipoprotein receptor-related protein 1 (LRP) is required for phagocytosis of targets bearing LRP ligands but is not required for C1q-triggered enhancement of phagocytosis. The Journal of Immunology, 181(1), pp.364-373.

Liu, F., Si, Y., Liu, G., Li, S., Zhang, J. and Ma, Y., 2015. The tetravalent anti-DR5 antibody without cross-linking direct induces apoptosis of cancer cells. Biomedicine & Pharmacotherapy, 70, pp.41-45.

Lu, **I** Wu, X. and Teh, B.K., 2007. The regulatory roles of C1q. Immunobiology, 212(4-5), pp.245-252.

Lubbers, R., Van Essen, M.F., Van Kooten, C. and Trouw, L.A., 2017. Production of complement components by cells of the immune system. Clinical & Experimental Immunology, 188(2), pp.183-194.

Lyons, T.R., Schedin, P.J. and Borges, V.F., 2009. Pregnancy and breast cancer: when they collide. Journal of Mammary Gland Biology and Neoplasia, 14(2), pp.87-98.

Maas, P., Barrdahl, M., Joshi, A.D., Auer, P.L., Gaudet, M.M., Milne, R.L., Schumacher, F.R., Anderson, W.F., Check, D., Chattopadhyay, S. and Baglietto, L., 2016. Breast cancer risk from modifiable and nonmodifiable risk factors among white women in the United States. JAMA Oncology, 2(10), pp.1295-1302.

Macedo, A.C.L. and Isaac, L., 2016. Systemic lupus erythematosus and deficiencies of early components of the complement classical pathway. Frontiers in Immunology, 7, p.55.

Mali, P., Yang, L., Esvelt, K.M., Aach, J., Guell, M., DiCarlo, J.E., Norville, J.E. and Church, G.M., 2013. RNA-guided human genome engineering via Cas9. Science, 339(6121), pp.823-826.

Mangogna, A., Agostinis, C., Bonazza, D., Belmonte, B., Zacchi, P., Zito, G., Romano, A., Zanconati, F., Ricci, G., Kishore, U. and Bulla, R., 2019. Is the complement protein C1q a pro-or anti-tumorigenic factor? Bioinformatics analysis involving human carcinomas. Frontiers in Immunology, 10, p.865.

Mantovani, A., Biswas, S.K., Galdiero, M.R., Sica, A. and Locati, M., 2013. Macrophage plasticity and polarization in tissue repair and remodelling. The Journal of Pathology, 229(2), pp.176-185.

Marchan, J., 2019. In silico identification of epitopes present in human heat shock proteins (HSPs) overexpressed by tumour cells. Journal of Immunological Methods, 471, pp.34-45.

Markiewski, M.M. and Lambris, J.D., 2007. The role of complement in inflammatory diseases from behind the scenes into the spotlight. The American Journal of Pathology, 171(3), pp.715-727.

Marks, J.D., Hoogenboom, H.R., Bonnert, T.P., McCafferty, J., Griffiths, A.D. and Winter, G., 1991. By-passing immunization: human antibodies from V-gene libraries displayed on phage. Journal of Molecular Biology, 222(3), pp.581-597.

Martinez, F.O. and Gordon, S., 2014. The M1 and M2 paradigm of macrophage activation: time for reassessment. F1000prime Reports, 6.

Martinson, H.A., Jindal, S., Durand-Rougely, C., Borges, V.F. and Schedin, P., 2015. Wound healing-like immune program facilitates postpartum mammary gland involution and tumor progression. International Journal of Cancer, 136(8), pp.1803-1813.

Masciari, S., Dillon, D.A., Rath, M., Robson, M., Weitzel, J.N., Balmana, J., Gruber, S.B., Ford, J.M., Euhus, D., Lebensohn, A. and Telli, M., 2012. Breast cancer phenotype in women with TP53 germline mutations: a Li-Fraumeni syndrome consortium effort. Breast Cancer Research and Treatment, 133(3), pp.1125-1130.

Mathelin, C., Annane, K., Treisser, A., Chenard, M.P., Tomasetto, C., Bellocq, J.P. and Rio, M.C., 2008. Pregnancy and post-partum breast cancer: a prospective study. Anticancer Research, 28(4C), pp.2447-2452.

Mattsson, P.T., Vihinen, M. and Smith, C.E., 1996. X-linked agammaglobulinemia (XLA): A genetic tyrosine kinase (Btk) disease. Bioessays, 18(10), pp.825-834.

McComb, S., Chan, P.K., Guinot, A., Hartmannsdottir, H., Jenni, S., Dobay, M.P., Bourquin, J.P. and Bornhauser, B.C., 2019. Efficient apoptosis requires feedback amplification of upstream apoptotic signals by effector caspase-3 or-7. Science Advances, 5(7), p.eaau9433.

McGonigal, R., Cunningham, M.E., Yao, D., Barrie, J.A., Sankaranarayanan, S., Fewou, S.N., Furukawa, K., Yednock, T.A. and Willison, H.J., 2016. C1q-targeted inhibition of the classical complement pathway prevents injury in a novel mouse model of acute motor axonal neuropathy. Acta Neuropathologica Communications, 4(1), pp.1-16.

Medina, C.B. and Ravichandran, K.S., 2016. Do not let death do us part:'find-me'signals in communication between dying cells and the phagocytes. Cell Death & Differentiation, 23(6), pp.979-989.

Melino, G., Knight, R.A. and Nicotera, P., 2005. How many ways to die? How many different models of cell death?. Cell Death & Differentiation, 12(2), pp.1457-1462.

Menzies, F.M., Henriquez, F.L., Alexander, J. and Roberts, C.W., 2011. Selective inhibition and augmentation of alternative macrophage activation by progesterone. Immunology, 134(3), pp.281-291.

Michaelsen, T.E., Kolberg, J., Aase, A., Herstad, T.K. and Høiby, E.A., 2004. The four mouse IgG isotypes differ extensively in bactericidal and opsonophagocytic activity when reacting with the P1. 16 epitope on the outer membrane PorA protein of Neisseria meningitidis. Scandinavian Journal of Immunology, 59(1), pp.34-39.

Migneault, I., Dartiguenave, C., Bertrand, M.J. and Waldron, K.C., 2004. Glutaraldehyde: behavior in aqueous solution, reaction with proteins, and application to enzyme crosslinking. Biotechniques, 37(5), pp.790-802.

Mishra, A.K. and Mariuzza, R.A., 2018. Insights into the structural basis of antibody affinity maturation from next-generation sequencing. Frontiers in Immunology, 9, p.117.

Mohammed, H., Russell, I.A., Stark, R., Rueda, O.M., Hickey, T.E., Tarulli, G.A., Serandour, A.A., Birrell, S.N., Bruna, A., Saadi, A. and Menon, S., 2015. Progesterone receptor modulates ERα action in breast cancer. Nature, 523(7560), pp.313-317.

Monks, J., Rosner, D., Geske, F.J., Lehman, L., Hanson, L., Neville, M.C. and Fadok, V.A., 2005. Epithelial cells as phagocytes: apoptotic epithelial cells are engulfed by mammary alveolar epithelial cells and repress inflammatory mediator release. Cell Death & Differentiation, 12(2), pp.107-114.

Montaño, F., Grinstein, S. and Levin, R., 2018. Quantitative phagocytosis assays in primary and cultured macrophages. In Macrophages (pp. 151-163). Humana Press, New York, NY.

Morgan, B.P., 1996. Intervention in the complement system: a therapeutic strategy in inflammation. Biochemical Society Transactions, 24(1), pp.224-229.

Moses, H. and Barcellos-Hoff, M.H., 2011. TGF-β biology in mammary development and breast cancer. Cold Spring Harbor Perspectives in Biology, 3(1), p.a003277.

Muller, W.J., Sinn, E., Pattengale, P.K., Wallace, R. and Leder, P., 1988. Single-step induction of mammary adenocarcinoma in transgenic mice bearing the activated c-neu oncogene. Cell, 54(1), pp.105-115.

Murshid, A., Borges, T.J., Lang, B.J. and Calderwood, S.K., 2016. The scavenger receptor SREC-I cooperates with toll-like receptors to trigger inflammatory innate immune responses. Frontiers in immunology, 7, p.226.

Nagasawa, H., Yanai, R. and Taniguchi, H., 1976. Importance of mammary gland DNA synthesis on carcinogen-induced mammary tumorigenesis in rats. Cancer Research, 36(7 Part 1), pp.2223-2226.

Nahta, R., Hung, M.C. and Esteva, F.J., 2004. The HER-2-targeting antibodies trastuzumab and pertuzumab synergistically inhibit the survival of breast cancer cells. Cancer Research, 64(7), pp.2343-2346.

Nanjappa, V., Thomas, J.K., Marimuthu, A., Muthusamy, B., Radhakrishnan, A., Sharma, R., Ahmad Khan, A., Balakrishnan, L., Sahasrabuddhe, N.A., Kumar, S. and Jhaveri, B.N., 2014. Plasma Proteome Database as a resource for proteomics research: 2014 update. Nucleic Acids Research, 42(D1), pp.D959-D965.

Nayak, A., Pednekar, L., Reid, K.B. and Kishore, U., 2012. Complement and non-complement activating functions of C1q: a prototypical innate immune molecule. Innate Immunity, 18(2), pp.350-363.

Need, E.F., Atashgaran, V., Ingman, W.V. and Dasari, P., 2014. Hormonal regulation of the immune microenvironment in the mammary gland. Journal of Mammary Gland Biology and Neoplasia, 19(2), pp.229-239.

Nevanlinna, H. and Bartek, J., 2006. The CHEK2 gene and inherited breast cancer susceptibility. Oncogene, 25(43), pp.5912-5919.

Nguyen-Ngoc, K.V., Shamir, E.R., Huebner, R.J., Beck, J.N., Cheung, K.J. and Ewald, A.J., 2015. 3D culture assays of murine mammary branching morphogenesis and epithelial invasion. In Tissue morphogenesis (pp. 135-162). Humana Press, New York, NY.

Nikoletopoulou, V., Markaki, M., Palikaras, K. and Tavernarakis, N., 2013. Crosstalk between apoptosis, necrosis and autophagy. Biochimica et Biophysica Acta (BBA)-Molecular Cell Research, 1833(12), pp.3448-3459.

Noor Din, S.M., 2017. Effect of C1q null mutation on mammary gland development and breast cancer susceptibility (Doctoral dissertation).

Norsworthy, P.J., Fossati-Jimack, L., Cortes-Hernandez, J., Taylor, P.R., Bygrave, A.E., Thompson, R.D., Nourshargh, S., Walport, M.J. and Botto, M., 2004. Murine CD93 (C1qRp) contributes to the removal of apoptotic cells *in vivo* but is not required for C1q-mediated enhancement of phagocytosis. The Journal of Immunology, 172(6), pp.3406-3414.

Ó'Fágáin, C., Cummins, P.M. and O'Connor, B.F., 2017. Gel-filtration chromatography. In Protein Chromatography (pp. 15-25). Humana Press, New York, NY.

Ogden, C.A., deCathelineau, A., Hoffmann, P.R., Bratton, D., Ghebrehiwet, B., Fadok, V.A. and Henson, P.M., 2001. C1q and mannose binding lectin engagement of cell surface calreticulin and CD91 initiates macropinocytosis and uptake of apoptotic cells. Journal of Experimental Medicine, 194(6), pp.781-796.

Öhlund, D., Elyada, E. and Tuveson, D., 2014. Fibroblast heterogeneity in the cancer wound. Journal of Experimental Medicine, 211(8), pp.1503-1523.

Ortega-Gómez, A., Perretti, M. and Soehnlein, O., 2013. Resolution of inflammation: an integrated view. EMBO Molecular Medicine, 5(5), pp.661-674.

Palm, A.K.E. and Henry, C., 2019. Remembrance of things past: long-term B cell memory after infection and vaccination. Frontiers in Immunology, 10, p.1787.

Parker, J.M.R., Guo, D. and Hodges, R.S., 1986. New hydrophilicity scale derived from high-performance liquid chromatography peptide retention data: correlation of predicted surface residues with antigenicity and X-ray-derived accessible sites. Biochemistry, 25(19), pp.5425-5432.

Patten, D.A., 2018. SCARF1: a multifaceted, yet largely understudied, scavenger receptor. Inflammation Research, 67(8), pp.627-632.

Peerschke, E.I. and Ghebrehiwet, B., 2014. cC1qR/CR and gC1qR/p33: observations in cancer. Molecular Immunology, 61(2), pp.100-109.

Penberthy, K.K. and Ravichandran, K.S., 2016. Apoptotic cell recognition receptors and scavenger receptors. Immunological Reviews, 269(1), pp.44-59.

Phuan, P.W., Zhang, H., Asavapanumas, N., Leviten, M., Rosenthal, A., Tradtrantip, L. and Verkman, A.S., 2013. C1q-targeted monoclonal antibody prevents complement-dependent cytotoxicity and neuropathology in in vitro and mouse models of neuromyelitis optica. Acta Neuropathologica, 125(6), pp.829-840.

Polyak, K. and Kalluri, R., 2010. The role of the microenvironment in mammary gland development and cancer. Cold Spring Harbor Perspectives in Biology, 2(11), p.a003244.

Poon, I.K.H., Hulett, M.D. and Parish, C.R., 2010. Molecular mechanisms of late apoptotic/necrotic cell clearance. Cell Death & Differentiation, 17(3), pp.381-397.

Poon, I.K., Lucas, C.D., Rossi, A.G. and Ravichandran, K.S., 2014. Apoptotic cell clearance: basic biology and therapeutic potential. Nature Reviews Immunology, 14(3), pp.166-180.

PrabhuDas, M.R., Baldwin, C.L., Bollyky, P.L., Bowdish, D.M., Drickamer, K., Febbraio, M., Herz, J., Kobzik, L., Krieger, M., Loike, J. and McVicker, B., 2017. A consensus definitive classification of scavenger receptors and their roles in health and disease. The Journal of Immunology, 198(10), pp.3775-3789.

Ragupathi, G., 1996. Carbohydrate antigens as targets for active specific immunotherapy. Cancer Immunology, Immunotherapy, 43(3), pp.152-157.

Ramirez-Ortiz, Z.G., Pendergraft, W.F., Prasad, A., Byrne, M.H., Iram, T., Blanchette, C.J., Luster, A.D., Hacohen, N., El Khoury, J. and Means, T.K., 2013. The scavenger receptor SCARF1 mediates the clearance of apoptotic cells and prevents autoimmunity. Nature Immunology, 14(9), pp.917-926.

Raschke, W.C., Baird, S., Ralph, P. and Nakoinz, I., 1978. Functional macrophage cell lines transformed by Abelson leukemia virus. Cell, 15(1), pp.261-267.

Rastogi, R.P., Kumar, A., Tyagi, M.B. and Sinha, R.P., 2010. Molecular mechanisms of ultraviolet radiation-induced DNA damage and repair. Journal of Nucleic Acids, 2010.

Ratko, T.A. and Beattie, C.W., 1985. Estrous cycle modification of rat mammary tumor induction by a single dose of N-methyl-N-nitrosourea. Cancer Research, 45(7), pp.3042-3047.

Ravichandran, K.S., 2011. Beginnings of a good apoptotic meal: the find-me and eat-me signaling pathways. Immunity, 35(4), pp.445-455.

Richardson, H., O'Keefe, L.V., Marty, T. and Saint, R., 1995. Ectopic cyclin E expression induces premature entry into S phase and disrupts pattern formation in the Drosophila eye imaginal disc. Development, 121(10), pp.3371-3379.

Roth, D.B., 2015. V (D) J recombination: mechanism, errors, and fidelity. Mobile DNA III, pp.311-324

Roos, A., Nauta, A.J., Broers, D., Faber-Krol, M.C., Trouw, L.A., Drijfhout, J.W. and Daha, M.R., 2001. Specific inhibition of the classical complement pathway by C1q-binding peptides. The Journal of Immunology, 167(12), pp.7052-7059.

Rosen, J.E., Chan, L., Shieh, D.B. and Gu, F.X., 2012. Iron oxide nanoparticles for targeted cancer imaging and diagnostics. Nanomedicine: Nanotechnology, Biology and Medicine, 8(3), pp.275-290.

Rőszer, T., 2015. Understanding the mysterious M2 macrophage through activation markers and effector mechanisms. Mediators of Inflammation, 2015.

Roumenina, L.T., Sène, D., Radanova, M., Blouin, J., Halbwachs-Mecarelli, L., Dragon-Durey, M.A., Fridman, W.H. and Fremeaux-Bacchi, V., 2011. Functional complement C1q abnormality leads to impaired immune complexes and apoptotic cell clearance. The Journal of Immunology, 187(8), pp.4369-4373.

Roy, R., Chun, J. and Powell, S.N., 2012. BRCA1 and BRCA2: different roles in a common pathway of genome protection. Nature Reviews Cancer, 12(1), pp.68-78.

Russo, J., Ao, X., Grill, C. and Russo, I.H., 1999. Pattern of distribution of cells positive for estrogen receptor α and progesterone receptor in relation to proliferating cells in the mammary gland. Breast Cancer Research and Treatment, 53(3), pp.217-227.

Ryu, J.M., Yu, J., Kim, S.I., Kim, K.S., Moon, H.G., Choi, J.E., Jeong, J., Do Byun, K., Nam, S.J., Lee, J.E. and Lee, S.K., 2017. Different prognosis of young breast cancer patients in their 20s and 30s depending on subtype: a nationwide study from the Korean Breast Cancer Society. Breast Cancer Research and Treatment, 166(3), pp.833-842.

Sano, K., Mitsunaga, M., Nakajima, T., Choyke, P.L. and Kobayashi, H., 2012. *In vivo* breast cancer characterization imaging using two monoclonal antibodies activatably labeled with near infrared fluorophores. Breast Cancer Research, 14(2), pp.1-8.

Santulli-Marotto, S., Gervais, A., Fisher, J., Strake, B., Ogden, C.A., Riveley, C. and Giles-Komar, J., 2015. Discovering molecules that regulate efferocytosis using primary human macrophages and high **c**ontent imaging. PLoS One, 10(12), p.e0145078.

Sasmono, R.T. and Williams, E., 2012. Generation and characterization of MacGreen mice, the Cfs1r-EGFP transgenic mice. In Leucocytes (pp. 157-176). Humana Press.

Schejbel, L., Skattum, L., Hagelberg, S., Åhlin, A., Schiller, B., Berg, S., Genel, F., Truedsson, L. and Garred, P., 2011. Molecular basis of hereditary C1q deficiency—revisited: identification of several novel disease-causing mutations. Genes & Immunity, 12(8), pp.626-634.

Schwartz, L.H., Litière, S., De Vries, E., Ford, R., Gwyther, S., Mandrekar, S., Shankar, L., Bogaerts, J., Chen, A., Dancey, J. and Hayes, W., 2016. RECIST 1.1—Update and clarification: From the RECIST committee. European Journal of Cancer, 62, pp.132-137.

Seino, J., Fukuoka, Y., Okuda, T. and Tachibana, T., 1984. Isolation, Molecular Properties and Allotype of Mouse Clq. The Tohoku Journal of Experimental Medicine, 142(4), pp.351-361.

Seitz, H.M., Camenisch, T.D., Lemke, G., Earp, H.S. and Matsushima, G.K., 2007. Macrophages and dendritic cells use different Axl/Mertk/Tyro3 receptors in clearance of apoptotic cells. The Journal of Immunology, 178(9), pp.5635-5642.

Selvarajan, V., Bidkar, A.P., Shome, R., Banerjee, A., Chaubey, N., Ghosh, S.S. and Sanpui, P., 2017. Studying *in vitro* phagocytosis of apoptotic cancer cells by recombinant GMCSF-treated RAW 264.7 macrophages. International Journal of Biological Macromolecules, 102, pp.1138-1145.

Shapiro, L. and Scherer, P.E., 1998. The crystal structure of a complement-1q family protein suggests an evolutionary link to tumor necrosis factor. Current Biology, 8(6), pp.335-340.

Sharp, J.A., Whitley, P.H., Cunnion, K.M. and Krishna, N.K., 2014. Peptide inhibitor of complement c1, a novel suppressor of classical pathway activation: mechanistic studies and clinical potential. Frontiers in Immunology, 5, p.406.

Shi, T., Wrin, J., Reeder, J., Liu, D. and Ring, D.B., 1995. High-affinity monoclonal antibodies against P-glycoprotein. Clinical Immunology and Immunopathology, 76(1), pp.44-51.

Shulman, M., Wilde, C.D. and Köhler, G., 1978. A better cell line for making hybridomas secreting specific antibodies. Nature, 276(5685), pp.269-270.

Sidaway, P., 2020. Neoadjuvant therapy improves pCR rate. Nature Reviews Clinical Oncology, 17(12), pp.718-718.

Simkins, S.G., Knapp, S.L., Brough, G.H., Lenz, K.L., Barley-Maloney, L., Baker, J.P., Dekking, L., Wai, H. and Dixon, E.P., 2011. Generation of monoclonal antibodies to the AML1-ETO fusion protein: strategies for overcoming high homology. Hybridoma, 30(5), pp.433-443.

Son, M., Diamond, B. and Santiago-Schwarz, F., 2015. Fundamental role of C1q in autoimmunity and inflammation. Immunologic Research, 63(1), pp.101-106.

Son, M., Diamond, B., Volpe, B.T., Aranow, C.B., Mackay, M.C. and Santiago-Schwarz, F., 2017. Evidence for C1q-mediated crosslinking of CD33/LAIR-1 inhibitory immunoreceptors and biological control of CD33/LAIR-1 expression. Scientific Reports, 7(1), pp.1-13.

Son, M., Porat, A., He, M., Suurmond, J., Santiago-Schwarz, F., Andersson, U., Coleman, T.R., Volpe, B.T., Tracey, K.J., Al-Abed, Y. and Diamond, B., 2016. C1q and HMGB1 reciprocally regulate human macrophage polarization. Blood, The Journal of the American Society of Hematology, 128(18), pp.2218-2228.

Son, M., Santiago-Schwarz, F., Al-Abed, Y. and Diamond, B., 2012. C1q limits dendritic cell differentiation and activation by engaging LAIR-1. Proceedings of the National Academy of Sciences, 109(46), pp.E3160-E3167.

Southey, M.C., Goldgar, D.E., Winqvist, R., Pylkäs, K., Couch, F., Tischkowitz, M., Foulkes, W.D., Dennis, J., Michailidou, K., Van Rensburg, E.J. and Heikkinen, T., 2016. PALB2, CHEK2 and ATM rare variants and cancer risk: data from COGS. Journal of Medical Genetics, 53(12), pp.800-811.

Spivia, W., Magno, P.S., Le, P. and Fraser, D.A., 2014. Complement protein C1q promotes macrophage anti-inflammatory M2-like polarization during the clearance of atherogenic lipoproteins. Inflammation Research, 63(10), pp.885-893.

Spring **L.**M., Fell, G., Arfe, A., Sharma, C., Greenup, R., Reynolds, K.L., Smith, B.L., Alexander, B., Moy, B., Isakoff, S.J. and Parmigiani, G., 2020. Pathologic complete response after neoadjuvant chemotherapy and impact on breast cancer recurrence and survival: a comprehensive meta-analysis. Clinical Cancer Research, 26(12), pp.2838-2848.

Stein, T., Salomonis, N. and Gusterson, B.A., 2007. Mammary gland involution as a multi-step process. Journal of Mammary Gland Biology and Neoplasia, 12(1), pp.25-35.

Stöhr, R., Deckers, N., Schurgers, L., Marx, N. and Reutelingsperger, C.P., 2018. AnnexinA5-pHrodo: a new molecular probe for measuring efferocytosis. Scientific Reports, 8(1), pp.1-9.

Sun, X., Bernhardt, S.M., Glynn, D.J., Hodson, L.J., Woolford, L., Evdokiou, A., Yan, C., Du, H., Robertson, S.A. and Ingman, W.V., 2021. Attenuated TGFB signalling in macrophages decreases susceptibility to DMBA-induced mammary cancer in mice. Breast Cancer Research, 23(1), pp.1-16.

Sun, X., Robertson, S.A. and Ingman, W.V., 2013. Regulation of epithelial cell turnover and macrophage phenotype by epithelial cell-derived transforming growth factor beta1 in the mammary gland. Cytokine, 61(2), pp.377-388.

Suzuki, M., Kato, C. and Kato, A., 2015. Therapeutic antibodies: their mechanisms of action and the pathological findings they induce in toxicity studies. Journal of Toxicologic Pathology, 28(3), pp.133-139.

Tang, D.C., DeVit, M. and Johnston, S.A., 1992. Genetic immunization is a simple method for eliciting an immune response. Nature, 356(6365), pp.152-154.

Tang, Y.T., Hu, T., Arterburn, M., Boyle, B., Bright, J.M., Palencia, S., Emtage, P.C. and Funk, W.D., 2005. The complete complement of C1q-domain-containing proteins in Homo sapiens. Genomics, 86(1), pp.100-111.

Tang, D., Kang, R., Coyne, C.B., Zeh, H.J. and Lotze, M.T., 2012. PAMP s and DAMP s: Signal 0s that spur autophagy and immunity. Immunological Reviews, 249(1), pp.158-175.

Taylor, J.S. and Raes, J., 2004. Duplication and divergence: the evolution of new genes and old ideas. Annual Review of Genetics, 38, pp.615-643.
199.

Thielens, N.M., Tedesco, F., Bohlson, S.S., Gaboriaud, C. and Tenner, A.J., 2017. C1q: A fresh look upon an old molecule. Molecular Immunology, 89, pp.73-83.

Thompson, A.M. and Moulder-Thompson, S.L., 2012. Neoadjuvant treatment of breast cancer. Annals of Oncology, 23, pp.x231-x236.

Thorn, C.F., Oshiro, C., Marsh, S., Hernandez-Boussard, T., McLeod, H., Klein, T.E. and Altman, R.B., 2011. Doxorubicin pathways: pharmacodynamics and adverse effects. Pharmacogenetics and Genomics, 21(7), p.440.

Tichy, E.D., Stephan, Z.A., Osterburg, A., Noel, G. and Stambrook, P.J., 2013. Mouse embryonic stem cells undergo charontosis, a novel programmed cell death pathway dependent upon cathepsins, p53, and EndoG, in response to etoposide treatment. Stem Cell Research, 10(3), pp.428-441.

Tirumalai, R.S., Chan, K.C., Prieto, D.A., Issaq, H.J., Conrads, T.P. and Veenstra, T.D., 2003. Characterization of the Low Molecular Weight Human Serum Proteome* S. Molecular & Cellular Proteomics, 2(10), pp.1096-1103.

Toong, C., Adelstein, S. and Phan, T.G., 2011. Clearing the complexity: immune complexes and their treatment in lupus nephritis. International Journal of Nephrology and Renovascular Disease, 4, p.17.

Tworoger, S.S. and Hankinson, S.E., 2006. Prolactin and breast cancer risk. Cancer Letters, 243(2), pp.160-169.

Unsworth, A., Anderson, R. and Britt, K., 2014. Stromal fibroblasts and the immune microenvironment: partners in mammary gland biology and pathology?. Journal of Mammary Gland Biology and Neoplasia, 19(2), pp.169-182.

Unverdorben, F., Richter, F., Hutt, M., Seifert, O., Malinge, P., Fischer, N. and Kontermann, R.E., 2016, January. Pharmacokinetic properties of IgG and various Fc fusion proteins in mice. In MAbs (Vol. 8, No. 1, pp. 120-128). Taylor & Francis.

van den Berg, R.H., Faber-Krol, M.C., van Wetering, S., Hiemstra, P.S. and Daha, M.R., 1998. Inhibition of activation of the classical pathway of complement by human neutrophil defensins. Blood, The Journal of the American Society of Hematology, 92(10), pp.3898-3903.

van Essen, H.F., Verdaasdonk, M.A., Elshof, S.M., De Weger, R.A. and Van Diest, P.J., 2010. Alcohol based tissue fixation as an alternative for formaldehyde: influence on immunohistochemistry. Journal of Clinical Pathology, 63(12), pp.1090-1094.

van Schaarenburg, R.A., Suurmond, J., Habets, K.L., Brouwer, M.C., Wouters, D., Kurreeman, F.A., Huizinga, T.W., Toes, R.E. and Trouw, L.A., 2016. The production and secretion of complement component C1q by human mast cells. Molecular Immunology, 78, pp.164-170.

Vandivier, R.W., Ogden, C.A., Fadok, V.A., Hoffmann, P.R., Brown, K.K., Botto, M., Walport, M.J., Fisher, J.H., Henson, P.M. and Greene, K.E., 2002. Role of surfactant proteins A, D, and C1q in the clearance of apoptotic cells *in vivo* and *in vitro*: calreticulin and CD91 as a common collectin receptor complex. The Journal of Immunology, 169(7), pp.3978-3986.

Varadan, V., Gilmore, H., Miskimen, K.L., Tuck, D., Parsai, S., Awadallah, A., Krop, I.E., Winer, E.P., Bossuyt, V., Somlo, G. and Abu-Khalaf, M.M., 2016. Immune signatures following single dose trastuzumab predict pathologic response to preoperative trastuzumab and chemotherapy in HER2-positive early breast cancer. Clinical Cancer Research, 22(13), pp.3249-3259.

Vazquez-Lombardi, R., Nevoltris, D., Luthra, A., Schofield, P., Zimmermann, C. and Christ, D., 2018. Transient expression of human antibodies in mammalian cells. Nature Protocols, 13(1), pp.99-117.

Verma, A., Ngundi, M.M., Meade, B.D., De Pascalis, R., Elkins, K.L. and Burns, D.L., 2009. Analysis of the Fc gamma receptor-dependent component of neutralization measured by anthrax toxin neutralization assays. Clinical and Vaccine Immunology, 16(10), pp.1405-1412.

Verneret, M., Tacnet-Delorme, P., Osman, R., Awad, R., Grichine, A., Kleman, J.P. and Frachet, P., 2014. Relative contribution of c1q and apoptotic cell-surface calreticulin to macrophage phagocytosis. Journal of Innate Immunity, 6(4), pp.426-434.

Visvader, J.E., 2009. Keeping abreast of the mammary epithelial hierarchy and breast tumorigenesis. Genes & Development, 23(22), pp.2563-2577.

Vonderheide, R.H., 2020. CD40 agonist antibodies in cancer immunotherapy. Annual Review of Medicine, 71, pp.47-58.

Wang, Y.A., Jian, J.W., Hung, C.F., Peng, H.P., Yang, C.F., Cheng, H.C.S. and Yang, A.S., 2018. Germline breast cancer susceptibility gene mutations and breast cancer outcomes. BMC Cancer, 18(1), pp.1-13.

Wang, Y., Martins, I., Ma, Y., Kepp, O., Galluzzi, L. and Kroemer, G., 2013. Autophagy-dependent ATP release from dying cells via lysosomal exocytosis. Autophagy, 9(10), pp.1624-1625.

Wang, T., Wu, X., Guo, C., Zhang, K., Xu, J., Li, Z. and Jiang, S., 2018. Development of inhibitors of the programmed cell death-1/programmed cell death-ligand 1 signaling pathway. Journal of Medicinal Chemistry, 62(4), pp.1715-1730.

Wang, B., Yang, C., Jin, X., Du, Q., Wu, H., Dall'Acqua, W. and Mazor, Y., 2020, January. Regulation of antibody-mediated complement-dependent cytotoxicity by modulating the intrinsic affinity and binding valency of IgG for target antigen. In MAbs (Vol. 12, No. 1, p. 1690959). Taylor & Francis.

Watson, C.J., 2006. Key stages in mammary gland development-Involution: apoptosis and tissue remodelling that convert the mammary gland from milk factory to a quiescent organ. Breast Cancer Research, 8(2), pp.1-5.

Welling, G.W., Weijer, W.J., van der Zee, R. and Welling-Wester, S., 1985. Prediction of sequential antigenic regions in proteins. FEBS letters, 188(2), pp.215-218.

Wijeyesakere, S.J., Bedi, S.K., Huynh, D. and Raghavan, M., 2016. The C-terminal acidic region of calreticulin mediates phosphatidylserine binding and apoptotic cell phagocytosis. The Journal of Immunology, 196(9), pp.3896-3909.

Wilson, C.L., Sims, A.H., Howell, A., Miller, C.J. and Clarke, R.B., 2006. Effects of oestrogen on gene expression in epithelium and stroma of normal human breast tissue. Endocrine-related Cancer, 13(2), pp.617-628.

Wines, B.D., Powell, M.S., Parren, P.W., Barnes, N. and Hogarth, P.M., 2000. The IgG Fc contains distinct Fc receptor (FcR) binding sites: the leukocyte receptors FcγRI and FcγRIIa bind to a region in the Fc distinct from that recognized by neonatal FcR and protein A. The Journal of Immunology, 164(10), pp.5313-5318.

Wu, Q., Li, B., Li, Z., Li, J., Sun, S. and Sun, S., 2019. Cancer-associated adipocytes: key players in breast cancer progression. Journal of Hematology & Oncology, 12(1), pp.1-15.

Yannakakis, M.P., Simal, C., Tzoupis, H., Rodi, M., Dargahi, N., Prakash, M., Mouzaki, A., Platts, J.A., Apostolopoulos, V. and Tselios, T.V., 2017. Design and synthesis of non-peptide mimetics mapping the immunodominant myelin basic protein (MBP83–96) epitope to function as T-cell receptor antagonists. International Journal of Molecular Sciences, 18(6), p.1215.

Yao, L., Chen, Y., Wang, X., Bi, Z., Xiao, Q., Lei, J., Yan, Y., Zhou, J. and Yan, L., 2020. Identification of antigenic epitopes in the haemagglutinin protein of H7 avian influenza virus. Avian Pathology, 49(1), pp.62-73.

Yuan, Y., Xu, Y., Xu, J., Ball, R.L. and Liang, H., 2012. Predicting the lethal phenotype of the knockout mouse by integrating comprehensive genomic data. Bioinformatics, 28(9), pp.1246-1252.

Yue, W., Wang, J.P., Li, Y., Fan, P., Liu, G., Zhang, N., Conaway, M., Wang, H., Korach, K.S., Bocchinfuso, W. and Santen, R., 2010. Effects of estrogen on breast cancer development: Role of estrogen receptor independent mechanisms. International Journal of Cancer, 127(8), pp.1748-1757.

Zahavi, D. and Weiner, L., 2020. Monoclonal antibodies in cancer therapy. Antibodies, 9(3), p.34.
Golay, J. and Taylor, R.P., 2020. The role of complement in the mechanism of action of therapeutic anti-cancer mAbs. Antibodies, 9(4), p.58.

Zeitelhofer, M., Li, H., Adzemovic, M.Z., Nilsson, I., Muhl, L., Scott, A.M. and Eriksson, U., 2018. Preclinical toxicological assessment of a novel monoclonal antibody targeting human platelet-derived growth factor CC (**p**DGF-CC) in PDGF-CChum mice. PloS One, 13(7), p.e0200649.

Zhao, Y.L., Tian, P.X., Han, F., Zheng, J., Xia, X.X., Xue, W.J., Ding, X.M. and Ding, C.G., 2017. Comparison of the characteristics of macrophages derived from murine spleen, peritoneal cavity, and bone marrow. Journal of Zhejiang University-Science B, 18(12), pp.1055-1063.

Zheng, A., Kallio, A. and Härkönen, P., 2007. Tamoxifen-induced Rapid Death of MCF-7 Breast Cancer Cells is mediated via ERK Signaling and can be abrogated by Estrogen. Endocrinology, 148(6), pp.2764-2777.

Zhou, A.Y., Ichaso, N., Adamarek, A., Zila, V., Forstova, J., Dibb, N.J. and Dilworth, S.M., 2011. Polyomavirus middle T-antigen is a transmembrane protein that binds signaling proteins in discrete subcellular membrane sites. Journal of Virology, 85(7), pp.3046-3054.

Zijlstra, M., Bix, M., Simister, N.E., Loring, J.M., Raulet, D.H. and Jaenisch, R., 1990. β2-microglobulin deficient mice lack CD4− 8+ cytolytic T cells. Nature, 344(6268), pp.742-746.

Zinonos, I., Labrinidis, A., Lee, M., Liapis, V., Hay, S., Ponomarev, V., Diamond, P., Zannettino, A.C., Findlay, D.M. and Evdokiou, A., 2009. Apomab, a fully human agonistic antibody to DR5, exhibits potent antitumor activity against primary and metastatic breast cancer. Molecular Cancer Therapeutics, 8(10), pp.2969-2980.